Determination of Organ Specific Pharmacokinetic Data for the Anti-Tuberculosis Drugs in Guinea Pigs Using Microdialysis

Thesis

DETERMINATION OF ORGAN SPECIFIC PHARMACOKINETIC DATA FOR THE ANTI- TUBERCULOSIS DRUGS IN GUINEA PIGS USING MICRODIALYSIS

OU PERSONAL IDENTIFIER: D0997213

AFFILIATED RESEARCH CENTRE: PUBLIC HEALTH ENGLAND, PORTON DOWN

REGISTERED DISCIPLINE: LIFE AND BIOMOLECULAR SCIENCE

SCHEME OF STUDY: PART TIME

SUBMITTED FOR THE DEGREE OF DOCTOR OF PHILOSOPHY

FAYE RACHEL LANNI

SUPERVISED BY:

DR. ANN RAWKINS

DR. STUART ARMSTRONG

PROFESSOR. GERAINT DAVIES

SEPTEMBER 2019

ABSTRACT

Optimised pre-clinical models are required for TB drug development to better predict the pharmacokinetics of anti-TB drugs to shorten the time taken for novel drugs and combinations to be approved for clinical trial.

Microdialysis can be used to measure unbound drug concentrations in awake freely moving animals in order to describe the pharmacokinetic behaviour of drugs in the organs as a continuous sampling technique. The aim of this PhD was to develop and optimise the microdialysis methodology in the guinea pig model to better understand the pharmacokinetics of anti-TB drugs in the lung.

Meticulous *in vitro* experiments were performed with each drug before progressing into *in vivo* experiments because the recovery (concentration of the drug in the tissue fluid related to that in the collected dialysate) of the drug was dependent upon a variety of experimental conditions. Mass spectrometry of the dialysate was used to determine the impact of flow rate, perfusion fluid, and the molecular weight cut-off and membrane length of probes on the recovery of rifampicin at physiologically relevant concentrations. Following identification of a correlation between rifampicin concentrations in lung and skeletal muscle and determination of probe efficiency, experiments were conducted to measure rifampicin in the sacrospinalis of guinea pigs using microdialysis. This demonstrated feasibility to use microdialysis in the guinea pig to generate organ-specific pharmacokinetic data. The data were robust and reproducible especially when compared to those generated from blood sampling. Lung concentrations were estimated from the sacrospinalis enabling calculation of AUC:MIC and Cmax:MIC ratios (PK/PD parameters associated with mycobacterial killing). Human-like values for these ratios were obtained in the lung but not in blood, indicating the power of the microdialysis to more accurately measure the PK parameters of drugs in organs. These studies established the microdialysis methodology and demonstrated its potential in developing predictive pre-clinical models.

For Neil and Luther

ACKNOWLEDGMENTS

Foremost, I would like to express my sincere gratitude to Dr. Ann Rawkins for the continuous support she has given me throughout the duration of my PhD, both professionally and personally. I honestly could not have wished for a better Director of Studies and mentor.

I would like to thank my other two supervisors, Professor Gerry Davies and Dr. Stuart Armstrong for their invaluable knowledge on pharmacokinetics and microdialysis.

I am indebted to Neil Burton, without whom this PhD would not have been possible. Thank you for continued use of both the mass spectrometers and Nespresso machine.

The *in vivo* aspects of this PhD were heavily dependent upon the experience and expertise of Mike Dennis, Irene Taylor and their incredibly talented team of staff led by Mark Cornwall, Susan Fotheringham, Nathan Wiblin, Ollie Skinner and Debbie Harris.

I would also like to acknowledge Emma Rayner for her veterinary skills, Rich Orledge for all his help in setting up the TRENDnet system and the TB group (past and present) for moral, emotional and practical support.

A special mention must be given to the PreDiCT TB consortium especially Henry Pertinez and Fatima Ortega-Muro for their input into these studies and continually prompt email responses. I would also like to thank Anne Lenaerts for sharing data with me.

I would like to thank Public Health England for funding my studies, it has been a wonderful and unique opportunity to complete these studies part-time whilst also furthering my career as a research scientist.

My parents, Michaela and John, my brother Joseph (and dog Oscar) have been a constant support, I couldn't have done it without you. I would like to mention my friends Helen, Hannah, Ele, Sam and Chris to thank them for listening to me talk about guinea pigs an obscene amount.

And finally, Daniel, you are a daily inspiration to me. Your continued support, even in the darkest hours, is what has kept me going. Obrigada,

TABLE OF CONTENTS

TABLE OF FIGURES

TABLE OF TABLES

ABBREVIATIONS

%CoV: % co-efficient of variation

%RR: %Relative Recovery

(RR-)(M-)(X-)DR-TB: (Rifampicin Resistant-) (Multi-) (Extensively-) Drug resistant -TB

°C: Degrees Centigrade

µl: microlitre

µm: micrometre

ADME: Absorption, Distribution, Metabolism, Excretion

AIDS: Acquired immune deficiency syndrome

ART: Anti-Retroviral Therapy

AUC: Area Under the Curve

B: Bound

BSA: Bovine Serum Albumin

$CaCl_2$: Calcium chloride

CAD: Collision activated dissociation

CE: Collision energy

CFU: Colony forming units

cm: centimetre

Cmax: Maximum Concentration

CNS: Central nervous system

CT: Computerised tomography

CUR: Curtain gas

CXP: Collision cell exit potential

Da: Daltons

DDI: Drug-drug interaction

DMSO: Dimethyl sulfoxide

DP: Declustering potential

DS-TB: Drug susceptible TB

DXT: Dextromethorphan

EMA: European Medicines Agency

ESI: Electrospray ionisation

ETH: Ethambutol

FDA: Food and Drug Administration

FEP: Fluorinated Ethylene Polypropylene

FP: Focussing potential

g: gram

Ga: Gauge

GI: Gastrointestinal

GSK: GlaxoSmithKlein

h: hour

HIV: Human immunodeficiency virus

HPLC: High Performance Liquid Chromatography

INH: Isoniazid

IS: Ion spray voltage

KCl: Potassium chloride

kDa: kilodalton

kg: kilogram

L: litre

LC-MS/MS: Liquid Chromatography Mass Spectrometry

LHS: Left Hand Side

LLOQ: Lower Limit of Quantitation

MDR: Multi-Drug Resistant TB

mg: milligram

$MgCl_2$: Magnesium chloride

MIC: Minimum Inhibitory Concentration

min: minute

ml: millilitre

mm: millimetre

mmol/L: millimoles per litre

Mo: Month

MRM: Multiple Reaction Monitoring

MS: Mass Spectrometry

Mw: Molecular Weight

NaCl: Sodium chloride

NADH: Nicotinamide adenine dinucleotide

NEB: nebuliser gas

ng: nanogram

nm: nanometres

NSAID: Non -steroidal anti-inflammatory drug

PanACEA: Pan-African Consortium for the Evaluation of Antituberculosis Antibiotics

PAS: Para-amino salicylic acid

PD: Pharmacodynamic

PK: Pharmacokinetics

PPB: Plasma Protein Binding

PZA: Pyrazinamide

ReMoxTB: Rapid Evaluation of Moxifloxacin in Tuberculosis

RHS: Right Hand Side

RIF: Rifampicin

RNA: Ribonucleic Acid

SD: Standard Deviation

SKM: Skeletal Muscle

TEM: Temperature of ion source

Tmax: Time at which maximum concentration occurs

TNF: Tumour Necrosis Factor

UB: Unbound

UK: United Kingdom

UPLC-MS/MS: Ultra-high performance liquid chromatography-mass spectrometry/mass spectrometry

UV: Ultra-violet

WHO: World Health Organisation

CHAPTER 1

INTRODUCTION

1.1 TUBERCULOSIS

1.1.1 GLOBAL BURDEN OF TB DISEASE AND IMPACT OF INTERVENTIONS.

Tuberculosis (TB), still, kills more people than any other infectious disease with 1.7 million deaths in 2017 alone[1]. It is the oldest infectious disease known to man and despite the causative agent, *Mycobacterium tuberculosis*, being identified by Robert Koch in 1882[2] and studied ever since, tuberculosis kills more people every three days than the whole of the West African Ebola outbreak in 2015. This continuing vast global burden can be attributed to a number of reasons including; the ability of the organism to enter a latent state[3], susceptibility to disease being strongly linked with social and economic inequalities[4], the association with and exacerbation of TB disease in persons co-infected with other diseases, especially HIV[5] and diabetes[6], the ability of the bacterium to manipulate host immunity in order to ensure survival[7], and to adapt to resist drug treatment leading to the emergence of drug-resistant strains[8].

Mycobacterium tuberculosis (M.tb), is a bacterium (Order: Actinomycetales, Genus: Mycobacteria) which is part of the *Mycobacterium tuberculosis* complex (MTBC). The MTBC also contains *M. bovis, M. canetti, M. africanum, M. microti* and *M. marinum*, all of which (except *M. bovis*) are adapted to a particular host species and share a common African ancestor which originated 35,000-15,000 years ago[9]. There are currently seven main circulating lineages of M.tb, classified using large sequence polymorphisms (LSPs) and single nucleotide polymorphisms (SNPs)[10] . The lineages are associated with distinct geographical regions and each differs genotypically and phenotypically including differences in virulence and drug resistance[11]. The highest burden of TB disease is found in East and South East Asia (caused mainly by Lineages 1, 2 and 3) whereas Lineage 4 causes the majority of disease in Europe,

North Africa and the Americas. Lineages 5 and 6 are classified as *M. africanum* and these lineages are limited to West-African regions, where they are responsible for 50% of the TB disease burden[12], and Lineage 7 is localised to Ethiopia and associated with immigrants from Ethiopia[13]. TB is, therefore, a heterogeneously distributed disease with certain regions of the world having higher disease burdens than others.

It is evident why TB is referred to as the 'Plague of Poverty[14]' when eight low and middle income countries account for 60% of TB associated deaths; India, China, Indonesia, Nigeria, Pakistan, Bangladesh, The Phillipines and South Africa. South Africa is also the location of the world's largest HIV epidemic[15]. 12% of all new active tuberculosis cases and 25% of all tuberculosis related deaths are due to HIV co-infection and active tuberculosis is the primary cause of hospitalisation in HIV infected adults and children[1]. There are numerous other pre-disposing and precipitating factors that contribute to the global TB burden which are shown in Figure 1.1.

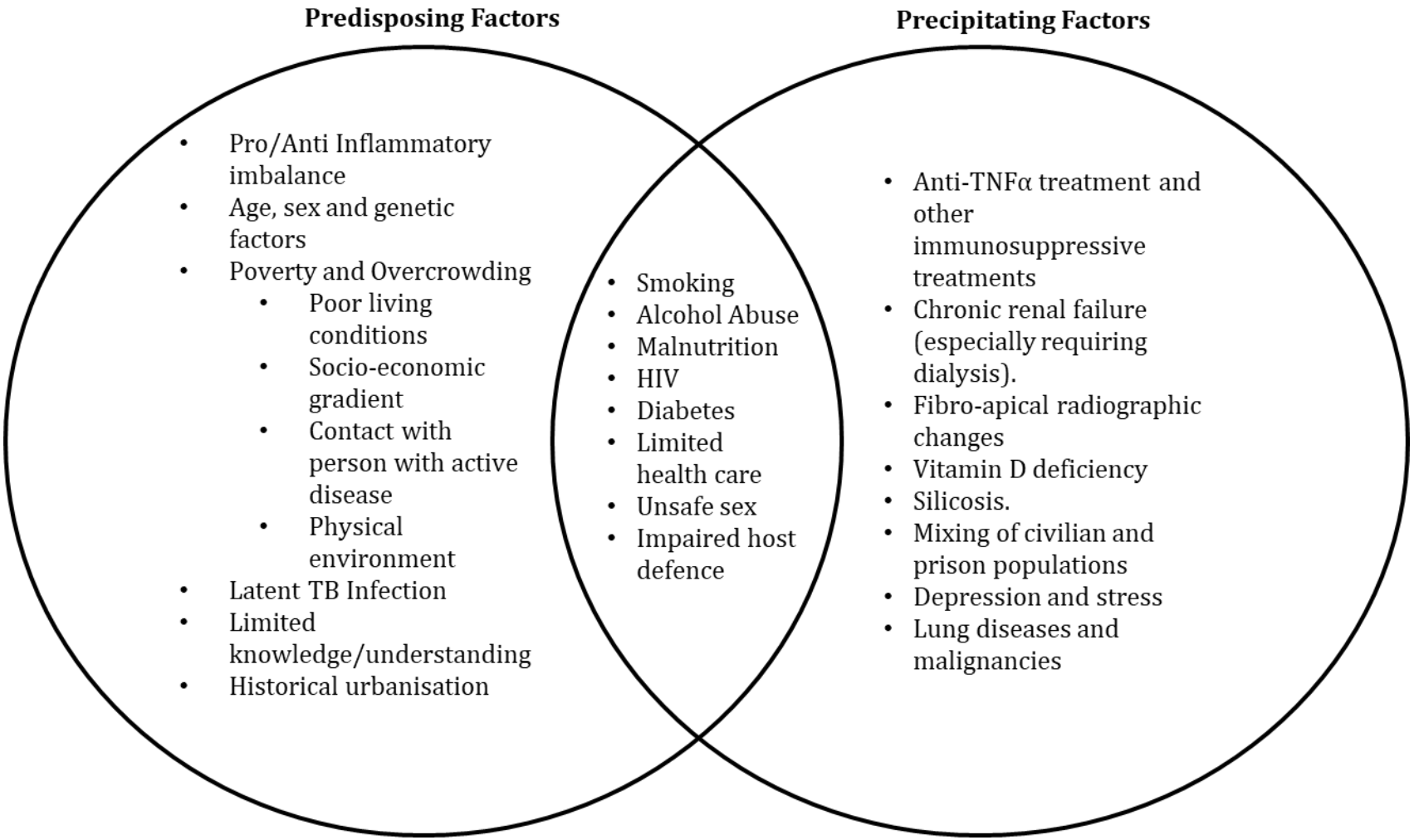

FIGURE 1.1: PRE-DISPOSING AND PRECIPITATING FACTORS THAT HAVE INCREASED THE GLOBAL TB BURDEN. This diagram was based on information found in 'Risk Factors for Tuberculosis[16]' and 'The Ongoing Challenge of Latent Tuberculosis[17]'.

The influence of socio-economic factors on TB is evidenced by the fact that between the late 1940's and 1980, the global burden of TB declined due to the combination of socio-economic growth and reform, declining poverty, improved living conditions, and increased hygiene but this period also saw the introduction of mass vaccination of the population with the BCG (Bacille Calmette Guerin) vaccine[18]. BCG has proven efficacy at preventing extra-pulmonary TB in children, although in adults the efficacy of BCG is variable dependent upon numerous factors including host, environmental and mycobacterial, yet still to this day it is the only licenced vaccine for TB[19].

The incidence of TB disease declined even further when the anti-tuberculosis drugs were introduced, with streptomycin co-administered with bed-rest as early as 1944 and the first drug regimen of streptomycin, para-amino salicylic acid (PAS) and isoniazid used in 1952[20]. However, in the 1990s, catalysed by the global HIV outbreak in the 1980s, an increase of poor living conditions especially in the former USSR, and patient non-compliance with the lengthy and toxic anti-TB drug regimens, the global burden of TB again increased and TB was declared a global health emergency in 1991[21]. This resurgence of disease burden highlights that in order to reduce the incidence of TB disease social, economic and environmental interventions need to be considered as well as medical interventions, such as drugs, diagnostics and vaccines.

1.1.2 HOST-PATHOGEN FACTORS THAT INFLUENCE TREATMENT OF TB DISEASE

Infection with M.tb is established in the lung following inhalation of one or more droplet nuclei, each of which is estimated to contain between 1-3 bacilli[22]. Once inhaled, the bacteria lodge in the alveoli where ingestion by alveolar macrophages occurs. Within macrophages, the bacteria deploy several mechanisms to resist intracellular killing including blocking of phagosome-lysosome fusion[23]. In addition to resisting killing by macrophages, M.tb has an array of strategies for survival and adaptation to the host environment which involve manipulation of the innate and acquired immune system[23]. In the lungs, a consequence of the host-pathogen interaction is the development of granulomas which form following recruitment of

lymphocytes and monocytes to the initial site of infection[7]. These granulomas may resolve upon successful eradication of the bacteria or, as bacteria replicate and cause cell damage which stimulates further host responses, the granuloma matures to an organised aggregation of different cell types which form around a central core of bacteria and cell debris, collectively described as the caseum. The necrotic caseum can fuse with the airway structure to form a cavity, which also contains a large number of slow growing and non-replicating mycobacteria[24].

Whilst granulomas are a host defence mechanism to enclose the bacteria and restrict spread, M.tb is able to survive and persist within these structures and this environment can be a protective niche, for example from drugs which, due to destruction of the vasculature, are unable to reach the bacteria[25]. It is known that genetically drug sensitive bacteria can be found persisting in granulomas throughout the treatment duration in different locations[26]. These lesions are also associated with different types of microenvironments such as oxygen tension, low pH and nutrient supply, which are known to affect drug efficacy[27]. Any or a combination of these host factors are responsible for the fact that drug treatment regimens are not always successful in complete eradication of M.tb from the host. The ability of M.tb to resist immune-mediated killing and persist means that relapse of disease can occur following the end of treatment[28]. The aim of a therapeutic regimen is therefore not just to treat and resolve the symptoms and consequences of active disease but also to prevent relapse by killing persisting organisms[29].

The process by which M.tb resists host defences and initiates a progressive infection leading to active disease is thought to occur in only a small proportion of those infected, approximately 5-10% with the remaining 90% becoming latently infected[17] with none of the clinical symptoms associated with active disease. It is estimated that 23% of the world's population is latently infected with M.tb[1]. The precise mechanisms by which the bacteria are maintained in a quiescent state are not fully understood but it is clear that there is a spectrum of disease states in latently infected individuals[30]. People that have latent TB infection (LTBI), are at risk of developing active disease, especially if immunosuppressed through disease or malnutrition

or by being exposed to immunosuppressive therapies. Individuals with LTBI are therefore, in some instances, treated with a preventative antibiotic regimen. This regimen involves daily treatment with isoniazid for a period of 6-9 months[31], with new regimens introduced that replaced isoniazid with rifampicin to shorten treatment duration and improve patient compliance[32].

Other host factors such as age (babies, children, adults and elderly) can influence the clinical manifestations of disease yet the approach taken to treatment is similar. Co-morbidities such as HIV/AIDS, not only alter the course or severity of disease but have an impact upon TB therapy due to drug-drug interactions. Thus, there is huge complexity in TB disease which brings significant challenges in the design and implementation of drug treatment regimens.

1.2 DRUG THERAPY FOR TUBERCULOSIS DISEASE

Before the advent of drug therapy, the treatments for TB disease were best described by George Bernard Shaw as a 'commercial system of quackery and poison'. Treatment could be bestowed by the touch of monarchs, artificial pneumothorax and operations intended to collapse the lung (i.e. thoracoplasty, plombage or phrenic crush) were conducted and often curative, but most famously used were the Sanatoriums. The Sanatoriums were known as 'waiting rooms of death' and bed rest, for 18 months minimum, in the open air with the presence of air-purifying pine trees was the main treatment. The last Sanatorium (Cheshire Joint Sanatorium, Loggerheads, Staffordshire) was closed in 1969 when it was confirmed that open air treatments had no significance in relation to drug therapy [33].

The first drug to be used to treat TB, streptomycin, was introduced in 1944 but it was quickly apparent that this drug alone was not sufficient to cure patients. A second drug with activity against TB, para-amino salicylic acid was identified around the same time and, when used in combination with streptomycin was more effective than streptomycin alone. This success in combination therapy initiated an era of TB drug discovery and clinical trials, during which several new drugs, and drug combinations were tested between 1952 and 1963, as illustrated in Figure 1.2. Rifampicin was discovered in 1963 and the current four front-line anti-TB drugs,

isoniazid, pyrazinamide, rifampicin and ethambutol, were introduced as a combination regimen in the 1980s (Figure 1.2). This regimen is still in use today, 40 years later and involves a combination of isoniazid and rifampicin for six months, with the first two months supplemented with pyrazinamide and ethambutol[34]. The doses administered are based on pharmacokinetics, previous historical clinical trial efficacy data, toxicity, cost and availability of the drugs during the 1980s when the regimen was initially introduced[35]. Further details of the drugs in the front-line regimen is given in the following sections. Table 1.1 shows all the drugs that have been used over time including those used now.

Anti-TB drugs for drug sensitive TB need to be taken daily for a six month period (as a minimum) and it is the duration, expense, availability of the drugs in the poorest countries and toxic side effects of the treatment that often leads to patient non-compliance. A key issue associated with patient non-compliance is the emergence of multi- and extensively- drug resistant TB (MDR and XDR-TB respectively)[24]. The introduction of novel diagnostic technologies such as Xpert MTB/RIF that can rapidly identify resistance to rifampicin and first-line line probe assays (LPA) that detect both isoniazid and rifampicin resistance, not only ensure the patient is receiving the right treatment, but also aid in decreasing the growing resistance to these important front-line drugs[35,36].

Additionally, the front-line drugs are likely to be ineffective against 1 bacillus in a population of 10^8 (varies between 10^6 - 10^9 bacteria for different drugs) which could select for resistance in the persisting population[37]. Therefore, regimens that clear these persistent bacteria are instrumental in controlling resistance, and also may lead to shorter treatment durations improving patient compliance[29]. Strategies have been implemented to help with patient compliance, such as directly observed therapies (DOTS) and novel strategies such as 99DOTS which uses smart phones, both approaches have been implemented with success [38].

MDR-TB which accounts for 3.5% of all new TB cases[1], is resistant to treatment with isoniazid and rifampicin and must be treated with a second-line drug regimen. XDR-TB, which has been identified in 127 WHO member states, is defined as MDR-TB with resistance to at least one fluoroquinolone or second-line injectable agent (amikacin, capreomycin or kanamycin)[1]. The

minimum treatment period for MDR-TB is 20 months, adding to issues of poor compliance due to cost and toxicity. In 2018, the WHO released new guidance for treatment of drug-resistant (DR) TB categorising second line and novel drugs into three categories based on safety and efficacy. The drugs to be prioritised and used in combination for the treatment of DR-TB are levofloxacin or moxifloxacin, bedaquiline and linezolid[39]. Kanamycin and capreomycin are no longer recommended due to associations with treatment failure (relapse) and the fact that they are injectable agents[39].

As highlighted in Figure 1.2, after the discovery of rifampicin in 1963, there was a lull in anti-TB drug discovery until the 1990s when rifapentine, rifabutin and the widely used fluroquinolones for MDR-TB were discovered, however no new drugs were discovered for the treatment of TB until pretonamid in 2000[40]. Even with these discoveries, it takes a minimum of six years to get a novel TB drug to market, and at least 20 years for the introduction of a novel regimen[41]. Hence, over time drugs were re-purposed for use of the treatment of TB and throughout history, many drugs have been used. However due to the continued emergence of drug resistance and toxicity of the treatment regimens there remains a need for new anti-TB drugs and regimens that are shorter, less expensive and less toxic.

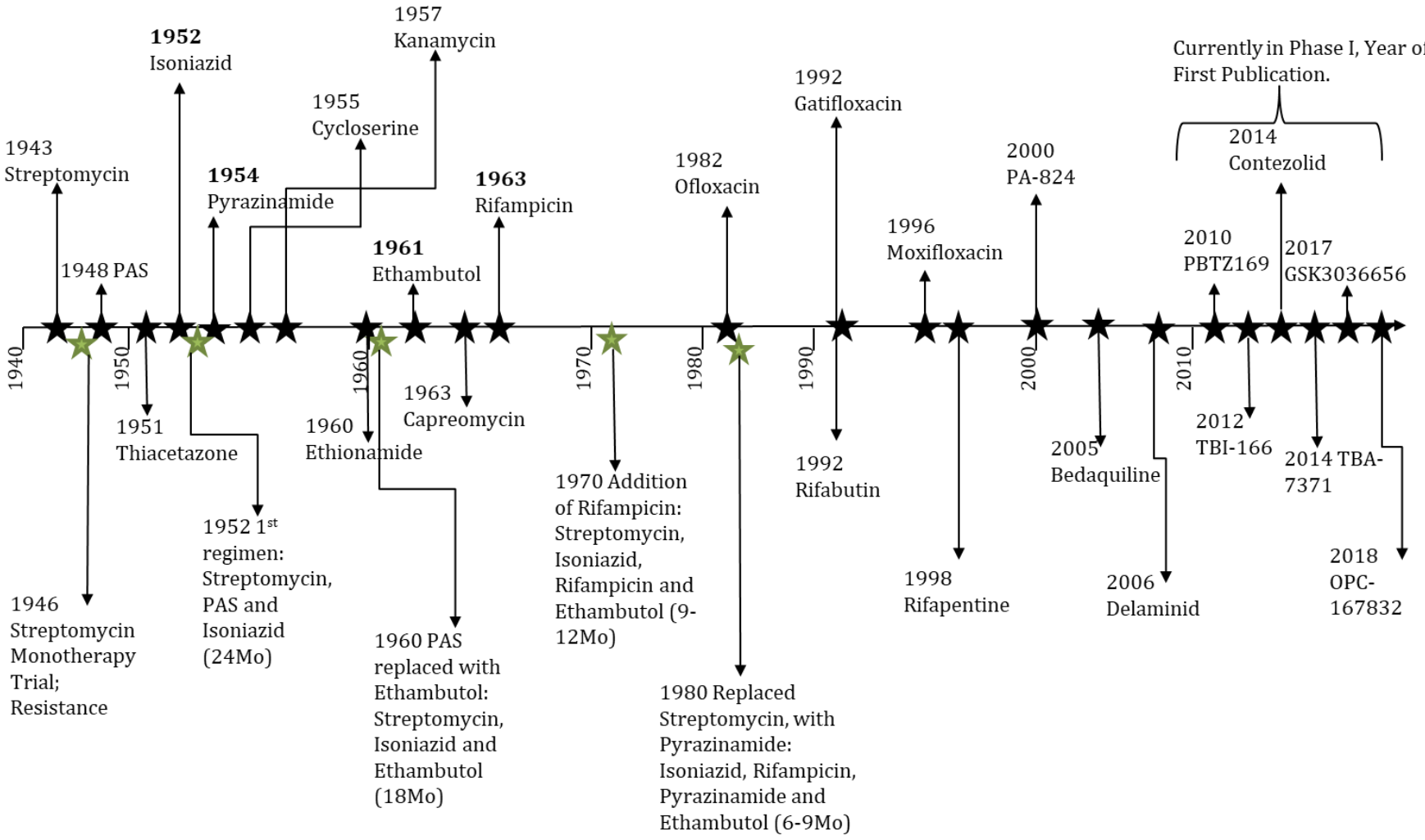

FIGURE 1.2: TIMELINE OF ANTI-TUBERCULOSIS DRUGS SHOWING WHEN THEY WERE INITIALLY DISCOVERED. Diagram adapted from Global TB Drug Development Pipeline[40] and WHO Global TB Report 2018[1]

Antibiotic	**Type of TB** (DS, MDR, XDR)	**Antibiotic Class**	**Target**	**Treatment Uses/ Comments**
Amikacin	Broad Spectrum Antibiotics/ MDR-TB	Aminoglycoside Injectable Agents	Protein synthesis (via 30s ribosomal subunit)/ Bactericidal with bacteriostatic properties at low concentrations	Downgraded to Group C medication for MDR-TB [42].
Capreomycin				August 2018, no longer recommended for treatment of MDR-TB[39].
Gentamicin				Use limited by serious adverse effects (ototoxicity and nephrotoxicity)[43] however aerosolised gentamicin significantly reduced bacterial burden in mouse model [44].
Kanamycin				August 2018, no longer recommended for treatment of MDR-TB[39].
Streptomycin				Not licenced for treatment of TB in UK as half of UK cases are resistant.
Tobramycin				Synergism with clarithromycin [45].
Cycloserine	MDR-TB	Small molecule; analogue of amino acid D-alanine.	Cell wall (peptidoglycan) synthesis	Also used for treatment of Mycobacterium Avium complex[46].
Terizidone		Pro-drug of cycloserine.		Re-purposed drug. Treatment of urogenital TB [47].
Enviomycin	X	Tuberactinomycin Injectable Agents	Protein synthesis (via 30s and 70S ribosomal subunit)	Bactericidal against M. avium complex [48].
Viomycin	XDR-TB			Rarely used. Structural basis for capreomycin.
Ethionamide	MDR-TB	Thioamide	Cell wall (mycolic acid) synthesis (similar mechanism to isoniazid) although largely unknown/ Bacteriostatic	Treatment of tuberculous meningitis and tuberculoma.
Prothionamide				Interchangeable with ethionamide as similar efficacy between the two, but prothionamide is better tolerated [49].

TABLE 1.1: DRUGS THAT HAVE BEEN OR CURRENTLY ARE USED FOR THE TREATMENT OF TB.

Antibiotic	**Type of TB** (DS, MDR, XDR)	**Antibiotic Class**	**Target**	**Treatment Uses/ Comments**
Ciprofloxacin	Broad Spectrum Antibiotics/ MDR-TB	Fluoroquinolone	Cell division via DNA gyrase and topoisomerase	Used for treatment of numerous bacterial infections.
Gatifloxacin				Withdrawn from market due to association with dysglycemia[50].
Levofloxacin				Second choice fluoroquinolone [51]. Less likely to be metabolically induced by rifamycins that moxifloxacin [52].
Moxifloxacin				First choice fluoroquinolone and has been incorporated into novel regimens [53].
Ofloxacin				Used when drug-susceptibility test results are not available before starting treatment [54]. Associated resistance with inadequate dosing.
Sparfloxacin				High associated toxicity [55].
Linezolid	MDR and XDR-TB	Oxazolidinone	Protein synthesis (via 50S) at early stage of translocation.	Approved for use with bedaquiline and pretonamid (BPaL) by FDA for XDR/ non responsive MDR-TB[56].
Sutezolid				Currently in Phase II Trials. Superior antimycobacterial activity than linezolid in vitro and in mouse [57]; better safety profile than linezolid [58].
Rifabutin	RR-TB	Rifamycin	DNA-dependant RNA polymerase suppressing RNA synthesis.	Recommended for active TB if rifampicin intolerance. Less DDIs than rifampicin, can be taken with ART [59].
Rifampicin	DS-TB			See Section 1.2.2
Rifapentine				Long acting derivative of rifampicin requiring once weekly administration. Currently in Phase III trials with/out Moxifloxacin to shorten treatment of DS-TB to 4 months[1].

CONTINUATION OF TABLE 1.1: DRUGS THAT HAVE BEEN OR CURRENTLY ARE USED FOR THE TREATMENT OF TB.

Antibiotic	**Type of TB** (DS, MDR, XDR)	**Antibiotic Class**	**Target**	**Treatment Uses/ Comments**
Delamanid	MDR-TB	Nitroimidazole	Cell wall (mycolic acid) synthesis	Phase III clinical trials[60]. Approved for use by EMA 2014.
Pretonamid			Dual activity depending on growth rate; cell wall and NO respiratory effects	Phase III clinical trials, incorporated into novel regimens and shows efficacy with bedaquiline and linezolid[61]. See Table 1.2
Para-amino salicylic acid	XDR-TB	Antimycobacterial	Folic acid synthesis.	Use in front-line regimen discontinued due to discovery of INH &RIF. High associated toxicity [62].
Ethambutol	DS-TB		Synthesis of cell wall components	See Section 1.2.4
Thioacetazone	Isoniazid Resistant-TB	Thiosemicarbazone	Cell wall (mycolic acid) synthesis (similar mechanism to isoniazid) although largely unknown	Rarely used as associated adverse reactions especially with HIV co-infection [63].
Clofazimine	MDR-TB	Riminophenazine	Cell division via binding to guanidine bases	Currently in Phase III trials. Used for treatment of leprosy [64]. Not licenced for treatment of TB in UK.
Clarithromycin	MDR-TB	Macrolide	Protein synthesis via 50S ribosomal subunit.	Associated with drug interactions including rifabutin [65]. Not licenced for treatment of TB in UK.
Bedaquiline	MDR-TB	Diarylquinalone	ATP synthase.	Phase III clinical trials, incorporated into novel regimens. See Table 1.2.
Isoniazid	DS-TB	Hydrazide	Cell wall (mycolic acid) synthesis	See Section 1.2.1
Pyrazinamide	DS-TB	Pyrazinoic acid amide	Membrane potential disruption and inhibition of trans-translation	See Section 1.2.3
Doxycycline	X (R)	Tetracycline	Protein synthesis (via 30s ribosomal subunit)	Not considered effective against TB until 2012 as shown to directly inhibit bacterial growth in guinea pigs [66].
Fusidic acid	X (R)	Fusidane	Protein synthesis via elongation factor	Activity shown *in vitro* [67].

CONTINUATION OF TABLE 1.1: DRUGS THAT HAVE BEEN OR CURRENTLY ARE USED FOR THE TREATMENT OF TB. X indicates not currently used against TB. (R) indicates repurposed.

1.2.1 ISONIAZID

Isoniazid (isonicotinylhyradrazine) is an orally delivered mycobactericidal drug, introduced for human use in 1952. The action of INH is biphasic in humans, exerting bactericidal activity on rapidly growing mycobacteria, and bacteriostatic action on slow growing mycobacteria[68]. The precise mechanism of action of isoniazid is poorly understood[69]. It is known that INH is a prodrug which is activated to the active form of the drug via peroxidation by the catalase-peroxidase enzyme *KatG* found in mycobacteria [70,71]. Activation via oxidation of INH via *KatG* creates carbon, oxygen and nitrogen free radicals which are central to the action of INH due to damage of a range of cellular components (lipids, proteins and nucleic acids[72]). This oxidation occurs in the presence of NADH which leads to the formation of an intra-cellular INH-NADH complex which binds and inhibits enoyl-acyl carrier protein reductase InhA[73] . The cell wall structure of M.tb is comprised of a mycolic acid-arabinogalactan-peptidoglycan complex, this has minimal permeability which aids M.tb survival and is an additional barrier to drug treatment[74]. The inhibition of InhA disrupts mycolic acid synthesis, a key component of the mycobacterial cell wall leading to death of the bacteria. The chemical structure of isoniazid is shown in Figure 1.4.

Resistance to INH developed shortly after its introduction and involves mutations in a number of genes, however the main mutations that contribute to INH resistance are within the *KatG* gene or the *inhA* regulatory region[69]. Mutations in *KatG* confer high level isoniazid resistance, which means INH is ineffective against M.tb with this mutation. However, mutations in the *inhA* regulatory region cause low level resistance which indicates that administration of high dose INH may be effective[75]. Recently due to this resistance, moxifloxacin has been used in place of INH and this led to superior sterilising activity and hence shortened treatments regimens when compared to HRZ in BALB/C and C3HEB/Fej mice[76], however moxifloxacin failed to clear persistent bacteria in the Cornell mouse model[77]. This was also true in humans as when this regimen was tested as part of the REMoX-TB trial, with the hope of reducing treatment

duration to four months, it did not show non-inferiority due to a higher relapse rate than current front-line regimen[78].

1.2.2 RIFAMPICIN

Rifampicin, a semisynthetic derivative of the rifamycins, is part of the ansamycin family of antibiotics which have activity against gram positive bacteria (Chemical Structure; Figure 1.4). It has the most potent sterilising activity in the front-line anti-TB drug regimen and is the most effective against persistent bacteria[79]. Hence, when rifampicin was incorporated into regimens in the 1970s and 1980s the treatment period decreased from 18 to 6-9 months. Rifampicin is effective against both growing and stationary phase bacilli[80] and exerts its therapeutic effects by binding to the β-subunit of RNA polymerase via 4-methyl-1-piperazinaminyl, thereby inhibiting RNA transcription in-turn preventing protein synthesis in bacterial cells[81].

Resistance to rifampicin is associated with mutations in the *rpoB* gene which codes for the β-subunit of RNA polymerase (the target of rifampicin)[82]. It is interesting to note that unlike isoniazid, rifampicin mono-resistance is rare, hence usually rifampicin resistance is a strong indicator of multi-drug resistance[1].

It is known that rifampicin was introduced at suboptimal doses due to cost, availability and proposed toxicity and this dose is still in use today[35,83]. However, humans can tolerate daily doses of 35mg/kg (as opposed to the currently used 10mg/kg) and this increased dose is known to increase bacterial elimination[84]. It is known that the maximum tolerated dose of rifampicin in humans is 40mg/kg and doses higher than this have led to the development of unconjugated hyperbilirubinemia (G. Davies, Personal communication). It has also been shown that BALB/C mice can tolerate up to 50mg/kg daily. This higher dose was associated with a shortened treatment duration of 6 weeks from the usual 14 weeks with no occurrence of relapse when trialled in the Cornell mouse model[79]. High dose rifampicin is currently in both Phase II and Phase III clinical trials for drug-sensitive TB.

1.2.3 PYRAZINAMIDE

Pyrazinamide (Pyrazine-2-carboxamide, PZA) is used during the initial treatment phase with isoniazid and rifampicin for drug- sensitive tuberculosis treatment. It was primarily added to the regimen to reduce the rate of relapse [85] as well as enhancing the activity of rifampicin, thereby shortening treatment duration from 9 to 6 months. It is also part of the majority of regimens for multi-drug resistant TB due to its possible *in vitro* synergism with the newly developed drugs [86]. The structure of PZA is shown in Figure 1.4. The mechanism of action of PZA is poorly understood, however it is a prodrug known to be converted in an acidic environment to pyrazinoic acid via the pyrazinamidase enzyme [87]. A mechanism of PZA resistance is associated with defects in this enzyme due to mutations in the *pncA* regulatory gene[88]. Pyrazinoic acid, which accumulates intracellularly appears to have no specific targets[87] but it diffuses out of the bacteria and is then protonated. The protonated form (HPOA) re-enters the bacterium and accumulates and disrupts homeostasis[89]. PZA/ Pyrazinoic acid is known to be poorly active against multiplying bacteria and the proposed target is dormant or persistent bacilli [90].

It is well known that PZA shows minimal activity *in vitro* and this is primarily related to pH, a key factor in determining the activity of PZA[87]. However, there are conflicting reports of its activity *in vivo* in animal studies. Ahmad *et al* state that pyrazinamide shows sterilising, dose-dependent activity and synergism with rifampicin against chronic TB infection in guinea pigs as it does it humans [90], however this is in contrast to data generated by Dickinson[91] and Steenken[92]. In mice, PZA had a dose dependant response for the first three weeks of treatment but did not confer any additional protection at later time points[27]. However, despite these conflicting data in animals, it is found in humans that PZA acts as a sterilising drug for the first two months of treatment[93].

1.2.4 ETHAMBUTOL

Ethambutol (2*S*,2'*S*)-2,2'-(Ethane-1,2-diyldiimino)dibutan-1-o) is a synthetic compound (structure shown in Figure 1.4) discovered in 1961. It was introduced into the anti-TB drug

regimen to prevent the emergence of drug resistance as ethambutol was found to be active against isoniazid and streptomycin resistant strains of TB[94]. The mode of action is to inhibit arabinosyl transferase the enzyme responsible for arabinogalactan and arabinomannan biosynthesis, which are two key components of the mycobacterium cell wall[95]. Ethambutol is efficacious against the majority of strains of the MTBC including *M. bovis* [96].

1.2.5 NEW DRUG DEVELOPMENT AND CLINICAL TRIALS

For 40 years, no novel drugs were introduced for the treatment of TB until bedaquiline (BDQ) was approved by FDA in 2013. The safety and efficacy of BDQ is still being evaluated in Phase III trials as part of the STREAM (Evaluation of Standardised Treatment Regimen of Anti-tuberculosis Drugs for Patients with Multidrug-resistant Tuberculosis) trial where bedaquiline was incorporated into a number of regimens with pre-existing and repurposed anti-TB drugs with the aim of shortening the treatment of MDR-TB[97]. However, due to success in earlier trials, over 70 countries have already started using BDQ to improve treatment outcomes of those with MDR or XDR-TB[1]. BDQ is a relatively well tolerated drug and only 0.6% of patients had treatment discontinuation due to adverse events[98]. Other promising drugs both in Phase III trials as part of novel regimens for MDR-TB are delamanid and pretonamid. A novel combination regimen containing pretonamid, moxifloxacin and pyrazinamide demonstrated more effective sterilisation in the mouse model than the current front-line regimen [99]. Other novel drugs being investigated have different modes of action to the traditional drugs, such as the indazole sulfanomides[100] and DprE1 inhibitors[101]. The TB drug development pipeline is shown in Table 1.2.

The majority of on-going anti-TB drug trials focus on MDR and XDR-TB, such as Nix-TB, STREAM and MDR-END with the overarching aim of shortening the duration of drug treatment. Another aim of these trials is to identify regimens that are compatible with Anti-Retroviral Therapy such as the RAFA trial in which an increased daily dose of rifampicin showed an 80% decrease in mortality associated with advanced HIV/TB co-infection compared with the standard daily dose of rifampicin[102].

As highlighted in Figure 1.2, tuberculosis drug development is a slow process and contributing factors are the slow growth of the organism, the complicated spectrum of TB disease in humans, including latent infection (adding at least another two years to the length of the drug development pipeline) and a lack of well-validated models and tools for pre-clinical development, especially those that recapitulate the diverse heterogenous states of TB disease. Some of the issues which surround the evaluation of new drugs pre-clinically include a limited understanding of the pharmacokinetics of drugs and how these relate to anti-mycobacterial activity. It is clear that to improve and eventually shorten the time taken for new drugs to be approved for use in the TB drug development pipeline there is a need for improved and better pre-clinical models to predict the pharmacokinetics of the anti-TB drugs both *in vitro* and *in vivo*.

Phase I	Phase II	Phase III
Contezolid (MRX-1) Oxazolidinone	**Delpazolid (LCB01-0371)** Oxazolidinone; LegoChem Biosciences	**Bedaquiline** (TMC-207)
GSK-3036656 Oxaborole; GSK	**SQ109** Small molecule drug; Sequella Inc & NIH	**Delamanid** (OPC-67683)
Macozinone (PBTZ169) Benzothiazinone; Nearmedic Plus	**Sutezolid (PNU-100480)** Oxazolidinone	**Pretomanid** (PA-824)
OPC-167832 Carbostyril; Otsuka	**Linezolid dose-ranging** Oxazolidinone	**Clofazimine** Riminophenazine
TBA-7371 Enzyme inhibitor (DprE1); TB Alliance	**High Dose Rifampicin** for DS-TB PanACEA	**High Dose Rifampicin** for treatment of DS-TB
TBI-166 Riminophenazine; TB Alliance with Institute of Materia Medica, Chinese Academy of Medical Sciences & Peking Union Medical College.	Bedaquiline and Delaminind (Deliberate Trial)	**Rifapentine** for treatment of DS-TB
BTZ-043 Benzothiazone; DprE1 inhibitor; University of Munich	Bedaquiline-Pretonamid-Moxifloxicin-Pyrazinamide (**BPaMZ**)	Bedaquiline – Pretomanid – Linezolid (**NiX-TB trial**)
	Bedaquiline- Pretonamid-existing and re-purposed anti-TB drugs for MDR-TB (**TB PRACTECAL Phase 2/3 trial**)	Bedaquiline – Pretomanid – Linezolid (**ZeNix trial**) – Linezolid optimization
	Delamanid-linezolid-levofloxacin-pyrazinamide for quinolone sensitive MDR-TB (**MDR-END trial**)	Bedaquiline with two optimised background regimens (oral, 9 months; with oral and injectables, 6 months) (**STREAM trial**)
	Levofloxacin with optimised background regimen (OBR) for MDR-TB (**OPTI-Q**)	Bedaquiline – Linezolid – Levofloxacin with OBR for MDR-TB (**NExT trial**)
		Bedaquiline and delamanid with various existing regimens for MDR-TB and XDR-TB (**endTB trial**)
		Pretomanid – Moxifloxacin – Pyrazinamide regimen (**STAND trial**)
		Rifapentine – Moxifloxacin for treatment of DS-TB (**TB Trial Consortium Study** 31/A5349)

TABLE 1.2: THE GLOBAL CLINICAL DEVELOPMENT PIPELINE FOR NEW ANTI-TB DRUGS AND REGIMENS. Adapted from WHO Global TB report[1]

1.2.6 PREDICT TB CONSORTIUM

A component of the studies required to address the aims of this PhD project were conducted within the PreDiCT TB consortium project funded by the EU Innovative Medicines Initiative (IMI) with in kind contributions from industry partners, predominantly GSK. The overall goal of PreDiCT TB was to develop and enhance an integrated set of pre-clinical *in vitro* and *in vivo* models that provide critical data for the purpose of identifying decision criteria for the progression of novel drugs and combinations to innovate early phase drug development and clinical trials. This was achieved by evaluating a defined set of anti-TB drugs in a set of novel and enhanced pre-clinical experimental systems, that encompass the range of physiological states of M.tb, and relating these data to human clinical trial data via *in silico* modelling. The impact of the PreDiCT TB consortium has been a comprehensive analysis of pre-clinical and clinical databases which will ultimately inform the predictive value of pre-clinical tools accelerating the drug development pathway to the clinic.

Eighteen *in vivo* models were used in the consortium; zebrafish, mouse models that span multiple aspects of TB disease, non-human primates and guinea pigs. The experiments that were conducted in guinea pigs are those that relate to this project. There were a number of PK experiments conducted (in uninfected guinea pigs) to optimise the dose of drug administered with an aim to identify drug doses that reflect human exposures. Those PK experiments are described in Chapter 2 of this thesis and the results obtained were used as the basis for drug concentrations tested in the *in vitro* microdialysis work up studies (Chapter 3) and the *in vivo* microdialysis studies (Chapter 5).

1.3 PHARMACOKINETICS

1.3.1. OVERVIEW OF PHARMACOKINETICS

The time-dependant bactericidal activity of penicillin and the concentration-dependant bactericidal activity of streptomycin, originally described by Eagle in 1948, were the first indication that pharmacokinetics (PK) and pharmacodynamics (PD) were inextricably linked to drug efficacy [103]. Three main PK/PD parameters are often calculated to predict drug efficacy:

- The ratio of peak drug concentration relative to Minimal Inhibitory Concentration (Cmax: MIC ratio)
- Area under the concentration time curve relative to MIC (AUC:MIC)
- Time during which the drug concentration exceeds MIC (T>MIC).

The parameter associated with microbial killing by the four front-line anti-TB drugs is AUC:MIC, although rifampicin activity also is consistent with a Cmax: MIC effect[104]. It is incredibly important to achieve MIC concentrations as sub-lethal treatment can cause bacterial resistance, but the MIC is a pre-determined, single value that does not account for patient, drug or pathogen factors which can affect therapy. Therefore, to better understand the drug and its effect, PK, which is the quantitation over time of a drug in the body, is measured. PK analyses should incorporate the physiochemical properties of the drug, blood flow, permeabilities of membranes and tissues, plasma protein and tissue binding [105].

There are four main components that contribute to the pharmacokinetic (PK) properties of a drug: absorption, distribution, metabolism and elimination (ADME), as shown in Figure 1.3.

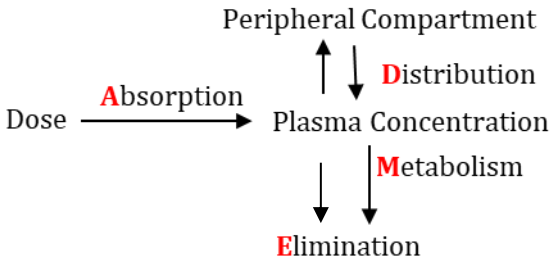

FIGURE 1.3: PHARMACOKINETICS. A basic schematic showing how absorption, distribution, metabolism and excretion/elimination (ADME) are interlinked to form the overarching pharmacokinetic profile of the drug.

1.3.2 ABSORPTION

Most pharmaceuticals, including the front-line anti-TB drugs (isoniazid, rifampicin, pyrazinamide and ethambutol) are taken orally; therefore following drug dissolution the sites of absorption are the gastrointestinal (GI) tract, the stomach and the small intestine. GI absorption of drugs involves the transport of the drug across the gut epithelium and the internal environment of the GI tract, especially the pH, is critical in determining the actual site of absorption. Other factors such as the physio-chemical properties of the drug affect absorption.

The biopharmaceutics classification system classifies drugs based upon aqueous solubility (LogS) and the associated bioavailability of the drug, as absorption is directly linked to bioavailability. The classes I-IV indicate how the drug will be absorbed and the subsequent bioavailability following oral administration. Class I drugs are highly soluble and permeable indicating high bioavailability, Class II are highly soluble with low permeability (rifampicin[106]), Class III are highly soluble and poorly permeable (ethambutol[107], isoniazid[108], pyrazinamide[109]) and Class IV are relatively insoluble and impermeable indicating low bioavailability. However, rifampicin is a zwitterion meaning that solubility increases in both acid and basic solutions and this means that absorption can occur at a number of GI sites[110].

As shown by the structure in Figure 1.4, isoniazid is a relatively simple drug with low molecular weight (137.14g/mol). It is highly soluble with a LogS of -0.56. Rifampicin has a very complex structure (Figure 1.4). This complexity means that rifampicin has the highest Mw of all the

front-line anti-TB drugs (822.94g/mol) as well as being the least soluble (LogS -8.18). There are structural similarities between pyrazinamide and isoniazid as shown in Figure 1.4. The physiochemical properties between the two are similar and pyrazinamide has a Mw 123.11g/mol and LogS of -0.65. In terms of physiochemical properties, ethambutol is similar to isoniazid and pyrazinamide (Figure 1.4), with a low Mw (204.31g/mol) and high solubility (LogS -0.46).

As tuberculosis is primarily a pulmonary disease, the delivery of drugs via the lungs has been considered for the development of novel anti-TB compounds[111,112]. The route of administration will have a direct impact on the absorption of the drug and subsequently their distribution and excretion; however, regardless of route, all drugs will enter the systemic circulation. Entering the systemic circulation means there is potential for drug to be 'lost' via first pass metabolism in the liver which greatly affects lipid soluble drugs and it is known that rifampicin undergoes first pass metabolism[113]**.** First pass metabolism, although hard to distinguish from poor absorption, means that the bioavailability of the drug decreases. Other losses in the GI tract also need to be considered, for example, 6-8% of the total dose of rifampicin degrades in the stomach due to the pH[106]. Ethambutol has an unusual absorption pattern, potentially due to its binding and chelation with molecules in GI fluids or tissues [114].

Following absorption, all drugs are distributed simultaneously to all tissues, including the organs of elimination, via the blood.

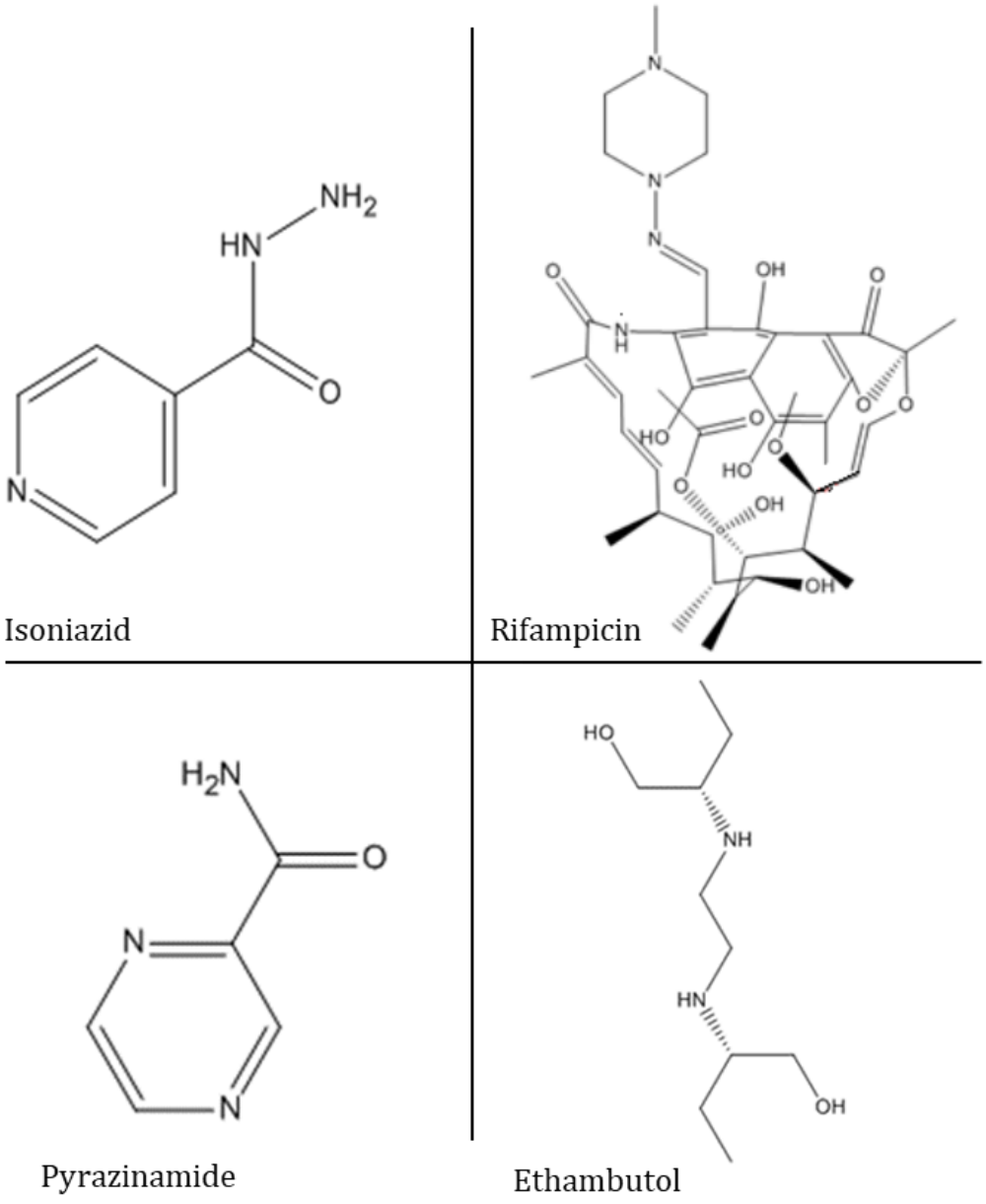

FIGURE 1.4: CHEMICAL STRUCTURES OF THE FRONT-LINE ANTI-TB DRUGS. Drawn in ChemBioDraw Version 12.

1.3.3 DISTRIBUTION

Distribution is a measured in L/Kg and provides an indication of the amount of drug which is distributed in the body in relation to the plasma concentration and is a critical determinant and predictor for drug activity [115]. There are large differences in the distribution of drugs to tissues, which are caused by differences in the physiochemical properties of the drug (primarily lipophilicity (LogP) and ionisation), perfusion rate, permeability of the tissue membranes and differences in protein binding in various tissues and plasma in the body. Perfusion rate is particularly important in relation to the lungs due to high vascularisation. Moderate to highly basic and lipophilic drugs are highly distributed to the lung and the rate of delivery is dependent upon blood flow.

The most important factor in relation to distribution is protein binding in the blood and tissues because the efficacy of the drug relies upon the unbound pharmacologically active fraction. Small Mw drugs are highly bound to plasma proteins but not to tissue proteins and highly polar drugs tend not to bind to any proteins. Acidic drugs commonly bind to albumin (the most abundant plasma protein), basic drugs bind to α1-acid-glycoprotein (which is largely restricted to plasma) and neutral lipophilic compounds are associated with lipoproteins (found in tissue extra cellular water). Basic drugs have a greater volume of distribution than acidic drugs due to higher tissue protein binding. Although binding is generally a reversible process, it can also affect the efficacy and toxicity of the drug, as well as modifying the time above MIC[116]. Rifampicin is the only front-line anti-TB drug which shows a relatively high level of plasma protein binding (92.2±1.1% (Humans))[117]; however it has been suggested that plasma protein binding is only problematic if it is over 95% as it is for the novel anti-TB drug bedaquiline (99.8±0.1% (Humans))[116]. Protein binding does differ between species and therefore it is imperative to know the degree of protein binding of the drug in the species being studied in order to fully describe the PK parameters, for example, in mice rifampicin is 97.1±0.2% plasma protein bound (PPB), in guinea pigs 69.5±2.3% PPB and in macaques 90.3±1.0% PPB[117].

1.3.4 METABOLISM

Metabolism, in general, renders compounds more polar and hydrophilic; however, there are exceptions to this. Metabolism can also activate prodrugs into the therapeutically active metabolite, as is the case with pyrazinamide (see Section 1.2). The majority of drug metabolism occurs in the liver and it can change the biological activity of the drug, by either decreasing the toxicity or increasing the chemical reactivity or toxicity. Most metabolic reactions, including those associated with the anti-TB drugs[118–120], involve induction or inhibition of cytochrome P450s (CYP 450s) which are intracellular monooxygenase enzymes. As with protein binding, it is important to understand species differences in relation to CYPs; rats and dogs primarily use CYP 2C enzymes for drug metabolism and humans primarily use CYP 3A. Non-human primates and guinea pigs have the highest total CYP 450s in the liver microsomes when compared to humans indicating that metabolism and clearance processes maybe faster in these species [121].

Rifampicin is a known inducer of enzyme systems, especially the CYP 450 enzymes and this is due to a high affinity of the drug for the Pregnane X receptor (PxR). The PxR, activated by a number of structurally diverse xenobiotics and drugs, mediates the induction of CYP 3A genes [122]. Rifampicin is also known to induce P-glycoprotein (Pgp), a protein pump which uses ATP to transport large hydrophobic molecules across the plasma membrane, via induction of the multidrug resistant (*mdr1* and *mdr2*) gene family[123]. It was shown that repeated administration of two different doses of rifampicin (15mg/kg and 50mg/kg), given twice daily for 7 days and 3 days respectively, induced *mdr2* and subsequently Pgp expression in NHPs. Interestingly, the lower dose (administered for longer) was associated with higher expression of liver *mdr2* and Pgp when compared to the control[124]. An increase in Pgp expression may lead to increased biliary clearance of rifampicin and can therefore alter the PK profile of the drug potentially leading to drug resistance[125].

In addition to inducing its own metabolism (via CYP 3A4), rifampicin causes the induction of other co-administered drugs and is a potent metabolic inducer of many other drugs including

bedaquiline and anti-retroviral agents[126]. This can change the assumed pharmacokinetic profiles of these drugs primarily reducing the AUC plasma-concentration time curve and decreasing drug efficacy[120]. Rifapentine and rifabutin are not as potent metabolic inducers as rifampicin.

The metabolism of isoniazid is unusual. It is a prodrug whose metabolism to acetylhydrazine is affected by genetic polymorphisms in humans. Isoniazid is metabolised in the liver via acetylation and the differences in metabolism and consequently elimination kinetics are due to polymorphisms of the N-acetyltransferase (NAT2) gene which can be predicted based upon ethnicity [127]. Individuals taking isoniazid with a fast acetylator status will have a decreased plasma concentration of INH and have a decreased risk of toxicity[128]. Individuals with a slow acetylator status will have a higher plasma concentration of INH and will accumulate InhA and are subsequently more susceptible to hepatoxicity especially those co-administered pyrazinamide[127,128]. Isoniazid can decrease the clearance of several drugs, including anti-retroviral efavirenz, via inhibition of the CYP 450s (2A6) even though this is not the primary route of isoniazid metabolism[119]. There are conflicting reports on the concomitant administration of rifampicin and isoniazid in regards to metabolism. There is evidence that isoniazid can decrease the bioavailability of rifampicin, however it has been shown that the induction effect of rifampicin on the CYPs far outweighs the inhibitory effects of isoniazid [129].

1.3.5 ELIMINATION

After the drug has been metabolised or bio-transformed into a more water soluble and therefore easily excretable compound, the drug can then be eliminated or cleared. Elimination rates can vary widely for different drugs due to differences in organ perfusion, plasma protein binding, disease state and other patient specific factors such as age. For instance, the PK of ethambutol is directly influenced by age, with lower clearance and longer elimination half-life with increasing age [130]. Isoniazid, pyrazinamide and ethambutol are all excreted via the kidney, whereas rifampicin is excreted via the biliary route because large polar molecules, or heavier protein bound molecules are more readily excreted via biliary excretion[131]. Rifampicin

clearance is a non-linear saturable process. Due to rifampicin's ability to induce its own metabolism, repeated oral administration increases the clearance[126]. Elimination, often defined as renal or non-renal excretion, is the primary PK parameter that is commonly measured. Renal excretion can be measured via the amount of unchanged drug or hydrophilic metabolites in the urine.

1.3.6 MODELLING OF PHARMACOKINETIC DATA

Most of the PK parameters of drugs are gained in animal model species and the overarching aim of such studies is to relate these PK parameters to humans. This is done by mathematical modelling and allometry. Allometry can only be used to predict human-based parameters if the parameter is fully dependant on body weight such as heat production[132]. Modelling is used to identify typical trends in PK data and to understand and quantify relationships between dose, concentration, therapeutic and adverse effects [133]. The models can then be predictive of drug responses for drugs that exhibit similar properties to those modelled without conducting *in vivo* experiments. It is stated by Hatton, that modelling could be improved by use of a multitude of different animal species intended to reflect different physiological functions [134]. There are different types of models that can be generated such as physiologically-based pharmacokinetic (PBPK) models that predict the PK of drugs using pre-clinical ADME data [135]. These models are comprised of organ representative compartments connected by circulating blood flow and incorporate drug specific parameters to predict the drug PK in humans[136] . There are also the conventional PK models which can be one, two or three compartment structures.

Modelling of the Population PK (PopPK) parameters of the anti-TB drugs has been described using conventional compartmental models based on blood drug concentration data following a single dose. These data were from mice[137]. Rifampicin PK parameters in blood were fitted with first order absorption and elimination in a one-compartment model. A one-compartment model was also used for isoniazid and showed dose dependant clearance. Both ethambutol and pyrazinamide required a two-compartment model and similarly to isoniazid, pyrazinamide showed dose dependant clearance. In humans, when the blood drug concentration data were

modelled a two-compartmental model was used for INH and ETH, a one-compartment model for PZA[130] and a one-compartment model for RIF[138,139]. The majority of models have been generated from PK data collected from the blood and it would be important to understand if organ PK data could be modelled in the same way (i.e. one-compartment model for RIF).

1.4 MICRODIALYSIS

1.4.1 METHODS FOR DETERMINING TISSUE PK

The majority of known drug pharmacokinetics are based upon total drug concentrations measured using blood and urine because the site of drug action is rarely accessible. It is often assumed that plasma drug concentrations are similar to organ drug concentrations, however there are examples where this is not the case, especially for well perfused organs such as the lung[140]. There are very few methods that allow quantitation of drug directly in the tissue compartments; they are non-invasive molecular imaging techniques such as PET (Positron emission tomography) scanning and semi-invasive microdialysis.

An advantage of microdialysis over the imaging techniques is the ability to directly measure the unbound pharmacologically active drug which is of key importance in pharmacokinetic studies. Microdialysis is also relatively inexpensive and requires less specialist equipment compared to the imaging techniques [141]. Imaging techniques do however have high temporal and spatial resolution and, similar to microdialysis can measure drug concentrations at multiple sites simultaneously. Other methods have been used to determine tissue pharmacokinetics of antimicrobials such as the skin blister technique, bronchoalveolar lavage and tissue biopsy. However, these methods are mostly static and can generally only provide total drug concentrations at one or very few time points per animal and therefore numerous animals are needed to provide multiple time points. The advantages and disadvantages of the methodologies used to measure organ or tissue PK are highlighted in Table 1.3.

	Microdialysis	PET	Tissue Biopsy
Matrix Sampled	ECF	Total Tissue	Total Tissue
Invasive?	Semi-invasive	No (Radioactive Exposure)	Yes
Measures UB Drug?	Yes	No (B and UB)	No (UB, B, vascular concentrations)
Continuous Monitoring? At multiple sites?	Yes	Yes	No
Expensive?	No (when compared to PET)	Yes (very technically complex; requires specialist centres)	No
Disadvantages	Time consuming calibration	Limited number of drugs that can be radio-labelled; inclusion of metabolite signal.	Invasiveness and hybrid tissue concentration owing to mixture of different compartments.

TABLE 1.3: COMPARISON BETWEEN MICRODIALYSIS, PET AND TISSUE BIOPSY. The key methods used to obtain pharmacokinetic data at the organ level. Adapted from Brunner and Langer 2006.

It is unlikely that there are any techniques superior to microdialysis for collecting only the unbound pharmacologically active and therefore clinically relevant portion of the drug.

1.4.2 INTRODUCTION TO MICRODIALYSIS

Microdialysis can be used to describe the pharmacokinetic behaviour of drugs in the organs rather than in circulation as a continuous monitoring and sampling technique. The concept of microdialysis was originally introduced by Professor Urban Ungerstedt (Karolinska Institute, Stockholm) in the early 1970's as a novel technique for neurological studies whereby the concentrations of neurotransmitters could be measured directly in the extracellular fluid of the central nervous system and brain using dialysis tubing as an artificial blood capillary[142]. Initially the data gained were not quantitative which proved problematic for pharmacokinetic research. To overcome this, calibration techniques were developed, originally by Lönroth *et al* (1987) who developed the 'no-net-flux' method for endogenous glucose[143]. Microdialysis was first used in clinical pharmacokinetic studies in 1991 to study acetaminophen disposition in anaesthetised rats [144].

Microdialysis is now used for a wide range of pharmacokinetic studies, as well as being included in the FDAs Critical Path Initiative (2004) which focusses on the implementation of new technologies in the development of drugs.

Microdialysis is a technique for sampling the chemistry of the interstitial fluid of tissues and organs. Hence microdialysis can be used to describe the pharmacokinetic behaviours of the drugs in organs, in live freely moving animals, as a continuous sampling technique. The continuous nature of the sampling is due to the fact microdialysis does not interfere with blood homeostasis, so the number of samples taken is not limited[145]. It can therefore have applications as a continuous real time monitoring technique, when coupled to online analysis, to measure analytes such as blood glucose.

Microdialysis sampling has been conducted in virtually every organ of the body in a wide range of species as evidenced by over 10,000 publications of which 1,600 involve human applications of the technique. A literature search focussing on publications between 2014 and 2019 with microdialysis being the main technique employed showed over 200 publications. The majority of these studies focus on brain microdialysis in rats and mice with the purpose of characterisation of neurotransmitters, but there are a few examples of microdialysis being employed in the brains of mice and rats to determine the pharmacokinetic profiles of drugs[146–149]. There are a number of publications using microdialysis in the bone and pulmonary epithelial lining fluid (PELF) of pigs[150–152]. Human microdialysis has been conducted in the brain with relation to neurotransmitters [153,154], skin for topical agents [155,156], one example of a study where linezolid was dialysed in soft tissue [157] but most relevant to this PhD is a microdialysis study conducted to better understand the pharmacokinetics of levofloxacin especially penetration into cavities of patients with multi-drug resistant TB [158]. Microdialysis has been conducted in guinea pigs, primarily in relation to the effects of nerve agents, but there are limited publications using this species between 2014 to 2019 and none identified that used microdialysis to study pharmacokinetics of drugs in the internal organs [159–161].

Microdialysis involves the insertion of a hollow fibre probe with a semi permeable membrane tip into peripheral or soft tissue. Although the probe insertion can be invasive (primarily

dependent upon the site of implantation), the probe is so small that even multi-slice CT scanning cannot detect the probe *in situ* [141]. This small size also enables the different compartments of complex organs to be distinguished as the concentrations of drugs (antimicrobials) may vary between these compartments [141]. Multiple probes can be used in different tissues simultaneously which enables drug distribution information to be collected within the same animal although this cannot be conducted in a freely moving animal.

The concept of microdialysis is based upon the passive diffusion of analytes across a semi-permeable membrane driven by a concentration gradient. The constant perfusion of the probe with a 'perfusion fluid' (a physiological salt solution) means that drugs of a certain size can pass into this fluid (dialysate) across the membrane of the probe tip, which has a molecular weight cut off that is dependent upon the pore size[162]. A schematic is shown in Figure 1.5. Following a variety of analytical techniques, most notably LC-MS/MS, the *in vivo* recovery of the drug can be calculated from the collected dialysate[145].

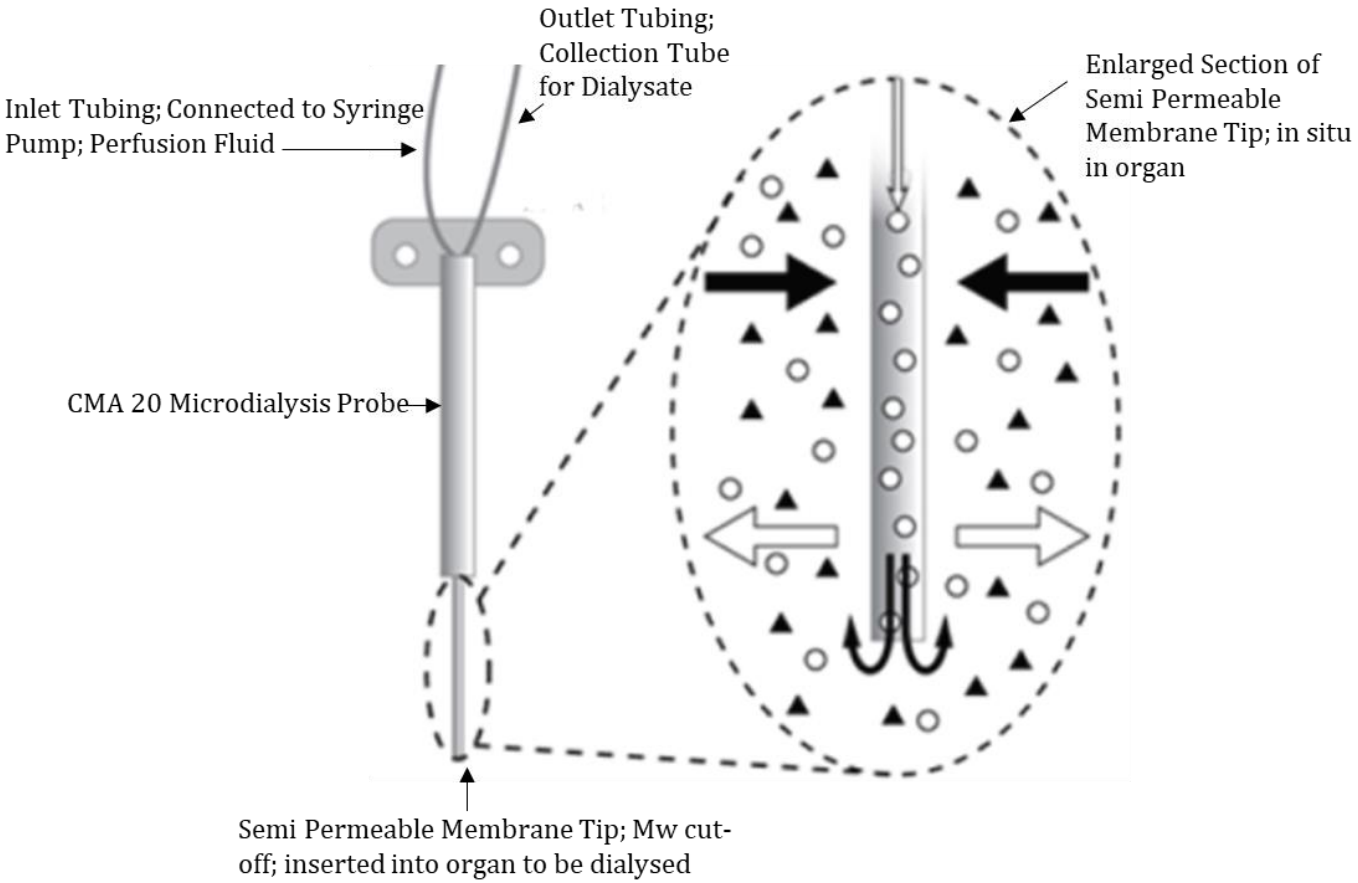

FIGURE 1.5: SCHEMATIC DRAWING OF THE CONCEPT OF MICRODIALYSIS METHODOLOGY CENTRED AROUND THE PROBE. Perfusion fluid is pumped from the syringe pump into the probe. The probe has a semi permeable membrane tip that is inserted into the tissue. As shown in the enlarged diagram of probe tip, the white arrows (and circles) indicate the direction and movement of the perfusion fluid. The black arrow (and triangles) indicate the movement of the unbound active drug or analyte. These molecules pass through the semi permeable membrane and the resulting dialysate is transported out to a collection tube via the outlet tubing.

1.4.3 MICRODIALYSIS METHODOLOGY

It is vitally important that meticulous *in vitro* experiments are carried out with each potential drug (or analyte) to determine the efficiency of the probe and optimisation of other microdialysis parameters including the analytical method, probe, perfusion fluid, tubing as well as tissue factors in order to calculate the relative recovery (described in Section 1.4.3.2).

1.4.3.1 ANALYTICAL METHODS

Initially the analytical methodology and the sensitivity of this methodology (the lower limit of quantitation (LLOQ)) to measure the drug concentrations in the dialysate needs to be identified. This is because the subsequent flow rate of perfusion fluid and sampling interval can only be optimised once it has been ensured that sufficient sample volume (and drug concentration) is available for the analytical methodology of choice[163]. The first step of the analysis is the separation of analytes that are in the dialysate, and (ultra) high performance liquid chromatography ((U)HPLC) is the most commonly used method[164,165]. Following separation of the analytes in the dialysate, a valid detection method needs to be employed and this is usually conducted using mass spectrometry (MS). MS can be used to analyse drug or analyte concentrations with very low detection limits; however, limitations can arise due to ion suppression as the sample matrix of the dialysate has a high ionic strength. However, specialist perfusion fluids can be created to eliminate the problems associated with the high salt concentrations found in microdialysis samples.

Most microdialysis samples are stored and analysed at a later date in order to calculate the concentration and recovery of the drug, especially during *in vivo* studies. Sample storage is important to ensure stability of the drug and to reduce the potential for losses such as evaporation prior to analysis. Fortunately, microdialysis generates protein-free samples due to the molecular weight cut-off of the probe, therefore reducing the likelihood of enzymatic degradation during storage as well as reducing time required for sample preparation prior to analysis [166].

Once the analysis and sample storage methods have been chosen and the required sample volume identified, the other *in vitro* factors that can affect relative recovery can be taken into account (as discussed in Chapter 3).

1.4.3.2 RECOVERY & CALIBRATION

The recovery of the drug is dependent upon a variety of experimental conditions which can be trialled including flow rate, membrane surface area, the material of the membrane, tubing materials and dimensions, temperature, tissue factors and the perfusion fluid [143,167,168]. Changing any one of these parameters can either increase or decrease the relative recovery of the probe and hence the resulting drug concentration in the dialysate.

The recovery is the relation between the concentrations of the drug in the periprobe fluid (the fluid surrounding the probe, and therefore concentration in the organ) and that in the collected dialysate[169]. These concentrations will be different because the constant flow of perfusion fluid means that a concentration equilibrium cannot be established, and hence the concentration of the drug in the dialysate is always a fraction of the actual drug concentration in the organ. Recovery can be calculated using the following equation:

$$Recovery\ (\%) = (Cdialysate \div Cperiprobe) \times 100$$

$C_{periprobe}$ is the concentration of drug in the fluid surrounding the probe; $C_{dialysate}$ is the concentration of drug in dialysate. The resulting percentage generated by the equation shows how efficiently the probe is recovering the drug. Once the recovery has been established this percentage can then be used as a correction factor and applied to the collected drug concentrations in order to calculate the concentration of drug in the organ. It is recommended that relative recoveries are over 20%[170].

The flow rate directly affects the efficiency of the probe as shown in Figure 1.6. The microdialysis probe is more efficient, with a greater recovery of drug in the resulting dialysate, at lower flow rates, decreasing from 100% at 0.1µl/min. However, these slow flow rates may

not give the desired temporal resolution or not produce sufficient sample volume for analytical methodology.

As mentioned, the continuous perfusion of the microdialysis probe with perfusate means that only a fraction of the drug concentration in the extracellular fluid is reflected in the dialysate, and therefore it is essential to understand at what efficiency the probe is extracting the drug from the tissue extracellular fluid. This is crucial for determination of true extracellular tissue concentrations. Calibration is initially performed *in vitro*; however, the *in vitro* recovery must be verified *in vivo* due to different tissue characteristics. There are a variety of methods for calibration.

One of the calibration methods to calculate relative recovery is the extraction efficiency method[166]. The perfusion fluid contains no drug and the probe is placed into a drug containing solution, with or without tissue, and the relative recovery of the probe is calculated and the error propagated over a series of experiments to calculate probe efficiency (how efficiently the probe is extracting the drug from the tissue). The main advantage to this methodology is that parameters can be changed to improve the relative recovery in a step-wise manner. The disadvantages are that it can be time consuming, requires dedicated analysis facilities and each drug will need to be trialled in the system and have a probe efficiency attributed to it. This was the method used in this PhD, as described in Chapter 3.

The most commonly used calibration method is retrodialysis in which the drug of interest is added to the perfusion fluid at a known concentration, and the *in vivo* loss of the drug from the perfusion fluid can be used as a measure for *in vivo* recovery[171]. The No Net Flux Method (also known as the 'Difference Method') involves the consecutive perfusion of varying concentrations of the drug into the perfusion fluid and measuring the resulting dialysate concentrations. The difference between the analyte concentrations in the perfusion fluid and the dialysate are calculated and regression analysis performed to calculate the perfusate concentration [145,143,172]. Although this method is time-consuming, it is the gold standard for microdialysis calibration.

Other calibration techniques include the 'zero flow' and 'ultraslow flow rate' methods; the 'extended or dynamic no net flux' method which in contrast to the 'no net flux' uses only one selected perfusion concentration of the drug[173]. There is also the 'internal standard' technique whereby an internal standard (urea or glucose) is added to the perfusion fluid[174,175] and the 'combined retrodialysis by drug or calibrator' technique which is a combination of retrodialysis and the internal standard method[167].

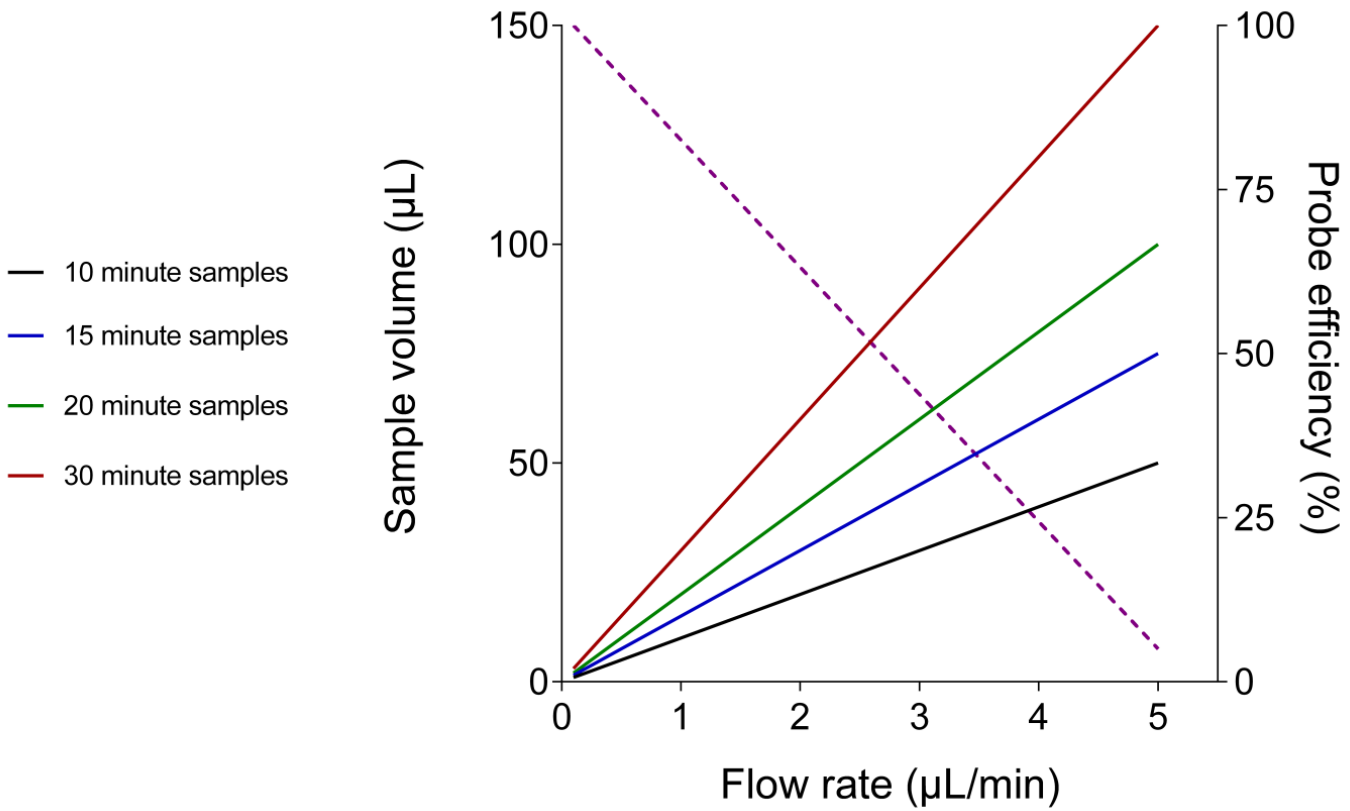

FIGURE 1.6: THE RELATIONSHIP BETWEEN FLOW RATE, SAMPLE VOLUME AND PROBE EFFICIENCY. As the flow rate increases from 1 to 5µl/min the sample volume increases as indicated by dashed line. The black (10min), blue (15min), green (20min) and red (30min) lines illustrate that decreasing the flow rate increases the probe efficiency and that increasing sample collection duration (from 10 to 30 min) means higher sample volume but decreased probe efficiency. Slow flow rates give good probe efficiency but small sample volumes for analysis. The converse is true for fast flow rates. Credit: Stuart Armstrong.

1.4.3.3 PROBES, TUBING AND PERFUSION FLUID

Microdialysis probes, which are commercially manufactured for various peripheral or soft tissues and brain, have a variety of characteristics that need to be considered. The most important factor is the molecular weight (Mw) cut-off of the probe membrane. It is imperative to know, before choosing a probe, the molecular masses of any drugs being investigated to ensure that the drug will be able to pass through the pores in the semi-permeable membrane. The main advantage of microdialysis is that the unbound portion of the drug is collected, if a Mw cut-off is too large it may allow serum proteins through, therefore both protein-bound and unbound drug would be collected. The probe membrane material must also be considered, as the drug of interest may interact or adsorb to the membrane, which therefore would affect the flow of perfusate and consequently the recovery of the drug. However, as the majority of probes used are commercially bought, it is not straightforward to change the probe membrane material. The membrane surface area is an additional characteristic to consider, as the surface area is proportional to the drug recovery; an increase in probe membrane surface area (an increase in the length of the probe) will increase recovery. However, the probe membrane may be too long to fit into the organ of interest.

The volume of dialysate collected in the desired time period can also be affected by the length of the inlet and outlet tubing. The tubing needs to be of sufficient length to incorporate parameters required for *in vivo* experiments such as the length of the harness spring. This highlights the need to perform *in vitro* studies incorporating all parameters that will be used for *in vivo* experiments. The material used in the manufacture of the tubing also needs consideration with respect to the adherence of drug to the tubing surface as well as the diameter and dimensions with regards to static and pulsatile pressures. The commercially bought CMA20 microdialysis probe comes pre-assembled with the tubing attached and therefore there is little choice in tubing material, hence other parameters will need to be altered to improve relative recoveries if the CMA20 probe is to be used.

The perfusion fluid must be similar in ionic strength, composition and pH to the surrounding extracellular fluid. It must also be compatible with the organ system and the drug being measured. There are commercially available perfusion fluids formulated for either brain or soft tissue microdialysis, yet Ringers Solution is often cited in the literature as the chosen perfusion fluid. Other components can be added to the perfusion fluid to increase recovery, such as Bovine Serum Albumin which can be used to block non-specific binding meaning that less drug will be adsorbed to tubing surfaces. It has been suggested that flushing the entire system with the drug eliminates the problem of loss due to adherence to plastic surfaces and that has been shown to be the case for rifampicin [176].

1.4.3.4 MATHEMATICAL PRINCIPLES

Mathematical principles can be applied to microdialysis to further understand the system. The principles of microdialysis are governed by an adaptation of Ficks Law of Diffusion and therefore predictions about how the drug will behave in the microdialysis system can be made[168]:

$$J = (\Delta C_{1-3}) \div R_{1-3}$$

Flux (J) which is the moles of drug in solution transported over the area of diffusion is calculated by dividing the overall concentration difference (C) between the three media (perfusate (1), probe membrane (2) and tissue (3)) by the resistance to diffusion of the drug through the each of the media (R). The factors that guide diffusion differ in each media therefore each concentration profile will differ and therefore all must be taken into account. Bungay *et al* developed 'mass transfer resistance' to calculate E_d which 'describes the proportional difference in analyte concentration between undisturbed external medium and perfusate' as a measure of probe efficiency. This calculation incorporates differential resistance and concentration gradient in tissue as well as gradient across width of the probe. This framework also incorporates additional factors that affect diffusion in tissue under steady-state conditions and hence can affect recovery such as degradation of the drug, reversible binding, hindrance and tortuosity of the tissue[177].

1.4.3.5 IN VIVO FACTORS

A good understanding and knowledge of the physiology of the organ to be dialysed is imperative since a number of factors including blood flow to and from the tissue, the ability of the drug to bind to cell surface proteins and also the complexity and tortuosity (diffusional path) of the organ will affect recovery. The geometry of the probe membrane means that an evenly distributed area of tissue is in contact with the probe membrane, which also acts as a physical barrier between the perfusion fluid and tissue protecting the tissue from the flow of the perfusate. Insertion of the probe into the tissue requires surgery, which can vary in invasiveness dependent upon which organ or area of the organ is being dialysed. Studies have investigated the effects of surgery and anaesthesia on microdialysis recovery, finding little evidence of any effect especially if a guide cannula is used to prevent damage to the probe membrane[141,178]. It has been shown that there is evidence of tissue trauma associated with probe insertion with probes inserted longer than 12 hours; this is associated with tissue necrosis, however linear probes are less damaging[179]. It is important to perfuse the microdialysis probe *in situ* for at least half an hour before beginning the microdialysis experiment to calibrate to the surrounding interstitial fluid[180].

Temperature is a key environmental parameter that needs to be taken into consideration when performing a microdialysis experiment. It has been reported that the higher the temperature, the greater the drug recovery, with a 1-2% increase in the diffusion coefficient observed for every 1°C increase in temperature[168]. de Lange demonstrated that microdialysis recovery at room temperature underestimated the *in vivo* recovery of the drug[180]. Therefore, it is of critical importance that the *in vitro* calibration studies which are conducted prior to the commencement of microdialysis *in vivo* are conducted at the specific body temperature of the species to be dialysed. This is also true of the perfusion fluid which should be warmed to the same body temperature before use.

As described in these sections, the development of the microdialysis methodology can be broken down into an almost sequential series of experiments. The experiments are conducted

in order to calculate and optimise the relative recovery and ultimately the efficiency of the probe associated with different drugs by changing different experimental parameters.

Thompson and Shippenberg[168] published a series of 11 steps that should be followed to design and conduct a successful microdialysis experiment, and these 11 steps were adapted to 7 steps for the purposes of this PhD as described in Chapter 3.

1.5 HYPOTHESIS AND AIMS

New drugs and shorter, less toxic drug regimens are urgently needed to control TB. Pre-clinical tools that are predictive of human responses to drugs are essential to ensure that drugs entering clinical development are optimised with respect to human-relevant PK/PD. This PhD sought to address the need for relevant, predictive pre-clinical tools by refinement of a pre-existing methodology to determine the PK of anti-TB drugs in guinea pigs and to develop and optimise the microdialysis technique in order to describe the organ-specific PK of drugs in the lung, the target organ for TB.

The hypotheses to be tested were:

1. Microdialysis methodology can be established to measure the concentration of drugs in the lung.
2. The concentrations and concentration-time curves (PK curves) of anti-TB drugs within the blood will be significantly different to the concentrations and PK curves in the lungs.

To address these hypotheses, the project had the following aims to:

- Establish PK of TB drugs (rifampicin, isoniazid etc) in peripheral blood (Chapter 2).
- Develop the microdialysis methodology *in vitro*; evaluation of probes, perfusion fluid and flow rates, development of calibration techniques and optimisation of analytical methods (mass spectrometry) with the overarching aim of calculating probe efficiency (Chapter 3).
- Investigate and optimise parameters for *in vivo* microdialysis including evaluation and selection of suitable organ for probe implantation, considerations and method development for surgery and pre-/ post- operative care including analgesia and housing requirements (Chapter 4).
- Determine the feasibility of measuring drug concentrations in organs (Chapter 4).
- Use optimised microdialysis methodology to determine organ-specific PK for TB drugs and compare PK profiles with those obtained in blood (Chapter 5).

- Investigate the potential for microdialysis to reproducibly measure concentrations of drug in organs of a single animal over a time course thus reducing the overall number of guinea pigs required for PK studies, addressing the 3Rs.

Development of microdialysis in the guinea pig model will give critical information to enable the PK of anti-TB drugs to be measured in the organs of disease and thereby generating an improved pre-clinical tool for dose and potentially regimen optimisation.

CHAPTER 2

PK PARAMETERS OF ANTI-TB DRUGS IN BLOOD

2.1 INTRODUCTION

Prior to the studies to establish the *in vitro* parameters (i.e. flow rate, probe type, perfusion fluid) for microdialysis, it was necessary to determine the concentration of drugs to be used in developing the microdialysis methodology. It was important that the concentration was in a range that was relevant to that which would be present *in vivo*.

Although there are similarities in biochemical, physiological and anatomical processes between species, there are also a number of differences. Hence for *in vivo* drug studies, the dose of drug to be administered to animal species must be optimised to be equivalent to human doses in order to model human drug exposure. There are various methods available to optimise doses between species and the primary method is allometric scaling based on weight. Although this method has been used with success, there are drugs whose behaviour is not well- predicted by allometric scaling, including drugs that have a molecular weight over 300Da and those that are excreted via the biliary route, such as rifampicin. This has led to the development of pharmacokinetically guided approaches to dose optimisation [135].

Physiology-Based PK (PBPK) models can be used to predict the PK of drugs in humans using pre-clinical data[136]. This is done by adjusting the model parameters to incorporate human-specific features following confirmation of PK in an animal species. These PBPK models can simulate and make predictions about drug behaviour in other species and can also enable doses to be scaled between species and within the same species (i.e. for specific populations) based on physiological data. An alternative PK guided approach is to choose a dose for use in an animal species based on the AUC_{0-t} (area under the concentration-time curve) in humans[132]. Different doses are applied in animal species in order to achieve the equivalent AUC_{0-t} in humans. The AUC_{0-t} is a measure of total systemic exposure to the drug integrated with time. For the front-line anti-TB drugs, the AUC_{0-t} is strongly associated with efficacy in pre-clinical

models and the PK/PD parameter that best describes the antimicrobial efficacy of the four drugs is AUC:MIC[104] though the Cmax: MIC is also associated with efficacy of rifampicin[181]. The PK parameter(s) which best associate with efficacy are therefore used as a benchmark to bridge between species, testing different doses of the drug in animals in order to achieve (if available), the equivalent human PK value. This approach was taken in these studies and the target was to achieve human-equivalent $AUC_{0\text{-}24}$.

2.1.1 ANIMAL MODELS OF TUBERCULOSIS

There are several different mammalian models that are used for TB drug development, this is because no one model recapitulates all the features of human TB disease[182]. The choice of animal model used is dependent upon the research question asked.

These same animal species have also been used for microdialysis studies, although not associated with TB research.

2.1.2 MOUSE

Mouse (*Mus musculus*) models are routinely used for TB drug evaluation and there are many different mouse models that can be used dependent upon the research question. There are models that can be used to show sterilisation[183] or early bactericidal activity[184] (EBA) or whether drugs can prevent disease relapse[185]. Mice can be genetically modified to 'humanise' the internal anatomy in order to more fully replicate TB disease in humans[186]. Pathologically, unlike humans, lung granulomas in mice lack structural organisation and rarely advance to caseous necrosis and cavitation, and although the presence of granulomas hinders bacterial growth, the disease does not reach a latent state and is associated with a progressive, chronic course of infection[187]. Mice can also maintain a high bacterial load throughout the disease time course[188].

Extensive studies have been conducted in various mouse models to characterise the PK of the anti-TB drugs with different parameter estimates being achieved for different strains. For

example, when the same dose of rifampicin was administered to three different mouse models, the terminal half-lives were reported as 4.4 hours for BALB/C mouse[189], 7.6 hours for the Swiss mouse[190] and 6.6 hours in C57BL/6[137].

Due to the small size of the mouse, the majority of microdialysis studies in mice have involved probe insertion into the brain as opposed to peripheral organs[147,191].

2.1.3 RABBIT

Rabbits (*Oryctolagus cuniculus*) are the largest small animal model used in TB research and are used to recapitulate the spectrum of disease outcomes and pathologies in humans. Upon infection with *M. tuberculosis*, rabbits form lung lesions with the human-associated features of necrosis, caseation and cavitation[192]. This species has been useful to demonstrate drug activity and penetration into lesions with novel imaging techniques[193]. These imaging techniques have also been used for drug distribution studies [192,194]. Similar to humans, rabbits have a varying level of resistance to *M. tuberculosis* disease although the commonly available strains of rabbit tend to be resistant (without pre-sensitisation) and this, along with the disadvantage of the larger size and cost of housing these animals at high containment, means that rabbits are less preferred for drug and method development studies.

Microdialysis has been routinely performed in the brain and the eye of the rabbit [195].

2.1.4 NON-HUMAN PRIMATE

Non-human primate (NHP) species are used for TB research due to their physiological, genetic and immunological similarities to humans. The most common species used are Cynomolgus (*Macaca fascicularis*) and Rhesus (*Macaca mulatta*) macaques. Upon infection with *M. tuberculosis,* macaques like humans, can present with the full spectrum of TB disease including acute and chronic progression as well as latent disease [196]. Imaging techniques for anti-TB drug distribution have been used in baboons (*Papio*) and a key finding of this study was that lung concentrations of total (bound and unbound) rifampicin were found to be 10 times above *M.*

tb MIC [115]. Drug doses administered to NHPs can be selected based on allometric scaling (based on weight) from the dose administered to humans due to the close similarity between the two species. The PK profiles of the current anti-TB drugs are very similar between humans and NHPs especially in relation to AUC_{0-t}. NHPs also show evidence of the fast/slow acetylator status associated with human isoniazid metabolism [197]. This highlights the relevance of this species in terms of anti-TB drug PK and associated toxicities. NHPs are rarely used for development of new methods such as microdialysis, especially without trials in smaller animal species first due to ethical reasons.

Microdialysis has been performed in NHPs, primarily in the brain, and the technique has been used successfully to add a wealth of data to the neuroscience field [198].

2.1.5 RAT

Although rats (*Rattus*) are used frequently for PK/PD studies, they are not frequently used in tuberculosis research due to their inherent resistance to the bacteria with few publications of studies with anti-TB drugs[199]. There are many examples of studies where rats have been used for microdialysis, primarily in the brain, for drugs (ie. Fluconazole[148], clozapine[200], ciprofloxacin[201]) and for other compounds (ie. Nicotine[202], antibodies[203], glutamate[204]). It is evident that the majority of the commercial microdialysis equipment has been developed for use with rats [165].

2.1.6 GUINEA PIG

Guinea pigs (*Cavia porcellus*) have been used in TB research since 1881 and they are still commonly used for TB pathogenesis studies and vaccine evaluation[205]. Disease progression, upon aerosol infection with *M. tuberculosis* in guinea pigs closely replicates several features of human TB, including the presence of caseous necrosis, granulomatous inflammation and occasionally pulmonary cavitation [206]. These lesions, which are hall marks of TB disease, have an influence on the bioavailability and penetration of drugs as well as on the mechanism of drug action. Similar to humans, guinea pigs show a concentration-dependant response with

rifampicin and isoniazid and also demonstrate the superior sterilising activity of rifampicin over isoniazid[207]. Additional advantages to the guinea pig model in relation to their similarities to humans, are that Dunkin-Hartley guinea pigs (the strain most commonly used for TB research) are genetically outbred which means there is heterogeneity associated with disease progression. Additional similarities are that guinea pigs have susceptibility to low dose aerosol infection [19] and show weight loss throughout disease progression, however, key differences between guinea pig and human disease is that upon aerosol infection all guinea pigs will have active disease progression (no latent disease) which is unlike humans, and that in the rare event of pulmonary cavitation in guinea pigs, which can be a common occurrence in human disease, the guinea pig usually dies before any small cavities can become larger and liquefy[208].

Despite the many advantages of the guinea pig model to study TB, guinea pigs have a very sensitive gut flora which means they are not an ideal model for drug studies. Drugs administered to guinea pigs often have to be co-administered with a lactobacillus probiotic which can change the gut microbiota and enzyme activities within the gut, ultimately affecting PK parameters[209]. Other disadvantages include the lack of accessible peripheral veins for blood collection; the marginal ear vein is the most easily accessed, but blood can also be collected from the tarsal vein and lateral saphenous vein. Blood collection from these venous sites are non-terminal procedures however only small volumes of blood can be collected, with no more than 1% of the guinea pigs blood volume or more than 4 blood samples removed over a 24 hour period. The collected blood also has a rapid coagulation time which can prove problematic when collecting small volumes for PK analysis[210].

There are almost 150 publications where microdialysis has been performed in guinea pigs. The majority of these studies involve microdialysis in the brain, inner ear and skin for numerous xenobiotics including drugs[211,212,213], nerve agents[214] and nerve agent treatments[215] as well as endogenous compounds such as serotonin[216]. Guinea pigs were the species of choice for this PhD with the intention of improving this model for anti-TB drug evaluation. Characterising the PK of novel and existing drugs in this model, with microdialysis, would be valuable to better

understand drug PK in this important model of TB disease and therefore to potentially predict effective drug concentrations for humans.

2.1.7 DEFINING BASIC PK PARAMETERS VIA BLOOD SAMPLING

Using guinea pigs as the species of choice, the studies described below were designed to understand and define drug doses in the guinea pig in order to achieve the equivalent human $AUC_{0\text{-}t}$. The aim was to describe human-relevant drug exposures of the four frontline anti-TB drugs (rifampicin, isoniazid, pyrazinamide and ethambutol) delivered as single drugs or in combination. These studies were conducted within the PreDiCT TB project (Chapter 1; 1.2.6). The short half-lives of the anti-TB drugs means that it was possible to describe the PK profile after one single oral dose[137]. External partners of the PreDiCT TB consortium contributed to this work with respect to the processing and UPLC-MS/MS analysis of blood samples to measure drug concentrations (GSK) and the analysis and interpretation of the data in R to generate $AUC_{0\text{-}t}$ data of the anti-TB drugs (University of Liverpool). The sample analysis and resulting data analysis were a central resource for the PreDiCT TB project to ensure harmonisation between the different partners within the consortium.

EQUIPMENT AND REAGENT LIST

Equipment	Comments	Source
2ml syringe	Oral administration of drug	BD574/GS576; Appleton Woods Ltd, Birmingham, UK
Scalpel	Ear bleeds	No. 15A; Product Code: 0320; Swann Morton, Sheffield, UK
20, 21, 23 gauge needles	Various uses	Terumo Agani, Surrey, UK
Chemical and Reagent	**Comments**	**Source**
0.1% Acetic Acid in HPLC water	Chromatographic Solvent	1005706; Sigma Aldrich Co LTD Dorset, UK
0.1% Heptafluorobutyric Acid	Chromatographic Solvent	52411; Sigma Aldrich Co LTD Dorset, UK
Acetonitrile	Chromatographic Solvent	PHR1551-3X1.2ml; Sigma Aldrich Co LTD Dorset, UK
Apple and Banana fruit puree	To help palatability of drugs for oral administration	Ella's Kitchen, Henley-on-Thames, UK
Butylhydroxytoluene		B1215000; Sigma Aldrich Co, Dorset, UK
Dimethyl sulfoxide (DMSO)		D2650; Sigma Aldrich, Dorset, UK
Ethambutol		E4630-25G; Sigma Aldrich Co LTD, Dorset, UK
HPLC (High Performance Liquid Chromatography) Grade Water	Many uses including diluting drug to create 'dose solution' This water is free from organic and inorganic compounds and has no UV absorbance.	270733-1L-M; Sigma Aldrich Co LTD, Dorset, UK
Isoniazid		I3377-250G; Sigma Aldrich, Dorset, UK
Midozolam	Internal Standard	BP722; Sigma Aldrich Co, Dorset, UK
Pyrazinamide		P7136 100G; Sigma Aldrich, Dorset, UK
Reserpine	Internal Standard	43530-4-5ML-F; Sigma Aldrich Co, Dorset, UK
Rifampicin		R3501-1G; Sigma Aldrich, Dorset, UK

UPLC/MASS SPECTROMETRY

GlaxoSmithKlein R&D, Diseases of the Developing World, Tres Cantos, Madrid, Spain	(UPLC) Aquity System with Sampler Manager	Waters, Hertford, UK
	(UPLC) Column; Aquity UPLC BEH C18 50x2.1mm, 1.7µm column	
	(Mass Spectrometer) API4000	Sciex, Warrington, UK
	(Data Collation) Mass Lynx	Waters, Hertford, UK

2.2.1 ETHICS STATEMENT

All of the guinea pig procedures were approved by UK Home Office legislation for animal experimentation as well as being approved by Public Health England, Porton Down local animal welfare and ethical review body (AWERB). All *in vivo* work was carried out under Project Licence: PPL NO. 30-3236. As far as possible principles of randomisation, non-bias and blinded analyses were adhered to, for example by using identification microchips.

2.2.2 GUINEA PIGS

Female full barrier-reared, out-bred Dunkin-Hartley guinea pigs (weighing between 200 and 250g; Envigo UK) arrived on site at least 72 hours prior to commencement of the first procedure. Throughout the duration of the study, guinea pigs were kept in a controlled environment and had access to food (Global Guinea Diet; Envigo, Enrichment Feed: Forage Mix; Envigo) and water *ad libitum*.

2.2.3 PREPARATION OF DRUGS FOR ORAL ADMINISTRATION

The drugs were orally administered and for the purpose of these studies as monotherapy, rather than in combination. The doses trialled were: isoniazid: 50mg/kg; rifampicin: 50 or 75 mg/kg; ethambutol: 100 or 250mg/kg. Animals were weighed immediately prior to administration of the drugs to the ensure accuracy of the dose. Due to the small volume of drug required per animal, a larger volume homogenous solution of the drug was prepared, with multiple doses created from the same stock solution. Solutions for administration were mixed with an apple and banana fruit puree, to make the drug more palatable for the guinea pigs. The drug and puree mixture was divided into 2ml volumes (in syringes) for administration.

2.2.4 ORAL ADMINISTRATION OF DRUGS TO GUINEA PIGS

Guinea pigs were gently restrained by hand and the syringe placed into the mouth, until the syringe end was at the rear of the buccal cavity. In a controlled manner 0.2ml of formulation

(drug+ puree) was administered into the back of the mouth. This was repeated until all the formulation had been consumed by the guinea pig. If the guinea pig was not consuming the formulation with ease, the syringe was removed from the mouth and a smaller volume of formulation introduced. Enough time was given for the guinea pig to consume the formulation. It was important to ensure that the guinea pigs were ingesting the formulation and not holding it in their cheeks. After all of the formulation had been consumed the time was recorded and the subsequent time of sample (blood and/or microdialysis fraction) collection was calculated from this point (t_0).

2.2.5 COLLECTION OF BLOOD FROM PERIPHERAL VEIN IN EAR

Blood was collected from the peripheral vein in the ear at 0.25, 0.5, 1, 2, 4, 7, 10 and 24 hours post drug administration. 12 guinea pigs were ear bled (2 blood sampling occasions each) for the studies detailed in this chapter. The guinea pig was gently restrained by hand and the ear gently held and rubbed with fingers to ensure maximum blood flow. A small incision was carefully made in a peripheral vein in the guinea pig ear using a scalpel. A 100µl sample was collected into a tube containing 200µl HPLC water. The blood was mixed thoroughly with the water using a vortex, placed into liquid nitrogen and stored at -80°C until protein precipitation and analysis. Residual blood flow from the vein was stopped using a sterile tissue.

2.2.6 UPLC-MS/MS SAMPLE ANALYSIS

The blood samples from these PK studies were analysed at GlaxoSmithKlein, Tres Cantos, Spain. A deliverable of the PreDiCT TB consortium was that all the *in vivo* samples be analysed in a harmonised and centralised resource, this was provided by GSK. The UPLC- MS/MS (Ultra-high Performance Liquid Chromatography-Mass Spectrometry/Mass Spectrometry) protocol and details of sample analysis given below was shared by Dr Fatima Ortega-Muro (Principal Scientist, GSK).

The UPLC system consisted of an Aquity UPLC System with Sampler Manager. The column used was an Aquity UPLC BEH C18 50x2.1mm, 1.7µm column. The mass spectrometer used was an

API4000 with electrospray ionisation source (ESI). Data were collected and processed using MassLynx. The chromatographic conditions are shown in Table 2.1.

Gradient	Acetonitrile	0.1% heptafluorobutyric acid + 0.1% acetic acid in HPLC grade water
Time (Min)	**%A**	**%B**
0	0.1	99.9
0.2	3	97
1.2	50	50
1.6	99	1
2	99	1
3.55	0.1	99.9
Flow Rate:	350µl/min	
Column Temperature:	5°C	
Injection Volume:	10µl	

TABLE 2.1: CHROMATOGRAPHIC CONDITIONS USED AT GSK for the rifampicin, isoniazid and ethambutol. The total run time was 3.55 minutes.

1mg/ml stock solutions of the front-line anti-TB drugs were made in 50:50 Methanol: Water. 1mg/ml internal standards reserpine and midazolam were prepared in dimethyl sulfoxide (DMSO) and further diluted in acetonitrile/methanol (80:20 v/v) to create 200ng/ml and 50ng/ml working standards respectively. Butylhydroxytoluene (1% w/v) was added as antioxidant agent.

Using the ESI, the mass spectrometer (MS) was operated in the positive ionisation mode (Nebuliser gas (NEB) 50PSI, Curtain gas (CUR) 10PSI, Collisionally Activated Dissociation (CAD) 5PSI, Ion-spray Voltage (IS) 2550V, Temperature of ion source (TEM) 500°C). The determined multiple reaction monitoring (MRM) transitions (m/z) were 138.02/120.98 for isoniazid, 205.4/115.9 for ethambutol and 823.5/791.2 for rifampicin. For the internal standards transitions were 609.61/194.97 for reserpine and 326.41/291.21 for midazolam. Mass spectrometry parameters are shown in Table 2.2.

Compound	De-clustering Potential (V)	Entrance Potential (V)	Collision Energy (Electron-volt)	Collision Cell Exit Potential (V)	Retention Time (Minutes)
Rifampicin	56	10	23	24	2.02
Isoniazid	26	10	21	6	1.26
Ethambutol	76	10	15	6	1.44
Reserpine	76	10	35	6.3	1.90
Midazolam	76	10	35	6.3	1.77

TABLE 2.2: MASS SPECTROMETRY PARAMETERS FOR DRUGS AND INTERNAL STANDARDS AT GSK.

The UPLC-MS/MS methodology was validated by adherence to the following acceptance criteria; the signal in the blank sample was <20% of the signal of the lowest calibration standard, the internal standard area in calibration standards did not differ from the area in unknown samples by more than 30%, definition of the upper limit of quantitation ((ULOQ) which was the calibration standard that met the acceptance criteria immediately above the highest concentration sample) and lower limit of quantitation ((LLOQ) which was the lowest calibration standard which meets the acceptance criteria if the signal is 10-fold of the signal to noise ratio).

2.2.7 DATA ANALYSIS

The concentrations of drug measured in the blood samples at GSK were analysed using PK Solver which is a freely available add-in programme for Microsoft Excel (2003-2010) designed by Zhang *et al*[217]. It was developed for a range of PK/PD analyses including non-compartmental analysis for extravascular administration and compartmental analysis of concentration-time data.

The data (concentration in ng/ml inputted as µg/L (ng/ml=µg/L)) for each of the drugs were input into Microsoft Excel 2010. The PK Solver add-in programme was installed, and the concentration against time data was selected for analysis within the programme using the non-compartmental analysis following an extravascular dose. The results are shown in Figure 2.1 and Table 2.3.

The PK Solver add-in for Microsoft Excel can be found in the online version of the publication:

doi:10.1016/j.cmpb.2010.01.007

2.3 RESULTS

The data shown in Figure 2.1 are the concentration-time curves generated in PK Solver, for each drug and dose. The concentrations of drug from three guinea pigs bled at each time point were averaged. PK Solver was also used to generate the associated $AUC_{0\text{-}t}$ (0-24 hours) and $AUC_{0\text{-}inf}$ (AUC extrapolated to infinity time) using the linear trapezoidal method, these and other PK parameters are shown in Table 2.3.

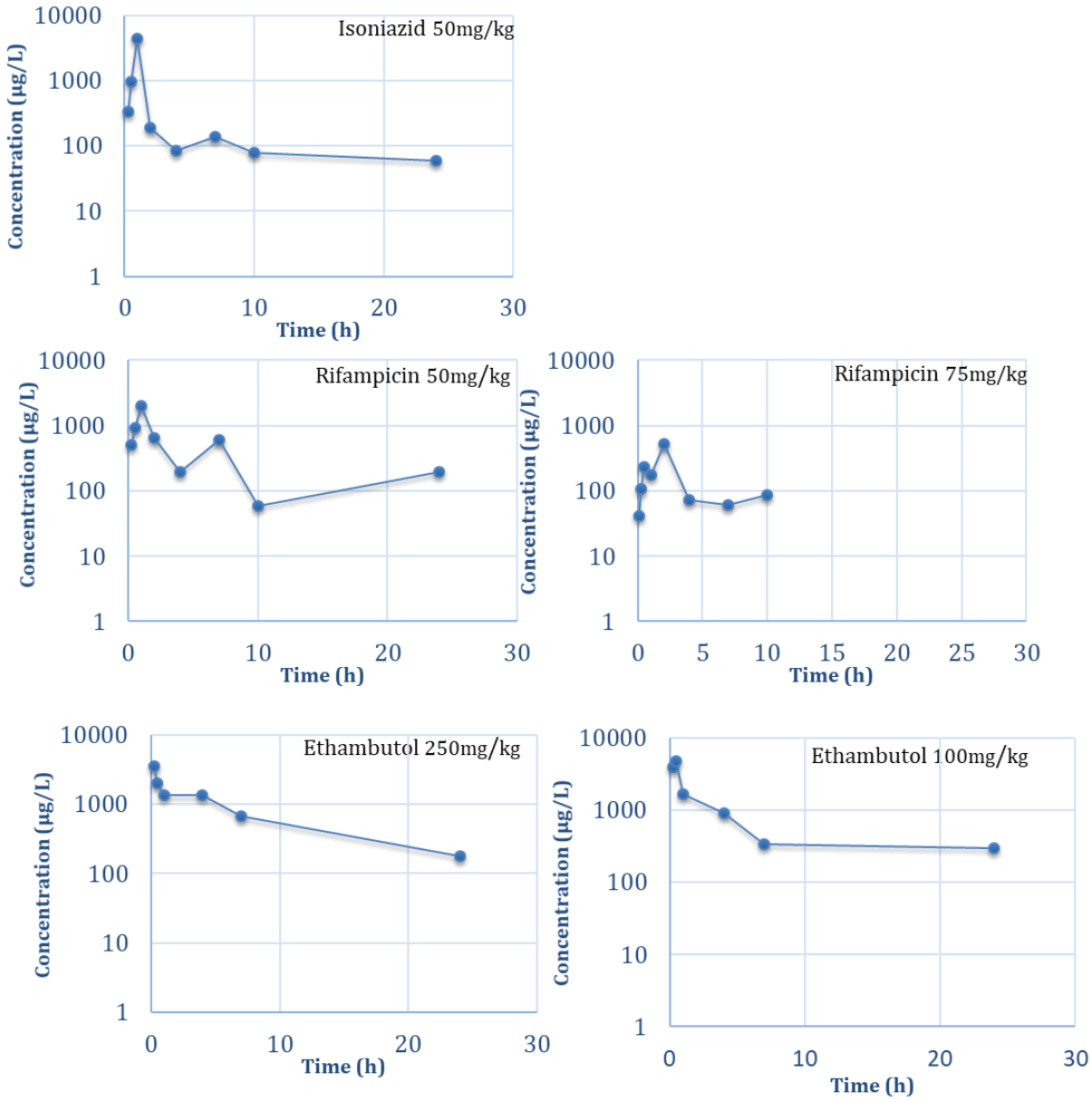

FIGURE 2.1: PK PROFILES GENERATED IN PK SOLVER. The concentrations of isoniazid (50mg/kg), rifampicin (50mg/kg vs 75mg/kg (no rifampicin measured after 10 hours post drug administration)) and ethambutol (100 vs 250 mg/kg) in blood over 24 hours.

Non-Compartmental Analysis						
Drug		**Rifampicin**		**Isoniazid**	**Ethambutol**	
Dose	**mg/kg**	**50**	**75**	**50**	**250**	**100**
h	**$t_{1/2}$**	16.68	3.75	9.2	7.61	7.77
h	**Tmax**	1	2	1	0.25	0.5
mg/L	**Cmax**	4.3	0.5	1.9	3.4	4.8
mg/L*h	**AUC_{0-24}**	5.66	1.51	7.06	16.43	14.42
	AUC_{0-inf}	7.07	1.98	9.61	18.42	17.77

TABLE 2.3: PK PARAMETERS FOR RIFAMPICIN, ISONIAZID AND ETHAMBUTOL CALCULATED FROM CONCENTRATION IN GUINEA PIG BLOOD. The parameters shown, calculated using PK Solver are $t_{1/2}$ (half-life of the drug), Tmax (time at which maximum concentration occurs), Cmax (maximum concentration). AUC_{0-t} and AUC_{0-inf} are shown (mg/L*h).

Species	**Drug**	**Dose (mg/kg)**	**Median AUC_{0-24} (mg/L*h)**	**AUC_{0-24} Range (mg/L*h)**	**Cmax (mg/L) (Range)**	**Median Tmax (h)**	**$t_{1/2}$ (h) (Range)**	**Reference**
Human	Rifampicin	(Median) 9.8	35.4	26.8-49.9	9.0 (6.6-12.8)	3.0	1.6 (1.4-1.8)	[218]
	Isoniazid	(Median) 4.9	4.4	1.3-15.0	1.9 (1.0-3.5)	1.0	1.9 (0.9-4.0)	
	Ethambutol	(Median) 17.2	12	5.4-28.2	1.8 (0.9-3.7)	4	3.3 (2.5-7.4)	[130]

TABLE 2.4: PK PARAMETERS OF RIFAMPICIN, ISONIAZID AND ETHAMBUTOL IN HUMANS. Published data (from Burhan *et al* and Denti *et al*) calculated from measured drug concentrations in blood.

2.3.1. ISONIAZID

The concentration-time curve for isoniazid showed a biphasic profile and the AUC_{0-24} with a dose of 50mg/kg was 7.06mg/L*h, which was within the range of AUC_{0-24} data obtained in humans with a median dose of 4.9mg/kg. The Tmax and Cmax values for isoniazid in guinea pigs were 1h and 1.9mg/L respectively which are similar values as those obtained in the human study. The $t_{1/2}$ value obtained from the guinea pig data (9.2h) was greater than that measured in humans (1.9h).

2.3.2. RIFAMPICIN

At a dose of 50mg/kg, the PK properties of rifampicin in guinea pigs were different to the published human data. The AUC_{0-24} was 5.65mg/L*h which was lower than the value obtained in humans (35.4mg/L*h). The Cmax of rifampicin was also lower in guinea pigs (4.3mg/L) than in humans. The Tmax occurred later in the human PK profile than in the guinea pig profile (3 hours vs 1 hour) and the half-life ($t_{1/2}$) was longer (16.6h) in guinea pigs than humans (1.6h). A higher dose of rifampicin (75mg/kg) given to guinea pigs, did not result in an increase in the AUC_{0-24}, or Cmax, compared with the 50mg/kg dose, the values obtained were lower with the higher dose, which is an unexpected result.

2.3.2. ETHAMBUTOL

Following a 100mg/kg dose of ethambutol, the AUC_{0-24} was 14.4mg/L*h and with a 250mg/kg dose the AUC_{0-24} was 16.4mg/L*h and these values were within the range of values obtained in humans dosed with 17mg/kg. The Cmax values were 4.8mg/L and 3.4 mg/L respectively for the 100mg/kg and 250mg/kg doses and these values obtained in guinea pigs were around the higher end of the range of values obtained in humans. The $t_{1/2}$ in guinea pigs was also similar to values obtained in humans but at the higher end of the range. The Tmax occurred earlier in guinea pigs (0.25 and 0.5 h for the 100 and 250mg/kg doses respectively) than in humans (3.3h).

2.4 DISCUSSION AND CONCLUSIONS

The PK profiles and parameters of each drug in the guinea pig were compared with published data for humans as described by Burhan *et al*[218] and Denti *et al*[130] . A summary of these parameters are shown in Table 2.5.

	AUC_{0-24} mg/L*h		**Cmax mg/L**		**Tmax h**		**$t_{1/2}$ h**	
	Guinea Pig	**Human (Range)**	**Guinea Pig**	**Human**	**Guinea Pig**	**Human**	**Guinea Pig**	**Human (Range)**
Isoniazid	7.06	1.3-15.0	1.9	1.0-3.5 (median:1.9)	1	1	9.2	0.9-4
Rifampicin 50mg/kg	5.66	26.8-49.9	4.3	6.6-12.8	1	3	16.68	1.4-1.8
Rifampicin 75mg/kg	0.5		0.5		2		3.75	
Ethambutol 250mg/kg	16.43	5.4-28.2	3.4	0.9-3.7	0.25	4	7.61	2.5-7.4
Ethambutol 100mg/kg	14.42		4.8		0.5		7.77	

TABLE 2.5: SUMMARY PK PARAMETERS AS GENERATED IN BLOOD FOR GUINEA PIGS compared to PK parameters generated in humans as identified in the literature.

These publications describe studies to evaluate the PK of the anti-TB drugs in populations who were patients with pulmonary TB and provided a data set with which to compare the PK parameters between species, based upon concentrations of drug measured in the blood.

Of the PK parameters examined, the AUC_{0-24} and Cmax were the ones which were most similar between the human data and the data from guinea pigs at the doses given. This was particularly the case for isoniazid and ethambutol. With the exception of $t_{1/2}$, which was longer in guinea pigs than in humans, the PK parameters obtained when guinea pigs were given a dose of 50mg/kg of isoniazid were closely matched to those described in humans dosed at 4.9mg /kg. In humans, isoniazid concentrations were modelled using a two-compartment model[130] and these data in guinea pigs were modelled using a non-compartmental analysis, so the $t_{1/2}$ measured in guinea pigs most likely overestimates the initial apparent half-life. These data collectively demonstrate that allometric scaling is not appropriate for identifying the most appropriate doses for an animal species. Generally, in order to achieve human-like exposures, the drug dose required for guinea pigs was much greater than that which would have been predicted by scaling based upon weight.

The AUC_{0-24} and Cmax for rifampicin were the least closely matched between humans and guinea pigs with 50mg/kg and 75mg/kg doses in guinea pigs resulting in much lower values for these PK parameters than a human dose of 9.8mg/kg. Additionally, the 75mg/kg dose not only failed to increase systemic exposure (AUC_{0-24}) but resulted in a decrease. The differences in $t_{1/2}$ between 50mg/kg and 75mg/kg rifampicin doses were most likely an artefact of the unusual profile associated with 75mg/kg dose. The higher dose of rifampicin was tested after a one- week washout period in the same guinea pigs that received the 50mg/kg dose of rifampicin. The reduction in the systemic exposure could be explained by the auto-induction of rifampicins' metabolism. Auto-induction, whereby a drug induces enzymes that enhance its metabolism, is known to occur following secondary exposure to rifampicin, resulting in a more rapid clearance even though a higher dose was administered[219]. Auto-induction has not previously been reported in the guinea pig after a single dose or when dosed to a steady state[220] although auto-induction following rifampicin administration has been identified in mice[137].

Studies to investigate whether human-like exposures could be achieved with doses of rifampicin higher than 50mg/kg were not pursued due to potential toxicity of this drug in guinea pigs. Antibiotic-associated enteritis was observed in some of the animals, a phenomenon also observed by Ahmad *et al.* After 14 days of treatment with rifampicin, 7/61 guinea pigs were culled following colon distension and a directly toxic effect on the GI tract [207]. It has been reported that a dose of 100mg/kg rifampicin in guinea pigs achieved a median AUC_{0-24} of 71.0mg/L*h which indicates that exposures equivalent to or even higher than the human range of AUC_{0-24} can be achieved[220] but this comes with a risk of toxicity, especially in the GI tract which can limit the bioavailability of rifampicin.

The data generated in the studies described in this Chapter enabled key parameters to be established prior to initiating microdialysis method development and subsequent investigations of anti-TB drug PK in disease-relevant tissue. These data were:

- Identification of drug doses for guinea pigs that are relevant to human exposures and that can be used as a starting point for set-up and optimisation of the *in vitro* parameters of microdialysis, such as flow rate, selection of probe and perfusion fluid.

A dose of 50mg/kg isoniazid and the doses of ethambutol (100 and 250mg/kg) were selected because these gave human-like exposures in guinea pigs and the rifampicin dose of 50mg/kg was chosen although it did not achieve a human-like AUC, to ensure minimal adverse drug effects.

- Concentration-time curves for the drugs to define post-drug sampling time points and other aspects of study design (taking into account 3Rs principles) to measure and compare concentrations of drug in blood and tissues sampled using microdialysis. For example, it was shown for both rifampicin and isoniazid that the Tmax occurred before the four hour time point, and therefore a four hour dialysis period would be sufficient for microdialysis studies in guinea pigs.
- Blood PK parameters for the anti-TB drugs which serve as comparative data to evaluate consistency between guinea pigs that have undergone microdialysis or not and against which to compare tissue PK .

CHAPTER 3

IN VITRO MICRODIALYSIS METHOD DEVELOPMENT

3.1 INTRODUCTION

The main principles of microdialysis, including a detailed overview of the factors that can affect the relative recovery of drug, was described in Chapter 1. Microdialysis is a continuous sampling technique and therefore describes the pharmacokinetic (PK) behaviour of drugs within organs and tissues as opposed to the traditional PK data collection site (blood) and importantly can be used to quantify the amount of unbound pharmacologically active drug. For the anti-TB drugs, where the target site for drug action is the lung, PK data obtained by microdialysis are thus more clinically relevant than data from the blood.

Thompson and Shippenberg[168] published a series of 11 steps that should be followed to design and conduct a successful microdialysis experiment. An adaptation of these 11 steps was devised and used to guide the progression of experiments performed in this PhD project, this adapted scheme is shown in Figure 3.1. Thompson and Shippenberg[168] suggested that these steps be followed sequentially; however, in practice, the process of setting-up microdialysis for use with the anti-TB drugs was cyclical. For instance, whilst optimising the sensitivity of the analytical equipment; probe type (Mw cut-off) and membrane length, flow rate, perfusion fluid and other factors, including drug- specific and tissue- specific factors, needed to be considered to improve the efficiency of recovery.

The initial *in vitro* experiments described here aimed to characterise the microdialysis system through testing different probes (different membrane lengths and molecular weight (Mw) cut-offs), perfusion fluids and flow rates. These experiments were conducted in order to optimise the efficiency of microdialysis recovery for each of the drugs (ETH, INH, RIF). The data generated from these *in vitro* experiments enabled the calculation of the probe efficiency (a correction factor applied to organ drug concentrations recovered *in vivo*). Optimisation of the bioanalytical methods for the three drugs (ETH, INH and RIF) was also completed. These

studies provided the data to enable an understanding of the factors that affect the recovery of drugs both *in vitro* and *in vivo*.

The microdialysis system for all *in vitro* experiments was set up as shown in Figure 3.2. The syringe pump was fitted with a 1ml syringe that contained the perfusion fluid. The syringe was connected to the CMA 20 microdialysis probe using a Luer lock needle and tubing connector. The probe was placed in the dose solution (drug (volume µg or mg) + HPLC water). The refrigerated fraction collector was connected to the probe via the probe outlet tubing to collect the resulting dialysate. Samples were collected every 30 minutes for 4 hours to align with the *in vivo* PreDiCT TB experiments (Chapter 2). The collected dialysate was analysed via Liquid Chromatography- Mass Spectrometry/ Mass Spectrometry (LC-MS/MS) to calculate the relative recovery and ultimately the probe efficiency.

The aspects of the microdialysis system optimised in this Chapter are those related to Steps 1 through 4 of Figure 3.1. Prior to the description of the studies that relate to steps 1-4, the methods used to calculate %relative recovery and %co-efficient of variation (Section 3.2.1) as well as the initial calibrations of the syringe pump (Section 3.3) and an overview of microdialysis parameters (Section 3.3.2) are described. An equipment list which details all the equipment, materials and reagents used for these *in vitro* studies is shown in Section 3.2.

The drugs used in this Chapter were ethambutol (ETH), isoniazid (INH) and rifampicin (RIF) (3 of the 4 front-line anti-TB drugs). It was vitally important that meticulous *in vitro* experiments were carried out with each drug before moving into *in vivo* experiments.

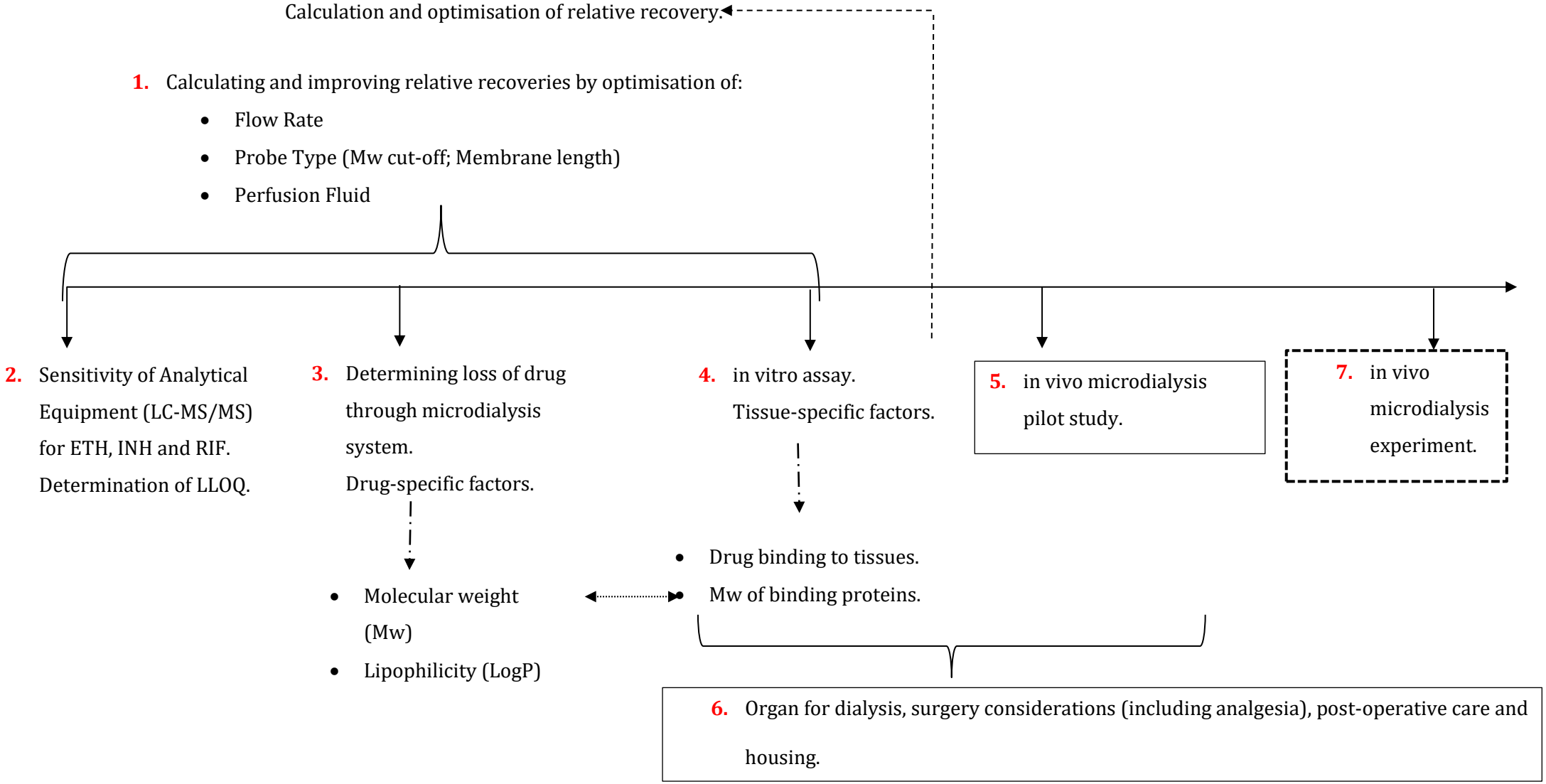

FIGURE 3.1: PROJECT SPECIFIC ADAPTATION OF 'AN OVERVIEW OF MICRODIALYSIS' TO REFLECT THE STEPS OF THIS PROJECT. This chapter details the results from steps 1 to 4. Black solid boxes represent results shown in Chapter 4, black dashed box represents results shown in Chapter 5.

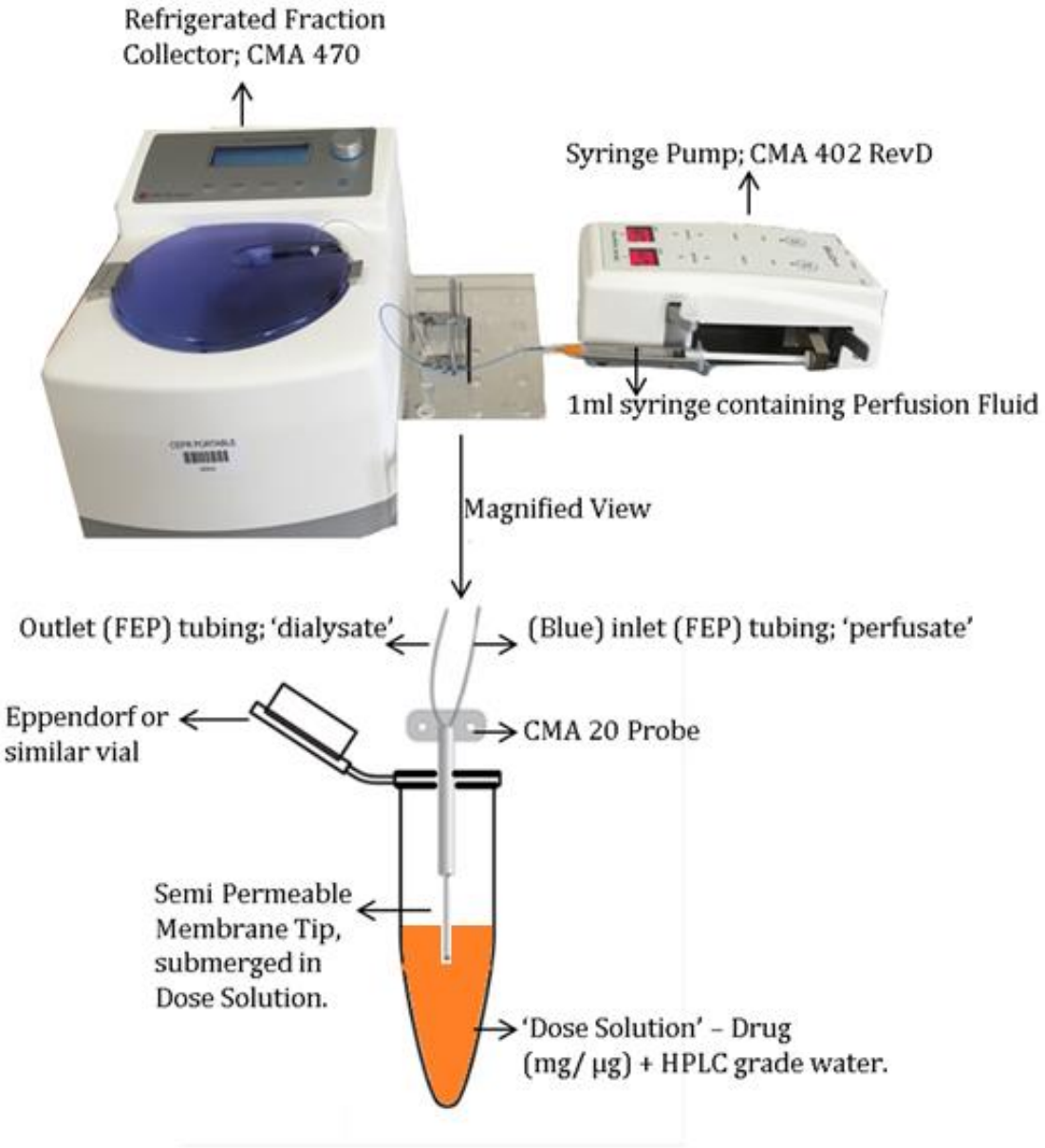

FIGURE 3.2: IN VITRO MICRODIALYSIS EQUIPMENT SET-UP. The syringe pump was fitted with a syringe (60mm stroke length) that was connected to the microdialysis probe. The probe was submerged in the dose solution. The refrigerated fraction collector was connected to the probe via outlet tubing to collect resulting dialysate in 300µl microdialysis tubes.

3.1.2 CALCULATING RELATIVE RECOVERY AND ERROR

The relative recovery (also known as the extraction efficiency) is the relation between the concentrations of the drug in the periprobe fluid (the fluid surrounding the probe) and that in the collected dialysate[169]. Recovery can be calculated using the following equation:

$$Recovery\ (\%) = \left(\frac{C_{dialysate}}{C_{periprobe}}\right) \times 100$$

$C_{dialysate}$ is the concentration of compound in dialysate, $C_{periprobe}$ is the concentration of compound in the fluid surrounding the probe (for these *in vitro* experiments the dose solution in which the microdialysis probe was sat).

As part of the characterisation of the microdialysis system, the experiments that determined the relative recovery of the probes were repeated three times (as a minimum) to enable a mean to be calculated and to obtain an error on these measurements. The recoveries of the replicate experiments were propagated to determine the efficiency (and associated error) of the probe. Subsequently, the relative recoveries obtained following *in vivo* microdialysis were corrected for using this calculated probe efficiency.

The co-efficient of variation was calculated to assess the reproducibility of the assay and with adequate calibration of the microdialysis probe, the within-probe co-efficient of variation for microdialysis measurements should be around 20% depending on the analyte [221].

$$CoV\ (\%) = (StdDev\ (All\ fractions) \div Mean\ (All\ fractions)) \times 100$$

3.2 IN VITRO EQUIPMENT LIST

Equipment	Comments	Source
300µl collection tubes	Compatible with refrigerated fraction collector. Polypropylene.	(1000/pack) 743110; Linton Instruments, Norfolk, UK.
CMA 20 Probe	Various molecular weight cut-offs; 4mm or 10mm membrane length.	(Various) CMA Microdialysis AB, Kista Sweden; Distributed by Linton Instruments, Norfolk, UK.
CMA 402 Rev D Syringe Pump	Designed for pulse-free low flow rates.	CMA Microdialysis AB, Kista Sweden.
CMA 470 Refrigerated fraction collector	Automatically changes tubes after desired collection period; maintains samples at 4°C.	CMA 8002770; CMA Microdialysis AB, Kista Sweden; Distributed by Linton Instruments, Norfolk, UK.
FEP Tubing	Fluorinated Ethylene Propylene; attached to probe.	BFEP-T22Q; Instech, Plymouth Meeting, USA; Distributed by Linton Instruments, Norfolk, UK.
Luer stubs blunt needle	Connect syringe to probe.	Fisnar QuantX 8001101; Ellsworth, Germantown, USA.
Tubing connectors		CMA 3409500; CMA Microdialysis AB, Kista Sweden; Distributed by Linton Instruments, Norfolk, UK.
Perfusion Fluid	**Composition**	**Source**
CNS Designed for microdialysis in central nervous system	NaCl 147 mmol/L, KCl 2.7 mmol/L, $CaCl_2$ 1.2 mmol/L, $MgCl_2$ 0.85 mmol/L	Harvard Apparatus, Holliston, USA distributed by Linton Instruments, Norfolk, UK
Ringers Solution +0.2% BSA	NaCl 147 mmol/L, KCl 4 mmol/L, $CaCl_2$ 2.25 mmol/L	BSA: Bovine Serum Albumin; A2058, Sigma Aldrich, Dorset, UK.
T1 Designed for microdialysis in soft tissues.	NaCl 147mmol/L, KCl 4mmol/L, $CaCl_2$ 2.3mmol/L	CMAP000034; Harvard Apparatus, Holliston, USA distributed by Linton Instruments, Norfolk, UK
Reagent	**Use**	**Source**
0.1% Formic Acid Aqueous	Chromatographic Solvent	5438040100; Sigma Aldrich Co LTD, Dorset, UK
Acetonitrile	Chromatographic Solvent	PHR1551-3X1.2ml; Sigma Aldrich Co LTD Dorset, UK
Dextromethorphan (DXT)	Internal standard	1180503-2G; Sigma Aldrich, Dorset, UK
Dimethyl sulfoxide (DMSO)		D2650; Sigma Aldrich, Dorset, UK
Ethambutol		E4630-25G; Sigma Aldrich Co LTD, Dorset, UK
HPLC Grade Water	Many uses including diluting drug to create 'dose solution'	270733-1L-M; Sigma Aldrich Co LTD, Dorset, UK
Isoniazid		I3377-250G; Sigma Aldrich, Dorset, UK
Rifampicin		R3501-1G; Sigma Aldrich, Dorset, UK

HPLC/ MASS SPECTROMETRY

Q3 Analytical, Porton Science Park, Porton Down, Salisbury, Wiltshire, SP4 0JG	(HPLC) Agilent 1100 Pump, Column heater, Degasser	Aligent, Cheadle, UK
	(HPLC) CTC HTS Autosampler	Presearch, Basingstoke, UK
	(HPLC) Column; Ethambutol; Ascentis Express C8 50x2.1MM	Phenomenex, Macclesfield, UK
	(HPLC) Column; Rifampicin; Kinetex C8 50x2.1MM, 5µm	
	(HPLC) Column; Isoniazid; Kinetex C18 150x2.1MM, 5µm	
	(Mass Spectrometer) API3000	Sciex, Warrington, UK

3.3.1 CALIBRATION OF THE SYRINGE PUMP BY WEIGHT

The volume of dialysate available for analysis is dependent upon the flow rate, therefore the syringe pump required calibration to ensure it was flowing at the expected flow rate (as described in Chapter 1). The initial stages of calibration of the syringe pump involved weighing of dialysate samples (every 10 minutes) as the syringe pump flowed at various rates (1, 2, 5, 10 µl/min). Deviations in the weight of the dialysate samples can indicate changes in the flow rate which can therefore affect the efficiency of the probe and therefore the concentration of drug in the dialysate.

It was evident that the syringe pump was flowing at a constant rate and was working as expected (Figure 3.3). The linearity of the data points indicate that the flow was continuous, and this was further emphasised by the cumulative weight of the samples being consistent with the flow rate. There were differences observed in sample collection at the different flow rates, and a faster flow rate resulted in an appropriately heavier sample being collected. All of this was indicative that the syringe pump was working as expected.

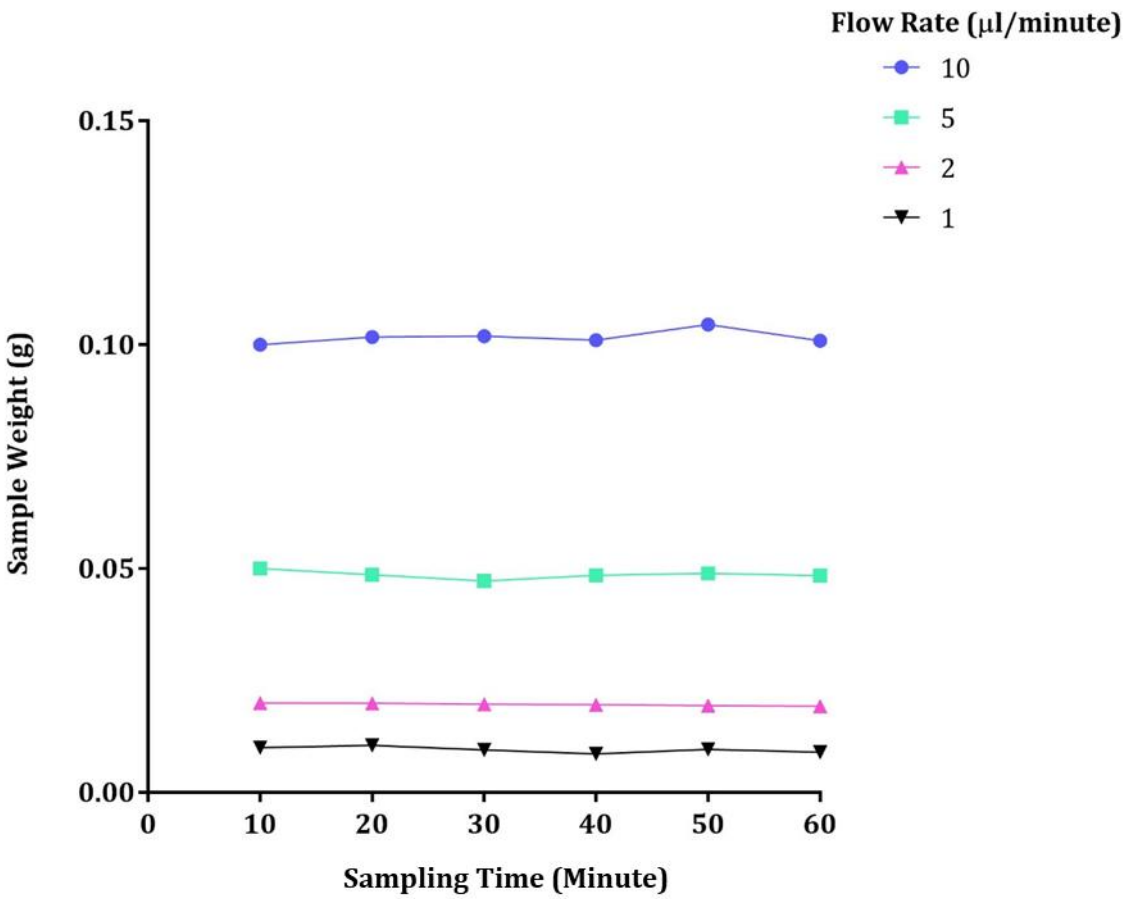

FIGURE 3.3: INITIAL SYRINGE PUMP CALIBRATIONS. Weight of samples collected at different flow rates over a 60-minute period.

3.3.2 OVERVIEW OF PROBES, PERFUSION FLUIDS AND FLOW RATES

Figure 3.4 shows a basic flow diagram of the microdialysis parameters (probe type, perfusion fluid and flow rate) which were evaluated and optimised with each drug (ETH, INH and RIF). These parameters were optimised with the aim of improving the relative recovery and hence calculating the probe efficiency associated with each of the different drugs.

For example, ethambutol was dialysed with a new CMA 20 probe (4mm membrane length, molecular weight cut-off of 20kDa) using T1 perfusion fluid at flow rates of 1 and 2µl/minute. As shown in Figure 3.4 the majority of the optimisation was completed with rifampicin; in total four different probes were evaluated, each had either a 4mm or 10mm membrane length with two different molecular weight cut-offs (20kDa or 100kDa), probes that had been re-used following previous exposure to the drug (rifampicin) after storage in demineralised water were also evaluated. Three different perfusion fluids and four different flow rates were tested.

The following parameters were evaluated and optimised to improve recoveries for the three drugs:

- Ethambutol; 4mm 20kDa probe, T1 perfusion fluid, 1 and 2µl/minute flow rates.
- Rifampicin; 4mm & 10mm, 20kDa & 100kDa probes (including previous exposure to rifampicin), T1, CNS and Ringers Solution (+BSA) perfusion fluids, 1, 2, 5 &10µl/minute flow rates. A rifampicin system flush was also evaluated.
- Isoniazid; 10mm 20kDa & 100kDa probes, T1 perfusion fluid, 2µl/minute flow rate.

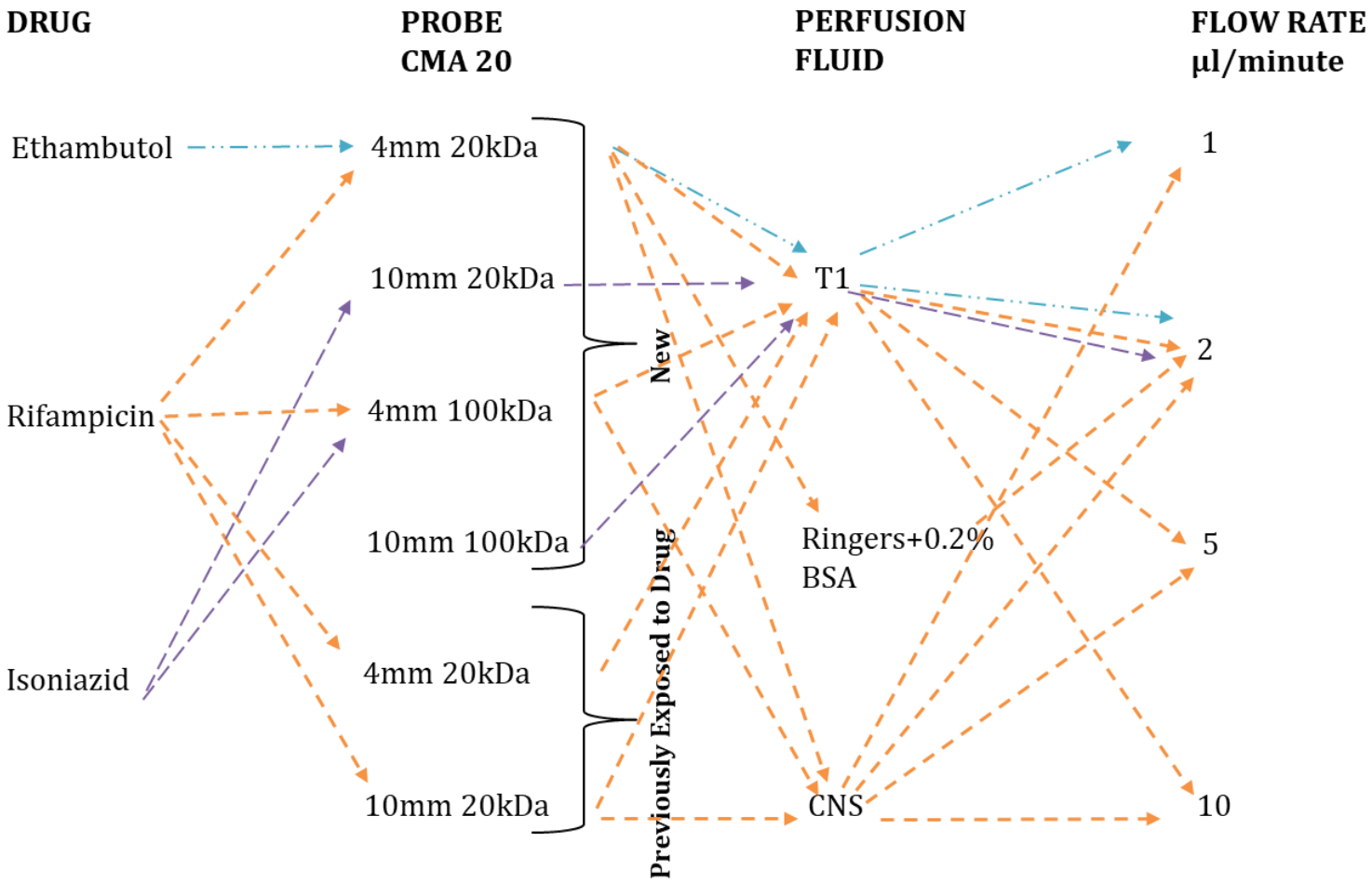

FIGURE 3.4: FLOW DIAGRAM SHOWING WHICH PROBES, PERFUSION FLUIDS AND FLOW RATES WERE TESTED WITH EACH DRUG. Orange arrows= rifampicin, purple arrows= isoniazid, blue arrows= ethambutol. BSA; bovine serum albumin, CNS; central nervous system. New; used directly, Previous exposure; re-used probe following primary exposure to drug.

3.4 SENSITIVITY OF ANALYTICAL EQUIPMENT

As shown in Figure 3.1, the first step in designing a microdialysis experiment is selection of analytical equipment. To quantify drug concentrations in dialysate fractions LC-MS/MS (Liquid Chromatography-Mass Spectrometry/Mass Spectrometry) was used. Sample analysis was conducted at Q3 Analytical (Porton Science Park). Each of the three drugs were analysed using a triple quadrupole mass spectrometer which was selected because of its high sensitivity and the potential to measure multiple compounds at the same time [222].

The LC-MS/MS system at Q3 Analytical consists of an HPLC (High Performance Liquid Chromatography) system comprised of an Agilent 1100 pump, column heater and degasser with a CTC HTS auto-sampler. The HPLC column used is specified for each drug. The mass spectrometer (MS) was an API 3000 with an ESI (Electro-spray Ionisation) source. Using ESI source, the MS was operated in the positive ionisation mode (Nebuliser Gas (NEB) 14PSI, Curtain Gas (CUR) 14PSI, Collisionally Activated Dissociation (CAD) 4PSI, Ion-spray Voltage (IS) 5500V, Temperature of ion source (TEM) 350°C) for all three drugs. The parent ion was observed in Q1(Quadrupole 1) and following collision-induced dissociation the product ion was observed in Q3 (Quadrupole 3).

Stock solutions of the drugs were made in dimethyl sulfoxide (DMSO) and further diluted to 10µg/ml in acetonitrile/0.1% formic acid to tune the MS. 10µl dextromethorphan (DXT) was added to stock solutions and samples as the internal standard. The multiple reaction monitoring (MRM) transition for DXT was 272.4/215.2 and DXT had an approximate retention time of 3.8 minutes. The chromatogram in Figure 3.5 shows the DXT peak.

Prior to beginning these *in vitro* studies, each drug was trialled in the LC-MS/MS system. Due to the resolution of the peak (shown in Figure 3.5) ethambutol was selected as the initial drug for optimisation studies. The HPLC column used for ethambutol analysis was an Ascentis Express C8 50 x 2.1MM. For ethambutol, the MRM transition was 205.3/116.4 and the approximate retention time was 3.2 minutes.

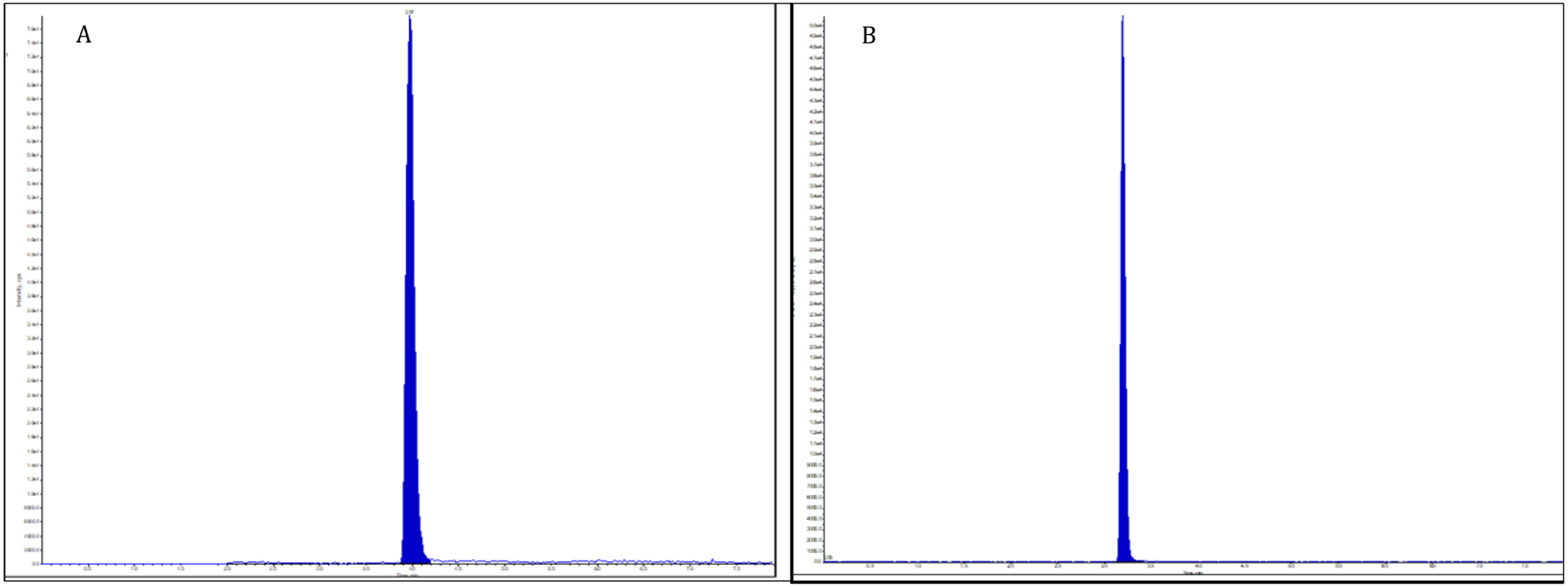

FIGURE 3.5: A; CHROMATOGRAM FOR THE INTERNAL STANDARD DXT. B; CHROMATOGRAM FOR ETHAMBUTOL. A; Peak at 3.8 minutes (x axis), peak intensity 7.64e4cps (y axis). B; peak at 3.2 minutes, peak intensity 5.04e4cps.

Compound	DP	FP	CE	CXP
Ethambutol	26	90	21	6
DXT	51	250	33	20

TABLE 3.1: MASS SPECTROMETRY PARAMETERS FOR ETHAMBUTOL AND DXT USED AT Q3 ANALYTICAL. DP; de-clustering potential (v), FP; focussing potential (v), CE; collision energy (electro-v), CXP; collision cell exit potential (v).

3.5.1 SELECTION OF ETHAMBUTOL CONCENTRATION FOR INITIAL MICRODIALYSIS STUDIES

The two ethambutol doses administered to the guinea pigs (100 and 250mg/kg) were used for initial *in vitro* microdialysis experiments. The microdialysis system was set up as shown in Figure 3.2. The probe used was a CMA 20 (4mm; 20kDa) with T1 perfusion fluid. A 2µl/min flow rate was chosen in the first instance, as recommended by Kloft and Simmel, in order to achieve adequate drug recovery as well as sufficient sample volume for analysis [170]. Samples were collected every 30 minutes for four hours, in duplicate.

Whilst conducting these experiments a sample was not collected at 30 minutes. This was potentially because of the lag time and dead space within the probe inlet and outlet tubing. The lag time for sample collection could be calculated as it was known that the dead volume of the inlet and outlet tubing was 1.8µl per 10cm. For these *in vitro* calibrations, the length of the inlet and outlet tubing was 20cm. Hence, the total dead volume was 7.2µl and using a flow rate of 2µl/minute meant there was a lag time of 3 minutes 36 seconds indicating that lag time and dead space within the system may not account for the lack of 30 minute sample collection. However, to negate any further issues associated with the lack of sample collection at 30 minutes, the syringe pump needed to continually flow for at least 30 minutes with the probe in a blank (no drug) solution prior to the collection of dialysate fractions for analysis. The fraction collector kept the samples at 4°C, for no longer than 4 hours, until they were stored at -80°C until analysis. Sample analysis was conducted as described above (Section 3.4) with the chromatographic conditions for ethambutol shown in Table 3.2. Concentrations of ethambutol above 10µg/ml cannot be quantified as this is above the upper limit of quantitation (2000ng/ml); therefore, the samples were diluted prior to analysis. Relative recovery and the co-efficient of variation were calculated as described in Section 3.1.2. The results from these initial experiments with ethambutol are shown in Table 3.3. Also shown in Table 3.3 is the concentration of ethambutol measured in each fraction and dose solution (mg/ml), the %

relative recovery and mean % relative recovery, the standard deviation (SD) and %Co-efficient of Variation (%CoV).

For these initial experiments the dose solutions used were chosen to reflect the oral dose of ethambutol that was administered to the guinea pigs *in vivo*. *In vitro* microdialysis conditions should be as close to *in vivo* as is practically possible and therefore the dose solutions should have been at the concentrations of ethambutol that were identified in the peripheral blood.

Gradient **Time (Min)**	0.1% Formic Acid (Aqueous) **%A**	0.1% Formic Acid (in Acetonitrile) **%B**
0	95	5
1	95	5
4	5	95
5	5	95
5.1	95	5
8	95	5
Flow Rate	250µl/minute	
Column Temperature	40°C	
Injection Volume	5µl	

TABLE 3.2: CHROMATOGRAPHIC CONDITIONS used for ethambutol analysis following microdialysis. Mass spectrometry parameters are shown in Table 3.1.

Dose	**Time (Min)**	**Conc (mg/ml)**	**% Relative Recovery**	**Mean % RR**	**SD**	**%CoV**
Conc of Dose Solution : 91mg/ml	60	16	17.6	35	11.93	34.4
	90	45.5	50.0			
	120	45.3	49.8			
	150	18.6	20.4			
	180	35.7	39.2			
	210	30.2	33.2			
	240	28	30.8			
Conc of Dose Solution: 56.5mg/ml	60	14	24.8	20	3.60	18.8
	90	12	21.2			
	120	10	17.7			
	150	11.4	20.2			
	180	7.81	13.8			
	210	12.5	22.1			
	240	13.9	24.6			

TABLE 3.3: ETHAMBUTOL RELATIVE RECOVERIES FOLLOWING IN VITRO MICRODIALYSIS. Two drug concentrations were compared (250mg/kg and 100mg/kg) over a period of 240 minutes using a flow rate of 2µl/minute. Conc (mg/ml); concentration of ethambutol measured in each fraction, SD; Standard Deviation, %CoV; Co-efficient of Variation.

3.5.2 REFINEMENT OF ETHAMBUTOL CONCENTRATION FOR INITIAL IN VITRO MICRODIALYSIS STUDIES

The median blood concentration of ethambutol as collected *in vivo* (Chapter 2) was 1.29µg/L (Cmax: 7214µg/L) following a 250mg/kg dose which indicated that a 1mg/ml solution of ethambutol was closer to the concentration of ethambutol expected in the organs. This lower concentration (1mg/ml) was therefore used for further *in vitro* experiments with ethambutol. An additional advantage to this lower starting concentration of ethambutol was that all fractions would contain less than 10µg/ml ethambutol which negates the need for the dilution series conducted prior to MS analysis, thereby reducing errors.

The equipment was set up as shown in Figure 3.2 and the probe used was a CMA 20 (4mm; 20kDa) with T1 perfusion fluid. Samples were collected using the same flow rate and collection period described in Section 3.5.1. Again, as in Section 3.5.1, no sample was collected at 30 minutes. Therefore, in order to collect a sample at 30 minutes for all future experiments, the syringe pump needed to continually flow for 60 minutes (as opposed to the 30 minutes mentioned in Section 3.5.1) with the probe in a blank (no drug) solution prior to collection of dialysate fractions for analysis. Relative recovery and the co-efficient of variation were calculated as described in Section 3.1.2. The results are shown in Table 3.4.

Replicate	Dose	Time (Min)	Conc (mg/ml)	%Relative Recovery	Mean %RR	SD	%CoV
1	Conc of Dose Solution: 1.24mg/ml	60	0.54	43.8	41.7	4.4	11.6
		90	0.54	43.1			
		120	0.54	43.4			
		150	0.47	37.7			
		180	0.48	38.4			
		210	0.57	46.2			
		240	0.40	32.4			
2	Conc of Dose Solution: 0.995mg/ml	60	1.58	159.1	59.3	52.0	89.4
		90	1.31	132.0			
		120	0.28	28.5			
		150	0.27	27.6			
		180	0.30	29.9			
		210	0.29	29.1			
		240	0.38	38.0			
3	Conc of Dose Solution : 1.17mg/ml	60	0.44	37.2	33.6	6.5	19.4
		90	0.41	35.2			
		120	0.48	41.3			
		150	0.46	39.4			
		180	0.41	35.1			
		210	0.37	31.3			
		240	0.33	28.5			

TABLE 3.4: ETHAMBUTOL RELATIVE RECOVERIES FOLLOWING IN VITRO MICRODIALYSIS. A dose solution of 1mg/ml ethambutol was used and dialysed with CMA20 probe (4mm, 20kDa). Samples were collected every 30 minutes for a period of 240 minutes in triplicate. Conc (mg/ml); concentration of ethambutol measured in each fraction, SD; Standard Deviation, %CoV; Co-efficient of Variation.

All the dose solutions were close to the expected 1mg/ml concentrations (0.995-1.24mg/ml) that were being aimed for. There was little effect of the different concentrations on %relative recovery demonstrating linear extraction efficiency over a concentration range. The % relative recoveries are sufficiently high as shown by the consistent collection of ethambutol in the individual fractions above the MS LLOQ of ethambutol (0.625µg/ml). The reproducibility of these experiments was generally good over the three replicates. These results indicated that the microdialysis parameters selected for use with ethambutol were fit for purpose.

The % relative recoveries for 2 samples were above 100% (Replicate 2; 159.1 & 132%) as the concentrations of these samples exceeded the concentration of the dose solution. This was indicative that there was residual ethambutol within the dialysis tubing or around the probe

membrane tip. This was confirmed by the fact that 101µg/ml of ethambutol was recovered within the 'flush' sample. The 'flush' sample is one that was collected after a brief flow of demineralised water at a 25µl/minute flow rate with the probe submerged in demineralised water. An additional reason for the above 100% relative recoveries (in Replicate 2) was that there was 'carry-over' of ethambutol between samples within the mass spectrometer, this was corroborated when a blank sample, in which only the internal standard DXT was present and no ethambutol, measured 0.0876µg/ml of ethambutol (data not shown).

3.5.3 FLOW RATE OPTIMISATION

Following optimisation of the concentration of the dose solution and adequate relative recoveries over the three replicates, the next parameter to be tested and optimised was flow rate. This was to understand if the probe was working more efficiently at a slower flow rate and whether sufficient sample volume was obtained for analysis (as described in Chapter 1). The experiment described in the previous section was repeated using a 1mg/ml dose solution and a 1µl/min flow rate. The other parameters remained the same; CMA 20 probe (4mm; 20kDa) and T1 perfusion fluid. The results are shown in Table 3.5.

Replicate	Dose	Time (Min)	Conc (mg/ml)	%Relative Recovery	Mean %RR	SD	%CoV
1	Conc of Dose Solution : 0.976mg/ml	30	0.55	56.8	53.8	9.7	19.2
		60	0.75	76.9			
		90	0.53	53.8			
		120	0.51	51.9			
		150	0.50	51.4			
		180	0.50	50.8			
		210	0.42	43.4			
		240	0.44	44.9			
2	Conc of Dose Solution: 0.913mg/ml	30	1.27	139.1	105.3	29.2	29.6
		60	1.21	132.5			
		90	1.15	126.0			
		120	1.02	111.7			
		150	0.98	107.0			
		180	0.87	95.6			
		210	0.82	89.3			
		240	0.38	41.2			
3	Conc of Dose Solution: 0.816mg/ml	30	0.67	81.5	65.6	11.0	17.9
		60	0.64	78.8			
		90	0.63	76.6			
		120	0.53	64.7			
		150	0.49	60.0			
		180	0.48	58.2			
		210	0.43	53.1			
		240	0.43	52.1			

TABLE 3.5: ETHAMBUTOL RELATIVE RECOVERIES FOLLOWING IN VITRO MICRODIALYSIS USING A 1µL/MIN FLOW RATE. A 1mg/ml dose solution with CMA20 (20kDa) probe and T1 perfusion fluid were used. Conc (mg/ml); concentration of ethambutol measured in each fraction, SD; Standard Deviation, %CoV; Co-efficient of Variation.

The dose solutions have similar concentrations for all three experimental replicates and, in these experiments a 30 minute sample was collected. Consistent with the data obtained for the

2µl/min flow rate (shown in Table 3.4) five of the %relative recoveries were over 100% adding strength to the observation that carry-over of ethambutol in the MS was occurring.

As the flow rate decreased (from 2µl/min to 1µl/min) the sample volume also decreased but there was still sufficient sample available for analysis. As expected when the flow rate was decreased to 1µl/min the %relative recovery increased, from 41%, 59% and 33% (mean relative recoveries at 2µl/min (Table 3.4)) compared with 53%, 105% and 65% (mean relative recoveries at 1µl/min). These data confirm what was stated in the literature in relation to slower flow rates leading to higher probe efficiencies[145]. However, over the 4 hour time period the concentration of ethambutol recovered using the 1µl/min flow rate decreased within all three experimental replicates. This trend is not shown with the 2µl/min flow rate experiments and therefore a 2µl/min flow rate was used for all future *in vitro* and *in vivo* microdialysis experiments.

3.5.4 OVERVIEW OF ETHAMBUTOL IN VITRO MICRODIALYSIS

In summary (as shown in Table 3.6), microdialysis with ethambutol was successful in recovering drug. There are no reports of suitable parameters for ethambutol (or any other TB drug) microdialysis and therefore these data are informative for future studies of ethambutol or any physiochemically similar drugs.

Concentration of Dose Solution	Probe	Perfusion Fluid	Flow Rate (µl/minute)	Recovery	Comments
91mg/ml (=250mg/kg)	CMA 20 4mm 20kDa	T1	2	Yes	Dose Solutions too high
56.5mg/ml (=100mg/kg)			2		
1mg/ml			2&1		System performing as expected.

TABLE 3.6: SUMMARY TABLE SHOWING WHICH PARAMETERS WERE TESTED WITH ETHAMBUTOL TO CALCULATE RELATIVE RECOVERIES.

The main parameters tested with ethambutol were optimisation of the dose solution and flow rate. It was shown that ethambutol was recovered across a range of concentrations and the reproducibility of the %relative recoveries were good and not influenced by concentration of

dose solution. As expected, the flow rate did have an impact with slower flow rates leading to increased recovery. However, the concentration of ethambutol recovered decreased over the four hour time course when using the 1µl/minute flow rate as there was less ethambutol in the dose solution to collect as time increased (i.e. the increased recovery meant more drug was removed from the dose solution earlier in the time course, so there was less available to collect later in the time course). These experiments also defined the initial experimental parameters to be used for *in vitro* microdialysis of isoniazid and rifampicin. It was concluded that all further *in vitro* experiments would be conducted with 1mg/ml dose solutions at a 2µl/minute flow rate.

3.6 ISONIAZID IN VITRO MICRODIALYSIS

Isoniazid is one of the four front-line anti-TB drugs and is used mono-therapeutically for the treatment of those infected with latent TB infection as discussed in Chapter 1. Isoniazid shares many physiochemical properties with ethambutol (Chapter 1) and hence the %relative recoveries with isoniazid should be similar to those achieved with ethambutol. The importance of isoniazid in the treatment of TB and the anticipated high recoveries (based on physiochemical properties) indicated that isoniazid could be an important drug to dialyse *in vivo* and PK data generated from blood sampling, as described in Chapter 2, would provide a comparator for PK data generated in organs, therefore isoniazid was characterised within the microdialysis system.

3.6.1 INITIAL IN VITRO EXPERIMENTS WITH ISONIAZID

Isoniazid *in vitro* microdialysis experiments were conducted using a 2µl/min flow rate using a dose solution of 1mg/ml of isoniazid as shown in Figure 3.2. These experiments were conducted using the left-hand side (LHS) and right-hand side (RHS) of the syringe pump and tested two probe types: Mw cut-off 20kDa, 10mm length and 100kDa, 4mm length. Replicates 1 and 2 for the same probe type used the LHS and RHS of the syringe pump. The perfusion fluid used was T1 perfusion fluid. Prior to beginning *in vitro* microdialysis with isoniazid the probes were placed in demineralised water for one hour using a 10µl/min flow rate which enabled samples to be reproducibly collected at 30 minutes. This was a refinement based on the results of the ethambutol *in vitro* experiments.

The samples were analysed as described in Section 3.4, and the column used for isoniazid analysis was a Kinetex C18 150x2.1mm, 5µm column. The MRM transition was 137.9/120.9 for isoniazid and the approximate retention time was 3.1 minutes. The chromatographic conditions used are shown in Table 3.7 and the chromatogram shown in Figure 3.6. Isoniazid mass spectrometry parameters are shown in Table 3.8. The LLOQ for isoniazid was 1ng/ml. The calibration curve was constructed as described in Section 3.7.1. DXT mass spectrometry

parameters are found in Section 3.4. The relative recoveries of isoniazid were calculated as described in Section 3.1.2. The results are shown in Table 3.9.

Gradient **Time (Min)**	0.1% Formic Acid (Aqueous) **%A**	0.1% Formic Acid (in Acetonitrile) **%B**
0	95	5
5	95	5
10	5	95
15	5	95
15.1	95	5
20	95	5
Flow Rate	400µl/minute	
Column Temperature	40˚C	
Injection Volume	5µl	

TABLE 3.7: CHROMATOGRAPHIC CONDITIONS FOR ISONIAZID.

Compound	DP	FP	CE	CXP
Isoniazid	31	270	19	2

TABLE 3.8: MASS SPECTROMETRY PARAMETERS USED WITH ISONIAZID.

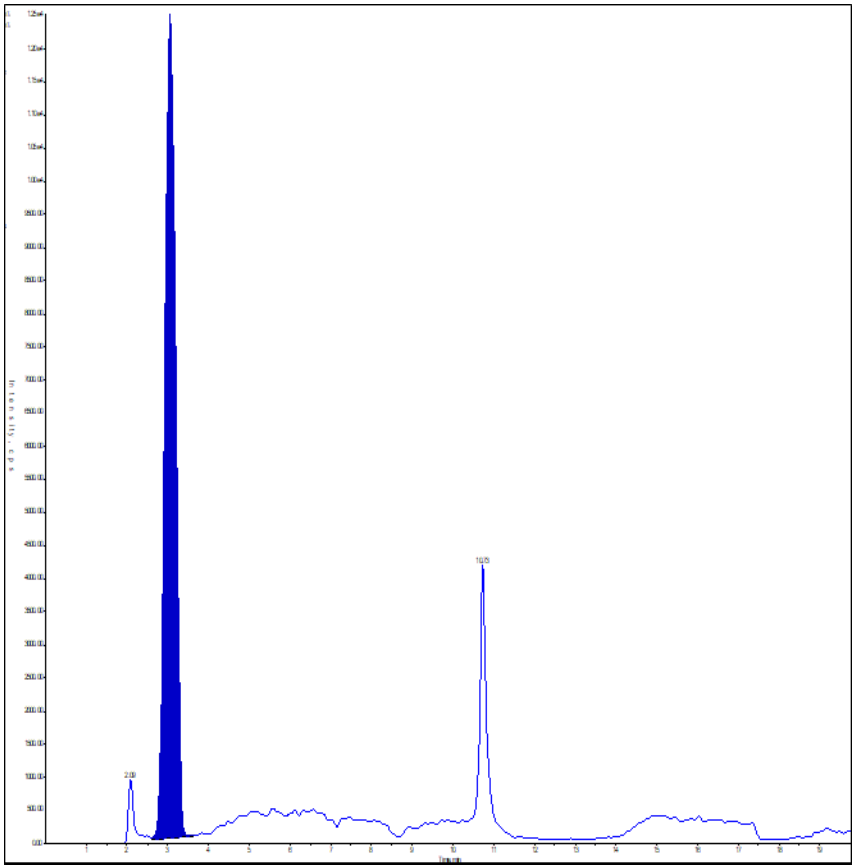

FIGURE 3.6: ISONIAZID CHROMATOGRAM FOLLOWING A 2000NG/ML ISONIAZID INJECTION. The peak is at 3.1 minutes (x axis) and the intensity of the peak is 1.25e4 (y axis). Additional peaks represent background interference.

20kDa Cut Off (10mm)								100kDa Cut Off (4mm)							
Replicate	**Dose**	**Time (Min)**	**Conc (mg/ml)**	**%Relative Recovery**	**Mean %RR**	**SD**	**%CoV**	**Replicate**	**Dose**	**Time (Min)**	**Conc (mg/ml)**	**%Relative Recovery**	**Mean %RR**	**SD**	**%CoV**
1 LHS	Conc of Dose Solution: 0.949mg/ml	30	0.339	35.7	40.9	10.1	24.7	1 LHS	Conc of Dose Solution: 1.070mg/ml	30	0.146	13.7	45.8	26.2	57.3
		60	0.553	58.3						60	0.795	74.3			
		90	0.504	53.1						90	0.98	91.5			
		120	0.447	47.1						120	0.664	62.1			
		150	0.371	39.1						150	0.505	47.2			
		180	0.329	34.7						180	0.358	33.5			
		210	0.296	31.2						210	0.263	24.6			
		240	0.267	28.1						240	0.206	19.3			
2 RHS	Conc of Dose Solution: 0.992mg/ml	30	0.582	58.7	44.3	11.2	25.3	2 RHS	Conc of Dose Solution: 1.804mg/ml	30	0.272	25.1	21.3	9.8	46.1
		60	0.566	57.1						60	0.457	42.2			
		90	0.494	49.8						90	0.308	28.5			
		120	0.521	52.5						120	0.228	21			
		150	0.422	42.6						150	0.183	16.9			
		180	0.339	34.2						180	0.151	13.9			
		210	0.289	29.2						210	0.134	12.4			
		240	0.3	30.2						240	0.114	10.5			
3 LHS	Conc of Dose Solution: 1.002mg/ml	30	0.645	64.4	64.4	5.8	9.1	3 LHS	Conc of Dose Solution: 1.128mg/ml	30	0.259	23	22.7	5.8	25.4
		60	0.738	73.7						60	0.37	32.8			
		90	0.664	66.3						90	0.327	29			
		120	0.7	69.8						120	0.296	26.3			
		150	0.661	65.9						150	0.228	20.2			
		180	0.561	55.9						180	0.192	17			
		210	0.642	64.1						210	0.177	15.7			
		240	0.556	55.5						240	0.201	17.8			

TABLE 3.9: ISONIAZID RELATIVE RECOVERIES FOLLOWING IN VITRO MICRODIALYSIS. Two different probes (Mw cut off 20kDa with 10mm membrane length and Mw cut off 100kDa with 4mm membrane length) and the left-hand side and right-hand side of the syringe pump were used. Conc (mg/ml); concentration of isoniazid measured in each fraction, SD; Standard Deviation, %CoV; Co-efficient of Variation.

The relative recoveries, as anticipated, due to the similar physiochemical properties were similar to those achieved with ethambutol (Table 3.4). The Mw cut-offs of the probes seem to have an effect on %CoV (24.7, 25.3 and 9.1% for 20kDa cut-off probe vs 57.3, 46.1, 25.4% for 100kDa cut-off probe) yet little effect on %relative recovery; as the lower Mw cut-off probe recovered more isoniazid in replicates 2 and 3, but less in replicate 1 (Table 3.9). As expected, use of the 10mm (longer) membrane resulted in increased recovery with a mean % relative recovery of 49% and a mean % relative recovery of 30% associated with the 4mm membrane.

Use of the LHS or RHS of the syringe pump had no effect on %relative recoveries which means that both sides can be used simultaneously enabling dialysis of two guinea pigs at the same time when dialysing *in vivo*.

The use of the higher Mw cut-off probe (100kDa) seemed to have little effect on relative recovery of isoniazid in these *in vitro* microdialysis experiments. There are no proteins in these *in vitro* samples, however if used *in vivo* this larger Mw cut-off would allow serum proteins (Mw of albumin in guinea pigs= ~64.9kDa[223]) to enter the dialysate. The isoniazid collected in the dialysate therefore could still be bound to proteins. As discussed in Chapter 1, a key advantage of the microdialysis methodology is the ability to collect only the pharmacologically unbound portion of the drug. Use of the 100kDa probe with isoniazid does not exclude the proteins and therefore may collect both unbound and bound drug. The lower Mw cut-off probes were sufficient to recover unbound isoniazid (Mw 137.14Da) and rifampicin (Mw 822.94Da). Therefore the 20kDa probes were used for all future microdialysis experiments as the lower Mw cut-off excluded all proteins from the dialysate thereby ensuring only the unbound portion of the drug was collected. An additional advantage to protein exclusion was that no additional sample processing was required prior to analysis.

The increased relative recovery associated with the longer membrane length was due to the larger surface area. The 10mm membrane should therefore recover more drug than the 4mm membrane when the probe was placed in the organ of interest *in vivo*.

The surface area of the probe membrane tip, even at the longer length, still fitted within the proposed organs for dialysis. It was preferable to use the longer membranes for all further *in vitro* and *in vivo* experiments due to the larger surface area for diffusion to occur (Chapter 1).

The co-efficient of variations for the lower Mw cut-off/ longer membrane probe were approximately 20% (Table 3.9), indicating that these results were reproducible and that no additional optimisation to improve isoniazid recoveries using a 1mg/ml isoniazid dose solution was required.

3.6.2 CONCLUSIONS OF IN VITRO MICRODIALYSIS WITH ISONIAZID

The main parameters tested for isoniazid were the probe membrane length and Mw cut-off. An additional parameter tested was use of the LHS and RHS of the syringe pump. The probes tested had a 10mm membrane, the first time this longer membrane had been tested within these studies. Relative recoveries associated with this longer membrane were higher than those associated with 4mm membrane. An additional parameter tested was molecular-weight cut-off of the probe membrane. The Mw cut-off appears to have no discernible differences in relation to isoniazid recovery.

Concentration of Dose Solution	Probe	Perfusion Fluid	Flow Rate (µl/minute)	Recovery	Comments
1mg/ml	CMA 20 10mm 20kDa	T1	2	Yes	Longer membrane has higher recovery.
	CMA 20 4mm 100kDa				Mw cut-off, no obvious effect on recovery.

TABLE 3.10: SUMMARY OF PARAMETERS TESTED FOR INITIAL IN VITRO MICRODIALYSIS WITH ISONIAZID.

Additional studies were performed using physiologically relevant dose solutions which showed that isoniazid could be recovered at these lower concentrations, with and without the presence of an organ. These studies have not been described here but can be found in the Appendix (A1). Therefore, the *in vitro* microdialysis parameters were optimised for use with isoniazid for preparation to move to *in vivo* experiments.

3.7 RIFAMPICIN IN VITRO MICRODIALYSIS

In previous *in vivo* studies (PreDiCT TB project) guinea pigs were orally administered rifampicin either mono-therapeutically or in combination with other drugs. An associated adverse effect of rifampicin administration, in some guinea pigs, was antibiotic related enteritis which resulted in animals being culled for welfare reasons. Further to this, studies described in Chapter 2 showed that a dose of 50mg/kg, which was largely well-tolerated was not sufficient to achieve human-equivalent exposures in the blood. This raised the issue that to obtain human- like exposures, as related to blood, the guinea pigs would need a higher dose of rifampicin which could not be tolerated. The question that remained is whether concentrations of rifampicin in the blood reflect those in the tissues and whether drug doses could be optimised more efficiently by measuring this drug in organs rather than blood. Therefore, to better understand rifampicin pharmacokinetics and answer this key question, rifampicin was used and optimised in the *in vitro* microdialysis system to enable this drug to be dialysed in the guinea pig *in vivo*.

Parameters for rifampicin microdialysis were evaluated using the systems described in Section 3.3 and equipment was set up as shown in Figure 3.2.

3.7.1 CHROMATOGRAPHIC CONDITIONS & MASS SPECTROMETRY PARAMETERS FOR RIFAMPICIN

The LC-MS/MS system used was the same as described in Section 3.4. The column used for rifampicin analysis was a Kinetex C8 50x2.1mm, 5µm column. The MRM transition was 823.6/95.3 for rifampicin and the approximate retention time was 4.3 minutes. The chromatographic conditions are shown in Table 3.11 and chromatogram shown in Figure 3.7. The mass spectrometry parameters for rifampicin are in Table 3.12. DXT mass spectrometry parameters are found in Section 3.4.

To prepare the standard curve a stock standard solution of 1mg/ml RIF was made in DMSO. Stock standard solutions were further diluted in DMSO to make final concentrations of 400, 40,

20, 10, 5, 2, 1, 0.5, 0.2, 0.1 and 0.02µg/ml. These dilutions were further diluted with T1 Perfusion Fluid (190µl T1 Perfusion Fluid to 10µl standard) to final concentrations of 2000, 1000, 500, 250, 100, 50, 25, 10, 5 and 1ng/ml. 10µl DXT was added to all samples as the internal standard. The calibration curves were made in 300µl microdialysis tubes following determination of rifampicin loss across passaging experiment (Section 3.8).

The HPLC-MS/MS methodology was validated by adherence to the following acceptance criteria; the signal in the blank sample was <20% of the signal of the lowest calibration standard, the internal standard area in calibration standards did not differ from the area in unknown samples by more than 15%, definition of the upper limit of quantitation ((ULOQ) which was the calibration standard that met the acceptance criteria immediately above the highest concentration sample if the standards gave a linear response) and lower limit of quantitation ((LLOQ) which was the lowest calibration standard which meets the acceptance criteria if the signal is 2 to 3 fold of the signal to noise ratio).

Gradient **Time (Min)**	0.1% Formic Acid (Aqueous) **%A**	0.1% Formic Acid (in Acetonitrile) **%B**
0	95	5
1	95	5
4	5	95
5	5	95
5.1	95	5
8	95	5
Flow Rate	250µl/minute	
Column Temperature	40˚C	
Injection Volume	5µl	

TABLE 3.11: CHROMATOGRAPHIC CONDITIONS FOR RIFAMPICIN.

Compound	DP	FP	CE	CXP
Rifampicin	11	180	105	8

TABLE 3.12: MASS SPECTROMTERY PARAMETERS USED WITH RIFAMPICIN.

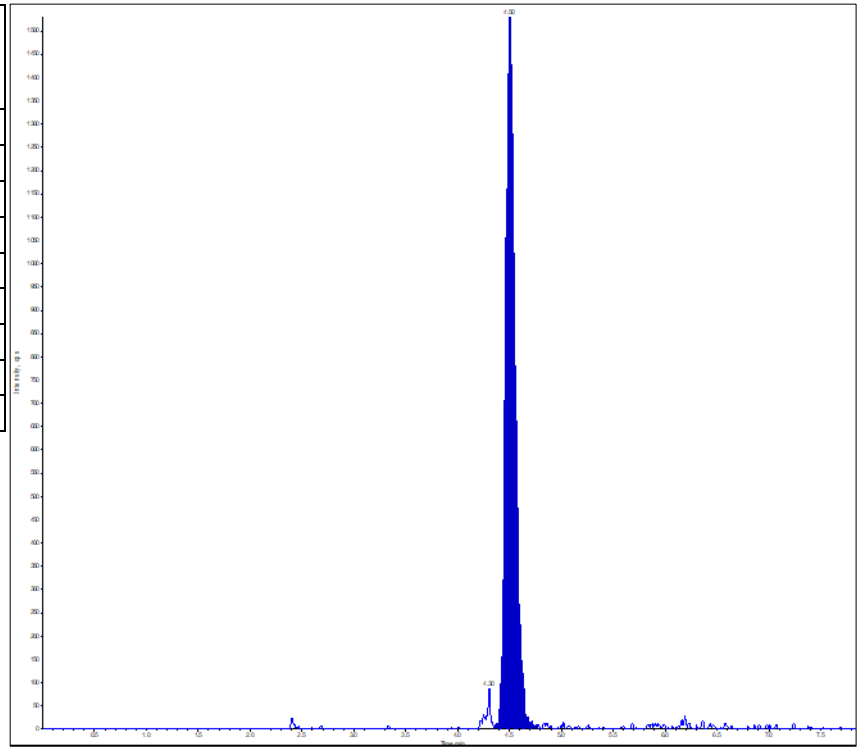

FIGURE 3.7: RIFAMPICIN CHROMATOGRAM FOLLOWING A 2000NG/ML RIFAMPICIN INJECTION. The peak is at 4.3 minutes (x axis) and the intensity of the peak is 1500 cps (y axis).

3.7.2 INITIAL IN VITRO EXPERIMENTS WITH RIFAMPCIN

Initial rifampicin *in vitro* experiments were conducted using the parameters that were optimised for ethambutol as described in Section 3.5.4. Briefly, the probe used was a CMA 20 (4mm; 20kDa) submerged in a 1mg/ml dose solution of rifampicin. T1 perfusion fluid flowed at a 2µl/min flow rate and the results are shown in Table 3.13.

Replicate	Dose	Time (Min)	Conc (mg/ml)	%Relative Recovery	Mean %RR	SD	%CoV
1	Conc of Dose Solution: 0.087mg/ml	30	No Sample		1.37	0.82	60
		60	<0	-			
		90	<0	-			
		120	<0	-			
		150	<0	0.4			
		180	0.002	1.9			
		210	0.001	1.0			
		240	0.003	2.2			
2	Conc of Dose Solution: 0.162mg/ml	30	No Sample		15.1	7.1	51.0
		60	<0	-			
		90	0.010	12.0			
		120	0.017	19.0			
		150	0.013	15.2			
		180	0.019	21.6			
		210	0.017	19.6			
		240	0.017	19.2			
3	Conc of Dose Solution: 0.125mg/ml	30	<0	-	10.1	6.1	63.8
		60	0.005	3.0			
		90	0.011	6.9			
		120	0.015	9.5			
		150	0.022	13.4			
		180	0.025	15.5			
		210	0.024	14.8			
		240	0.030	18.2			

TABLE 3.13: RIFAMPICIN RELATIVE RECOVERIES FOLLOWING IN VITRO MICRODIALYSIS IN TRIPLICATE. A 1mg/ml rifampicin dose solution was used with T1 perfusion fluid flowing at 2µl/min flow rate. Samples were collected every 30 minutes for a total of 240 minutes. Conc (mg/ml); concentration of rifampicin measured in each fraction, SD; Standard Deviation, %CoV; Co-efficient of Variation, <0 = below lower limit of quantitation.

Following LC/MS-MS analysis of the rifampicin-containing dialysate samples, there were three key results. The first of these was that the dose solutions were lower (mean dose solution = 0.124±0.03mg/ml) than the expected 1mg/ml (shown in Table 3.13) and only one 30 minute

sample was collected. Secondly, as time increased (between 0-240 minutes) the concentration of rifampicin recovered in the dialysate also increased. This was shown with all three experimental replicates. Thirdly there were 6 %relative recoveries which were below the lower limit of quantitation (5ng/ml), which was unexpected, but as these samples were collected at earlier time points it is indicative that there was not any rifampicin in the samples to measure due to the length of time taken for the rifampicin to move through the microdialysis tubing because of the physiochemical properties of the drug.

There were several possibilities for the measured concentrations of the dose solutions being lower than the concentration prepared; the (in)solubility of rifampicin in solution, a miscalculation whilst the dose solutions were prepared and a dilution of the dose solution with the constant perfusion of the perfusion fluid. This dilution of the dose solution potentially occurred because 60µl of T1 perfusion fluid passed through the probe into the dose solution every 30 minutes whilst a flow rate of 2µl/minute was used. However, this would not be unique to the rifampicin dose solutions and therefore given the concentrations of the dose solutions associated with isoniazid and ethambutol, this seems an unlikely explanation. Another possibility for the lower dose solution was that due to the lipophilic nature of rifampicin (LogP -3.85), it adhered to the Eppendorf which contained the dose solution.

The increased rifampicin concentration in the dialysate observed over time could also be due to adherence of rifampicin to the plastic of the Eppendorf and FEP tubing. The increased concentrations of rifampicin over time suggested that saturation of binding sites in the Eppendorf and the FEP tubing plastics with rifampicin had occurred leading to no further binding of rifampicin to the plastics. This subsequently allowed more rifampicin to flow through the tubing and be collected. This saturation of binding sites may not have occurred till after 60 minutes which is why no 30 minute sample was collected in replicates 1 and 2 and when a sample was collected at 30 minutes in replicate 3, the measured rifampicin was below the LLOQ. A visible crystallisation around the probe tip may have led to recoveries below the LLOQ and therefore highlighted the need to perform a flush with demineralised water prior to beginning dialysis in all future experiments.

It was evident from the co-efficient of variations that these experiments were variable and would need repeating before the true %relative recoveries could be calculated, but the mean %relative recoveries were close to the acceptable 20% recovery for replicates two and three (15.13% and 10.13% respectively). A probe efficiency greater than 20% is sufficient as this would recover rifampicin at concentrations above the LLOQ for MS analysis (5ng/ml).

3.7.3 REPEAT OF INITIAL EXPERIMENTS WITH RIFAMPICIN; IMPACT OF DOSE SOLUTION

In light of the results in Section 3.7.2, the experiment was repeated using a different method to prepare the dose solution. The same probe (CMA 20 (4mm; 20kDa)) and probe tubing used for the experiment described in Section 3.7.2 was used again for the repeat experiments. T1 perfusion fluid was used. To make the 1mg/ml solution, 10mg of rifampicin was added to 10ml of HPLC water to alleviate any errors associated with weighing out small amounts of drug. The absorbance of rifampicin for a 1mg/ml solution is 0.337nm and this was checked prior to commencing the experiments. The rifampicin solution was heated to 25°C to ensure solubilisation. The results of this repeat experiment are shown in Table 3.14.

Replicate	Dose	Time (Min)	Conc (mg/ml)	%Relative Recovery	Mean %RR	SD	%CoV
1	Conc of Dose Solution: 0.652mg/ml	30	No Sample		6.3	0.4	7
		60					
		90	0.047	7.2			
		120	0.041	6.2			
		150	0.040	6.1			
		180	0.040	6.1			
		210	0.042	6.4			
		240	0.039	6.0			
2	Conc of Dose Solution: 0.724mg/ml	30	0.0263	3.6	7.9	2.0	26.6
		60	0.082	11.3			
		90	0.061	8.5			
		120	0.058	7.9			
		150	0.056	7.7			
		180	0.057	7.8			
		210	0.057	7.8			
		240	0.060	8.2			
3	Conc of Dose Solution: 0.705mg/ml	30	No Sample		8.3	0.6	7.4
		60	0.064	9.1			
		90	0.064	9.0			
		120	0.058	8.3			
		150	0.056	7.9			
		180	0.056	7.9			
		210	0.059	8.4			
		240	0.053	7.4			

TABLE 3.14: RIFAMPICIN RELATIVE RECOVERIES FOLLOWING IN VITRO MICRODIALYSIS with a 1mg/ml dose solution. A 2µl/min flow rate was used. A different method of preparing dose solutions was used following low relative recoveries in initial experiment. Conc (mg/ml); concentration of rifampicin measured in each fraction, SD; Standard Deviation, %CoV; Co-efficient of Variation.

The relative recoveries were still lower than expected, when taking into account the relative recoveries obtained with ethambutol. The reproducibility of these experiments was increased compared to the initial rifampicin *in vitro* results (CoV: 60%, 51% and 63.82% for initial rifampicin experiments (Table 3.13)).

3.7.4 SUMMARY OF INITIAL RIFAMPICIN IN VITRO MICRODIALYSIS

These initial experiments showed that, when using the microdialysis parameters optimised for ethambutol, it was possible to recover rifampicin, although not consistently or at concentrations far enough above the LLOQ to be confident that this drug would be recovered *in vivo*. This indicates that parameters established for one drug are not necessarily optimal for use with another.

Concentration of Dose Solution	Probe	Perfusion Fluid	Flow Rate (µl/minute)	Recovery	Comments
1mg/ml	CMA 20 4mm 20 kDa	T1	2	Yes	Low recovery when compared to ethambutol
		Ringers + 0.2% BSA		No	Not repeated

TABLE 3.15: SUMMARY OF PARAMETERS TRIALLED FOR INITIAL IN VITRO MICRODIALYSIS WITH RIFAMPICIN.

With the aim of improving rifampicin relative recoveries, an additional perfusion fluid (Ringers+0.2% BSA) was tested, however, as all samples had concentrations of rifampicin below the limit of detection (Lower Limit of Quantitation (LLOQ): 5ng/ml) following MS analysis, this perfusion fluid was not used again.

As rifampicin was the focus for *in vivo* microdialysis, additional optimisation of microdialysis parameters needed to be conducted to improve rifampicin relative recoveries.

3.8 DETERMINING LOSS OF ANALYTE TO IMPROVE RIFAMPICIN RECOVERIES

To further understand why the recoveries of rifampicin had been so low (when compared to ethambutol and isoniazid) and with the intention of improving them, the first aim was to determine the loss of the analyte.

As shown in Figure 3.1, a key step in development of the microdialysis methodology is determination of the loss of drug within the microdialysis system. Whilst performing *in vitro* experiments with rifampicin, the relative recoveries were lower (mean recovery=9.54%) and more variable (mean %CoV=31.54%) than the relative recoveries generated with ethambutol (Table 3.4) and isoniazid (Table 3.9). A hypothesised reason for these lower relative recoveries is that rifampicin is a lipophilic drug and can adhere or non-specifically bind to the plastics within the microdialysis system. To better understand the properties of rifampicin and how rifampicin interacts with the microdialysis system, a series of experiments were conducted.

3.8.1 EVALUATION OF RIFAMPICIN ADHERANCE

To test the hypothesis that the lipophilicity of rifampicin was the cause of the lower relative recoveries, 1mg/ml rifampicin solutions were made in a plastic vessel (whereby rifampicin is expected to adhere to the plastic) and in a glass vessel (limited adherence of rifampicin). The plastic and glass vessels were left on the laboratory bench (not covered) for 8 hours at ambient temperature (approximately 20 °C). 25µl of 1mg/ml rifampicin solution was sampled from each vessel at 0, 0.25, 0.5, 1 ,2 ,4, 6 and 8 hours and analysed by LC-MS/MS as described in Sections 3.4 and 3.7.1. The results are shown in Figure 3.8 and represent a single experiment.

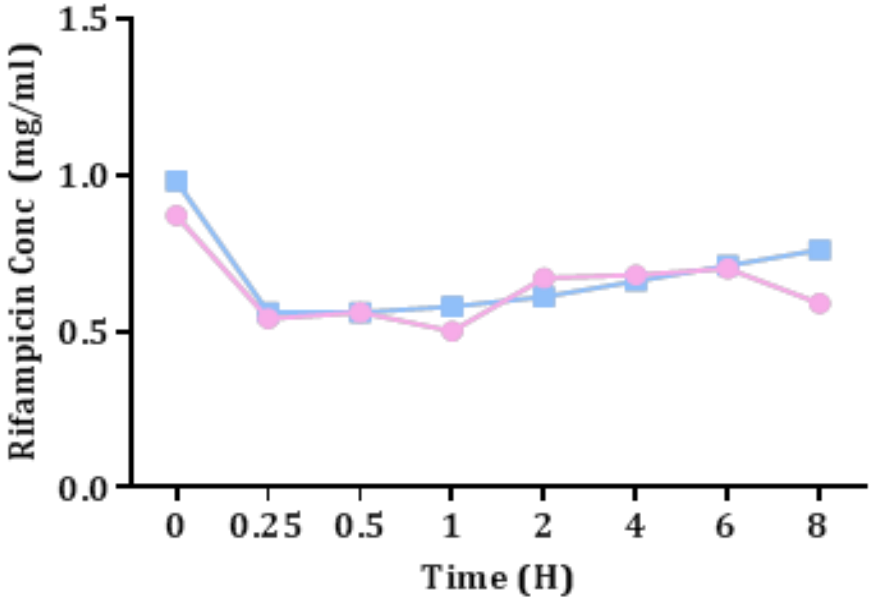

FIGURE 3.8: RIFAMPICIN CONCENTRATIONS MEASURED IN GLASS AND PLASTIC VESSLES. This experiment was conducted over an 8-hour period to identify if there was adherence of rifampicin to plastic. Pink circles are rifampicin concentrations measured using a glass vessel, blue squares are rifampicin concentrations measured using a plastic vessel. Each point represents a single sample.

In both the glass and plastic vessels, the measured rifampicin concentration at time zero was higher than at all other time points (Figure 3.8). This could be attributed to the incomplete dissolution of rifampicin. This explanation is corroborated by observations during the analysis process of a visible precipitate in some of the samples.

There was little difference (especially up to the four-hour time point; the length of a microdialysis experiment) between rifampicin concentrations measured in a glass or plastic vessel. An extension of this experiment was preparation of a 5µg/ml rifampicin solution by serial dilution or as a single dilution in both plastic and glass vessels. There were no discernible differences identified between the rifampicin concentrations recovered between the serial dilution and the direct dilution in either the plastic or glass vessels (data not shown).

To further investigate rifampicin non-specific binding, a passage experiment was conducted whereby a 10µg/ml rifampicin solution was made in T1 perfusion fluid and 200µl of this solution was passaged across 10 tubes sequentially (using a different polypropylene pipette tip each time). The 10 tubes used for the passage were either standard polypropylene Eppendorfs, glass vials or 300µl polypropylene microdialysis tubes. After passaging through 10th tube, 50µl rifampicin solution from each tube type was added to 50µl 1µg/ml DXT in DMSO in an HPLC glass vial and analysed via LC-MS/MS (as described in Sections 3.4 and 3.7.1). The amount of rifampicin recovered is related to the 10µg/ml RIF starting solution. These data were calculated by comparing peak area ratios (PAR; an example of which is seen in Figure 3.7) which can be done using HPLC. Three replicates of each passage through the different tube types were conducted and a mean (+standard deviation) PAR calculated. This average (mean) was then related to the starting concentration (10µg/ml) to calculate the percentage of rifampicin that had been recovered. Results are shown in Table 3.16.

	Mean PAR	SD	% of Starting Rifampicin Concentration
10µg/ml RIF in T1 Perfusion Fluid	1.607	0.098	**100**
10µg/ml RIF in Eppendorf (Polypropylene)	0.002	0.000	**0.125**
10µg/ml RIF in Glass Tube	0.030	0.004	**1.85**
10µg/ml RIF in 300µl Microdialysis Collection Tubes	0.470	0.042	**29.3**

TABLE 3.16: RIFAMPICIN MEASURED (% RECOVERED OF 10µG/ML SOLUTION) IN THREE DIFFERENT TUBE TYPES FOLLOWING SEQUENTIAL PASSAGE THROUGH TEN TUBES.

29.3% of the starting rifampicin concentration (10µg/ml) was recovered in the microdialysis tubes which was the highest observed recovery. This recovery was most likely associated with the smaller surface area of these 300µl tubes as there was less surface for rifampicin adherence.

All *in vitro* experiments with rifampicin, isoniazid and ethambutol were completed using plastic Eppendorfs for the dose solutions. The data indicated that there were no differences in adherence using glass or plastic (Figure 3.8), so plastic Eppendorfs were used for all remaining *in vitro* experiments. These data shown in Table 3.16 indicated that by using the 300µl microdialysis tubes to collect fractions the associated adherence of rifampicin to plastics was minimised. Hence, the 300µl collection tubes were used for all future *in vitro* optimisation experiments and *in vivo* microdialysis experiments with rifampicin.

3.8.2 FURTHER OPTIMISATION OF MICRODIALYSIS PARAMETERS TO IMPROVE RIFAMPICIN RECOVERIES

Having investigated loss of drug, a series of three experiments were completed (Experiments 1, 2 and 3). Each experiment was designed to test different parameters (probes, perfusion fluids, flow rates) in order to improve rifampicin recoveries.

For all three experiments, the dose solutions in which the probe(s) were submerged were 1mg/ml rifampicin. For each experiment, four flow rates were tested (1, 2, 5 and 10µl/minute). The tubing was cleared after each flow rate (throughout experiments 1-3) by flowing with demineralised water at a 25µl/min flow rate for 10 minutes. Samples were collected for

LC/MS-MS analysis (as in Section 3.4 and 3.7.1) every 30 minutes for 2 hours. Relative recoveries were calculated as described in Section 3.1.2.

Experiment 1 used two previously exposed CMA20 cut-off 20kDa, 4mm probes, cleared with demineralised water at a 25µl/min flow rate for 10 minutes. T1 perfusion fluid was used for the 10 and 5µl/min flow rates. CNS perfusion fluid was used for the 2 and 1µl/min flow rates. The results from this experiment are shown in Table 3.17.

Experiment 2 used two new CMA20 probes with different Mw cut-offs (20kDa or 100kDa), but the same membrane length (4mm). CNS perfusion fluid was used for all flow rates. Results are shown in Table 3.18.

Experiment 3 used one previously exposed CMA20 (20kDa, 4mm) probe, flushed with 1mg/ml rifampicin solution at a 10µl/min flow for at least 10 minutes. This experiment was devised following a publication in which rifampicin concentrations were measured in the human brain using microdialysis. To alleviate the issue of non-specific binding, a flush of the tubing with rifampicin was conducted by Mindermann *et al* (1998)[224]. T1 perfusion fluid was used for all flow rates. Flushes with rifampicin were conducted prior to beginning each new flow rate (1mg/ml solution of rifampicin flushed through probe and tubing at a 10µl/min for 10 minutes). Results are shown in Table 3.19. No rifampicin was detected in the dialysate at the 1µl/minute flow rate (all samples below LLOQ (5ng/ml)).

Experiment 1							
PF	**Flow Rate**	**Time (min)**	**Conc (mg/ml)**	**%Relative Recovery**	**Mean %RR**	**SD**	**%CoV**
T1	10µl/min	**0**	0.28				
			0.43				
		30	0.01	3.17	3.8	0.6	17.0
		60	0.01	3.43			
		90	0.01	4.06			
		120	0.01	4.61			
		30	0.01	3.26	2.9	0.5	19.8
		60	0.01	2.40			
		90	0.02	3.60			
		120	0.01	2.50			
	5µl/min	**0**	0.52				
			0.53				
		30	0.02	3.11	5.1	1.2	26.4
		60	0.03	5.95			
		90	0.03	5.90			
		120	0.03	5.35			
		30	0.05	9.27	6.8	1.4	24.3
		60	0.03	6.50			
		90	0.03	5.75			
		120	0.03	5.81			
CNS	2µl/min	**0**	0.36				
			0.47				
		30	0.06	17.66	17.3	2.9	19.5
		60	0.05	12.68			
		90	0.07	18.34			
		120	0.07	20.72			
		30	0.04	8.89	15.3	5.5	41.1
		60	0.05	11.15			
		90	0.09	19.18			
		120	0.10	22.05			
	1µl/min	**0**	0.26				
			0.31				
		60	0.08	29.99	50.6	17.9	36.3
		90	0.14	56.54			
		120	0.17	65.21			
		30	0.07	22.00	34.0	7.3	24.8
		60	0.11	34.23			
		90	0.13	40.77			
		120	0.12	38.83			

TABLE 3.17: RIFAMPICIN RELATIVE RECOVERIES CALCULATED FROM RIFAMPICIN CONCENTRATIONS COLLECTED DURING EXPERIMENT ONE. 2 previously exposed (to rifampicin) CMA 20 probes (4mm, 20 kDa) were tested at 4 different flow rates (1, 2, 5 and 10 µl/ minute) with two different perfusion fluids (T1 and CNS). PF; perfusion fluid, Conc (mg/ml); concentration of rifampicin measured in each fraction, SD; Standard Deviation, %CoV; Co-efficient of Variation.

Experiment 2							
PF	**Flow Rate**	**Time (min)**	**Conc (mg/ml)**	**%Relative Recovery**	**Mean %RR**	**SD**	**%CoV**
CNS	10µl/min	**0**	0.491				
			0.177				
		30	0.003	0.6	1.3	0.6	52.7
		60	0.004	0.8			
		90	0.010	1.9			
		120	0.009	1.9			
		30	0.002	0.3	3.7	0.6	52.3
		60	0.007	1.4			
		90	0.009	1.8			
		120	0.009	1.8			
	5µl/min	**0**	0.143				
			0.155				
		30	0.002	0.51	9.5	1.3	55.1
		60	0.016	3.18			
		90	0.019	3.78			
		120	0.017	3.55			
		30	0.013	2.65	8.8	0.2	7.4
		60	0.015	2.99			
		90	0.014	2.89			
		120	0.013	2.55			
	2µl/min	**0**	0.173				
			0.185				
		30	0.034	6.96	15.4	2.5	54.1
		60	0.005	1.05			
		90	0.032	6.52			
		120	0.035	7.20			
		30	0.057	11.63	37.0	1.9	16.1
		60	0.070	14.27			
		90	0.083	16.91			
		120	0.064	12.98			
	1µl/min	**0**	0.214				
			0.244				
		120	0.080	16.26	37.2		
		30	0.061	12.43	48.7	7.0	33.5
		60	0.139	28.32			
		90	0.125	25.57			
		120	0.150	30.53			

TABLE 3.18: RIFAMPICIN RELATIVE RECOVERIES CALCULATED FROM RIFAMPICIN CONCENTRATIONS COLLECTED DURING EXPERIMENT TWO. Two different Mw cut-off probes (20kDa or 100kDa; 4mm membrane). CNS perfusion fluid was used over four different flow rates. PF; perfusion fluid, Conc (mg/ml); concentration of rifampicin measured in each fraction, SD; Standard Deviation, %CoV; Co-efficient of Variation.

Experiment 3							
PF	**Flow Rate**	**Time (min)**	**Conc (mg/ml)**	**%Relative Recovery**	**Mean %RR**	**SD**	**%CoV**
Rif Flush	10µl/min	10m	0.1941				
		10m	0.2356				
T1		**0**	0.2866				
			0.2998				
		30	0.0062	2.18	0.9	0.8	97.7
		60	0.0016	0.56			
		90	0.0010	0.33			
		120	0.0014	0.48			
		30	0.0014	0.48	0.2	0.1	78.3
		60	0.0004	0.13			
		90	0.0005	0.16			
		120	0.0004	0.12			
Rif Flush		10m	0.1813				
		10m	0.1552				
T1	5µl/min	**0**	0.3371				
		30	0.3036	90.08	34.1	39.7	142.7
		60	0.0352	10.43			
		90	0.0061	1.81			
		120	ND				
T1	2µl/min	**0**	0.2479				
		30	0.3238	130.62	63.3	45.7	83.3
		60	0.1637	66.01			
		90	0.1344	54.20			
		120	0.0058	2.35			

TABLE 3.19: RIFAMPICIN RELATIVE RECOVERIES CALCULATED FROM RIFAMPICIN CONCENTRATIONS COLLECTED DURING EXPERIMENT THREE. One previously exposed CMA 20 probe (20kDa 4mm) was flushed with 1mg/ml rifampicin before use. T1 perfusion fluid was used over 4 different flow rates. ND: no drug detected. PF; perfusion fluid, Conc (mg/ml); concentration of rifampicin measured in each fraction, SD; Standard Deviation, %CoV; Co-efficient of Variation.

All three experiments showed that as the flow rate decreased from 10µl/min to 1µl/min, the relative recovery of rifampicin increased. This is a known characteristic of the microdialysis system. Another observation was that as the flow rate decreased the percentage co-efficient of variation increased highlighting that lower flow rates were associated with less reproducibility.

Reviewing the results in Table 3.17 in conjunction with Table 3.18, a comparison of perfusion fluids can be made. The T1 perfusion fluid and CNS perfusion fluid, although similar, do have different compositions (see Section 3.2). There seemed to be no pattern in relation to the relative recoveries and the perfusion fluid used. For the 10µl/ min flow rates, relative recoveries were higher with T1 (3.814% (T1) 1.313% (CNS)), yet for 5µl/min flow rate, the relative recoveries were higher with CNS perfusion fluid (5.0% (T1) 9.5% (CNS)). T1 perfusion fluid is designed specifically for microdialysis in peripheral tissues and demonstrated good recovery with ETH and INH, hence there was no rationale in selecting CNS over T1. T1 perfusion fluid was selected for use for all further *in vitro* and *in vivo* experiments.

Using the data in Table 3.13 in which a new 20kDa (4mm) probe was used with T1 perfusion fluid at a 2µl/min flow rate, the mean relative recoveries across the three experiments was 8.85%. The previously exposed probes (20kDa (4mm)) used with CNS perfusion fluid at a 2µl/min flow rate increased the relative recoveries to a mean of 16.37% (Table 3.17). The %relative recovery was higher with the probes that had been previously exposed to rifampicin and the results were less variable (mean %CoV with probes that had previous exposure to rifampicin: 35.1%; mean %CoV with new probes: 58.2%) , however this was an average (mean) of only two replicates as opposed to three.

The concept that higher recoveries were associated with probes that had previously been exposed to rifampicin were strengthened with use of the 10µl/min flow rate (Table 3.17) which showed a mean recovery over 2 hours of 3.35%. When comparing these results with those shown Table 3.18, in which a new probe was used and other parameters remained the same, the % relative recoveries were lower with the new probe (2.5%).

This increased % relative recovery associated with the probe which had been previously exposed to rifampicin was expected because of the lipophilic nature of rifampicin. It is likely that the prior use with rifampicin, would result in saturation of binding to the surfaces, hence when the probe was re-used there were no (or minimal) binding sites for the rifampicin to non-specifically bind (adhere) to, resulting in more drug being collected in the dialysate. For all further microdialysis experiments with rifampicin, probes were previously exposed to rifampicin. When performing *in vivo* microdialysis, the probe required flushing with rifampicin to ensure previous exposure[176], and due to the requirement of aseptic technique this flush was conducted *in situ.*

The effect on relative recovery in relation to the molecular weight cut-offs of the probes can be identified by comparing results in Table 3.17 (20kDa) and Table 3.18 (100kDa). The relative recovery for the 100kDa probe was 3.65% which was approximately 1% higher than the 2.94% for the 20kDa Mw probe. It is important to note here that the membrane length (4mm) and the length of the tubing (20mm) used was the same for both probes. As discussed in Section 3.6.1, use of the 100kDa probe would prove to be problematic when conducting microdialysis *in vivo*. In guinea pigs, rifampicin is 69.5% plasma protein bound, binding to α-1-acid glycoprotein (Mw: 23.2kDa), albumin (Mw: 64.9kDa) as well as serum proteins (Mw: ranges between 70 to 250kDa)[117]. Evidently, the 100kDa cut-off probe would allow many of these proteins into the dialysate, therefore, the 20kDa cut-off probe was used for the remainder of the studies reported in this thesis.

3.9 RIFAMPICIN IN VITRO MICRODIALYSIS WITH PHYSIOLOGICALLY RELEVANT DOSE SOLUTIONS

The previous experiments (Sections 3.7 and 3.8) used a 1mg/ml rifampicin solution in order to optimise the parameters to increase %relative recovery. It was important that *in vitro* microdialysis experiments were conducted closer to the concentration of drug that was expected in the guinea pigs' organs following oral drug administration. Using the data generated in Chapter 2, the Cmax (maximum concentration) measured in blood following a 50mg/kg oral dose of rifampicin was 6µg/ml. Therefore, a more physiologically relevant concentration of 10µg/ml was used as the dose solution for these experiments. A 100µg/ml dose solution was also used. These experiments were conducted to ascertain if the microdialysis system and the analytical equipment were sensitive enough to detect these lower concentrations of rifampicin collected in the dialysate.

Initially, a 100µg/ml rifampicin solution was dialysed with parameters optimised throughout this Chapter: CMA 20 probes (20kDa, 10mm tip) which had previously been exposed to rifampicin, T1 perfusion fluid and a flow rate of 2µl/min. The dose solution was heated to and maintained at 39.2°C (guinea pig body temperature) to replicate *in vivo* conditions. Samples were analysed as discussed in Section 3.7.1, and relative recoveries calculated as discussed in Section 3.1.2. The results are shown in Table 3.20.

Replicate	Dose	Time (Min)	Conc (µg/ml)	%Relative Recovery	Mean %RR	SD	%CoV
1	Conc of Dose Solution: 24.2µg/ml	30					
		60	4.57	18.9	15.9	2.0	14.0
		90	4.29	17.7			
		120	3.85	15.9			
		150	3.69	15.3			
		180	3.57	14.7			
		210	3.07	12.7			
		240					
2	Conc of Dose Solution: 30.04µg/ml	30	2.06	6.9	11.6	6.0	51.7
		60	6.83	22.7			
		90	4.57	15.2			
		120	1.97	6.5			
		150	4.35	14.5			
		180	1.93	6.4			
		210	4.23	14.1			
		240	1.97	6.5			

TABLE 3.20: RIFAMPICIN RELATIVE RECOVERIES FOLLOWING IN VITRO MICRODIALYSIS WITH A 100µG/ML DOSE SOLUTION. A previously exposed probe was used (20kDa 10mm) at 2µl/min flow rate with T1 perfusion fluid. Conc (µg/ml); concentration of rifampicin measured in each fraction, SD; Standard Deviation, %CoV; Co-efficient of Variation.

The %relative recoveries for the 100µg/ml dose solution were similar to %relative recoveries when a 1mg/ml solution of rifampicin was used (Table 3.17). The dose solutions were below the expected concentrations (30µg/ml and 24µg/ml) of 100µg/ml. An explanation for the lower than expected dose solution was described in Section 3.7.2 and with a 100µg/ml dose solution, 6µg of rifampicin was removed every 30 minutes (across 4 hour experiment) ultimately lowering the concentration by at least 48µg. As the relative recoveries for the individual fractions were related to the starting dose solution, the %relative recovery remained the same.

These experiments were repeated with the same parameters and a 10µg/ml dose solution was also dialysed. The results for both the 100 and 10µg/ml dose solutions are in Table 3.21. The concentrations of rifampicin in the dose solutions (132 & 82.8 µg/ml) were closer to the 100µg/ml dose solution that was aimed for. The dose solutions for 10µg/ml calibrations were similar between both experimental replicates. The mean relative recoveries were higher with

100μg/ml dose solution. One 30-minute sample had a rifampicin concentration much higher than the rest of the samples (Table 3.21; 10μg/ml Replicate 2; 19.9μg/ml). This high value could be due to rifampicin crystallisation on the probe or carry-over of rifampicin during MS analysis as 30-minute samples were analysed immediately after the dose solution. Recovering rifampicin from these low dose solutions via *in vitro* microdialysis gave confidence that the proposed rifampicin concentrations expected in the organs (based upon the concentration of rifampicin measured in blood) could be recovered during *in vivo* microdialysis. Therefore, no further optimisation for rifampicin microdialysis was conducted.

Replicate	Dose	Time (Min)	Conc (µg/ml)	%Relative Recovery	Mean %RR	SD	%CoV
1	Conc of Dose Solution (240 mins): 132µg/ml	30	No Sample		27.0	5.3	18.2
		60	37.3	28.1			
		90	47.5	35.8			
		120	42.7	32.2			
		150	36.0	27.2			
		180	25.7	19.4			
		210	30.3	22.9			
		240	30.6	23.1			
2	Conc of Dose Solution (240 mins): 82.8µg/ml	30	51.6	62.3	47.9	9.6	21.7
		60	46.2	55.8			
		90	43.2	52.2			
		120	24.7	29.8			
		150	36.0	43.5			
		180	37.4	45.2			
		210	38.1	46.1			
		240	No Sample				
1	Conc of Dose Solution: 19µg/ml	30	2.4	12.9	8.6	4.3	54.5
		60	2.9	15.4			
		90	1.7	8.7			
		120	0.6	3.0			
		150	1.5	8.1			
		180	1.8	9.6			
		210	0.5	2.6			
		240	No Sample				
2	Conc of Dose Solution: 21.7µg/ml	30	19.9	91.5	11.0	28.6	55.9
		60	4.7	21.6			
		90	3.7	17.0			
		120	0.9	4.2			
		150	2.3	10.8			
		180	1.7	7.8			
		210	1.5	6.8			
		240	1.9	8.8			

TABLE 3.21: RIFAMPICIN RELATIVE RECOVERIES FOLLOWING IN VITRO MICRODIALYSIS WITH PREVIOUSLY OPTIMISED PARAMETERS USING 100µG/ML AND 10µG/ML DOSE SOLUTIONS. A previously exposed probe was used (20kDa 10mm) at 2µl/min flow rate with T1 perfusion fluid. Conc (µg/ml); concentration of rifampicin measured in each fraction, SD; Standard Deviation, %CoV; Co-efficient of Variation

3.9.1 PROBE EFFICIENCIES

Table 3.22 shows all the calculated mean %relative recoveries gained for rifampicin *in vitro* microdialysis. These data were propagated to determine the efficiency (and associated error) of the probe. Subsequently, the *in vivo* microdialysis recoveries were corrected for using this calculated probe efficiency. Error was propagated using the method described in 'An Introduction to Error Analysis'[225]. Errors were propagated using standard error of the mean of relative recoveries. The equation used to calculate error was:

$$\sqrt{(a)^2 + (b)^2 + \ldots\ldots + (z)^2}$$

The error was then divided by mean %relative recovery to get the fractional uncertainty.

The results table column in Table 3.22 shows which results table (in Chapter 3) the %relative recovery data was obtained from. For 4 of the concentrations, the data is not shown in this Chapter. This is because a set of samples were analysed at the University of Liverpool. It was decided to include these data as the concentrations of the dose solutions and the associated %relative recoveries were very similar to those results shown in Table 3.21 hence these relative recoveries were included to strengthen the calculated probe efficiency.

Across all of the dose solutions (19µg/ml-724µg/ml; Table 3.22) the probe efficiency with rifampicin was calculated to be 15%±32%. This meant the associated error (CI) was ±32% which was very high. However, it was assumed (based on blood concentrations) that the expected *in vivo* organ concentration of rifampicin was going to be less than or close to 50µg/ml, and at these concentrations the probe efficiency was calculated to be 21%±9%. The probes used at these lower concentrations (19-30µg) were CMA20 (Mw cut-off 20kDa, 10mm membrane length) probes which were optimised for use *in vivo*. A probe efficiency greater than 20% is sufficient as this would enable rifampicin to be consistently recovered at concentrations above the LLOQ (5ng/ml) and hence it was concluded that no further optimisation would be required. Therefore, recovered rifampicin collected during *in vivo* microdialysis could be confidently corrected with this figure (21±9%).

Rif Conc (µg/ml)	%RR	Results Table	Probe Efficiency
19	8.6%	Table 3.21	21%±9%
21.7	11%	Table 3.21	
22	21%	Not Shown	
24.2	15%	Table 3.20	
30	25%	Not Shown	
30.04	11%	Table 3.20	
82	47%	Table 3.21	19%±10%
87	15%	Table 3.13	
132	27%	Table 3.21	
162	10%	Table 3.13	
173	15%	Table 3.18	
185	37%	Table 3.18	
249	16%	Not Shown	16%±15%
355	17%	Table 3,17	
466	15%	Table 3.17	
589	10%	Not Shown	8.12%±25%
652	6%	Table 3.14	
705	8%	Table 3.14	
724	8%	Table 3.14	

TABLE 3.22: ALL MEAN RELATIVE RECOVERIES ASSOCIATED WITH RIFAMPICIN PROPAGATED TO DETERMINE EFFICIENCY OF THE PROBE. An efficiency of 21±9% could be attributed to the probe as the concentration of rifampicin in the organs were expected to be less or approximately equal to 50µg/ml. Results table column shows where in this document the relative recoveries can be found. Data not shown is data that is not described in this document due to the samples being analysed at the University of Liverpool.

3.9.2 CONCLUSIONS FOLLOWING OPTIMISATION OF PARAMETERS TO IMPROVE RIFAMPICIN RECOVERIES

In this section the main aim was to improve rifampicin relative recoveries from those determined in Section 3.7. The main parameters tested were probes, perfusion fluid and flow rate. Initially, adherence and non- specific binding of rifampicin to plastics (an unavoidable component of the microdialysis system) were investigated. It was found that rifampicin concentrations were highest following passage through the 300µl microdialysis tubes, so these tubes were used throughout the remainder of this project. The other parameters tested are in Table 3.23.

Concentration of Dose Solution	Probe	Perfusion Fluid	Flow Rate (µl/minute)	Recovery	Comments
1mg/ml	CMA 20 4mm 20kDa Previously Exposed	CNS	1&2	Yes	Previously exposed probes had higher recovery than new probe.
		T1	5&10	Yes	
	CMA 20 4mm 20kDa New	CNS	1, 2, 5 &10	Yes	Low. Perfusion fluid had no effect on recovery.
	CMA 20 4mm 100kDa			Yes	Mw cut-off, no effect on recovery.
	CMA 20 4mm 20kDa	Rifampicin Flush; T1	1, 2, 5 &10	Variable	Useful in relation to exposing the probe to rifampicin.

TABLE 3.23: SUMMARY TABLE OF PARAMETERS TESTED TO IMPROVE RIFAMPICIN RECOVERIES.

The probes that had been previously exposed to rifampicin meant that higher concentrations of rifampicin were recovered, and the method for exposing sterile probes *in vivo* to rifampicin to ensure previous exposure was confirmed.

There were no discernible improvements in recoveries associated with CNS perfusion fluid, therefore T1 perfusion fluid was used for all future calibrations as it was optimised for use in peripheral tissues.

In vitro experiments were also conducted with more physiologically relevant concentrations (100 & 10µg/ml) of rifampicin with parameters optimised throughout this Chapter; Previously exposed probes (10mm, 20kDa), T1 perfusion fluid and 2µl/min flow rate were used. Rifampicin was recovered via microdialysis at these concentrations using these parameters, which enabled the probe efficiency associated with rifampicin to be calculated. The probe efficiency associated with rifampicin at the concentrations expected in the organs was 21±9% and this figure was used as a correction factor when microdialysis was conducted *in vivo*.

3.10 ORGAN EFFECTS ON %RELATIVE RECOVERY

All *in vitro* calibrations up to this point were conducted with dose solutions made of drug and water, however another factor that could affect relative recovery is the tissue in which the microdialysis will occur as shown in Figure 3.1. Hence, for the final *in vivo* microdialysis preparations, the equipment was set up as in Figure 3.2 and the probe was submerged in a drug and organ homogenate dose solution as opposed to a drug and HPLC water dose solution.

3.10.1 IN VITRO MICRODIALYSIS WITH ORGAN HOMOGENATES SPIKED WITH RIFAMPICIN

Three sets of guinea pig lungs, livers and skeletal muscles (organs of interest for probe insertion) were defrosted at room temperature and weighed on an analytical balance. To every 0.2g tissue, 1ml Ringers solution was added[192]. An Ystral homogeniser was used and post homogenisation the organ was spiked with 10µg/ml rifampicin. These spiked samples were vortexed for at least 2 minutes and maintained at 39.2°C in a water bath whilst the CMA20 microdialysis probe (20kDa; 10mm) which had been previously exposed to rifampicin were submerged into the homogenate. T1 perfusion fluid was used with a 2µl/minute flow rate and dialysate fractions were collected every 30 minutes for 4 hours. Samples were analysed as discussed in Section 3.7.1. Rifampicin was measured in all dialysate samples which gave reassurance that these low drug concentrations were able to be collected and analysed via LC-MS/MS in the presence of tissue homogenate.

The results are shown in Figure 3.9 and each point on the graph represents an average of three different replicates.

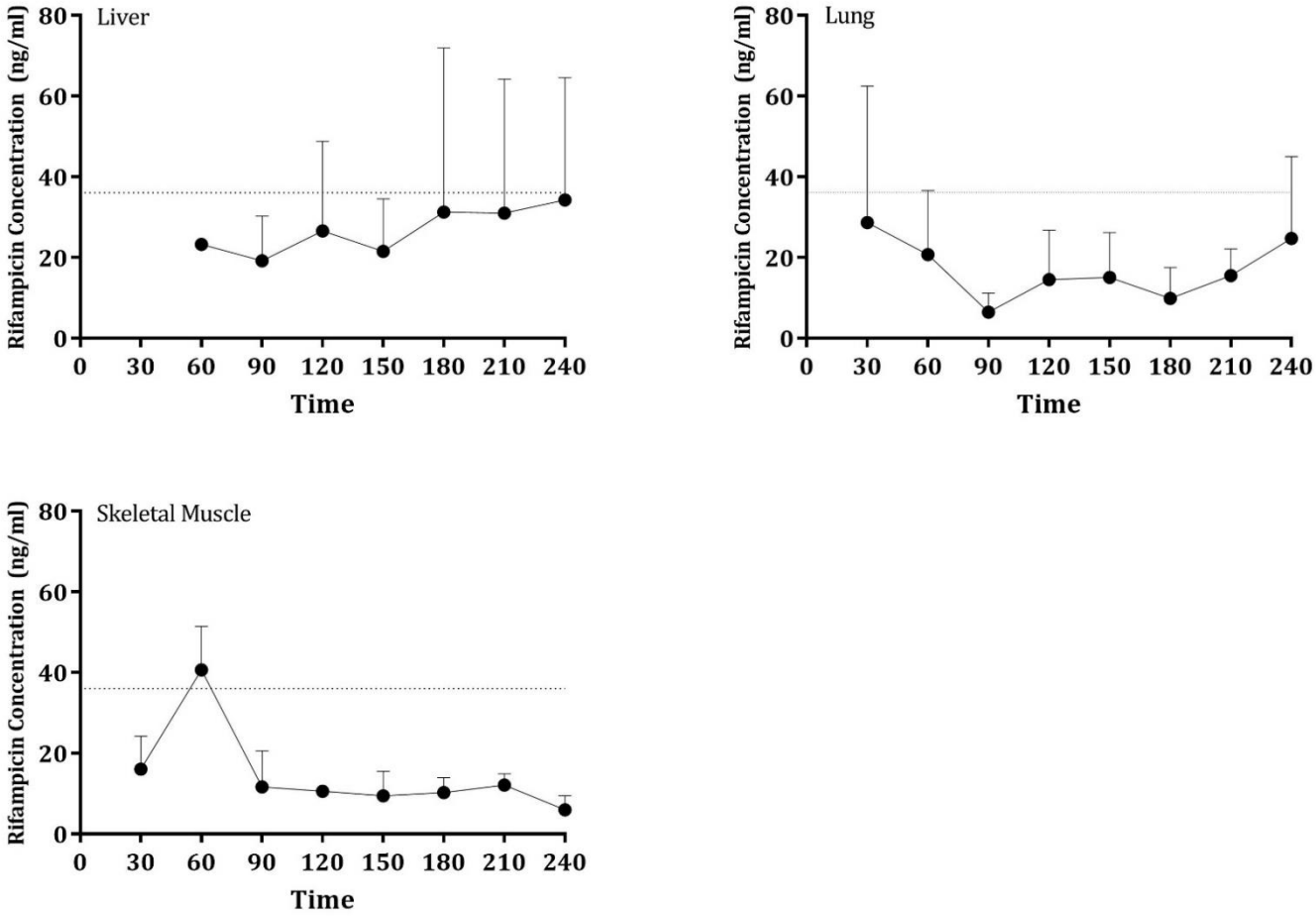

FIGURE 3.9: CONCENTRATIONS OF RIFAMPCIN RECOVERED IN FRACTIONS FOLLOWING MICRODIALYSIS IN ORGAN HOMOGENATES. Lungs, livers and skeletal muscle were spiked with 10µg/ml rifampicin in triplicate. Each point represents an average of three replicates. Additional line on graph show 21% (36ng) of the proposed unbound concentration of rifampicin (180ng).

Initially the unbound drug proposed to be in the spiked homogenates was calculated based upon plasma protein binding in blood which is 69.5% for rifampicin in guinea pigs. On this basis it was assumed that there was 0.18µg (180ng) of unbound rifampicin available in the homogenate for collection via microdialysis. Using the calculated probe efficiency of 21±9% (Table 3.22) and the proposed unbound drug in the homogenate, a line was drawn on the graphs in Figure 3.9 which shows 21% of 180ng which is 36ng.

It was evident in Figure 3.9, that over the time course, the probe was not consistently recovering 21±9% of the hypothesised unbound rifampicin. The reasons for this may be as this was a static system with no blood flow and the organs were spiked with the drug. However, at the 30 and 60-minute time points within the lung and skeletal muscle, the probe was working as expected recovering approximately 21% of the expected unbound rifampicin. The lower values at the later time points, as evidenced in the skeletal muscle, could be explained due to the static system whereby the majority of the unbound drug may have been already removed.

The lung results were more variable when compared to the skeletal muscle, as between 60 and 210 minutes the probe was recovering below the hypothesised 21%. This can be explained by the associated volume of blood that is present in the lungs, that when homogenised, could decrease the amount of unbound drug available to collect due to protein binding as well as potentially diluting the available drug. Within the liver, the probe was working close to the proposed 21% efficiency especially from 180 minutes onwards.

Rifampicin was recovered at approximately the expected probe efficiency (21%) from organ homogenates (30 and 240 minutes for lung, 60 minutes skeletal muscle and between 180 and 240 minutes in liver). Although these data were variable, the aforementioned limitations of the static system and use of homogenised tissue most likely contributed to this variability and hence these data support the use of 21±9% as the correction factor for probe efficiency for the rifampicin microdialysis data generated *in vivo.*

3.11 IN VITRO CONCLUSIONS PRIOR TO MOVING IN VIVO

This chapter describes the *in vitro* microdialysis experiments conducted with ethambutol, rifampicin and isoniazid with the overarching aim of calculating the efficiency of the probes to recover each drug prior to performing *in vivo* microdialysis. To calculate probe efficiency, the relative recovery of the drug was measured with probe. Recovery was optimised and improved by changing various parameters such as flow rate, perfusion fluid and probe type. Table 3.24 shows the parameters that were tested.

Drug	Concentration	Probe	Perfusion Fluid	Flow Rate (µl/min)	Recovery
ETH	91mg/ml (=250mg/kg)	CMA 20 (4mm; 20kDa)	T1	2	Yes- Very High
	56.5mg/ml (=100mg/kg)				Yes- Very High
	1mg/ml				Yes
				1	Yes
RIF	1mg/ml	CMA 20 (4mm; 20kDa)	T1	2	Yes- Very low
			Ringers +0.2% Bovine Serum Albumin		No
		Previously Exposed CMA 20 (4mm; 20kDa)	CNS	1 & 2	Yes- Very low
			T1	5 & 10	Yes
		CMA 20 (4mm; 20kDa)	CNS	1, 2, 5 & 10	Yes- Low
		CMA 20 (4mm; 100kDa)			Yes
		Flushed with rifampicin; CMA 20 (4mm; 20kDa)	T1	1, 2, 5 & 10	Variable
	100µg/ml	Previously Exposed CMA 20 (10mm; 20kDa)		2	Yes
	10µg/ml	Previously Exposed CMA 20 (10mm; 20kDa)			
INH	1mg/ml	CMA 20 (10mm; 20kDa)	T1	2	Yes
		CMA 20 (4mm; 100kDa)			Yes

TABLE 3.24: ALL PARAMETERS (PROBE TYPE, PERFUSION FLUID, FLOW RATE) THAT WERE TESTED IN THIS CHAPTER TO ENABLE PROBE EFFICIENCIES TO BE CALCULATED.

The calculated probe efficiency for rifampicin was 21±9% at the concentrations expected in the organs. An *in vitro* assay was conducted, primarily to understand matrix (organ) effects on the recovery of rifampicin. The recoveries for rifampicin were close to the expected 21±9% and these experiments gave confidence that the microdialysis methodology could recover low concentrations of the drug in the presence of organ/tissue components.

Therefore, the parameters that were proposed to be used for *in vivo* microdialysis were a previously exposed CMA 20 probe (20kDa, 10mm), T1 perfusion fluid and 2µl/minute flow rate.

CHAPTER 4

IN VIVO MICRODIALYSIS METHOD DEVELOPMENT

4.1 INTRODUCTION

Drug doses for *in vitro* microdialysis and for oral administration to guinea pigs were defined in Chapter 2. The key parameters for microdialysis, such as probe type, perfusion fluid and flow rate were defined during the *in vitro* studies detailed in Chapter 3. The aims of the studies described in this Chapter were to define the organ into which the microdialysis probe was to be implanted and to establish the *in vivo* microdialysis methodology. This methodology is comprised of *in vivo* study design and surgical considerations, as well as pre- and post-operative care including analgesia and housing requirements.

4.2 SELECTION OF ORGAN FOR MICRODIALYSIS

4.2.1 LIVER

The lungs (main target site for drug delivery during TB disease) were the original organ of interest to recover unbound (UB) anti-TB drug concentrations via microdialysis. The feasibility of microdialysis in the lung of an awake freely moving guinea pig was limited and could not be successfully conducted without the use of a specially designed proprietary MetQuant 'floppy' microdialysis probe (Thomas Cremers, Brains On-Line [226], Personal Communication). The liver was therefore proposed as an alternative organ to dialyse, primarily because of its large size and seemingly straightforward location for probe insertion.

Isoniazid and rifampicin are both metabolised in the liver, and are also associated with high levels of hepatotoxicity, which gave further justification for the liver as the site of probe implantation. Isoniazid is known to cause severe liver failure in 1% of people who are administered this drug, especially those with the slow acetylator status[127,128]. This toxicity is most likely associated with the bioactivation of the pro-drug into its reactive metabolites[227]

(Chapter 1). The practicality of microdialysis probe implantation into the liver of guinea pigs was investigated *post mortem*. A guinea pig was culled via an intra-peritoneal injection of sodium pentobarbitone as described later in this Chapter and then was laid on its right- hand side. The surgery area was prepared in advance by ensuring the table used was clean and covered. The area into which the probe was to be implanted was close clipped and cleaned. An incision was made along the midline of the guinea pig to expose the peritoneum. The xiphoid process was used as an anatomical 'land mark' and needle (23Ga x 5/8" 0.6x16mm) was inserted approximately 1mm below the xiphoid process, but above the ribs. An incision was made along the peritoneum to determine if the needle had entered the liver without disturbing or disrupting other internal anatomy of the guinea pig. The initial insertion did enter the liver of the guinea pig; however, it also exited out the other side. To ensure maintenance of the probe membrane and comfort for the guinea pig, the probe must be anchored in position with sutures. There were no suitable anchor points (points to suture the probe to) within the liver.

It was clear that insertion of the probe into the liver was a non-recoverable procedure and therefore would not be fit for the purpose of this project. As highlighted in this section, probe implantation into the liver or the lung was not feasible, hence an alternative tissue was investigated for probe implantation as detailed in the following sections.

4.3 SKELETAL MUSCLE AS A SURROGATE FOR LUNG

4.3.1 INTRODUCTION

It was identified that unbound drug concentrations within the lung and skeletal muscle were similar for gatifloxicin[228] and cefpodoxime[229]. Both of these drugs share physiochemical properties with isoniazid, and it was therefore decided to design an experiment to identify if the concentrations of anti-TB drugs were similar between lung (site of TB disease and therefore the most relevant organ for microdialysis) and skeletal muscle or if not, whether there was a correlation. Similar or correlated drug concentrations between the lung and skeletal muscle would enable the skeletal muscle to be used as a surrogate for lung microdialysis in the guinea pig. This experiment and the subsequent results are described in the following section.

An investigation into the feasibility of probe implantation into the skeletal muscle was also conducted (Section 4.4.5). The sacrospinalis is a large skeletal muscle that is located next to the spine, and due to its size, strength and proximity to the dermis there were anatomical advantages for probe implantation. There are several examples of microdialysis in the skeletal muscle [215,228,229] using minimally invasive surgical protocols, which ensured that animals can be awake and freely moving.

For the first investigation, skeletal muscle was collected from the hind leg (biceps femoris) of the guinea pig, because for the purposes of PK/PD modelling, skeletal muscle is not distinguished by anatomical location.

4.3.2 STUDY DESIGN AND METHODS

Following the methods described in Chapter 2, six guinea pigs were administered one oral dose of isoniazid (50mg/kg) or rifampicin (50mg/kg) and blood samples were taken from the ear, following the schedule in Table 4.1. Guinea pigs were cardiac bled and necropsied to remove lung, liver and skeletal muscle. The samples were processed via protein precipitation (Chapter 4) and analysed at Q3 Analytical, following the methods described in Chapter 3.

	Guinea Pig	Ear Bleed	Cardiac Bleed & Necropsy
One Oral Rifampicin Administration (50mg/kg)	1		1hr Post Drug Administration
	2		
	3	1hr Post Drug Administration	2hr Post Drug Administration
	4		
	5	1hr&2hr Post Drug Administration	4hr Post Drug Administration
	6		
	Guinea Pig	**Ear Bleed**	**Cardiac Bleed & Necropsy**
One Oral Isoniazid Administration (50mg/kg)	1		1hr Post Drug Administration
	2		
	3	1hr Post Drug Administration	2hr Post Drug Administration
	4		
	5	1hr&2hr Post Drug Administration	4hr Post Drug Administration
	6		

TABLE 4.1: STUDY DESIGN TO INVESTIGATE THE RELATIONSHIP BETWEEN DRUG CONCENTRATIONS IN THE LUNG AND SKELETAL MUSCLE. Six guinea pigs were administered a single oral dose (50mg/kg) of isoniazid or rifampicin and ear bled either at 1 and/or 2 hours post drug administration. Cardiac bleeds and necropsies (lung, liver, skeletal muscle removed) were performed either at 1, 2 or 4 hours post drug administration.

4.3.3 EQUIPMENT LIST FOR INVESTIGATION OF RELATIONSHIP BETWEEN LUNG AND SKELETAL MUSCLE DRUG CONCENTRATIONS

Equipment	Comments	Source
2ml/10ml syringe	Oral administration of drug/cardiac bleed	BD574/GS576; Appleton Woods Ltd, Birmingham, UK.
Scalpel	Ear bleeds	No. 15A; Product Code: 0320; Swann Morton, Sheffield, UK
Sterilin plates	Necropsy Procedure	SC274; Appleton Woods Ltd, Birmingham, UK
Various gauge needles	Various uses	Terumo Agani, Surrey, UK
Drug, Chemical or Reagent	**Comments**	**Source**
0.1% Formic Acid Aqueous	Chromatographic Solvent	5438040100; Sigma Aldrich Co LTD, Dorset, UK
Acetonitrile	Chromatographic Solvent	PHR1551-3X1.2ml; Sigma Aldrich Co LTD Dorset, UK
Apple and Banana fruit puree	To help palatability of drugs for oral administration	Ella's Kitchen, Henley-on-Thames, UK
Dextromethorphan (DXT)	Internal standard	1180503-2G; Sigma Aldrich, Dorset, UK
Dimethyl sulfoxide (DMSO)		D2650; Sigma Aldrich, Dorset, UK
HPLC Grade Water		270733-1L-M; Sigma Aldrich Co LTD, Dorset, UK
Isoniazid		I3377-250G; Sigma Aldrich, Dorset, UK
Isopropyl alcohol (IPA)	Necropsy Procedure	I0398; Sigma Aldrich, Dorset, UK
Rifampicin		R3501-1G; Sigma Aldrich, Dorset, UK
Sodium pentobarbitone	Dolethal 200mg/ml	Vetoquinol UK Ltd

HPLC/MASS SPECTROMETRY

Q3 Analytical, Porton Science Park, Porton Down, Salisbury, Wiltshire, SP4 0JG	(HPLC) Agilent 1100 Pump, Column heater, Degasser	Aligent, Cheadle, UK
	(HPLC) CTC HTS Autosampler	Presearch, Basingstoke, UK
	(HPLC) Column; Rifampicin; Kinetex C8 50x2.1MM, 5µm	Phenomenex, Macclesfield, UK
	(Mass Spectrometer) API3000	Sciex, Warrington, UK

4.3.4 CARDIAC BLEED AND NECROPSY PROCEDURE

Guinea pigs were euthanised via 2ml injection of 200mg/ml sodium pentobarbitone. Blood samples were withdrawn once the pedal withdrawal reflex was absent. A syringe with needle was used to withdraw 1ml of blood from the heart, which was then added to 2ml HPLC water. The tubes were closed, vortexed and snap frozen in liquid nitrogen. The guinea pig was then placed on its back and an incision made in the abdomen and thorax to remove the lungs and liver. The skeletal muscle from the hind leg (biceps femoris) was removed after removing the fur on the left hind leg and using the scissors to cut away the muscle from the bone. Organs were placed on Sterilin plates to remove excess connective tissue, weighed on an analytical balance and snap frozen.

4.3.5 SAMPLE PROCESSING FOR ANALYSIS OF ISONIAZID AND RIFAMPICIN CONCENTRATIONS IN BLOOD AND TISSUE

This method was adapted from Kjellson et al[192].

Blood, liver, lung and skeletal muscle samples were thawed at room temperature. To every 0.2g of tissue (as weighed at point of necropsy) 1ml of PBS was added. Each tissue was homogenised (Ystral) and the blade was cleaned between every sample with isopropyl alcohol and then demineralised water to ensure no carry-over of tissue or drug. Methanol (10µl) was added to 50µl of homogenate or blood and vortexed thoroughly. 440µl acetonitrile (containing 0.3µg/ml dextromethorphan (internal standard for LC-MS/MS (Chapter 3)) was added to the samples and vortexed for two minutes then centrifuged in a microfuge at 10,000g for 10 minutes. The supernatant was removed and stored at -80°C until samples were thawed, transferred to HPLC tubes and the liquid evaporated from samples (Genevac evaporator). When dry, 20µl of 0.1% formic acid was added to each HPLC tube and these samples were injected directly into the HPLC for analysis.

4.3.6 COMPARISON OF DRUG CONCENTRATIONS IN LUNG AND SKELETAL MUSCLE

The mean concentrations (μg/ml) of rifampicin and isoniazid in lung and skeletal muscle from six guinea pigs were plotted (GraphPad Prism V7) against one another as shown in Figure 4.1. These data represent both the bound and unbound (total) drug concentrations.

The concentration of rifampicin measured in the skeletal muscle was significantly lower than that found in the lung (Wilcoxon test; P=0.0313). The mean concentration of rifampicin in the lung was 22.67μg/ml (Standard Deviation (SD): 22.6) and in the skeletal muscle was 6.19μg/ml (SD:6.9). This meant that the concentration of rifampicin in the lung was approximately 3 times higher than in the skeletal muscle.

The concentration of isoniazid measured in the skeletal muscle was lower than that found in the lung (Wilcoxon test; P=0.1563). The mean concentration of isoniazid in the lung was 30.3μg/ml (SD: 36.9) and in the skeletal muscle was 6.01μg/ml (SD: 5.8). This meant that the concentration of isoniazid in the lung was approximately 5 times higher than in the skeletal muscle.

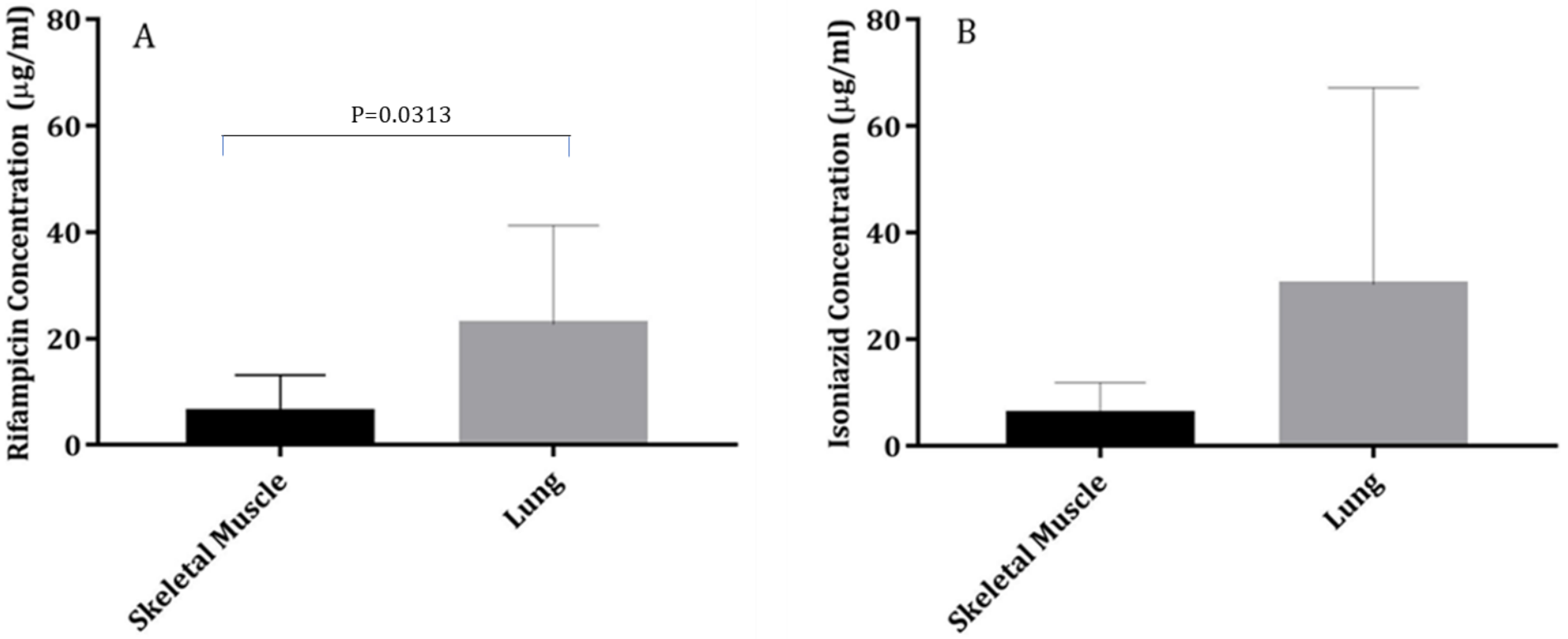

FIGURE 4.1: A) MEAN ORGAN CONCENTRATION OF RIFAMPICIN (BOUND AND UNBOUND) IN LUNG AND SKELETAL MUSCLE. B) MEAN ORGAN CONCENTRATION OF ISONIAZID (BOUND AND UNBOUND) IN LUNG AND SKELETAL MUSCLE. Six guinea pigs were dosed with either 50mg/kg of rifampicin or isoniazid and the concentration of drug in the lung and hind leg skeletal muscle were measured. Error bars represent standard deviation (SD).

4.3.7 RELATIONSHIP BETWEEN LUNG AND SKELETAL MUSCLE CONCENTRATIONS OF ISONIAZID

As the isoniazid concentrations in the lung and skeletal muscle were not sufficiently similar, the concentrations in the two organs were analysed to identify if there was a relationship or correlation between them that would enable the concentration in the lung to be derived from the skeletal muscle. There was no relationship identified between lung and skeletal muscle drug concentrations in animals dosed with isoniazid (Pearson R^2 value =0.1857 (P = 0.3936)). The data are shown in Figure 4.2.

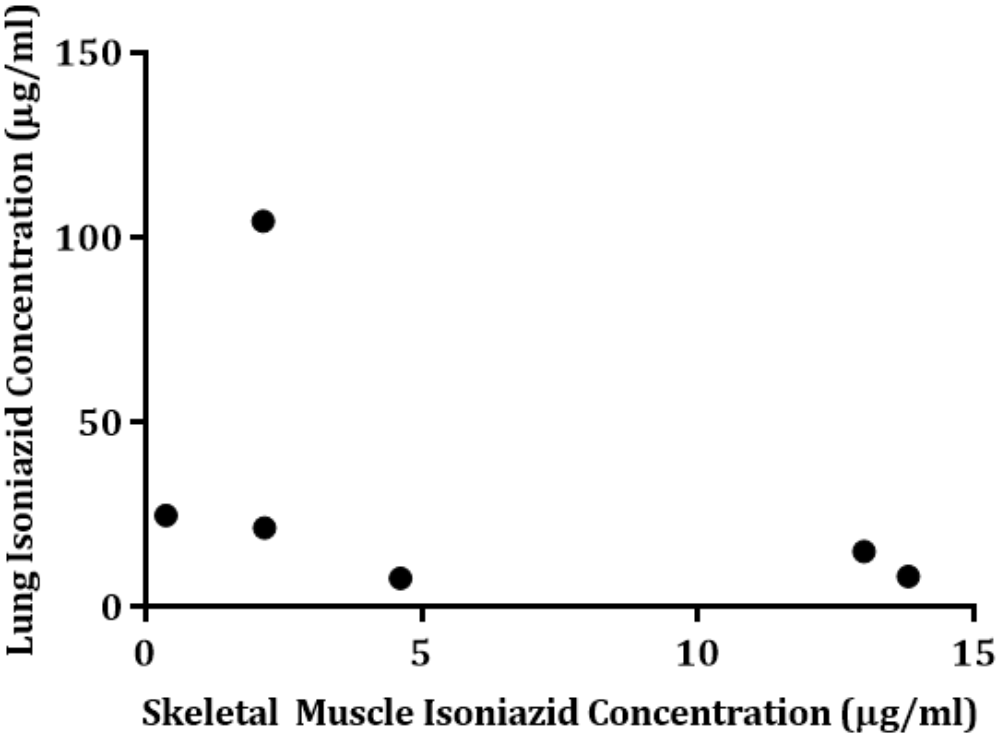

FIGURE 4.2: ISONIAZID CONCENTRATIONS MEASURED IN THE LUNG AND SKELETAL MUSCLE. There is no relationship between the concentrations of isoniazid within the two organs. The data from six guinea pigs is plotted.

Under the conditions tested (doses and timescale), it does not appear that lung concentrations of isoniazid could be estimated from skeletal muscle and therefore microdialysis of the sacrospinalis would not be a suitable for this drug. Further investigations would be required to optimise the methodology for *in vivo* microdialysis experiments with isoniazid.

4.3.8 RELATIONSHIP BETWEEN LUNG AND SKELETAL MUSCLE CONCENTRATIONS OF RIFAMPICIN

As the concentrations of rifampicin differed between the lung and skeletal muscle (P=0.0313), the individual animal data were analysed to identify if there was a relationship between the quantity of drug in the two tissues. The rifampicin concentrations in the lung and skeletal muscle were plotted and tested for correlation (Pearson correlation test) which generated an R^2 value of 0.8718 (p=0.0065).

A second order polynomial (quadratic function) (Figure 4.3) was used to fit all data points, generating an R^2 of 0.964 (Sy.x=4.5) highlighting the strength of the fit.

The use of a second order polynomial with these data (Figure 4.3) generated the following equation:

$$Y = B0 + B1 * X + B2 * X\text{^}2$$

where Y is the concentration of rifampicin in the lung, B0=-7.254, B1=7.848 and B2=-0.2361 (equation constants generated in GraphPad Prism) and X is concentration of rifampicin in the skeletal muscle. This meant that rifampicin concentrations measured in the skeletal muscle could be used to calculate rifampicin concentrations in the lung.

The second order polynomial was used to account for the data point at 20.1µg/ml in skeletal muscle and 55µg/ml in the lung. This data point was from a guinea pig that was culled two hours post drug administration. To understand if the time at which the samples were collected had an effect on the relationship between drug concentrations in the lung and skeletal muscle, the ratio of rifampicin concentrations between lung and skeletal muscle were plotted over time (Figure 4.4). The ratio varied minimally which indicated that the relationship of drug concentrations between the lung and skeletal muscle was true regardless of sampling timepoint and therefore suggested that differing rates of distribution following oral drug administration could be accountable for this apparent outlier.

These data provided confirmation that the sacrospinalis was a potentially suitable tissue to dialyse in order to estimate concentrations of rifampicin in the lung due to the strength of the relationship (R^2 =0.8718) between lung and skeletal muscle concentrations. Rifampicin was therefore selected for *in vivo* microdialysis studies using the sacrospinalis for probe insertion with the assumption that this relationship (between lung and skeletal muscle rifampicin concentrations) would remain true for unbound rifampicin concentrations as collected via microdialysis.

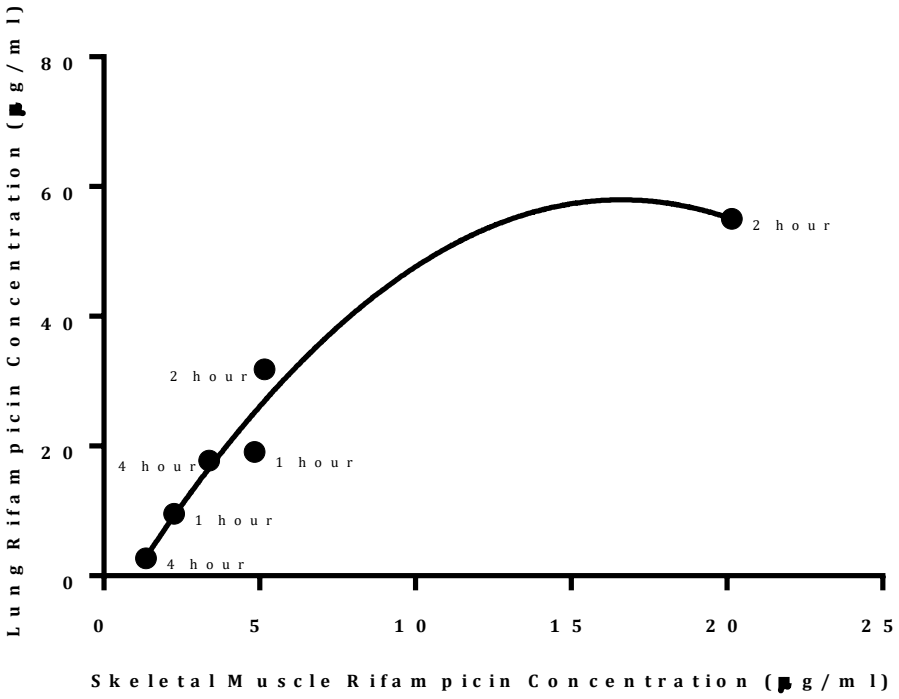

FIGURE 4.3: CORRELATION BETWEEN RIFAMPICIN CONCENTRATIONS IN THE LUNG AND SKELETAL MUSCLE. Data points for six guinea pigs were fitted with a second order polynomial. Each point is labelled with hour of collection. The equation Y=B0+B1*X+B2*X^2 where Y is the concentration of rifampicin in the lung, B0=-7.254, B1=7.848 and B2=-0.2361 (equation constants generated in GraphPad) and X is concentration of rifampicin in the skeletal muscle.

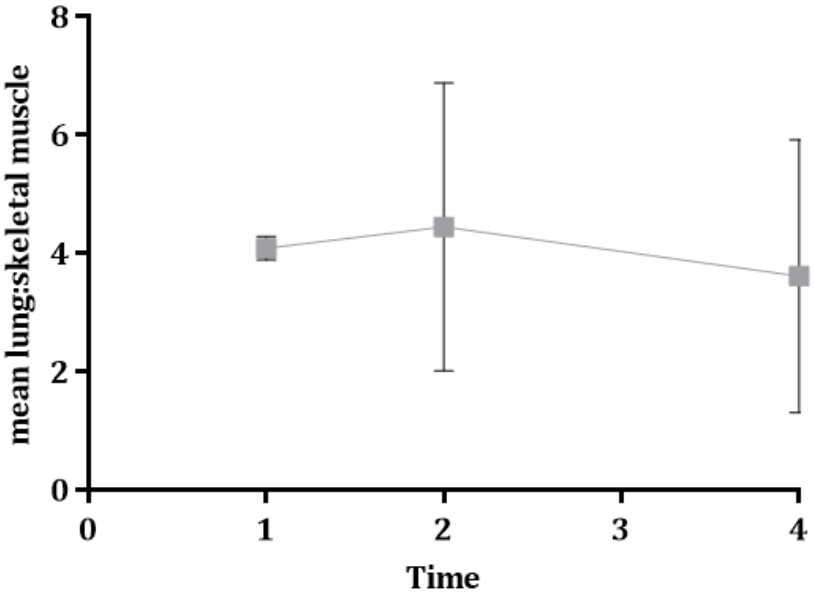

FIGURE 4.4: MEAN RATIO OF RIFAMPICIN CONCENTRATIONS BETWEEN LUNG AND SKELETAL MUSCLE PLOTTED OVER TIME. Each point is the mean data of two guinea pigs which were culled 1, 2 or 4 hours post drug administration. Error bars represent standard deviation.

4.4.1 INTRODUCTION TO PILOT STUDY

Following the determination and optimisation of the microdialysis parameters that best recover rifampicin, calculation of the probe efficiency (Chapter 3) and the determination of a correlation (R^2 =0.8718) between rifampicin concentrations in the lung and skeletal muscle (Section 4.3), it was decided that rifampicin was to be administered to the guinea pigs with the aim of being recovered via microdialysis *in vivo*. An initial *in vivo* microdialysis study with two guinea pigs was designed to prove that rifampicin concentrations could be measured via the microdialysis methodology from the sacrospinalis over time.

An essential component of this pilot study was determination of the methods required for *in vivo* microdialysis. The methods described in this section are for the following:

- Anaesthesia, as guinea pigs required anaesthesia for the implantation of the CMA20 microdialysis probe into the sacrospinalis.
- Surgical implantation of the probe into the sacrospinalis. As shown in Section 4.3 the sacrospinalis was selected as the site of microdialysis for rifampicin and therefore a protocol was devised for the insertion of the selected microdialysis probe (based on studies in Chapter 3 (CMA20 10mm 20kDa)) into the sacrospinalis. An important component of this pilot study was to determine whether the guinea pig would survive the surgical implantation of the probe and thrive thereafter to enable good quality data to be generated from healthy animals.
- Maintenance of the microdialysis probe *in situ* to ensure patency. The probe was flushed twice daily until patency (visible liquid in collection tube) was observed. The first flush occurred as soon as was practically possible following the guinea pig being placed into the warmed home cage for recovery post-surgery. The probe was flushed with a rifampicin containing solution to ensure that the probe had been previously exposed to rifampicin to limit non-specific binding of rifampicin to the microdialysis system plastics (Chapter 3).

Also described are the methods used for post-operative care, entry and exit into the guinea pig housing room, urine and faeces collection (as rifampicin is known to be excreted via these routes) and *ex vivo* microdialysis. The overarching *in vivo* microdialysis study schedule and method is shown in Section 4.5.

As part of this methodology, ear bleed samples were collected at set time points post drug administration as described in Chapter 2. These samples were collected to enable blood drug concentrations to be related to organ drug concentrations and as a comparator to the PK parameters of rifampicin in blood which were generated in Chapter 2. Collection of ear bleeds had to comply with the specified limits on frequency of ear bleeds in the Home Office Project Licence, which details that each guinea pig can have 2 ear bleeds (maximum blood volume of 100µl per occasion). An alternative approach for blood sampling was considered, involving blood vessel (jugular vein) cannulation so that blood samples could be collected at intervals time-matched to the microdialysis fractions. This would require an additional surgical procedure and since collection of blood from the peripheral vein in the ear (capillary blood) had been used previously (Chapter 2) and shown to be feasible, this less invasive method was preferred.

The lessons learnt from this pilot study are highlighted at the end of this chapter. The results from this initial *in vivo* microdialysis experiment were analysed in conjunction with additional data generated from further *in vivo* microdialysis experiments and these data are shown and discussed in Chapter 5.

4.4.2 IN VIVO MICRODIALYSIS EQUIPMENT LIST

Microdialysis Equipment	Comments	Source
300µl collection tubes	Polypropylene.	(1000/pack) 743110; Linton Instruments, Norfolk, UK
CMA 20 Probe	20kDa molecular weight cut-offs; 10mm membrane length.	CMA 8010436; CMA Microdialysis AB, Kista Sweden; Distributed by Linton Instruments, Norfolk, UK.
CMA 402 Rev D Syringe Pump	Designed for pulse-free low flow rates.	CMA Microdialysis AB, Kista Sweden
FEP Tubing	Fluorinated Ethylene Propylene; attached to probe.	BFEP-T22Q; Instech, Plymouth Meeting, USA; Distributed by Linton Instruments, Norfolk, UK
Harness	To tether guinea pigs	CIH95 Covance Infusion Harness for Rat; CMA Microdialysis AB, Kista, Sweden distributed by Linton Instruments, Norfolk, UK
Liquid swivel		CM375KRP; Instech, Plymouth Meeting, USA distributed by Linton Instruments, Norfolk, UK
Luer stubs blunt needle	Connect syringe to probe.	Fisnar QuantX 8001101; Ellsworth, Germantown, USA
Split tubing	For probe insertion *in vivo*	CMA 8309019; CMA Microdialysis AB, Kista, Sweden distributed by Linton Instruments, Norfolk, UK
T1 Designed for microdialysis in soft tissues.	NaCl 147mmol/L, KCl 4mmol/L, $CaCl_2$ 2.3mmol/L;	CMAP000034; Harvard Apparatus, Holliston, USA distributed by Linton Instruments, Norfolk, UK
Tubing connectors		CMA 3409500; CMA Microdialysis AB, Kista Sweden; Distributed by Linton Instruments, Norfolk, UK
Equipment	**Comments**	**Source**
Ethicon Sutures Mersilk 3/0	To stitch probe into place.	W328H; Ref: GSI003A; Johnson and Johnson, New Jersey, USA
TRENDnet Camera	To observe guinea pigs	TRENDnet TV IP310PI Outdoor 3 MP PoE Day/Night Network Camera; Insight, Salford, UK
Various gauge needles	Various uses	Terumo Agani, Surrey, UK
	Comments	**Source**
Buprenorphine	Opioid Analgesic	Vetergesic 0.3mg/ml; Ceva Animal Health Ltd, UK
Carprofen	NSAID Analgesic	Carpreive 5%w/v; Norbrook Laboratories, USA
Chlorhexidine	Disinfectant	Hibiscrub; 500ml EA; Ref: MOLN10008780; VWR International, Lutterworth, UK
Isoflurane	Anaesthetic agent (IsoFlo 100% w/v inhalation vapour)	Zoetis UK Ltd
Vetbond Tissue Adhesive	To close incisions	3M 1469sb

Additional equipment used is shown in Section 4.3.2.

4.4.3 ANAESTHESIA

Before any guinea pig was considered for surgical implantation of the microdialysis probe, a thorough health check (including acknowledgement of clear eyes, good coat, no swelling, normal respiratory sounds, food and water intake and evidence of mobility and activity) was undertaken. The weight of the guinea pig was recorded immediately prior to anaesthesia to ensure that an accurate dose of isoflurane (2-2.5%/0.4-0.8L/min oxygen) was given. Immediately prior to anaesthesia, a subcutaneous injection of buprenorphine ((opioid) 0.3mg/kg) was administered in order to minimise pain upon recovery from anaesthesia.

The concentration of isoflurane was gradually increased (starting with 0.5%) to reduce adverse reactions such as hypersalivation. The guinea pigs were placed in a position with their head and neck extended to help the airway remain clear and unobstructed, and a rodent sized facemask was used for maintenance of the anaesthesia. Following the initial induction of anaesthesia, a subcutaneous injection of carprofen ((NSAID) 4mg/kg) was administered to relieve any inflammation associated with the surgical procedure.

Depth of anaesthesia was continually monitored using the pedal withdrawal reflex and an absence of this reflex was indicative that the appropriate depth of anaesthesia had been achieved.

4.4.4 SURGICAL IMPLANTATION OF MICRODIALYSIS PROBE INTO SACROSPINALIS OF GUINEA PIG

Initially a guinea pig cadaver was used to demonstrate the implantation of a microdialysis probe (CMA 20, 10mm, 20kDa) into the sacrospinalis muscle (Figure 4.5). Following additional refinements on cadavers, this protocol was used to implant probes into anesthetised guinea pigs.

The following surgical procedure was completed in approximately 15 minutes.

m. erector spine; also known as *m. sacrospinalis*

Erector muscle of spine (22).

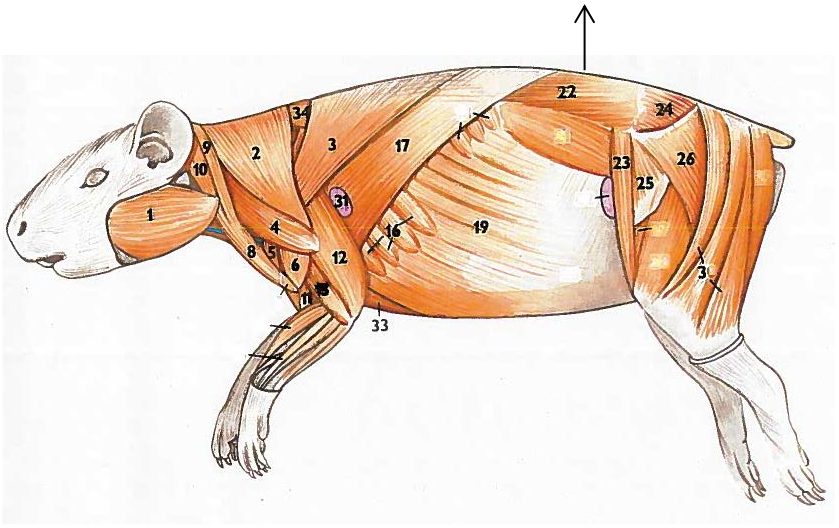

FIGURE 4.5: LOCATION OF THE SACROSPINALIS MUSCLE WITHIN THE GUINEA PIG BODY (MUSCLE LABELLED #22[230]).

Surgical procedures were carried out using sterile instruments and following good aseptic technique. Guinea pigs were anesthetised as described in the previous section and warmth was generated via a heat mat set to 55˚C and maintained via a surgical drape.

Initially the sacrospinalis was located using the spine as a reference point, and the area around the sacrospinalis and between the shoulder blades was close clipped and cleaned with warmed chlorhexidine. A scalpel was used to make two incisions, one which was between the shoulder

blades (approximately 5mm long) and the other incision was made at the side of the spine, directly above the location of the sacrospinalis (approximately 1 to 1.5cm long).

A trocar which functioned as a portal for the subsequent placement of the microdialysis tubing was inserted into the incision made directly above the sacrospinalis and tunnelled carefully under the skin where it emerged through the incision between the shoulder blades. The inner stylet from the lumen of the trocar was carefully removed and the inlet and outlet tubing of the microdialysis probe was gently inserted into the trocar. The trocar was then pulled cranially through the incision between the shoulder blades so that the inlet and outlet tubing of the probe emerged through this incision.

The spine was used as the point of reference and introducer (comprised of a guide needle (21Ga x 1$^{1/2"}$ 0.8mm x 40mm) & split tubing) was inserted in a caudal direction at a 45° angle into the incision above the sacrospinalis. Resistance was encountered as the myelin sheath was pierced. Once the myelin sheath was pierced no more resistance was met and the angle of the guide needle was reduced until parallel with the spine.

The needle was carefully removed, ensuring the split tubing remained *in situ*, and the microdialysis probe was introduced into the sacrospinalis. The split tubing was then carefully pulled apart, leaving the microdialysis probe *in situ*.

The microdialysis probe was sutured in place via the suture points on the probe to the subcutaneous muscle. Once sutured, the remaining suture thread was tied off. Both of the incision holes were then sutured closed and sealed with tissue glue.

At this point, two additional pieces of tubing (full length) were connected to the inlet and outlet tubing of the microdialysis probe using modified blue tubing connectors (fluted ends removed) which had been previously soaked in ethanol. The probe tubing and additional tubing were threaded up through the harness spring and the guinea pig gently placed into the harness as shown in Figure 4.6. The harness was tightened gently.

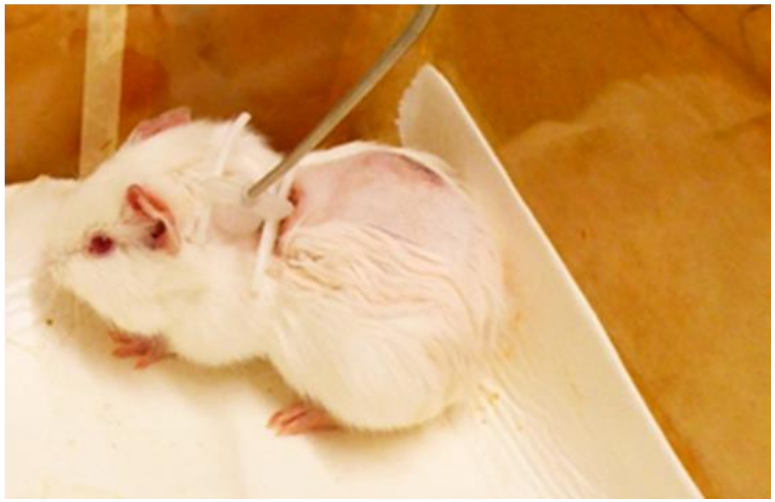

FIGURE 4.6: GUINEA PIG WEARING HARNESS FOLLOWING COMPLETION OF SURGICAL PROCEDURE. The close clipped area is visible in this photo as well as the location of the sacrospinalis incision. The probe tubing was threaded up through harness spring and is attached to the liquid swivel.

FIGURE 4.7: EXAMPLE OF TRENDNET SURVEILLANCE CAMERA DISPLAY. LHS; day time view of guinea pigs in cages, RHS; night time view of guinea pigs in cages. Both cages are clearly visible.

4.4.5 ENTRY AND EXIT INTO GUINEA PIG HOUSING ROOM

Throughout the duration of the experiment guinea pigs were housed in a room that was quiet and warm with minimal foot traffic. The guinea pigs being dialysed were the only animals kept in the room. As the guinea pigs were tethered, entry and exit into the housing room needed to be done in calm and controlled manner to not frighten the guinea pigs and cause them to make any sudden movements. To minimise the entry and exit to the room, guinea pigs were monitored via a network surveillance camera allowing them to be monitored throughout the time that they were tethered. An example of the TRENDnet display is seen in Figure 4.7.

4.4.6 POST-OPERATIVE CARE (RECOVERY)

Immediately following completion of surgery, individual guinea pigs were placed into their warmed home cages (30-35°C) which were previously modified to create an anchor point for attachment of the harness. Maintenance of temperature was important as a significant amount of fur was removed as part of the surgical procedure which increased the risk of hypothermia. Therefore, heat was generated via a heat mat placed under the cages and via a 'hand warmer' inside the cages. Home cages were lined with tray liner and Vetbed (medical grade bedding with 28mm pile for warmth and comfort) along the bottom. Guinea pigs had access to food and water *ad libitum*.

The animals were constantly monitored until fully awake and movement was observed. Comprehensive monitoring was conducted via TRENDnet camera and physically to identify any post-operative complications.

The general condition (appearance, posture, coat, vocalisation) and activity/ mobility of the guinea pigs were monitored via TRENDnet system as well as physically. The camera was an integral component of this experiment in order to observe the natural behaviour of the guinea pigs. Being a prey species, they naturally hid discomfort when being physically monitored and it was therefore important that they were remotely observed in order to show evidence of discomfort.

The harness was monitored for fit (tightness or looseness). It was important to strike the right balance between ensuring the harness was tight enough as to not allow the guinea pigs access to the tubing and ensuring that it was not so tight that it was causing discomfort. The harness needed to be tightened throughout the tethered duration as the constant movement of the guinea pigs and decrease in swelling (post-surgery) loosened it. The harness straps proved to be an irritant (as evidenced via TRENDnet system) as the straps became longer (upon tightening) evidenced by the guinea pigs constantly turning their heads to try and reach them. The harness straps were trimmed as short as possible to minimise this. Incision wounds were also checked for presence of infection.

Food and fluid intake as well as urine and faeces output were monitored both physically and via the TRENDnet system. There was more evidence of guinea pigs eating than drinking so to alleviate any potential dehydration, the food was then mixed with water. Faeces were found in the guinea pig cages. It was decided not to remove the faeces because guinea pigs are caecotrophs and the faeces are covered in a mucus, that contains vitamins that have benefits upon re-ingestion. Note that immediately prior to oral drug administration all faeces were cleared from the cages.

Both buprenorphine (0.03mg/kg) and carprofen (4mg/kg) were administered to the guinea pigs prior to surgery (following collection of guinea pig weight) and then every 8-12 hours for buprenorphine and every 24 hours for carprofen. Buprenorphine and carprofen were administered via subcutaneous injection in a 300µl volume with Ringers Solution. This volume of Ringers Solution was selected in order to administer additional fluids to counter dehydration and also to maximise the volume of analgesic given in each dose. A smaller total volume would require a very small volume of the active ingredient which may be difficult to dispense accurately resulting in potential under-dosing. Table 4.2 shows the relative doses of each drug based on body weight.

Buprenorphine (Vetergesic)					Carprofen (Carpreive)				
Guinea Pig Weight (kg)	Dose of Analgesia (mg/kg)	Volume to Administer (µl)	Volume of Ringers Solution (µl)	Final Dose Volume (µl)	Guinea Pig Weight (kg)	Dose of Analgesia (mg/kg)	Volume to Administer (µl)	Volume of Ringers Solution (µl)	Final Dose Volume (µl)
0.2	0.03	20	280	300	0.2	4	16	284	300
0.3		30	270		0.3		24	276	
0.4		40	260		0.4		32	268	

TABLE 4.2: DOSE OF BUPRENORPHINE AND CARPROFEN ADMINISTERED TO GUINEA PIGS, PRE AND POST SURGERY. Doses of carprofen and buprenorphine, and hence Ringers solution, were dependant on guinea pig weight. Guinea pigs received buprenorphine every 8 hours and carprofen every 24 hours.

4.4.7 MAINTENENCE OF MICRODIALYSIS PROBE IN SITU

20cm (approximately) of sterile FEP tubing was used to connect a 1ml syringe (in the syringe pump) via a Luer stubs blunt needle and clear tubing connector to the liquid swivel (Figure 4.8). The liquid swivel was clipped into the counter balanced lever arm (Figure 4.8). The inlet tubing (which exited the top of the tether spring) was looped and attached via a clear tubing connector to the rear of the liquid swivel. The outlet tubing (which also exited at the top of the tether spring) was placed into a collection tube which was connected to the tether spring via a tubing clip (No longer manufactured).

The syringe contained a warmed (in an oven to approximately 39°C; guinea pig body temperature) rifampicin containing solution (10µg/ml in Ringers solution). A 2µl/minute flow rate was used, and the flow continued until there was evidence of fluid on the outlet tubing.

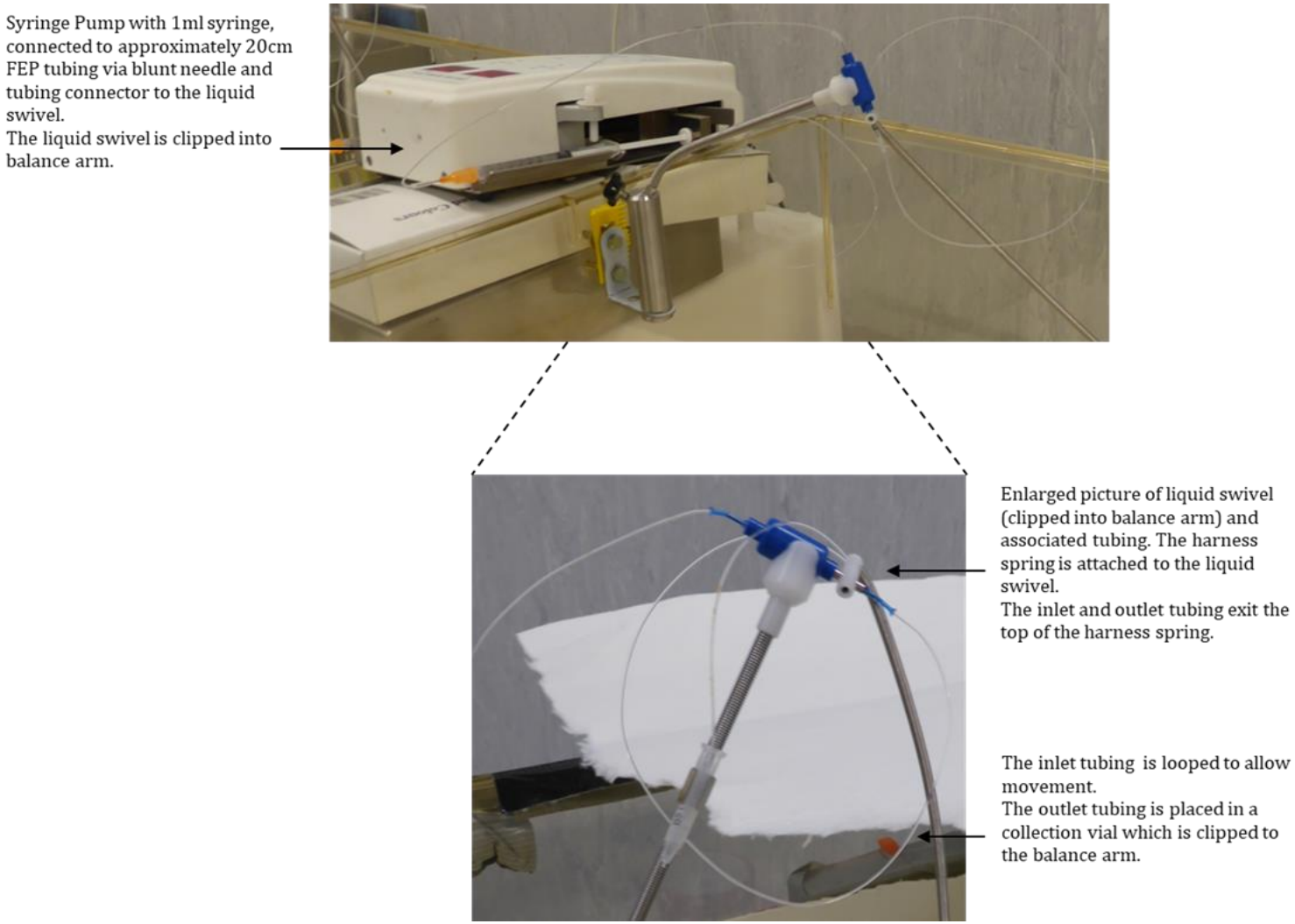

FIGURE 4.8: SET UP OF MICRODIALYSIS EQUIPMENT. The syringe was connected to the liquid swivel. The liquid swivel was connected to the harness spring which contained the inlet and outlet tubing. The inlet tubing was looped to allow movement. The outlet tubing was placed in a collection vial.

4.4.8 URINE & FAECES COLLECTION

During the 4 hour microdialysis experiment, cages were lined with hydrophobic (reflective) tray liners. A Pasteur pipette was used to immediately collect all urine and the time (post drug administration) and volume (directly measured) recorded. Faeces were collected by sterile forceps and the time (post drug administration) recorded. Both urine and faeces samples were snap frozen in liquid nitrogen and stored at -80°C until protein precipitation and analysis (Section 4.3.5).

4.4.9 EX VIVO MICRODIALYSIS

Following removal of lungs at the point of necropsy, lungs were dialysed whole as shown in Figure 4.9. The syringe pump was set up as described in Chapter 3 and CMA 20 probe (10mm, 20kDa) was inserted into the lung. The syringe contained T1 perfusion fluid with a flow rate of 2µl/min and a single sample was collected at 30 minutes.

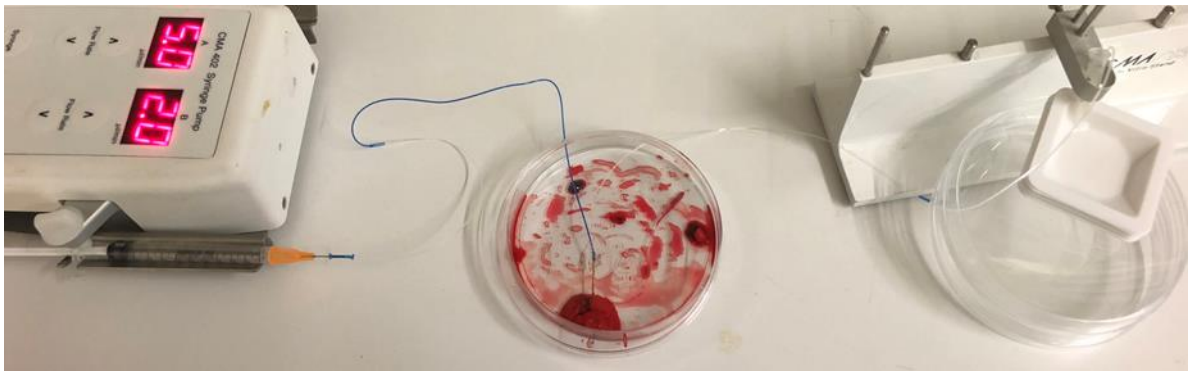

FIGURE 4.9: EX VIVO MICRODIALYSIS SET UP. The syringe pump contained a 1ml syringe containing T1 perfusion fluid. The syringe was connected to blue inlet tubing. The CMA20 probe was inserted into the lungs and the outlet tubing was placed in a collection vial for 30 minutes.

4.5 PILOT IN VIVO MICRODIALYSIS EXPERIMENT

Prior to performing *in vivo* microdialysis an additional *in vitro* calibration was conducted using an equipment set-up that reflected that of the final *in vivo* set-up (including the liquid swivel). The lag time was calculated to be 3 minutes 36 seconds (same as Chapter 3). *in vivo*, the lag time is calculated from the point of sample collection within the guinea pig (i.e. the time taken for the perfusion fluid to flow down inlet tubing is discounted). As 20cm of additional tubing was added to the outlet tubing (to enable tubing to be threaded up through harness spring) the total outlet tubing was the same length (40cm) as the combined length of the inlet and outlet tubing for *in vitro* calibrations. This calibration showed that the probe was working at 30% efficiency (data not shown) which was concordant with the probe efficiency as calculated using the *in vitro* set up described in Chapter 3 (21±9%).

The microdialysis equipment was set up as shown in Section 4.4.7. The two guinea pigs arrived on site at least 72 hours before the commencement of the procedures. Both guinea pigs underwent the surgical protocol under anaesthesia as detailed in Section 4.4.3 for probe implantation into the sacrospinalis (Figure 4.10). Guinea pigs were placed into their home cages where they remained for the duration of the experiment. Approximately two hours post-surgical completion, a rifampicin flush was conducted to ensure probe patency and limit non-specific binding (Section 4.4.7). This was then repeated later that day and twice the following day. Eight hours post-surgery (and in subsequent eight hour intervals) guinea pigs were administered buprenorphine via subcutaneous injection. 24 hours post-surgery guinea pigs were administered carprofen. Throughout this recovery period the guinea pigs were constantly observed remotely via a camera and twice- daily health checks were performed in person when the microdialysis probes were flushed (Section 4.4.6).

Guinea pigs were dialysed on day 3 post-surgery following a one hour pre-flush with warmed T1 perfusion fluid. Oral drug administration of a single 50mg/kg rifampicin dose (Chapter 2) occurred following the one hour pre-flush. The following *in vitro* optimised microdialysis parameters were used:

Probe	(*in situ*) CMA 20, 10mm Membrane, 20kDa Mw Cut-Off
Perfusion Fluid	T1 warmed to approximately 39°C; guinea pig body temperature.
Tubing	(*in situ*) FEP Tubing for Microdialysis
Flow Rate	2µl/minute
Sample Storage	Samples were stored on ice throughout the experiment and stored at -80°C until point of analysis.
Pre-collection Flow	1 hour at 2µl/minute prior to drug administration with T1 perfusion fluid. It was important not to stop the flow to allow sufficient sample volume for 30 minute sample.
Number of samples	8 per guinea pig, samples were collected every 30 minutes.

TABLE 4.3:MICRODIALYIS PARAMETERS USED FOR IN VIVO EXPERIMENT

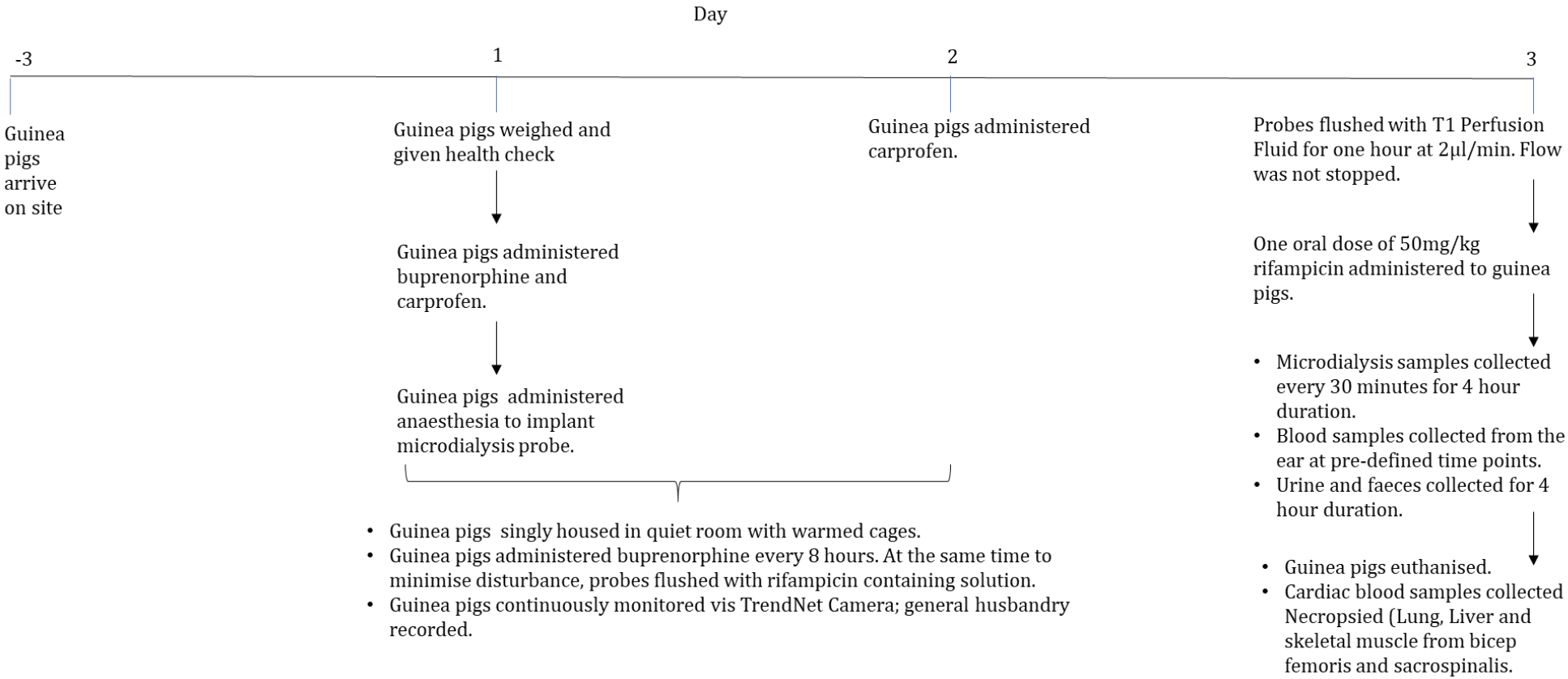

FIGURE 4.10: STUDY SCHEDULE FOR IN VIVO MICRODIALYSIS EXPERIMENT. Guinea pigs arrived on site at least 72 hours before the first procedure. On day 1 guinea pigs underwent surgery for probe implantation, and on day 3 guinea pigs underwent *in vivo* microdialysis following oral administration of 50mg/kg rifampicin.

During the dialysis period, ear bleeds were collected at set time points post drug administration (Section 4.4.1) to provide a control. As guinea pigs were singly housed, all urine and faeces from the individual guinea pigs were collected over the four-hour microdialysis experiment (Section 4.4.8).

Following completion of the four-hour dialysis experiment, guinea pigs were euthanised, cardiac bled and lungs, liver and skeletal muscle from the hind leg and sacrospinalis removed (Section 4.3.4) with the following modification; the guinea pig was initially placed on its front, sprayed with IPA and an incision made along the spine. The sacrospinalis was removed using sterilised scissors and forceps. Following necropsy, lungs were dialysed prior to homogenisation as in Section 4.4.9. Organ samples were processed as in Section 4.3.5, and blood, organ samples and microdialysis samples were analysed for drug concentrations as in Chapter 3.

4.5.1 CONCLUSIONS FOLLOWING PILOT STUDY

Both guinea pigs tolerated the surgery and analgesia well. The recovery period was adequate with no need to elongate for future studies. This pilot study also confirmed there was adequate healing time to enable handling of guinea pigs for collection of ear bleeds. The Named Veterinary Surgeon examined the guinea pigs and had no cause for concern. Rifampicin was recovered in all microdialysis fractions following microdialysis in the sacrospinalis of one guinea pig which confirmed that the microdialysis equipment and methods established in Chapter 3 were applicable *in vivo*.

Upon necropsy it was shown that the probe was implanted correctly. For the other guinea pig, it was evident that there was no probe patency on day 2 as no liquid was recovered. This guinea pig was still administered one oral dose of rifampicin and culled at 2 hours post drug administration to add data to the correlation data set (Chapter 5). Upon necropsy it was evident that the probe had snapped *in situ* as shown in Figure 4.11. All organs from both guinea pigs contained rifampicin, as did the sample collected via *ex vivo* microdialysis.

FIGURE 4.11: PROBE SNAPPED IN SITU. The red box indicates the head of the probe, the shaft and membrane tip are missing, and it was clear as to why the probe showed no evidence of patency in Guinea Pig B.

Following completion of the pilot study, several refinements were made prior to conducting subsequent experiments (which are detailed in Chapter 5):

- Cage sides were covered to ensure they were opaque and cages sides were elongated with wire to restrict any possible vertical movement.
- Cages were truncated to relieve additional pressure on the balance arm.
- Guinea pigs were handled throughout the pilot experiment to administer analgesia. It was decided that for the subsequent study to minimise handling when administering analgesia.
- The ability to handle the guinea pigs throughout the study duration gave confidence that the guinea pigs could be handled to conduct ear bleeds without causing them any additional pain.
- Probes were flushed for evidence of patency at point of analgesia administration (every 8 hours) removing the need for additional entrance into the housing room.
- Once the guinea pig was secured in the harness, the straps were trimmed, as it was shown that the straps were in the guinea pigs eyeline causing irritation.
- Lower food and water bowls were used to ensure ease of access.

CHAPTER 5

EVALUATION OF RIFAMPICIN PK IN GUINEA PIGS USING MICRODIALYSIS

5.1. INTRODUCTION

Microdialysis can be used to describe the pharmacokinetic behaviour of drugs in organs as a continuous sampling technique, in awake freely moving animals. Microdialysis is the only methodology available to collect the unbound pharmacologically active portion of the drug. Traditional methodologies for pharmacokinetic analysis such as blood collection are a measurement of total drug concentrations (unbound and bound). The aim of this PhD was to develop the microdialysis methodology for use with rifampicin to determine the organ PK of this drug over a four-hour time period in an awake freely moving guinea pig and compare the results gained via the microdialysis methodology with those gained via traditional methods.

Meticulous *in vitro* microdialysis experiments were performed with rifampicin before progressing to *in vivo* experiments because drug recovery (concentration of the drug in the tissue related to that in the collected dialysate) is dependent upon a variety of experimental and environmental conditions. The impact of flow rate, temperature, perfusion fluid, molecular weight cut-off and tubing materials on the recovery of rifampicin at physiologically relevant concentrations were determined using mass spectrometry to measure rifampicin concentrations in the dialysate (Chapter 3). *In vitro* calibrations with rifampicin have shown that the efficiency of the probe is 21% ± 9%. Rifampicin was recovered from tissue homogenates at the concentrations expected and following difficulties associated with insertion of the probe into the guinea pig lung and liver, experiments were conducted to investigate skeletal muscle as a surrogate for lung microdialysis. A correlation (R^2 = 0.8718) was identified between rifampicin concentrations in the lung and skeletal muscle with stable ratios of drug between the two organs (Chapter 4). It was therefore determined that using microdialysis to quantify the unbound pharmacologically active part of rifampicin in the

skeletal muscle would enable the unbound concentration of rifampicin to be quantified in the lung, the main target site for drug delivery during tuberculosis disease.

An initial pilot *in vivo* microdialysis experiment was conducted with two guinea pigs (Chapter 4). Guinea pigs tolerated the surgery well and were healthy throughout the duration of the experiment. Unbound rifampicin was collected every 30 minutes over a four-hour duration from the skeletal muscle (sacrospinalis) of one guinea pig. Rifampicin was detectable in all collected fractions. Total rifampicin concentrations measured in the lung and skeletal muscle were added to the pre-existing correlation data set (Chapter 4).

Having proven that the microdialysis technique could be successfully applied, further experiments were performed to provide a complete data set in order to determine the PK of rifampicin in the target organ (lung) via microdialysis of skeletal muscle to compare organ PK profiles with those obtained in peripheral blood. Technical refinements discussed in Chapter 4 were incorporated into the additional experiments.

The data presented and analysed in this chapter include the measurements from experiments described in Chapter 4.

5.2. EXPERIMENTAL OVERVIEW

The experimental schedule shown in Figure 4.10 (Chapter 4) was followed. Each guinea pig was attributed a letter (A-F). A total of six guinea pigs underwent surgery to have a microdialysis probe (CMA20, 10mm, 20kDa) implanted into the sacrospinalis on Day 1 (as described in Chapter 4). The surgery and microdialysis were performed on pairs of guinea pigs. All six guinea pigs tolerated the surgery, anaesthesia and recovery well, subcutaneously administered buprenorphine (every 8 hours) and carprofen (every 24 hours) was used successfully for pain relief with no adverse effects.

Consistent with the pilot study, all guinea pigs showed evidence of movement, vocalisation, food and water intake and urine and faeces output. As previously noted, due to guinea pigs being a prey species, when physically in the room with them, guinea pigs limited their

movement. Observation of the guinea pigs through the TRENDnet system showed the guinea pigs eating, drinking and being significantly more mobile. An additional benefit to observing the guinea pigs remotely was that it was possible to observe and rectify any discomfort they were experiencing (such as a too tight harness). The guinea pigs were seen by the Named Veterinary Surgeon and Home Office Inspector with no cause for concern.

The rifampicin-containing solution for *in situ* probe flushing and the rifampicin for oral administration were prepared separately for each pair of guinea pigs. The microdialysis equipment was set up as described in Chapter 4 and checked to ensure it was working as expected i.e. correct volume of sample being collected. The *in situ* probes were flushed with the rifampicin-containing solution every 8 hours at the point of buprenorphine administration to ensure probe patency and to minimise adherence of rifampicin to plastic (as described in Chapter 3). On Day 3 (Day 2 post- surgery), the syringe pump was switched on in order to flow at 2µl/minute for one hour prior to the dialysis period with T1 perfusion fluid to ensure equilibration of the perfusion fluid with the surrounding muscle and sufficient sample volume for the 30 minute sample.

Four of the six guinea pigs were successfully dialysed for four hours, with samples collected every 30 minutes following oral administration of 50mg/kg rifampicin. Samples were analysed via LC-MS/MS as described in Chapter 3. Microdialysis sample volumes were sufficient for analysis, and rifampicin was recovered in all of the collected fractions. One of the guinea pigs died at the point of drug administration (Guinea Pig C) and was subsequently diagnosed as having unexpected heart failure. Upon histological examination, all examined tissues were normal including the probe implantation site which had no associated inflammation. The other guinea pig (Guinea Pig B) showed no evidence of probe patency on Day 2, however it was successfully administered drug and necropsied at two hours post drug administration with a view to add additional data to the correlation data set. This was particularly important because the outlying datapoint in Figure 4.3 (Chapter 4) was from a guinea pig that was culled at two hours post drug administration. At the point of necropsy it was evident that the probe had snapped *in situ* (Chapter 4).

The five guinea pigs (A, B, D, E, F) were bled from the ear at pre-defined time points to time match the microdialysis fractions. It was possible to handle these animals, in a controlled manner, to enable ear bleeding. Rifampicin was not recovered in all ear bleed samples. Urine and faeces were collected during the four-hour dialysis period, and the volume and time of excretion were recorded. Upon necropsy it was evident that all probes had been successfully implanted into the sacrospinalis. Guinea pigs were cardiac bled and lungs, livers and two types of skeletal muscle (collected from the biceps femoris and sacrospinalis) were removed, weighed and processed as described in Chapter 4.

5.3. IN VIVO MICRODIALYSIS RESULTS

5.3.1 RIFAMPICIN RECOVERED IN SACROSPINALIS

The rifampicin concentrations (μg/ml) recovered from the sacrospinalis from the four dialysed guinea pigs are shown in Figure 5.1.

No samples were collected at 30 and 60 minutes post drug administration for Guinea Pig D. The probe showed patency when flushed with the rifampicin-containing solution and during the one-hour pre-drug administration flush, however at the point of oral drug administration, upon handling the guinea pig, the outlet tubing had to be trimmed because it was causing an obstruction. The process of trimming the tubing caused it to be crushed such that no liquid was collected. Re-cutting the tubing with a scalpel rectified this and samples were collected from 90 minutes onwards.

The data shown in Figure 5.1 indicated that there was a similar profile of change in rifampicin concentrations over time in all 4 guinea pigs. Samples from Guinea Pigs E and F contained the approximately the same concentrations at 30 and 60 minute time points (E; 132 and 65μg/ml F; 126 and 72μg/ml). The recovered rifampicin concentrations in Guinea Pigs D and F were very similar between 120 and 240 minutes.

Whilst the kinetics (change over time) of the datasets from each of the four guinea pigs was similar, there were variations in the actual values. As mentioned, samples from Guinea Pigs D and F contained similar quantities of rifampicin between 120 and 240 minutes (D; 40, 32, 35, 27, 25μg/ml and F; 38, 28, 32, 21,19μg/ml) but these concentrations were higher than those recovered from Guinea Pigs A (17, 14, 17, 12, 17μg/ml) and E (21, 19, 15, 10, 11μg/ml) with the exception of the higher drug concentration at the 30 minute time point associated with Guinea Pig A (250μg/ml).

As previously described, the efficiency of the probe was calculated to be 21±9% by *in vitro* studies (Chapter 3). Hence, the measured unbound concentrations of rifampicin in these samples (Figure 5.1) were used to calculate the estimated concentration of unbound drug by

correcting for the efficiency of the probe, which therefore represented an estimate of the actual unbound rifampicin concentration expected *in vivo* in the sacrospinalis. This is shown in Figure 5.2 where the mean rifampicin concentrations from the sacrospinalis of all 4 guinea pigs was plotted either at the measured concentration (21%±9%) or at the estimated concentrations with the corrected values to account for probe efficiency. Applying this correction factor resulted in an increase in mean rifampicin concentrations from 170μg/ml to 809μg/ml at 30 minutes and 18μg/ml to 87μg/ml at 240 minutes. Note this is only the concentration of unbound rifampicin.

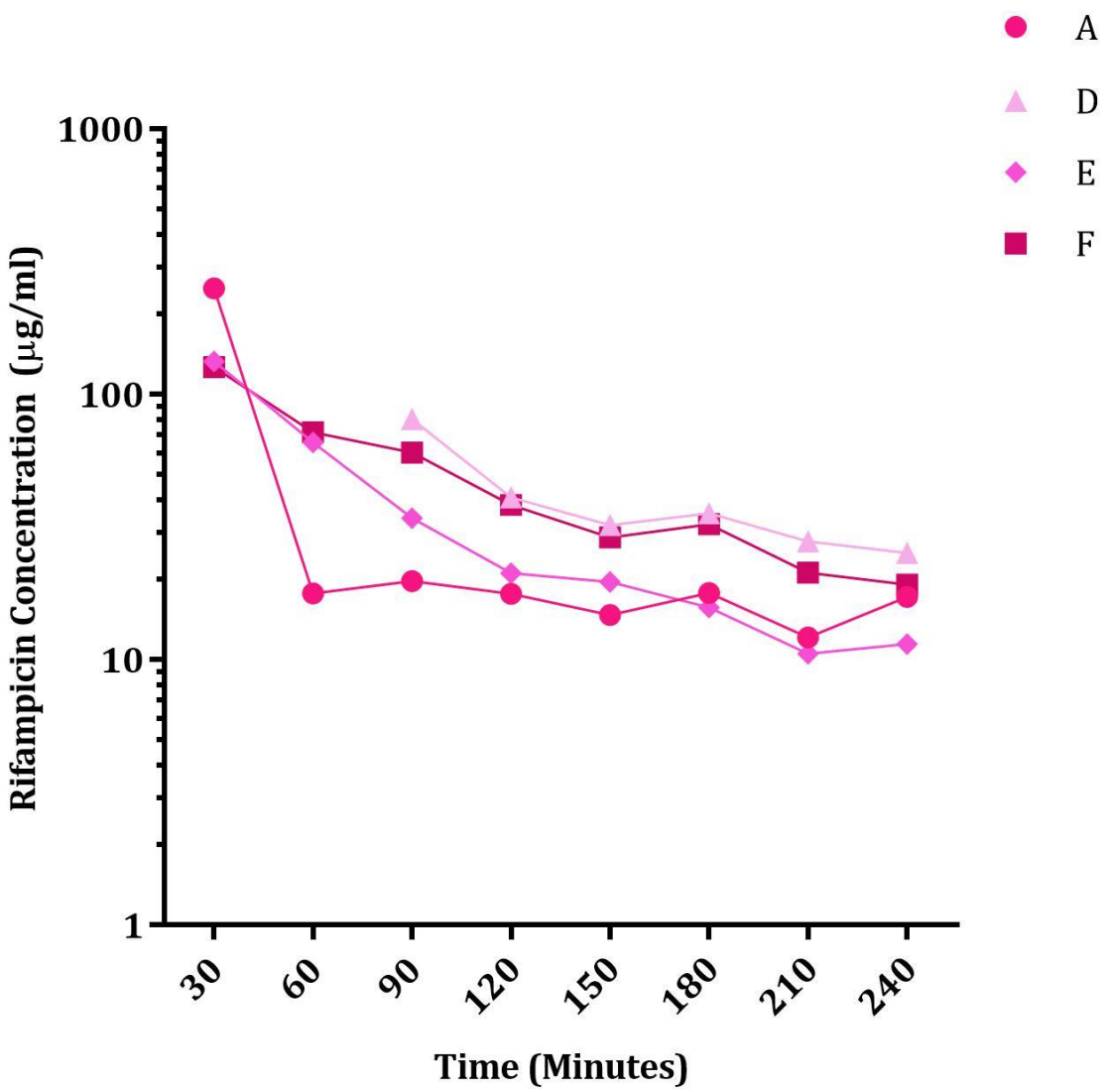

FIGURE 5.1: RIFAMPICIN CONCENTRATIONS RECOVERED FROM SACROSPINALIS. Fractions were collected over a four-hour (240 minute) period from four guinea pigs (A, D, E, F) every 30 minutes. The measured rifampicin concentrations in each fraction are shown.

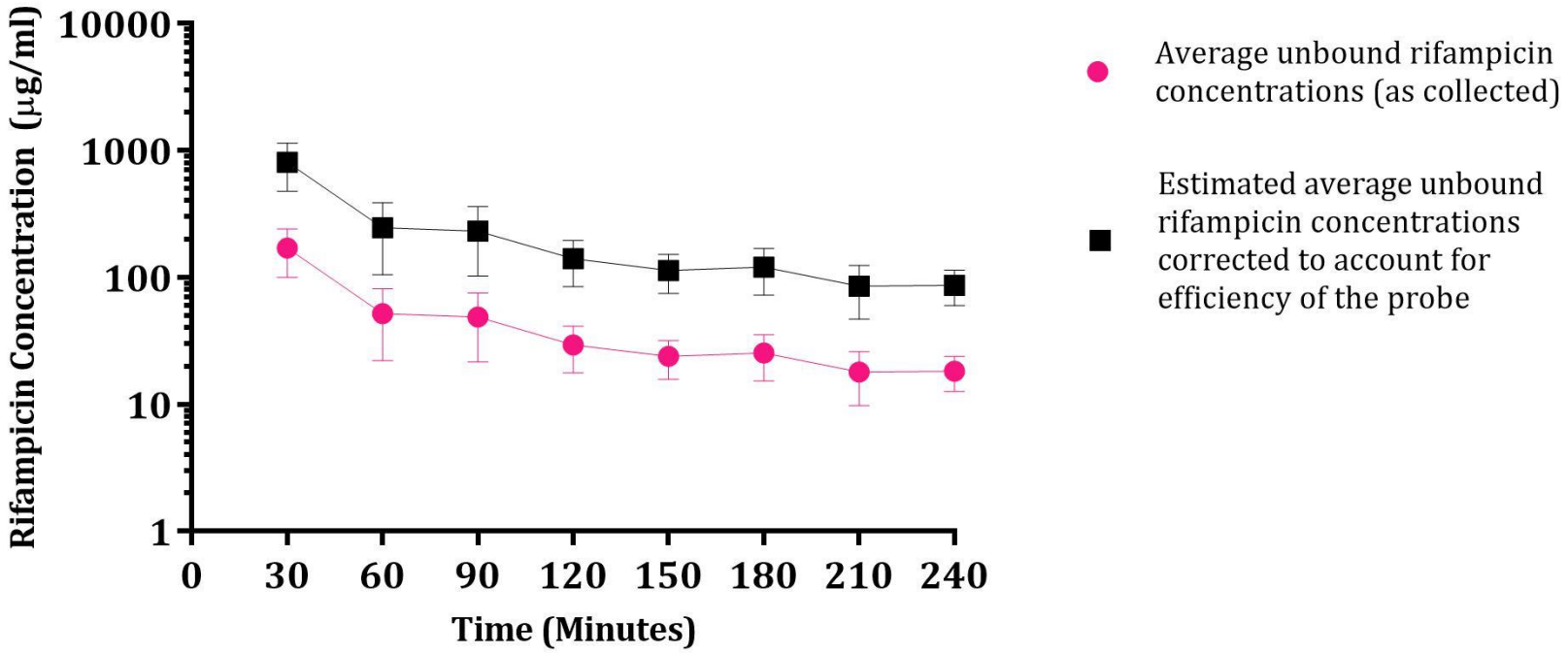

FIGURE 5.2: MEAN RECOVERED UNBOUND RIFAMPICIN CONCENTRATIONS (µG/ML) as collected via microdialysis from all four guinea pigs with a probe efficiency of 21±9% (pink line) and the corrected values of estimated unbound rifampicin concentrations to account for the probe efficiency (black line). Error bars show the standard deviation.

5.3.2 RELATIONSHIP BETWEEN RIFAMPICIN CONCENTRATIONS MEASURED BY MICRODIALYSIS AND TOTAL DRUG IN SACROSPINALIS

At the point of necropsy, the sacrospinalis was collected and processed to measure both bound and unbound rifampicin concentrations in order to relate these data to the unbound rifampicin concentrations collected via microdialysis. This comparison was conducted between samples collected at the four-hour (240 minute) time point.

Figure 5.3 shows the rifampicin concentrations associated with the sacrospinalis (for each guinea pig). The rifampicin concentration in the sacrospinalis was measured following removal and homogenisation at 240 minutes. The unbound rifampicin available to collect via microdialysis was calculated assuming that 31% of the total measured rifampicin in the sacrospinalis was unbound, as rifampicin is 69% plasma protein bound and this was assumed to be equivalent to tissue binding. The mean unbound rifampicin concentrations as collected at 240 minutes with the probe operating at 21±9% efficiency and the estimated rifampicin concentrations corrected for probe efficiency are also shown.

The rifampicin concentrations in the sacrospinalis were most similar between Guinea Pigs A & F (20 and 22μg/ml respectively) and D & E (10 and 6μg/ml respectively). The unbound rifampicin, measured at 240 minutes with the probe operating at 21% efficiency, was approximately 150% higher than the total rifampicin concentrations measured in the sacrospinalis for Guinea Pig D and approximately 83% higher for Guinea Pig E. For Guinea Pigs A and F, the unbound rifampicin collected with the probe operating at 21% efficiency at 240 minutes, was 17μg/ml and 19μg/ml respectively which is approximately 3 times higher than the rifampicin that was available for collection based upon 69% protein binding. When adjusting the measured unbound concentrations to account for probe efficiency, the unbound rifampicin concentrations associated with the sacrospinalis are much higher than expected for all guinea pigs based upon total rifampicin concentrations in the sacrospinalis (approximately 4 times the total concentration for Guinea Pigs A and F, 9 times the total concentration for Guinea Pig E and 12 times the total concentration for Guinea Pig D).

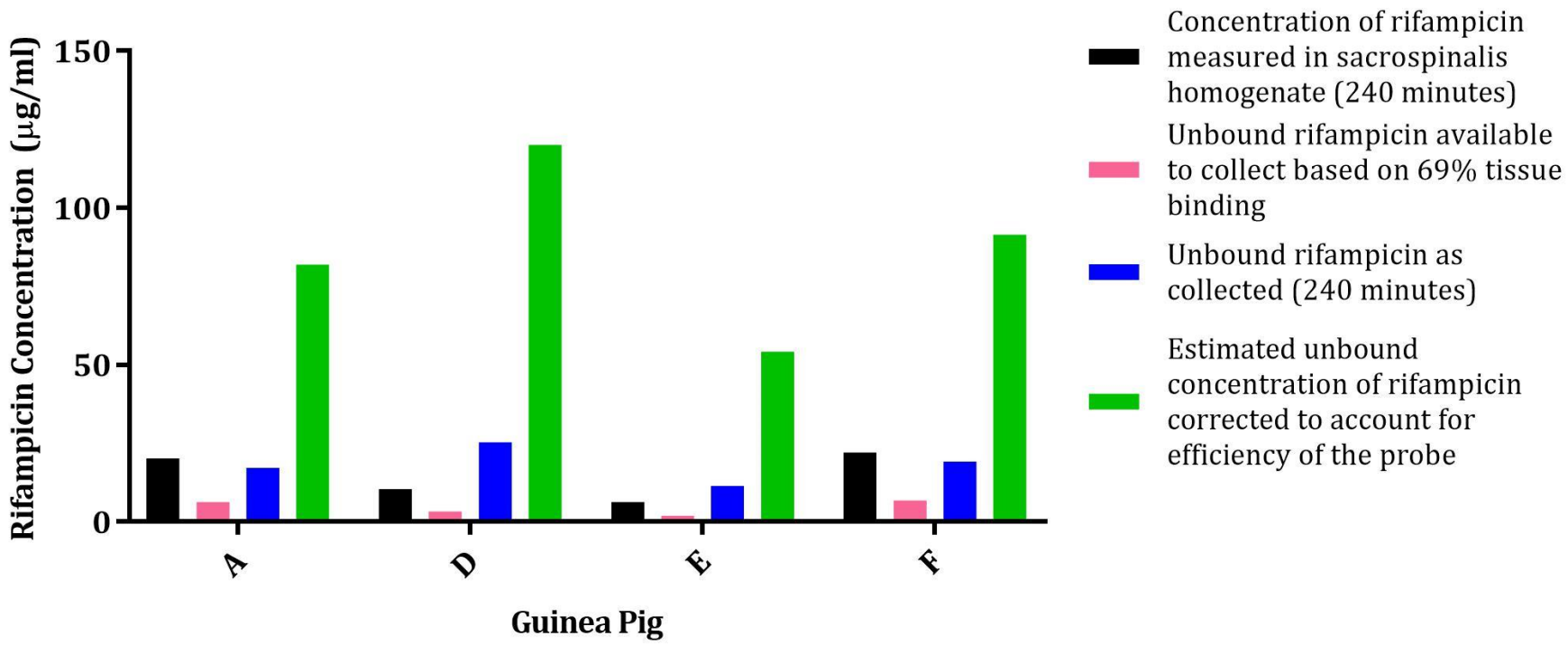

FIGURE 5.3: RIFAMPICIN CONCENTRATIONS (µG/ML) IN SACROSPINALIS. Black bars represent rifampicin concentrations measured in the sacrospinalis homogenate following necropsy at 240 minutes, pink bars represent unbound rifampicin available to collect based on 69% plasma protein binding, blue bars represent the unbound rifampicin concentration as collected via microdialysis at 240 minutes whilst the probe was operating at 21% efficiency (equivalent time point to sacrospinalis collection time point), green bars represent estimated unbound rifampicin concentration in sacrospinalis corrected for probe efficiency.

5.3.3 RELATING SACROSPINALIS CONCENTRATIONS TO LUNG CONCENTRATIONS

5.3.3.1 CORRELATION BETWEEN SKELETAL MUSCLE AND LUNG- ADDITIONAL DATA

In Chapter 4, a correlation was identified between the concentration of rifampicin in the lung and the biceps femoris (skeletal muscle in the hind leg). This relationship formed the basis of the rationale to perform microdialysis in the sacrospinalis in order to generate data that could be related to the lungs, the target organ for drugs to treat TB. On completion of the microdialysis experiments described in this chapter, lung and skeletal muscle samples were taken at necropsy, after the final 240 minute microdialysis sample, and processed and analysed to measure concentrations of rifampicin, using the methods described in Chapter 4. Thus additional data points could be added to the correlation data set and the full data set is shown in Figure 5.4A.

The Pearson correlation R^2 value of the data shown in Figure 5.4A was 0.4696 (P value = 0.02). The strength of this correlation was weaker than that obtained with a minimal data set (Chapter 4), however the second order polynomial fitted the data well with an R^2 value of 0.8432. There was a notable outlying data point which contrasted with the data set as a whole by the fact that the concentration of rifampicin was the same (29.20µg/ml) in both lung and skeletal muscle, whereas the lung concentration was generally found to be higher than in the skeletal muscle in all other guinea pigs. Additionally, with this data point included, when the rifampicin concentration in the skeletal muscle was greater than 20.4µg/ml the concentration in the lung decreased, which was an unlikely scenario.

Removing the outlying data point strengthened the correlation (Pearson R^2 = 0.8595 (P value = 0.0001)) and a second order polynomial also fitted these data well (Pearson R^2 =0.8735 (data not shown)). However, the unlikely scenario described above of high skeletal muscle concentrations equalling decreasing lung concentrations remained when the data was fitted with the second order polynomial. In this case, skeletal muscle rifampicin concentrations over 35µg/ml calculated negative rifampicin concentrations in the lung. Therefore, linear

interpolation was used to fit the data with R^2 value of 0.8595 (Sy.x=6.91) as shown in Figure 5.4B. Although there was one outlier excluded from this data set, data from all other guinea pigs was incorporated.

The equation generated by fitting the data with linear interpolation, as shown Figure 5.4B, was used to estimate the rifampicin concentrations in the lung as calculated from the measured rifampicin concentrations within the skeletal muscle (sacrospinalis). This equation gave realistic lung concentrations at high skeletal muscle concentrations (primarily 30 minute skeletal muscle concentrations as shown in Figure 5.1).

The equation used was:

$$Y = B0 + B1 * X$$

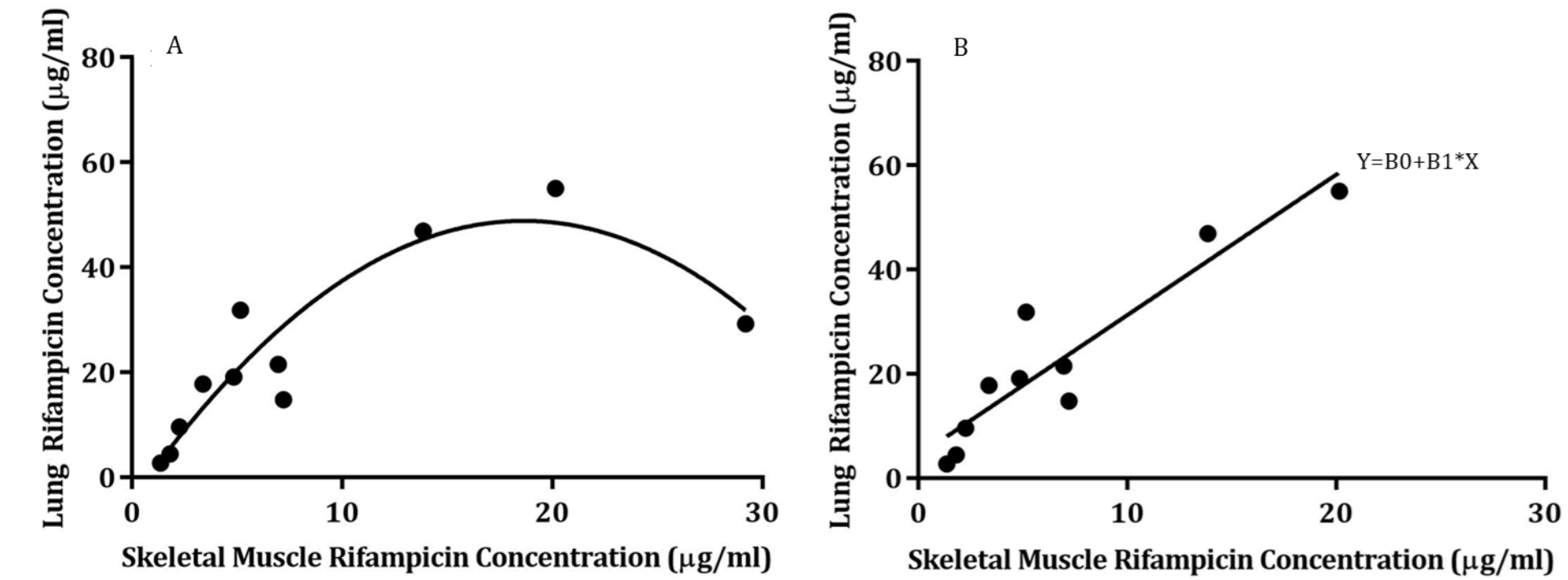

FIGURE 5.4: A; CORRELATION BETWEEN RIFAMPICIN CONCENTRATIONS MEASURED IN LUNG AND BICEPS FEMORIS (SKELETAL MUSCLE FROM HIND LEG). All data points are shown from experiments described in chapter 4 and the animals used for in vivo microdialysis. B; CORRELATION BETWEEN RIFAMPICIN CONCENTRATIONS MEASURED IN LUNG AND BICEPS FEMORIS (SKELETAL MUSCLE FROM HIND LEG). Data from pre-existing correlation data set as shown in Chapter 4 and from guinea pigs used for in vivo microdialysis. Data point at 29.20μg/ml in both lung and skeletal muscle removed. Data fitted with linear interpolation and the following equation generated; Y=B0+B1*X, where B0= 4.317, B1= 2.695, X= unbound rifampicin concentration (μg/ml) recovered from sacrospinalis can be used to calculate Y, the estimated unbound rifampicin concentration in lung (μg/ml).

5.3.3.2 ESTIMATED LUNG CONCENTRATIONS OF RIFAMPICIN FROM MICRODIALYSIS OF SKELETAL MUSCLE

Using the equation generated by linear interpolation of the data points (Figure 5.4B) (Y=B0+B1*X), Y which is the estimated unbound rifampicin concentration (μg/ml) in the lungs could be calculated using the equation constants generated by GraphPad Prism (B0= 4.317 (±3.381), B1= 2.695 (±0.38)) and the unbound rifampicin concentration (μg/ml) recovered from sacrospinalis (X). It is important to note that the data set in Figure 5.4B is comprised of total rifampicin concentrations measured in the organs whereas samples collected via microdialysis contain only the unbound pharmacologically active rifampicin. An assumption has been made that the relationship between the lung and skeletal muscle associated with total drug concentrations will remain the same for unbound drug concentrations. Therefore, it was valid to extrapolate unbound drug concentrations in the lung from unbound drug concentrations measured in the skeletal muscle by microdialysis.

Rifampicin concentrations measured via microdialysis from the sacrospinalis (21% probe efficiency) were thus used to calculate the unbound rifampicin concentrations in the lung (Pink line; Figure 5.5). An estimate of actual *in vivo* rifampicin concentrations in the lung was made by correcting for probe efficiency. This is the gold line in Figure 5.5. Rifampicin is 69% protein bound in guinea pigs therefore a further adjustment was made to estimate the total (B+UB) rifampicin concentrations in the lung (Black line; Figure 5.5).

Mean rifampicin concentrations in the lung from all four guinea pigs, over the 240 minute dialysis period, are shown in Figure 5.5.

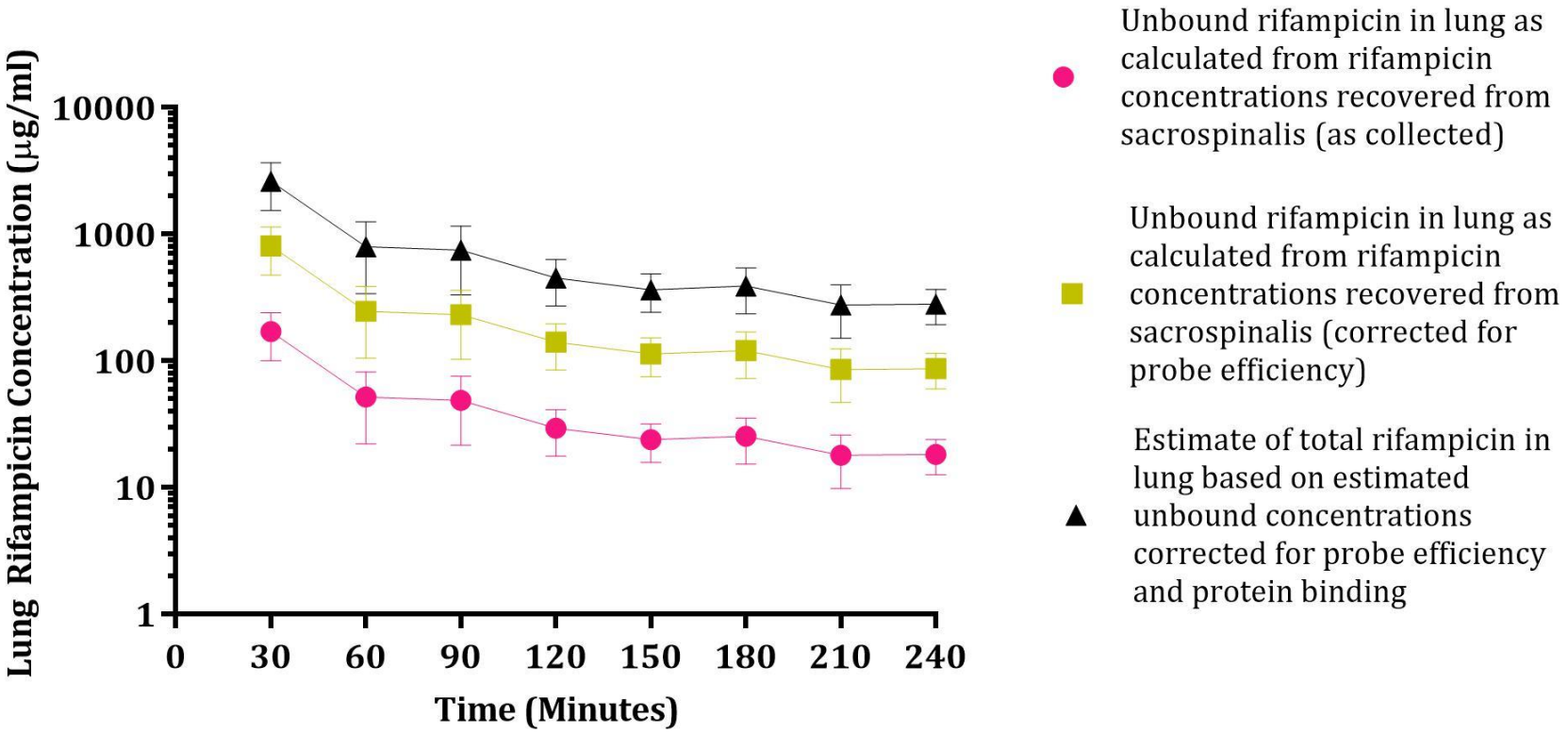

FIGURE 5.5: MEAN LUNG CONCENTRATIONS (µG/ML) GENERATED USING THE EQUATION Y=B0+B1*X. Pink line shows unbound rifampicin in lung calculated from the unbound rifampicin concentrations recovered from the sacrospinalis. Gold line represents estimated unbound rifampicin concentrations in the lung corrected for probe efficiency. Black line is an estimate of total (B+UB) rifampicin concentrations in the lung based on the estimated unbound rifampicin corrected for probe efficiency and 69% plasma protein binding. Error bars show standard deviation.

5.3.3.3 RELATING ESTIMATED LUNG CONCENTRATIONS TO MEASURED TOTAL LUNG CONCENTRATIONS

Prior to homogenisation, lungs were dialysed *ex vivo* as shown in Chapter 4. One *ex vivo* sample was collected after 30 minutes. Taking these *ex vivo* concentrations, the data generated in Figure 5.5 whereby rifampicin concentrations in the lung were estimated by correlating the measured unbound rifampicin in the sacrospinalis (probe efficiency of 21%) via the equation generated in Figure 5.4B, as well as the measured concentration of total drug in lung tissue at necropsy, it was possible to test the ability of skeletal muscle microdialysis to estimate unbound lung concentrations. These data are shown in Figure 5.6.

The total rifampicin concentration measured in the lung homogenate was lower in each guinea pig (~1.75 times for Guinea Pigs A and D; ~2.5 times for Guinea Pigs E and F) than the estimated unbound rifampicin in the lung at 240 minutes (21% probe efficiency). The estimated unbound lung concentrations were even higher when extrapolated to correct for probe efficiency (~ 8 times for Guinea Pigs A and D; ~12 times for Guinea Pigs E and F) than the total rifampicin measured in the lung homogenate. The estimated unbound rifampicin concentrations in the lungs were generally higher than the concentrations collected via *ex vivo* microdialysis (at equivalent probe efficiencies), however, the estimated concentration in the lung and the measured *ex vivo* concentrations of unbound rifampicin were similar (44, 31 and 28μg/ml unbound rifampicin collected *ex vivo* for Guinea Pigs D, E and F respectively; 72, 35, and 56μg/ml unbound rifampicin as estimated in lungs (UB by correlation) for Guinea Pigs D, E and F respectively at 21% probe efficiency).

The unbound concentration of rifampicin in the lung as collected directly from the pre-homogenised lung *ex vivo* (21% probe efficiency) was on average 1.5 times higher, than the total concentrations for Guinea Pigs D, E and F. The concentration recovered *ex vivo* was lower for Guinea Pig A than for the other three guinea pigs, which may be an exceptional result when considering the similarities between all animals with respect to the total rifampicin in the lung homogenate and the estimated concentrations in the lung based on microdialysis data. When the concentrations were corrected for probe efficiency, the unbound concentrations (as

collected via *ex vivo* microdialysis) were 1.6, 5.3, 10.6 and 6.5 times higher (for Guinea Pigs A, D, E and F respectively) than the total for all animals. This indicated that the total rifampicin concentration measured in the lung homogenate was unexpectedly low when compared to the estimated unbound rifampicin concentration in the lung as calculated by sacrospinalis microdialysis *in vivo* and also lower than the unbound rifampicin collected by *ex vivo* microdialysis.

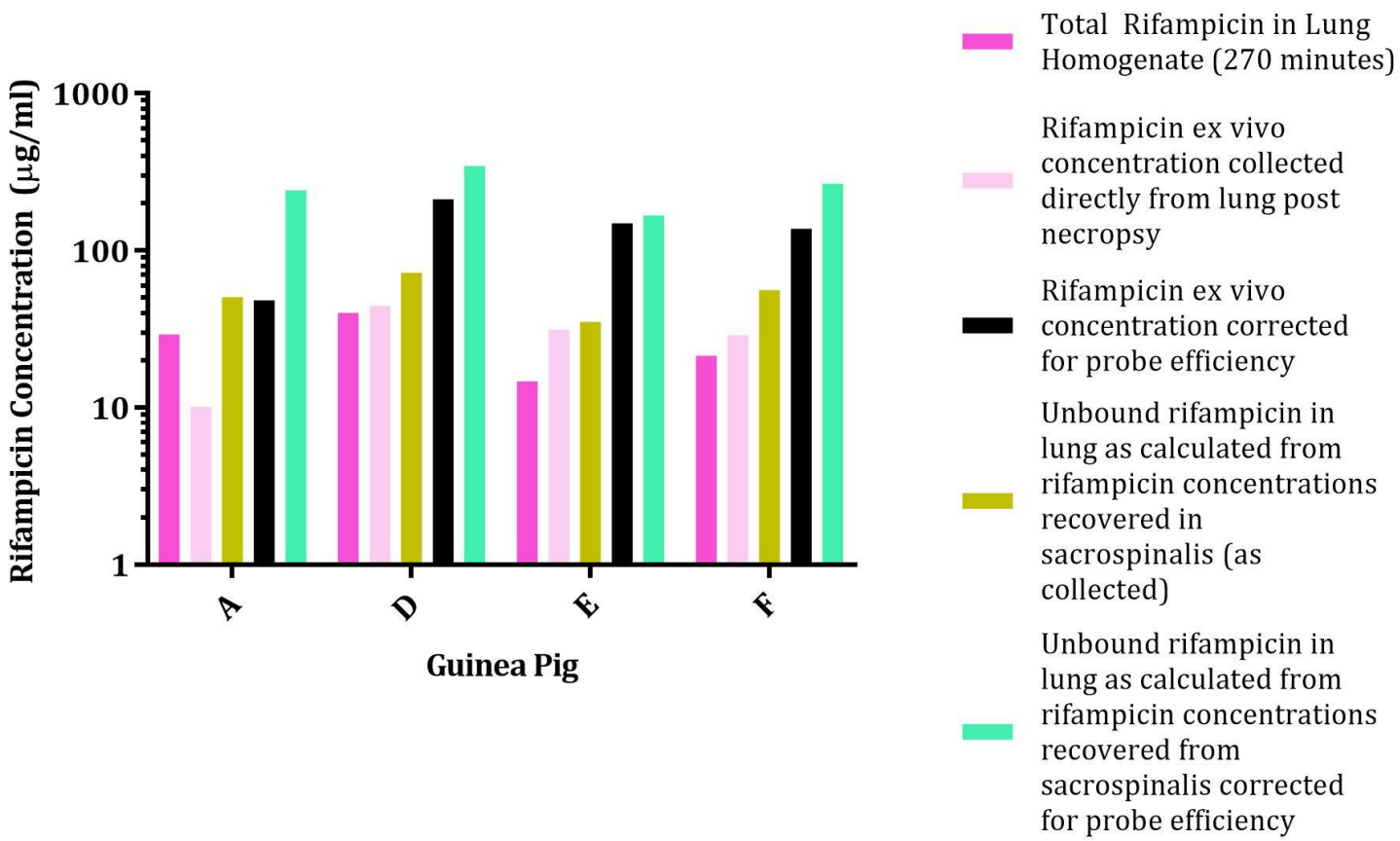

FIGURE 5.6: RIFAMPICIN CONCENTRATIONS (µG/ML) IN THE LUNG. Dark pink bar represents the total (bound and unbound) rifampicin in the lung homogenate collected at necropsy at 240 minutes and then dialysed for an additional 30 minutes prior to homogenisation. Light pink bar is the unbound concentration of rifampicin recovered from the lung via ex vivo microdialysis post necropsy and pre-homogenisation with the probe operating at 21% efficiency and the black bar is the estimated ex vivo unbound rifampicin concentration corrected for probe efficiency. One sample was collected at 30 minutes. Gold bar is the lung concentration of rifampicin at the 240 minute time point as calculated from the unbound rifampicin concentrations recovered from the sacrospinalis using the 21% efficiency value and the aquamarine bar is the concentration corrected for probe efficiency.

Total (B+UB) rifampicin concentrations in the lung from dialysed guinea pigs were compared against total rifampicin concentrations in the lungs of guinea pigs that were not dialysed (animals used for the study described in Chapter 4) to understand if the removal of drug via microdialysis was causing the total rifampicin concentrations in the lung to be lower than expected. The concentrations of rifampicin measured in the lungs of the two un-dialysed guinea pigs, at 4hours post 50mg/kg rifampicin administration, were 17.7 and 2.7µg/ml. These data indicate that the total rifampicin concentrations measured in the lung homogenate of Guinea Pigs A, D, E and F are not lower than expected, when related to the estimated unbound rifampicin concentrations, because of the microdialysis methodology. These data also demonstrate the animal to animal variation associated with measuring drug concentrations in homogenate, whereas the concentrations measured via microdialysis are much more reproducible.

5.3.3.4 COMPARISON OF HOMOGENATE VS ESTIMATED LUNG AND SACROSPINALIS CONCENTRATIONS

In addition to measuring the total rifampicin concentration in the lungs removed at necropsy, the total drug in the sacrospinalis was also measured. It was thus possible to compare the measured total concentrations of drug in these two organs, and to relate these values to those estimated by *in vivo* microdialysis. The data shown in Figure 5.7 are total (B +UB) rifampicin concentrations as measured in the organ homogenate or an estimated total (B+UB) rifampicin concentration based on the unbound rifampicin concentrations collected via microdialysis at 240 minutes post-drug administration. The measured unbound concentrations have been corrected for probe efficiency and 69% protein binding.

Figure 5.7 shows that the rifampicin concentrations measured in the homogenate were similar between the lung and sacrospinalis at the 240 minute time point, although (apart from Guinea Pig F) there was a tendency for the lung concentration to be higher (between 1.4 to 4 times) than that measured in the muscle. When comparing the homogenate concentrations of rifampicin with the estimated concentrations of rifampicin based on microdialysis data, it is

evident, in both organs, that the total concentration as measured in the homogenate was lower than expected.

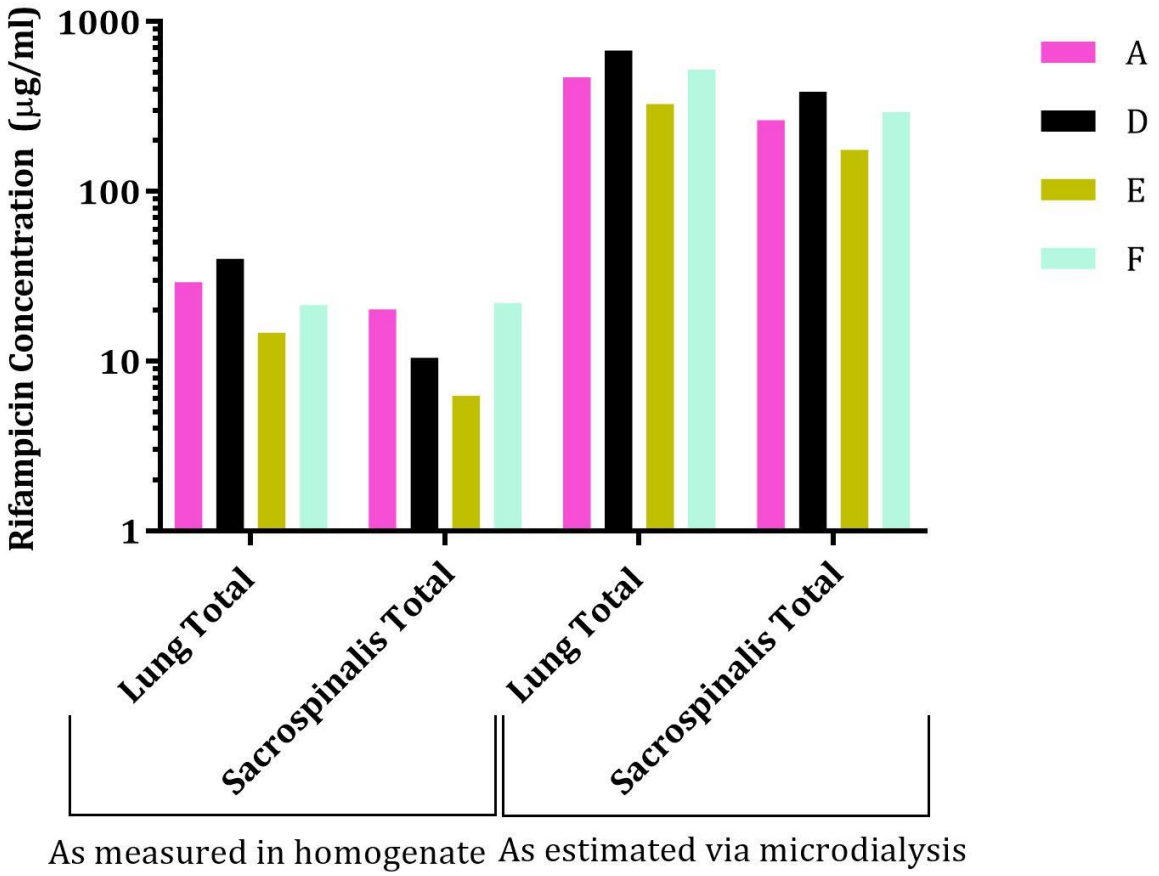

FIGURE 5.7: TOTAL (BOUND AND UNBOUND) RIFAMPICIN CONCENTRATIONS (µG/ML) IN THE LUNG AND SACROSPINALIS AT 240 MINUTES. Total (B+UB) rifampicin concentrations as measured following necropsy and homogenisation are shown against the estimated total rifampicin concentrations in the organs based on unbound rifampicin concentrations as measured via microdialysis in the sacrospinalis. UB concentrations have been corrected for probe efficiency and 69% protein binding.

5.3.5 COMPARISON OF TOTAL SKELETAL MUSCLE CONCENTRATIONS OF RIFAMPICIN

Muscle is often grouped together for PK modelling as it is assumed that skeletal muscle throughout the body will contain the same concentration of drug. The sacrospinalis and bicep femoris (skeletal muscle from the spine and hind leg respectively) were collected from the dialysed guinea pigs at necropsy. The biceps femoris was the skeletal muscle used to generate the data set in Figure 5.4B and the sacrospinalis was the anatomical location of the probe implantation. Total (bound and unbound) rifampicin concentrations were compared for each guinea pig in Figure 5.8.

When comparing the concentration of rifampicin in the two skeletal muscle samples from the four guinea pigs (Figure 5.8), there were similarities between them, particularly in Guinea pigs A, D and E (sacrospinalis concentrations; 20.2, 10.49 and 6.26μg/ml; biceps femoris concentrations; 29.2, 12.5 and 7.2μg/ml for Guinea Pigs A, D and E respectively). The concentration of rifampicin in the sacrospinalis was slightly lower than in the biceps femoris for Guinea Pigs A, D and E, but this might be explained by the fact that the sacrospinalis muscle was dialysed. Guinea Pig F is the only animal in which the concentration of rifampicin in the sacrospinalis (22.03μg/ml) was higher than the concentration in the biceps femoris (6.96μg/ml). This was likely due to an unexpectedly high concentration of drug in the sacrospinalis, which is supported by the data in Figure 5.7 (lung vs sacrospinalis) where the sacrospinalis concentration of rifampicin in Guinea Pig F was higher than expected, given an overall trend of lower concentrations of drug in the muscle compared to the lung.

When the mean total organ concentrations of rifampicin were compared, as shown in Figure 5.9, the concentration of rifampicin was relatively similar regardless of the anatomical location yet the lung concentration was higher (lung (26.4μg/ml) than the biceps femoris (13.9μg/ml) or sacrospinalis (14.75μg/ml)).

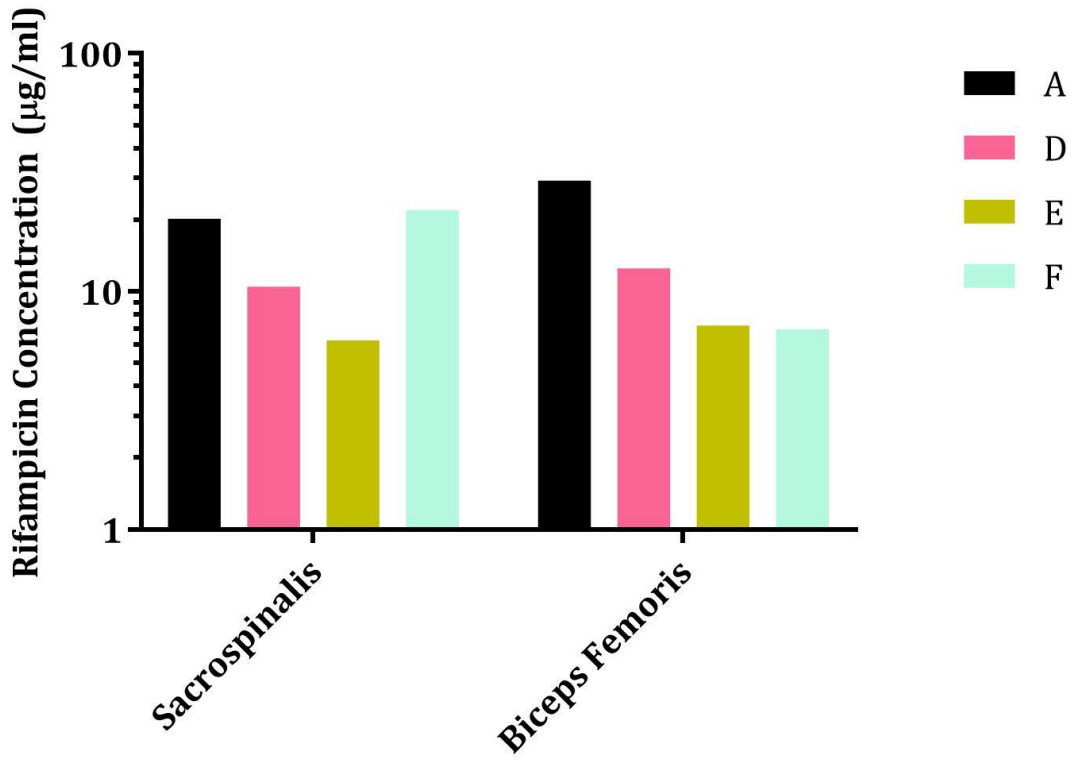

FIGURE 5.8: TOTAL RIFAMPICIN CONCENTRATIONS (µG/ML) IN SKELETAL MUSCLE COLLECTED FROM TWO DIFFERENT ANATOMICAL LOCATIONS. At the point of necropsy the biceps femoris and the sacrospinalis were homogenised, processed and analysed to measure total (bound and unbound) rifampicin concentrations. The concentrations for each guinea pig are shown.

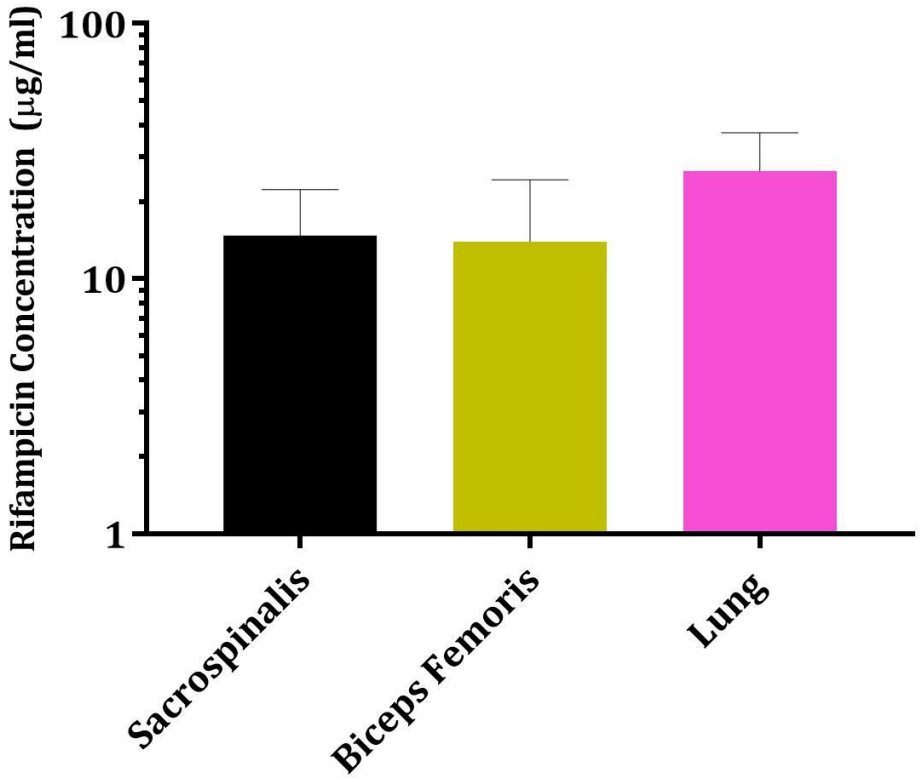

FIGURE 5.9: MEAN RIFAMPICIN CONCENTRATIONS (µG/ML) IN THE TWO DIFFERENT ANATOMICAL SITES OF SKELETAL MUSCLE (BICEPS FEMORIS AND SACROSPINALIS) AND THE LUNG FOR GUINEA PIGS A, D, E AND F. Lungs and skeletal muscle were taken at the point of necropsy (240 minutes), homogenised, processed and analysed to measure total rifampicin concentrations. Error bars show standard deviation.

5.3.7 BLOOD CONCENTRATIONS (EAR BLEED AND CARDIAC BLEED)

Blood samples were taken from the guinea pigs that were dialysed in order to compare drug concentrations in tissues with those in the circulating blood. Ear bleeds were collected as a representation of total (B+UB) rifampicin concentrations in peripheral blood, as the marginal vein in the ear is relatively easy to collect blood from in the guinea pig. Rifampicin was not recovered in all of the ear bleed samples which meant that not all microdialysis fractions could be time matched to blood concentrations. The data are shown in Figure 5.10 alongside the mean unbound rifampicin as collected from the sacrospinalis via microdialysis, the mean rifampicin concentration measured in cardiac blood (at four hours post drug administration) and the estimated unbound lung concentration as calculated via the equation generated in Figure 5.4B. Also plotted are the estimated total rifampicin (B+UB) concentrations in the sacrospinalis and lung corrected for probe efficiency and 69% protein binding.

The drug concentrations measured in ear bleeds were lower than those recovered via microdialysis in the skeletal muscle. The same trend of decreasing concentration over time was observed in both skeletal muscle and blood with the exception of the 240 minute time point, where the drug concentration in blood was higher than at any other time point. This was an unusual result. These data show that rifampicin concentrations measured in the peripheral blood are not indicative of those in the organs, as they are substantially lower, particularly when the organ concentrations were corrected for probe efficiency and 69% protein binding. This was unexpected as blood contains bound and unbound drug, and only the unbound drug was measured in the organs.

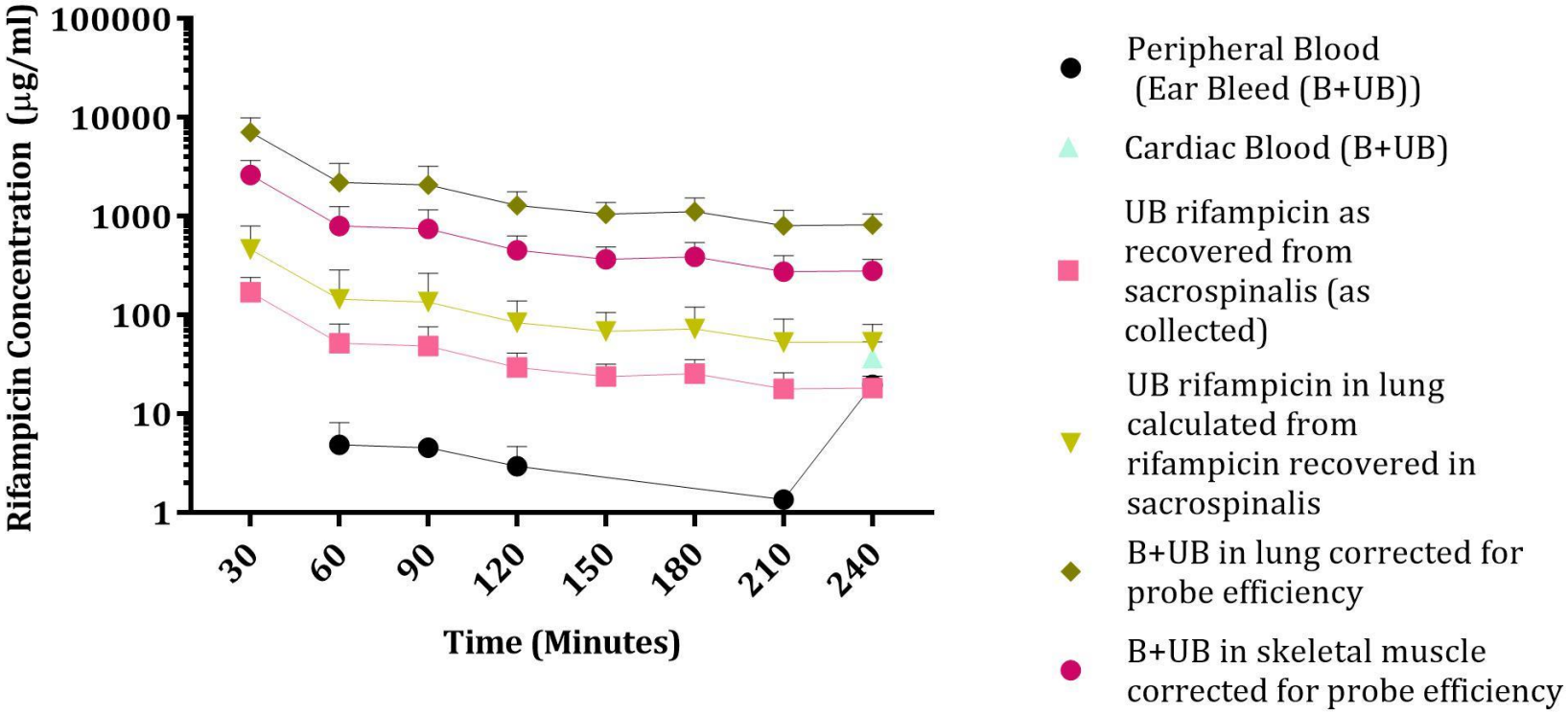

FIGURE 5.10: A COMPARISON BETWEEN RIFAMPICIN CONCENTRATIONS (µG/ML) MEASURED IN GUINEA PIGS A, D, E AND F. Black line indicates mean concentrations in peripheral blood as collected from ear bleeds, pink line is mean unbound rifampicin concentrations as recovered from the sacrospinalis via microdialysis (21% probe efficiency), dark pink line is the mean total rifampicin concentrations as recovered from the sacrospinalis via microdialysis corrected for 69% tissue binding and probe efficiency, mean cardiac bleed concentrations at 240 minutes are indicated as well as mean estimated unbound rifampicin concentrations in the lung as calculated from the equation generated in Figure 5.4B(gold line). Dark gold line is the mean total rifampicin concentrations in the lung as calculated by the equation corrected for 69% tissue protein binding and probe efficiency. Error bars represent standard deviation.

The mean total (B+UB) rifampicin concentration measured in the cardiac blood at 240 minutes (36.8µg/ml) was similar to the estimated (by the equation generated in Figure 5.4B) unbound concentration of drug in the lung at the same time point (53.5µg/ml) before any corrections were applied for probe efficiency and protein binding. It is assumed that 79% more drug is in the tissue than measured with the microdialysis probe working at 21±9% efficiency. Therefore with corrections applied, the cardiac blood, although containing a higher concentration of rifampicin than the ear bleed samples, did not represent the drug concentrations estimated in the lung.

In Chapter 2, ear bleeds were collected to enable calculation of the AUC_{0-t} to understand if human -like exposures were achieved post drug administration. Additional ear bleed data were obtained in the study described in Chapter 4. All of these data were collated with the ear bleed data generated as part of the microdialysis studies to form a more robust data set to enable a comparison between total rifampicin concentrations measured in the peripheral blood (ear bleeds) and the cardiac blood with estimated unbound rifampicin concentrations in the organ (lung). All guinea pigs received a dose of 50mg/kg rifampicin. These data are shown in Figure 5.11.

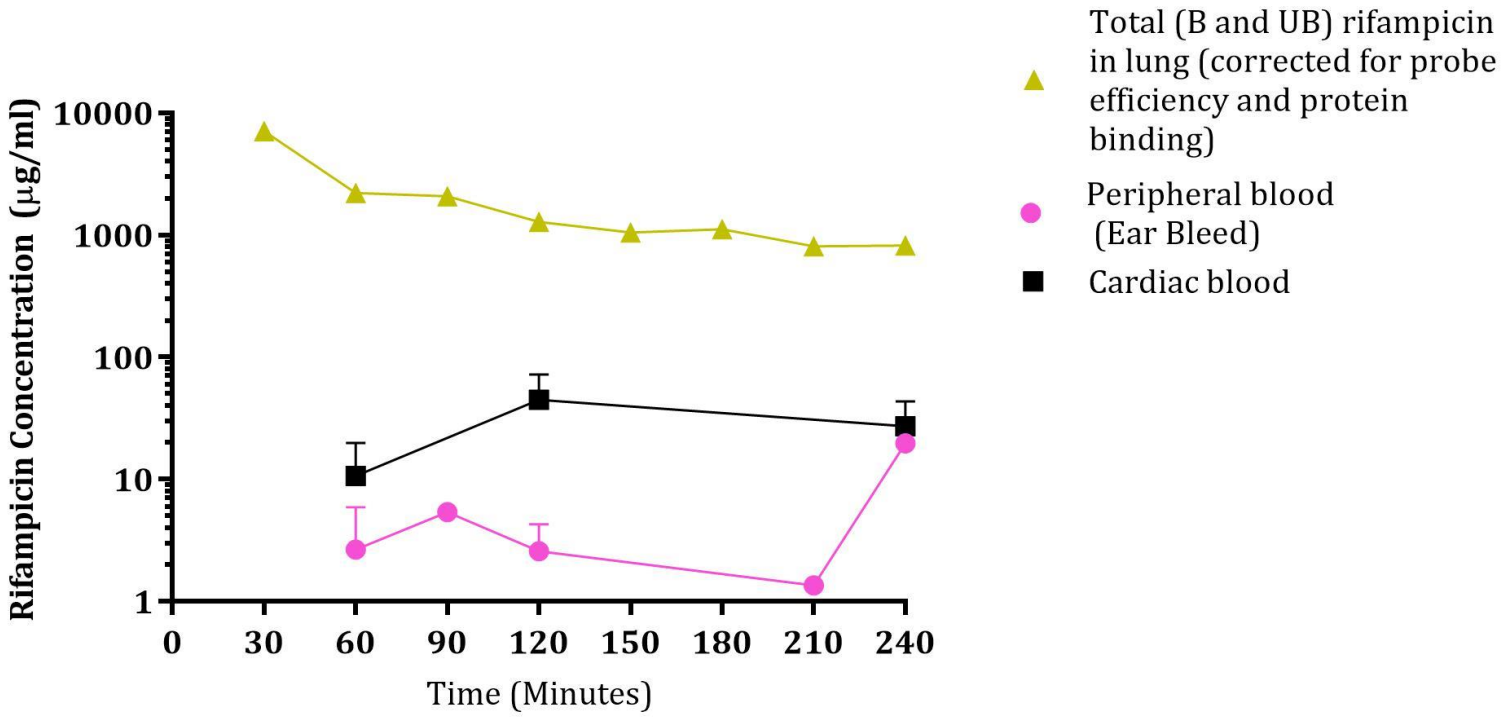

FIGURE 5.11: MEAN RIFAMPICIN CONCENTRATIONS (µG/ML) AS RECOVERED FROM EAR BLEEDS AND CARDIAC BLEEDS FROM GUINEA PIGS THAT RECEIVED 50MG/KG DOSE OF RIFAMPICIN. Pink line indicates total rifampicin concentrations in the peripheral blood (collected via ear bleed) and black line indicates total rifampicin concentrations cardiac blood. Gold line represents total rifampicin in the lung calculated from unbound rifampicin concentrations in the sacrospinalis recovered via microdialysis. These data were then corrected to total concentrations by correcting for probe efficiency and assuming 69% tissue binding.

The additional blood sample data points (Figure 5.11) reinforce the interpretation of the data shown in Figure 5.10 in relation to cardiac blood, demonstrating over the time course that rifampicin concentrations measured in the cardiac blood (60 to 240 minutes), did not match (i.e were lower) the corresponding rifampicin concentration in the lung (calculated via microdialysis). The rifampicin concentrations in the cardiac blood were closer to the estimated concentration of rifampicin in the lung than those measured in ear bleed samples but were still much lower. Furthermore, the kinetics of concentration over time for both blood sample type did not match that of the organ concentrations.

5.3.8 LIVER, URINE & FAECES CONCENTRATIONS OF RIFAMPICIN

Liver, urine and faeces were collected to aid in characterisation of elimination (Chapter 1). Rifampicin concentrations in the liver were measured in the six guinea pigs used in Chapter 4 and the five guinea pigs used in the *in vivo* microdialysis study in order to obtain data at 1, 2 and 4 hours post drug administration. These data are shown in Figure 5.12.

The highest mean rifampicin concentration in the liver was at one-hour post drug administration (508µg/ml). The concentrations in the liver then decreased between one and two hours (233µg/ml) and then remained relatively static. This trend is similar to that seen with recovered rifampicin in the microdialysis fractions.

Urine and faeces were collected throughout the four-hour dialysis experiment. Not all guinea pigs produced urine and faeces and none of the collected urine samples contained rifampicin. The recovered concentrations of rifampicin in the faeces were relatively consistent over time, especially at three and four-hour time points (three samples; 15.3, 18.4, 18.4µg/ml rifampicin) indicating that rifampicin was being eliminated at a similar rate.

Relating the liver concentrations to those found in faeces, it is evident that approximately 10% of the total rifampicin concentration in the liver was eliminated into the faeces (Table 5.1). Guinea Pig B which was culled at two hours post drug administration eliminated 2% of total rifampicin concentration recovered in the liver.

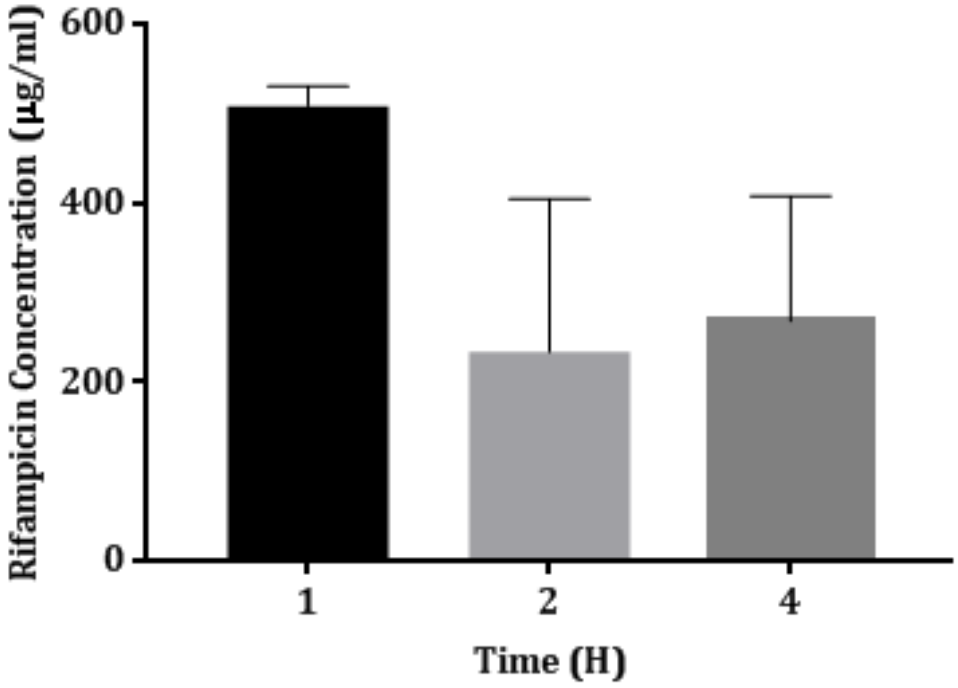

FIGURE 5.12: MEAN RIFAMPCIN CONCENTRATIONS (µG/ML) recovered in the liver of guinea pigs culled at 1, 2 or 4 hours post drug administration. Error bars show standard deviation.

	Rifampicin Concentration µg/ml		
	Liver	Faeces	% Eliminated
Guinea Pig F	152	15.6	10.3
Guinea Pig B	416	42.5	10.2

TABLE 5.1: RIFAMPICIN CONCENTRATIONS (µG/ML) MEASURED IN THE LIVER AND FAECES. At the point of necropsy (4 hours post drug administration) livers were removed, processed and analysed for rifampicin concentrations. All collected faeces from guinea pigs F and B were processed, analysed and the concentrations from all faeces samples were totalled. % eliminated is concentration of rifampicin eliminated in faeces related to rifampicin concentrations measured in the liver.

5.4 PHARMACOKINETIC DATA

To generate pharmacokinetic parameters, rifampicin concentrations as measured via microdialysis in the sacrospinalis at 21±9% probe efficiency were inputted into PK Solver (as described in Chapter 2) [217]. A one-compartment analysis was conducted using first order kinetics for each dialysed guinea pig, the strength of the fit of the data to the model is indicated by the R^2 value. PK Solver generated a number of PK parameters and the key parameters that were deduced from this analysis are the $AUC_{0\text{-}t}$, $AUC_{0\text{-}inf}$, Cmax and Tmax. The PK graphs generated in PK Solver are shown in Figure 5.13. PK parameters are shown in Table 5.2. The CV% and geometric mean are shown as an indication of the robustness of the data.

Table 5.2 and Figure 5.13 show that the amount of drug (A; µg/ml) was similar between Guinea Pigs D, E and F which was consistent with the fact that all guinea pigs were administered the same dose of drug. The data obtained for Guinea Pig A was markedly different as evidenced by the profile shown in Figure 5.1 and 5.13. Absorption rates (ka; 1/h) were similar between Guinea Pigs A, E and F, Guinea Pig D was lower but this can be explained by the fact the first sample collected for Guinea Pig D was at 90 minutes. Elimination rates (k10) were similar between Guinea Pigs D and F, and the steep decline in rifampicin concentration between 30 and 60 minutes seen with Guinea Pig A explains why the highest elimination rate is associated with this guinea pig. Guinea Pig E had a faster elimination rate than D and F as evidenced by the steeper decline in recovered rifampicin in microdialysis fractions as seen in Figure 5.1 and Figure 5.13. Guinea Pig D had the highest total rifampicin concentration in the liver at four hours which could be an explanation for the lowest elimination rate of the four guinea pigs, and conversely Guinea Pig E has the highest elimination rate (excluding Guinea Pig A) and the lowest total rifampicin concentration in the liver at four hours.

The half-life of absorption ($t_{1/2}$ ka; h) was similar between all four guinea pigs, but the half-life of elimination ($t_{1/2}$k10; h) was most similar between Guinea Pigs A and E, and Guinea Pigs D and F mimicking the profiles observed in Figure 5.1. Guinea Pig A had the lowest elimination half-life as expected due to the steep decline in rifampicin concentration between 30 and 60 minutes.

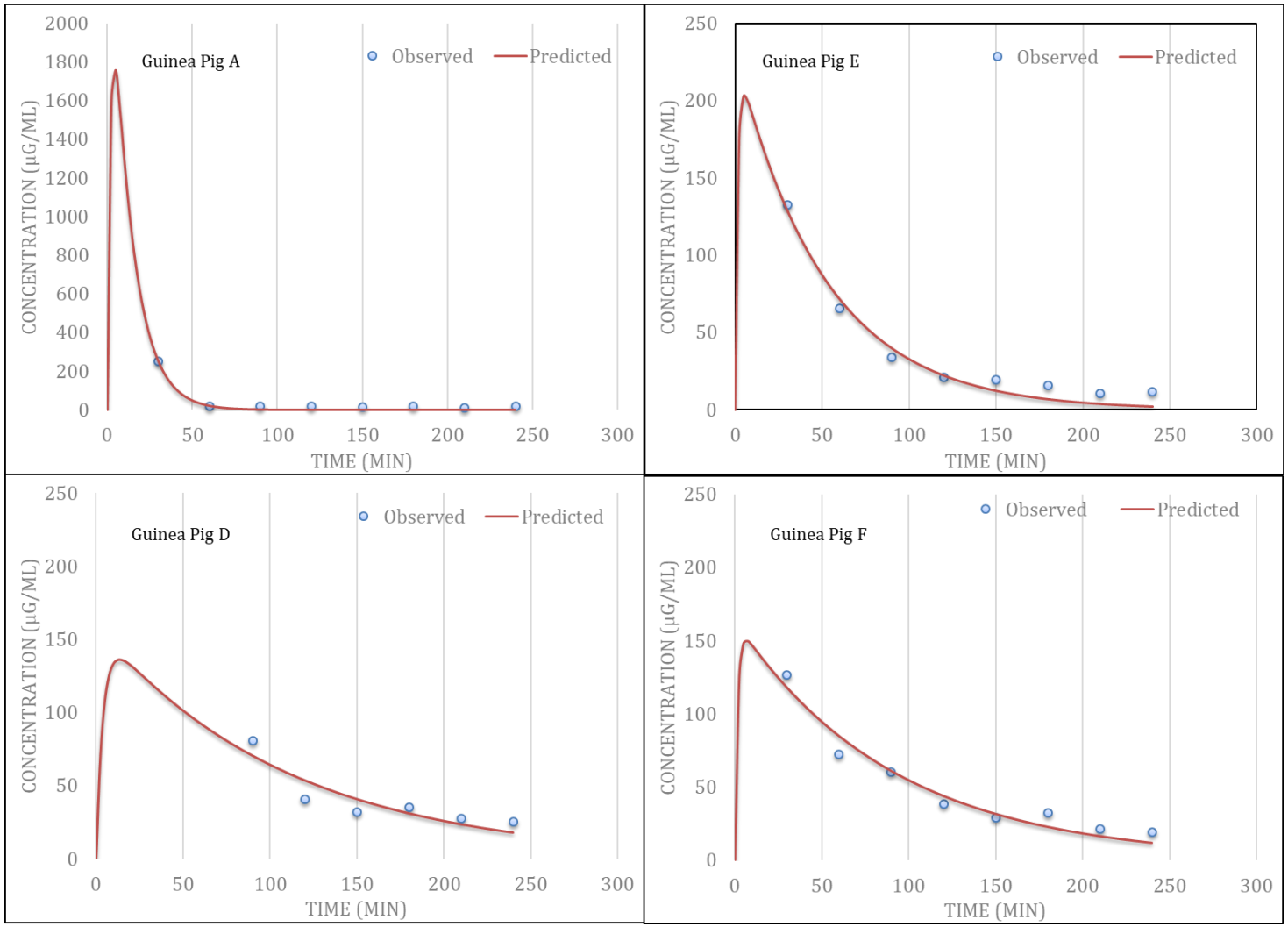

FIGURE 5.13: PK GRAPHS OF RIFAMPICIN CONCENTRATIONS IN THE SACROSPINALIS FOR GUINEA PIGS A, D, E AND F generated in PKSolver using a one-compartment analysis with first order kinetics. Red circles indicate observed (recovered from sacrospinalis) rifampicin concentrations. Note different axis scale for GP A.

(first-order kinetics) One-Compartment Analysis Parameters												
		A	D	E	F							
	R^2	0.985	0.963	0.985	0.984	Mean	SD	Min	Median	Max	CV%	Geometric Mean
µg/ml	A	2960.5	159.6	231.7	163.8	878.9	1388.13	159.60	197.75	2960.50	157.9	365.94
1/min	ka	0.528	0.257	0.69	0.65	0.53	0.20	0.257	0.59	0.69	36.8	0.50
1/min	k10	0.08	0.009	0.0195	0.011	0.03	0.03	0.009	0.02	0.08	112.9	0.02
min	$t_{1/2}$ ka	1.311	2.695	0.99	1.065	1.515	0.798	0.990	1.188	2.695	52.7	1.4
	$t_{1/2}$k10	8.42	76.51	35.4	63	45.833	30.245	8.420	49.200	76.510	66.0	34.6
µg/ml*min	AUC $_{0\text{-}t}$	30361.89	15000.28	11412.79	13578.56	17588.4	8642.5	11412.8	14289.4	30361.9	49.1	16299.3
	AUC $_{0\text{-}inf}$	30361.89	17004.36	11521.51	14641.17	18382.2	8296.1	11521.5	15822.8	30361.9	45.1	17178.8
µg/ml*min^2	AUMC	426287	1943204.2	605971.7	1353438.1	1082225.2	700455.5	426287.0	979704.9	1943204.2	64.7	907878.7
(mg/kg)/(µg/ml)	V/F	0.02	0.32	0.22	0.31	0.218	0.139	0.020	0.265	0.320	64.0	0.14
(mg/kg)/(µg/ml)/min	Cl/F	0.0016	0.0029	0.0043	0.0034	0.003	0.001	0.0016	0.0032	0.0043	36.9	0.00
min	Tmax	4.16	13.48	5.29	6.37	7.32		4.16		13.48		
mg/L	Cmax	1773.4	136.3	203	150.1	565.7	805.6	136.3	176.6	1773.4	142.4	293.0

TABLE 5.2: PHARMACOKINETIC PARAMETERS GENERATED IN PKSOLVER BASED UPON RIFAMPICIN CONCENTRATIONS IN THE SACROSPINALIS (21% PROBE EFFICIENCY) AGAINST TIME (every 30 minutes for four hour period). Each guinea pig is attributed a colour to indicate which was associated with the maximum and minimum values for each PK parameter. a; amount of drug in body at one time, ka; first order absorption rate constant, k10; clearance, $t_{1/2}$ ka/ $t_{1/2}$ k10; half-lives of absorption and elimination, $AUC_{0\text{-}t}$; systemic exposure over four hour time period, $AUC_{0\text{-}inf}$; systemic exposure over infinity; AUMC; area under first moment of the plasma concentration time curve from 0-infinity, V/F; volume of distribution, CL/F; clearance, Tmax; time at which maximum concentrations occurs; Cmax; maximum concentration.

The average Tmax (time that the maximum concentration occurs) was 7 minutes, indicating that rifampicin penetration into the tissues occurred rapidly, however this is based on the predicted as opposed to observed rifampicin concentrations used to generate the PK curves shown in Figure 5.13. The data for Guinea Pig D, due to the lack of collected samples at 30 and 60 minutes, caused the Tmax average to increase, because excluding the data from Guinea Pig D lowers the average Tmax to approximately 5 minutes. Although the microdialysis sampling scheme is much richer than that associated with ear bleed and cardiac bleed sampling due to samples being collected every 30 minutes, each collected fraction represents all the drug collected between 0 and 30 minutes. For the purpose of generating PK parameters, the measured rifampicin concentration was inputted at each 30 minute time segment (30, 60, 90, 120, 150, 180, 210, 240 minutes) however the Tmax and Cmax could be different if these parameters occurred at a point in between the 30 minute collection period i.e. at 15 or 20 minutes. The Cmax is the maximum measured concentration and the mean Cmax for all four guinea pigs was 565mg/L.

Other generated PK parameters were as expected (AUMC and Volume of distribution (V/F)) based on the data in Figure 5.1. Guinea Pig E has the highest rate of clearance (Cl/F) as it has the steepest decline over time, and Guinea Pig A has the lowest rate as concentrations remain relatively static after 60 minutes.

The AUC_{0-t} and AUC_{0-inf} is a measure of total systemic exposure to rifampicin over time and can be used to identify if human-like exposures (human AUC) are achieved indicating whether the dose of rifampicin administered to the guinea pigs is clinically relevant. AUC_{0-t} and AUC_{0-inf} (μg/ml*min) are highest for Guinea Pig A. The mean AUC_{0-t} and AUC_{0-inf} for all four guinea pigs was corrected to account for probe efficiency in order to estimate the actual *in vivo* concentration. At 21% probe efficiency the mean unbound rifampicin AUC_{0-t} was 17.58mg/ml*min and AUC_{0-inf} was 18.38mg/ml*min and when corrected for probe efficiency the AUC_{0-t} was 64.1mg/ml*min and AUC_{0-t} was 64.5mg/ml*min.

Key PK parameters (AUC_{0-t}, AUC_{0-inf} and Cmax) were also generated in PKSolver for the mean estimated unbound rifampicin concentrations in the lung as shown in Figure 5.5 as well as for blood concentrations of rifampicin as collected via ear bleeds and cardiac bleeds as used for Figure 5.11. Blood data were analysed using a non-compartmental analysis. These parameters were compared against those generated for the average rifampicin concentrations as recovered by microdialysis for all four guinea pigs. Table 5.3 shows the AUC and Cmax data calculated in PKSolver for the different sampling sites. The human AUC values (based on total rifampicin concentration in blood) are also shown in Table 5.3. To compare the quoted AUCs in Table 5.3, the data needed transforming to mg/L*hour, these data are also shown in the table.

	Sample Site		AUC_{0-t} (mg/ml*min)	mg/L*h	AUC_{0-inf} (mg/ml*min)	mg/L*h	Cmax mg/L
Unbound	**Sacrospinalis**	As Collected (21%)	17.58	1.05	18.3	1.09	565
		Corrected value for probe efficiency	64.1	3.84	64.5	3.87	1230
	Lung	Based on sacrospinalis (21%)	37.20	2.23	37.4	2.24	680
		Corrected value for probe efficiency	177.16	10.62	178.5	10.68	3270
Total (B+UB)	**Sacrospinalis**	Corrected value for probe efficiency +69% protein binding	206.7	12.4	208	12.48	3960
	Lung	Corrected value for probe efficiency +69% protein binding	571.4	34.2	575.8	34.5	10500
	Blood (Ear Bleed)	As measured	0.813	0.048			5.41*
	Blood (Ear Bleed/ Chapter 2)			5.66		7.07	4.3
	Blood (Cardiac Bleed)		6.30	0.37			44.9
	Human Blood (range)			26.8-49.9			6.6-12.8

TABLE 5.3: CALCULATED AUC PARAMETERS FOR DIFFERENT SAMPLING SITES. These parameters were generated in PKSolver. Shown is sampling site and whether the AUC is for total or unbound drug. Also highlighted is whether the measured value has been corrected for probe efficiency and protein binding. A column converting mg/ml*min to mg/l*h is shown. Also shown is the human AUC and Cmax in blood as published the literature. * = Cmax was calculated excluding outlying data point at 240 minutes.

The calculated AUCs associated with the lung and sacrospinalis were based on unbound rifampicin concentrations. These data have been corrected for probe efficiency and further corrected with a protein binding factor of 69% to enable a direct comparison between the estimated lung AUC_{0-t} and the human blood AUC_{0-t} range. Applying these correction factors to

the estimated lung AUC_{0-t} (37.20mg/ml*min) generated an estimated lung AUC_{0-t} of 34.2mg/L*h. This indicated that with a dose of 50mg/kg rifampicin human-like exposures were achieved in the lung. Human-like exposures, in relation to Cmax, were achieved in the sacrospinalis and lungs of the dialysed guinea pigs. However in the blood, by removing the outlying data point at 240 minutes (19.68mg/L; as shown in Figure 5.10 and Figure 5.11) meant that human-like exposures were not matched in the blood. The data shown in Table 5.3 were variable with few similarities observed between the different sampling sites.

The AUC:MIC and Cmax: MIC are the PK parameters that best predict the efficacy of rifampicin in humans. The Cmax: MIC ratio associated with suppression of rifampicin resistance in humans is ≥175[181]. The rifampicin MIC used for these analyses is 45ng/ml[231].The AUC: MIC ratio in mice associated with a 1 log reduction in colony forming units (CFU) upon infection with M.tb is 271[232]. The AUC and Cmax data shown in Table 5.3 were analysed against the MIC to calculate if either of these ratios were achieved in the lung or blood of guinea pigs. The results are shown in Table 5.4.

	Sampling Site	AUC mg/L*h	MIC ng/ml	AUC: MIC	Cmax mg/L	MIC ng/ml	Cmax: MIC
B+UB	**Mouse**			**271**	**Human**		**175**
UB	**Lung Corrected value for probe efficiency**	10.62	45	237	3270	45	7.27E+04
	Lung Corrected value for probe efficiency +69% protein binding	34.2		760	10500		2.33E+05
B+UB	**Blood (Ear Bleed)**	5.66		125	5.41		120.2

TABLE 5.4: AUC:MIC AND CMAX:MIC RATIOS ASSOCIATED WITH GUINEA PIG LUNG CORRECTED FOR PROBE EFFICIENCY WITH AND WITHOUT PROTEIN BINDING CORRECTIONS AND BLOOD. Also shown are human and mouse thresholds for rifampicin efficacy.

Correcting for probe efficiency in the lung calculates an AUC: MIC of 237 which is close to the ratio associated with a 1 log reduction in CFU, however when the lung AUC is corrected for protein binding the AUC: MIC ratio is 760. The Cmax: MIC ratio in the blood (Chapter 2; Cmax: MIC 95.5) following a 50mg/kg dose of rifampicin in guinea pigs does not reach the threshold

associated with suppression of resistance. However, within the lung, the Cmax: MIC ratios are far above the threshold (≥175).

A dose of 50mg/kg rifampicin in guinea pigs was curative (i.e. decreased bacterial load over time course) as shown in Figure 5.14. Briefly, guinea pigs were aerosol challenged with 50-100 CFU M.tb (H37Rv) and 4 weeks post challenge guinea pigs were administered 50mg/kg rifampicin (in fruit puree as was done for these studies) five days a week. Three guinea pigs from each treatment group were necropsied at weeks 5, 6, 7 and 8 post-challenge. Lungs were homogenised, serially diluted, plated on agar plates and incubated for 3-4 weeks until colonies were enumerated. As shown over the time course, rifampicin treated guinea pigs had a reduction in bacterial load when compared to the untreated group. These data indicate that guinea pigs do not need to receive a dose higher than 50mg/kg rifampicin in order to benefit from the therapeutic effects.

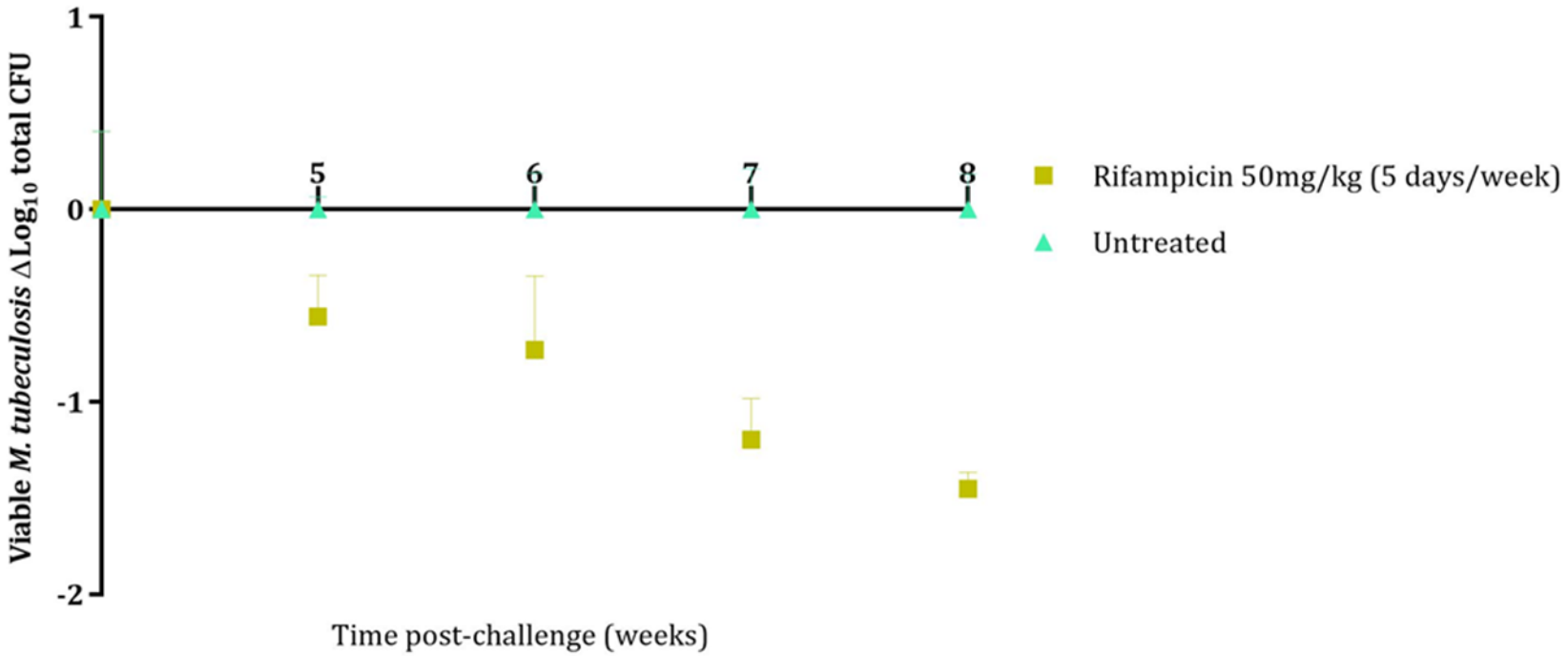

FIGURE 5.14: VIABLE M.TUBERCULOSIS AS MEASURED IN THE LUNGS OF GUINEA PIGS TREATED WITH 50MG/KG RIFAMPICIN. Delta Log_{10} total CFU is shown for rifampicin treated guinea pigs related to untreated guinea pigs following aerosol infection with 50-100CFU of H37Rv. Each point represents the mean CFU measured in three guinea pigs.

5.5 DISCUSSION

Microdialysis, the only methodology available to measure unbound drug concentrations in organs, was used to measure rifampicin concentrations in the lungs of guinea pigs. These data were analysed to derive PK parameters which were compared to the equivalent parameters within blood in both guinea pigs and humans.

In the skeletal muscle of all four dialysed guinea pigs, the measured unbound rifampicin concentrations and the associated kinetic profile, over 240 minutes, were very similar as shown in Figure 5.1. This highlights the reproducibility and robustness of the microdialysis methodology. When comparing the results generated using microdialysis and those generated via blood collection (Figure 5.10), the robustness of the microdialysis methodology is further highlighted. Figure 5.10 also indicated the irreproducibility of blood samples as the total concentration of rifampicin in the peripheral blood (until 240 minutes post drug administration) was lower than the unbound rifampicin collected from the sacrospinalis even when 100% recovery was not assumed. This was unexpected as it was assumed that the blood would contain more rifampicin (bound and unbound) than a sample collected via microdialysis which contained only unbound rifampicin. At 240 minutes, the ear bleed concentration was similar to the concentration measured via microdialysis (21% efficiency), however the only conclusion that can be attributed to this was that peripheral blood data is unreliable and varied. Microdialysis consistently recovered unbound rifampicin which generated a much more detailed profile of the kinetics of rifampicin in the guinea pig, using less animals than required to generate the less adequate blood kinetic profile (Figure 5.11). This is partly due to the design of the studies in Chapter 2 but also because rifampicin concentrations were not always recovered in the ear bleed samples. 12 guinea pigs were used to generate the kinetic profiles in blood and 4 guinea pigs were used to generate the kinetic profile in organs seen in Figure 5.11.

An interesting and unexpected result was that in all animals, the unbound concentration of rifampicin when corrected for probe efficiency (representing actual *in vivo* concentrations) in the sacrospinalis and lung was higher than the total rifampicin concentration measured in the

equivalent organ homogenates following necropsy. This is highlighted in Figure 5.7. It could therefore be concluded that the estimated concentrations based on the unbound rifampicin collected from the sacrospinalis are over-representing the drug concentrations in the organs, potentially due to incorrect assumptions being applied to correct for protein binding or probe efficiency. Rifampicin plasma protein binding figures are varied and range between 43% and 94% in humans [233]. In animal models of TB, guinea pigs have the lowest plasma protein binding figure (69%) when compared to C57 mice (97.1% PPB) and macaques (90.3% PPB)[117]. This between- species and within- species variation associated with protein binding does suggest that the protein binding figure used to correct these data could be lower or higher. A lower tissue protein binding factor, meaning there was more unbound drug available to collect via microdialysis, would make sense in relation to these data.

It was assumed (based on blood concentrations) that the expected *in vivo* organ concentration of rifampicin was going to be less than or close to 50µg/ml, and at these concentrations the CMA 20 (10mm, 20kDa) probe efficiency was calculated to be 21%±9%. This assumption was correct when total organ concentrations were measured as shown in Figure 5.7, Figure 5.8 and Figure 5.9. If it was assumed that the probe was operating at 30% efficiency (higher end of the calculated 21±9% efficiency), using the data in Figure 5.3, the unbound concentrations of rifampicin in the sacrospinalis when corrected for probe efficiency were 57, 84, 38 and 64µg/ml as opposed to 81.9, 120, 54.2 and 91.4µg/ml (corrected for probe efficiency based on 21% probe efficiency) for Guinea Pigs A, D, E and F respectively. Although correcting the measured unbound rifampicin concentrations with this higher figure (30%) lowered the concentration closer to the total concentration as measured in the organ (20.2, 10.49, 6.26, 22.03µg/ml for Guinea Pigs A, D, E and F respectively), the total rifampicin concentration measured in the sacrospinalis was still lower than expected based on the unbound concentration as measured by microdialysis. There were a number of hypothesised reasons for this.

One reason could be that the unbound rifampicin has been dialysed out of the sacrospinalis and as such there was less total rifampicin in the sacrospinalis at the point of necropsy. In the

lung, an additional *ex vivo* sample was collected (270 minutes) and therefore removed more rifampicin from the lungs. As this was completed following necropsy, there was no blood supply to the lungs hence the distribution equilibrium could not be re-established and therefore the measured total rifampicin concentration could be low. Collection of the additional 30 minute sample via *ex vivo* microdialysis could also have caused degradation of the remaining rifampicin in the lung.

Another highly likely reason for the lower than expected total drug concentrations in organs was that the organs required homogenisation. The homogenisation process destroys tissue compartments and can release large blood volumes, especially in the lung. The homogenisation and protein precipitation process could be a source of drug loss due to the lipophilic nature of rifampicin and the associated non-specific binding to plastics. Plastics are an unavoidable component of the homogenisation and protein precipitation processes and therefore use of these methods for sample preparation may have underestimated the total rifampicin concentration in the organ. The homogenisation process could also be why the measured total rifampicin concentrations in the organs were variable (20.2, 10.49, 6.26, 22.03μg/ml in the sacrospinalis of Guinea Pigs A, D, E and F respectively). Given the similarity of the microdialysis data (Figure 5.1) in animals that were dosed separately, it seemed unlikely that the varying concentrations of rifampicin in the sacrospinalis were due to different drug doses. Samples collected via microdialysis (due to the exclusion of proteins) require no processing, therefore it could be deduced that the concentrations as measured by microdialysis are a more accurate estimate of rifampicin concentrations in the organs.

The main reason to dialyse the sacrospinalis was to use the measured unbound concentrations to estimate the unbound rifampicin concentration in the lung (μg/ml) (Figure 5.4B). This was possible after fitting the data in Figure 5.4B with a linear interpolation after the removal of an outlying data point. However, this data point could be indicative of distribution equilibrium being reached in the lung and skeletal muscle at 2 hour post drug administration. This, again, highlighted the animal to animal variation associated with measuring organ concentrations of drug in guinea pigs post necropsy. This variation has not been associated with the collected

microdialysis samples. The kinetic profile associated with the estimated rifampicin concentrations in the lung matched that in the sacrospinalis (Figure 5.1), which indicated that the linear interpolation used to fit the data was the best model. Further support for the use of the linear interpolation to accurately predict unbound concentrations in the lung from those in the skeletal muscle was that the unbound rifampicin concentrations collected *ex vivo* from the lung were similar to the estimated unbound concentration of rifampicin in the lung as calculated from the equation in Figure 5.4B. These data strengthened the use of skeletal muscle as a surrogate for lung. As evidenced in Figure 5.8, the total rifampicin concentrations measured in the sacrospinalis and biceps femoris (two skeletal muscles from different anatomical sites) were similar for all guinea pigs. This indicated that the relationship between rifampicin concentrations in the lung and skeletal muscle was not dependent upon the site of skeletal muscle sampled. This was not unexpected as there is no difference in the structure of skeletal muscle at different anatomical sites. The data in Figure 5.8 are concordant with the literature, in which muscle is not delineated by anatomical site (as concentrations should be the same) for PBPK modelling. When the measured total concentrations of rifampicin in the skeletal muscle were averaged the concentrations were similar to that measured in the lung (Figure 5.9). This similarity between lung and skeletal muscle unbound drug concentrations was identified by both Liu[229] and Tasso[228], when measured via microdialysis in anesthetised rats. The similarities in rifampicin concentrations shown in Figure 5.9 was unlike the data generated in Chapter 4, whereby the total rifampicin concentrations (as measured) were not sufficiently similar and an assumption could not be made that rifampicin concentrations in the lung and skeletal muscle were the same. However, even with the differences between the relationships (same concentrations in both organs vs correlated relationship between both organs), these data further strengthened the use of skeletal muscle as a surrogate for lung.

The measured and estimated unbound drug concentrations in the lung and sacrospinalis were inputted into PKSolver and PK parameters were generated as shown in Table 5.2. This is the first time that the pharmacokinetics of unbound rifampicin have been described in the organs of guinea pigs. The PK parameters associated with blood were defined in Chapter 2 and enable

a comparison to the PK parameters associated with the organs as defined in this chapter. The strength of these generated organ PK parameters are reinforced by a number of reasons. One reason is that more samples were collected via microdialysis to generate the PK parameters. During the four-hour experiment, 8 microdialysis samples were collected and only two ear bleed samples, this is due to the fact microdialysis does not interfere with blood homeostasis whereas the number of blood samples that can be collected is determined by the project licence. As mentioned in Chapter 4, guinea pigs can be cannulated to enable more intensive blood sampling, however project licence restrictions still apply and expense as well as feasibility need to be considered. The continuous serial sampling of organ drug concentrations is a key advantage of the microdialysis methodology. Although the microdialysis methodology is able to collect samples more frequently than in the blood, each sample, although analysed as a 30 (or 30 minute increment) minute sample, actually represents the concentration of rifampicin recovered between 0 and 30 minutes. It is known that the lag time of the system is 3 minutes 36 seconds and although the pharmacokinetic profiles of rifampicin in the organs would remain the same, the timing of sample collection would shift by 3 minutes. Use of a one compartment model accounts for this. The microdialysis methodology could be adapted to collect samples every 15 minutes, although this would require additional *in vitro* optimisation due to the smaller sample volume that would be available for LC-MS/MS analysis. However, using the microdialysis methodology enabled the Tmax to be reported in minutes (Table 5.2) as opposed to hours for the first time following a single dose of rifampicin in the guinea pig. Note that these data are based upon the 'predicted' values as oppose to the measured 'observed' values used to generate the PK curves in PKSolver.

The differences in blood PK parameters generated between Chapters 2 and 5 of this thesis highlight the variability associated with these samples (Table 5.3). The Cmax for the blood data in Chapter 2 was 4.3mg/L. The Cmax data generated from peripheral blood samples collected from guinea pigs that were also dialysed was relatively similar (5.41mg/L) when the outlying data point at 240 minutes was excluded, although when this point was included (19.68mg/L) the Cmax data were vastly different. The Cmax data associated with the cardiac blood

(44.9mg/L) were much higher than that associated with the peripheral blood. Cardiac blood concentrations of rifampicin (at 240 minutes) seemed more relevant to organ drug concentrations than peripheral blood concentrations (Figure 5.10). However, when the data were corrected for probe efficiency the cardiac blood underestimated the concentrations of unbound rifampicin in the organs. Collection of cardiac blood at necropsy is usually a single sample that cannot be easily collected sequentially from the same animal. The kinetic profile of rifampicin in cardiac blood (compiled from all guinea pigs bled in Chapter 4 as well as the guinea pigs used for *in vivo* microdialysis) was similar to that generated via microdialysis between 120 and 240 minutes, however it still underestimated the estimated unbound rifampicin in the organs when these concentrations were corrected for probe efficiency. The measured $AUC_{0\text{-}t}$ in blood generated during Chapter 2 was 5.66mg/L*h, and for the dialysed guinea pigs was 0.0048mg/L*h and 0.37mg/L*h in peripheral and cardiac blood respectively. The $AUC_{0\text{-}t}$, was generated over 24 hours in Chapter 2 and over 4 hours in Chapter 5. Unfortunately, the peripheral blood data set generated in Chapter 5 was not robust enough to generate $AUC_{0\text{-}inf}$ hence blood AUC parameters cannot be directly compared.

An additional difference between the blood samples in Chapter 2 and Chapter 5 was that they were analysed at two different sites (Chapter 2; GSK, Chapter 5; Q3 Analytical). There were two main differences between the analytical methodologies at the two sites, one was that at GSK UPLC was used as opposed to HPLC (Q3 Analytical) and UPLC analysis is known to be more sensitive. The other difference was that at GSK, butylhydroxytoluene was added to the samples to prevent rifampicin loss by oxidation. It could therefore be assumed that the data generated at Q3 Analytical may underestimate the amount of rifampicin in the samples, however the similarities between the Cmax data in blood from the two sites (4.3mg/L GSK and 5.41mg/L at Q3 Analytical) and the acceptance criteria for method validation gave confidence that both methodologies were measuring similar concentrations of rifampicin. All samples generated via *in vivo* microdialysis were analysed at Q3 Analytical and hence measured rifampicin concentrations were directly comparable in terms of analytical methodology.

The Tmax values generated in blood (4 hours for peripheral blood, 2 hours for cardiac blood) were vastly different to those associated with microdialysis (generated in minutes). Based upon the measured rifampicin concentrations in blood and the associated blood PK parameters it could be concluded that a 50mg/kg dose does not achieve human-like exposures in the guinea pig (Table 5.3). This conclusion based on PK in blood is strengthened by an unpublished data set shared by Anne Lenaerts (Colorado State University)[234]. Three guinea pigs were administered a 50mg/kg oral dose of rifampicin. The Cmax data ranged from 1.38 to 4.36mg/L. The individual AUC_{0-t} for each guinea pig ranged between 2.79 and 19.37mg/L*h and Tmax values in blood were 4.23, 2.03 and 4.07 hours for the three guinea pigs. In another data set where guinea pigs were administered a single dose of 50mg/kg rifampicin, the Cmax was 2.9±2.0mg/L, the Tmax was 2.0±0.01h and the AUC_{0-inf} was 13.4±5.8mg/L*h[207] in serum. In all datasets whereby the PK of rifampicin was measured in blood, neither the measured Cmax or AUC_{0-t} PK parameter indicated human-like exposures had been achieved in guinea pigs following a 50mg/kg dose. Interestingly, in BALB/C mice, a dose of 50mg/kg rifampicin generated a Cmax of 52±10mg/L and AUC_{0-24} of 600±81mg/L*h in blood which are far above the human range[235]. In a data set where guinea pigs were administered a 100mg/kg oral dose of rifampicin, the mean Cmax in blood was 14.80mg/L (range 6.27-16.86mg/L)[220] which was inside the human range (6.6-12.8mg/L) but still lower than the parameters achieved following a 50mg/kg dose in mice. The AUC_{0-t} range (32.66-124.24mg/L*h) in guinea pigs that were administered 100mg/kg of rifampicin, although wide, were within the human range (26.8-49.9mg/L*h)[220]. It is important to mention a recent publication which used meta-analysis to estimate PK parameters associated with human blood at standard rifampicin doses, and the estimated AUC following a single dose of rifampicin was calculated to be 72.56mg/L*h[236]. Based on these data it would be acceptable to conclude that guinea pigs needed to be administered an oral dose of 100mg/kg rifampicin to achieve human-like exposures, although doses of 100mg/kg of rifampicin have been associated with directly toxic effects in the guinea pig[207].

The calculated AUCs associated with the organs were more relevant to the human data than those associated with the blood. Figure 5.9 indicated that mean total rifampicin concentrations were similar between lung and skeletal muscle. However, the PK data associated with unbound rifampicin show differences in the $AUC_{0\text{-}t}$ between the sacrospinalis and the lung especially when the data is corrected for probe efficiency. If the relationship between the rifampicin concentrations (Figure 5.4B) in the lung and skeletal muscle had not been identified, an assumption would have been made that the $AUC_{0\text{-}t}$ in guinea pigs did not achieve human-like exposures even when a 69% protein binding factor is applied (12.4mg/L*h). The estimated unbound rifampicin $AUC_{0\text{-}t}$ in the lung (10.62mg/L*h) is close to that of the lower end of the human range (26.8-49.9mg/L*h)[218], especially as the $AUC_{0\text{-}t}$ associated with the lung was calculated for only the unbound drug and the human range was calculated for total drug concentrations. To enable a direct comparison between the estimated lung and human $AUC_{0\text{-}t}$ range, the estimated lung data were corrected for protein binding which calculated the total lung $AUC_{0\text{-}t}$ to be 34.2mg/L*h. This therefore indicated that with a dose of 50mg/kg rifampicin human-like exposures (26.8-49.9mg/L*h) were achieved in the lungs, which are the target organ of rifampicin, negating the need for higher doses to be administered to the guinea pig and hence reducing the chances of toxic drug effects occurring.

The PK parameters that are associated with rifampicin efficacy are the AUC:MIC ratio and Cmax: MIC ratio (Table 5.4). The Cmax: MIC ratios associated with blood following a 50mg/kg dose of rifampicin in guinea pigs does not reach the threshold associated with suppression of resistance (≥175). However, Cmax: MIC ratios associated with the organs are above this threshold (271) in the organs again suggesting that a 50mg/kg dose is sufficient in guinea pigs. Correcting for probe efficiency in the lung calculated an AUC:MIC of 237. This is the unbound rifampicin AUC: MIC ratio and was close to 271 which is the figure associated with total (bound and unbound rifampicin) AUC:MIC. These data suggest that a dose of 50mg/kg rifampicin was sufficient to achieve a 1 log reduction in CFU in the lung, as although the unbound AUC in the lung is not at 271, the AUC: MIC ratio when corrected for protein binding was 760. These data

indicated that although therapeutic concentrations of rifampicin are not obtained in the blood, therapeutic concentrations are achieved in the lungs.

Microdialysis was used to describe the pharmacokinetic behaviour of unbound rifampicin in the lungs as a continuous sampling technique in awake freely moving guinea pigs for the first time. Microdialysis generated more robust, reproducible and human relevant PK data when compared to traditional methods such as blood collection and total organ concentrations measured post necropsy. This more robust data set compiled by microdialysis was generated using less animals which is in line with the 3Rs principles associated with use of animals in scientific research. The development of this methodology has significance for pre-clinical development of novel anti-TB drugs because the organ PK data was different to the PK data generated in blood, and PK data generated in the blood underestimated the equivalent parameters in the organs. Blood data indicated that a dose higher than 50mg/kg would need to be administered to guinea pigs to achieve human-like exposures, however, use of the microdialysis methodology has shown that human-like concentrations are achieved in the lungs of guinea pigs following a 50mg/kg dose.

CHAPTER 6

GENERAL DISCUSSION

Two main hypotheses were tested in the studies detailed in this thesis. The first hypothesis was centred around the establishment of the microdialysis methodology in guinea pigs to measure the concentration of drugs in the lung. The second hypothesis was that the concentrations and concentration-time curves (PK curves) of anti-TB drugs within the blood will be significantly different to the concentrations and PK curves in the lungs.

In relation to the first hypothesis, the microdialysis methodology was successfully established for use in the guinea pig and the microdialysis system was optimised with rifampicin, a key component of the front-line anti-TB drug regimen. The use of this methodology has enabled the successful completion of reproducible and robust experiments to measure unbound drug concentrations and therefore generate PK parameters, within the organs of guinea pigs (Figure 5.13). A clear advantage to the microdialysis methodology over traditional methods (i.e. blood collection) was that four guinea pigs were used to generate a data set (Figure 5.1), which would have required approximately 16 guinea pigs in order to generate the equivalent data set using blood sampling due to the constraints around frequency of blood collection. Hence, the microdialysis methodology adheres to the 3Rs principles associated with use of animals in scientific research, because microdialysis enabled more (quality and quantity) information to be gathered from each guinea pig therefore reducing the amount of animals required and refining the information gained from a single animal.

Whilst development and optimisation of the microdialysis system was successful, several technical challenges needed to be overcome. A significant amount of *in vitro* optimisation was required, not only to optimise the microdialysis-specific parameters to improve probe efficiencies, but also in the identification of a site for probe implantation. The latter was largely dependent on the requirement for guinea pigs to be awake and unanaesthetised and therefore there were minimal sites for implantation especially those which were relevant to the lung. A

thorough understanding of the physiochemical properties of the drugs was imperative in the optimisation of microdialysis-specific parameters and in the identification of a relationship between lung and skeletal muscle drug concentrations to enable probe implantation into the sacrospinalis. Having performed *in vitro* microdialysis with three of the four front-line anti-TB drugs, important data were generated enabling assumptions to be made based upon the physiochemical properties of other anti-TB drugs. Probe efficiencies could be estimated and whether skeletal muscle could be used as a surrogate for lung. As an example, it would be expected that the probe efficiency associated with pyrazinamide would be very similar to that of isoniazid (~67%) due to the similarities in physiochemical properties between the two drugs. The probe efficiency associated with the other rifamycins (rifabutin and rifapentine) is estimated to be around 21% due to the shared similarities with rifampicin. However, caution must be exercised when making assumptions about drugs based solely upon their physiochemical properties. This was highlighted in this thesis with isoniazid, because no relationship was identified between lung and skeletal muscle isoniazid concentrations. This was unexpected as isoniazid has similar physiochemical properties to gatifloxicin[228] (Mw:375.39, LogS:-1.71, LogP:1.31) and cefpodoxime[229] (Mw:427.188, LogS:-1.47, LogP:-0.32) and both of these drugs showed similar concentrations in the lung and skeletal muscle. A relationship between lung and skeletal muscle rifampicin concentrations was shown which might not have been predicted based upon the physiochemical properties of rifampicin which differ from those of gatifloxicin and cefpodoxime.

In order to use the microdialysis methodology with other anti-TB drugs, *in vitro* optimisation would need to be conducted to ascertain the probe efficiency associated with the drug. Hence, a significant disadvantage to the microdialysis methodology is that it is more time consuming to implement than traditional methods and also requires the use of specialist equipment. However, the microdialysis-specific parameters optimised in these studies with rifampicin, serve as an important starting point. For example, the same parameters were used for isoniazid and achieved high relative recoveries, even though rifampicin and isoniazid share few physiochemical properties. An interesting drug to trial and optimise in the microdialysis

system to measure the unbound concentration of in organs would be bedaquiline. In guinea pigs and humans, bedaquiline is ~99% plasma protein bound[117], and it would be important to understand if this is similar in tissues and measure the actual quantities of unbound bedaquiline via microdialysis. The high LogP value associated with bedaquiline (6.24) indicates that there would be non-specific binding of the drug to the plastics within the microdialysis system. However, it has been shown in these studies that such issues associated with rifampicin can be overcome by prior exposure of the probes to drug and use of the 300µl microdialysis collection tubes. The PK of bedaquiline has been previously established in the plasma and lungs of BALB/C and C3HeB/FeJ mice with similar results between the two sampling sites in both species[27]. However, the lung PK data in those studies was based upon total drug concentrations in homogenate. Use of the microdialysis methodology in guinea pigs would enable unbound bedaquiline to be measured *in vivo* and to identify whether blood concentrations truly reflect the amount of unbound drug in the lungs. This has the potential to optimise dosing regimens for this important new TB drug.

Technical refinements can be made to further optimise the microdialysis system with the anti-TB drugs. A simple and easy to implement refinement would be the use of a slower flow rate or to decrease the lag time (3 minutes 36 seconds). This would enable more temporal resolution to further define Tmax parameters in the organs. As discussed in Chapter 5 the Tmax data were reported in minutes, however this was based on the predicted as opposed to observed (measured) drug concentrations (i.e. use of a one compartment model). Adjusting the microdialysis system to enable the collection of fractions every 10 or 15 minutes (using 2µl minute flow rate) could be completed with minimal optimisation as 5µl is the minimum sufficient sample volume for LC-MS/MS. Incorporation of online analysis into the microdialysis methodology, whereby dialysate is directly injected into the HPLC, would reduce sample volumes even further as well as providing near real time information[165]. This online directly coupled analysis is a unique feature of microdialysis, due to the generation of protein free samples and hence the lack of requirement to process the samples prior to analysis[237].

However, incorporation of online analysis could only be conducted in a dedicated microdialysis facility.

Another technical refinement to improve the data generated using microdialysis would be to further characterise the PK of drugs by sampling for a longer period of time (~24 hours). This longer dialysis period would be especially important for drugs with longer half-lives such as bedaquiline[27]. The microdialysis experiments performed with rifampicin were conducted over a period of 4 hours. In terms of animal welfare, there was no evidence of guinea pig discomfort during the dialysis period and no welfare concerns were raised by either the Home Office Inspector or Named Veterinary Surgeon upon inspection of the guinea pigs. There has been evidence of associated tissue trauma following probe implantation especially if the probe is implanted for longer than 12 hours[169], however in the guinea pigs used for these studies where the probe had been *in situ* for ~50 hours there was no evidence of tissue inflammation identified (as shown via histopathological analysis) at the probe implantation site. This suggests that microdialysis is a minimally invasive method. Hence, the microdialysis experiments could be easily adjusted to incorporate a longer dialysis period.

An important conclusion from the data generated in these studies is that blood samples (collected via ear bleeds) no longer need to be collected as part of the microdialysis experiments because the data generated via blood sampling was less reliable than that generated by microdialysis. If blood samples are required, a more robust method for sampling (i.e. jugular vein catherization) must be employed, however this would require amendments to the Home Office licence as well as ensuring that more frequent collection of blood samples would not affect the associated PK parameters. A similar disparity between blood and organ drug concentrations has also been shown in the rabbit model where it was found that plasma and lung homogenate were not a suitable surrogate for drug concentrations in lesions within the lungs of rabbits infected with M.tb[192]. Verification of the amount of total drug in an organ following microdialysis was found to be important and is recommended for future studies. However, there was evidence that drug concentrations were underestimated in organ homogenates. As highlighted in Figure 5.3, there was a disparity between drug concentrations

measured in the homogenate and those measured via microdialysis (especially when the microdialysis concentrations were corrected for probe efficiency). It is hypothesised that the concentrations measured via microdialysis (due to the lack of requirement for sample processing) are more representative of *in vivo* drug concentrations. To address this hypothesis, different methods of tissue homogenisation could be used to more efficiently measure total drug concentrations. The Ystral homogeniser used in these studies to homogenise every 0.2g tissue in 1ml PBS should have achieved a uniform subcellular particle size of 10µm which can be extracted efficiently, however with tougher tissue such as muscle a uniform homogenate may not have been created. Alternative methods such as bead beating could be used to more efficiently break down the tissue, although this may increase the available surface area for non-specific drug binding, however addition of an organic solvent (phosphate buffer) can aid in drug recovery by reducing this binding[238].

The studies performed in this thesis showed definitively that a dose of 50mg/kg rifampicin in guinea pigs did not achieve human-like exposures in the blood, yet human-like exposures were achieved in the lung. A dose of 50mg/kg was shown to be therapeutic (Figure 5.14) which suggests that sufficient drug concentrations are achieved in the lung and microdialysis is the most efficient way of measuring this. As TB is a predominantly pulmonary disease, there is interest in delivering anti-TB drugs by aerosol in order to deliver them directly to the lung [44, 111.112]. Studies were focussed on the aerosolisation of aminoglycosides as it is known that parenteral administration of these drugs is associated with low total drug concentrations in the lung[239]. Aerosolised capreomycin administered to guinea pigs resulted in a high drug exposure in the lung as measured via bronchiolar lavage but a significantly reduced systemic exposure based upon plasma measurements[111]. Although the PK parameters have been measured in the lungs of guinea pigs following aerosolisation of capreomycin, the data where obtained at a single time point. Microdialysis could be used to measure the PK parameters (especially the AUC_{0-t}) associated with aerosolised drugs over a time course within the same guinea pig. These data could be compared to the same PK parameters generated for orally administered drugs. However, a limitation associated with the microdialysis methodology

established in this thesis is that sampling the sacrospinalis via microdialysis may underestimate the associated lung concentrations and therefore the unbound drug concentrations in the lung following aerosol administration may only be established via *ex vivo* microdialysis (if unanesthetised guinea pigs are to be used).

The main advantage to using guinea pigs as a model species for drug evaluation against TB, is that upon aerosol infection with M.tb, the disease progression recapitulates the main pathologies of human TB disease including the presence of primary and secondary lesions[206]. The morphological features of lesions impact the drugs ability to enter the lesion and gain access to the bacteria. For example, granulomas in guinea pigs, similarly to humans, have a reduced vascular supply impeding drug delivery. Bacterial persistence is also associated with these lesions, and hence lesions are an important feature to factor into the associated pharmacokinetics of the anti-TB drugs[240]. It would therefore be very important to understand the effects of TB disease on the unbound rifampicin concentrations measured via microdialysis, especially to measure if human-equivalent exposures can still be achieved within the lungs of TB infected guinea pigs. Given the specific nature of TB disease in the lung, skeletal muscle may be a less relevant surrogate to measure drug concentrations in infected lungs. It would therefore need to be ascertained prior to performing *in vivo* microdialysis if the relationship between drug concentrations in the lung and skeletal muscle still existed following infection with M.tb, which most likely will require the use of further animals to establish this relationship between drug concentrations. If this relationship remained, following aerosol infection and a period of time for disease establishment, guinea pigs could undergo surgery to insert the microdialysis probe into the sacrospinalis. The surgery would need to be conducted at Containment Level 3 (CL3) and protocols and associated risk assessments would need to be established to reflect this. There is no evidence in the literature of lung microdialysis in awake, freely moving small animals. *In vivo* microdialysis of the lung has only been performed in anesthetised animals following a thoracic rib resection[228,229].

The effects of anaesthesia would need to be investigated to identify any effects on drug concentrations although it has been shown by others that there was no effect of anaesthesia on

the PK of bromosulfophthalein, a drug with similar physiochemical and metabolism properties as rifampicin, in rats[241].

An alternative to dialysing the lungs *in vivo* would be to dialyse them *ex vivo* following necropsy. *ex vivo* dialysis of the lungs gave meaningful results (Figure 5.6), albeit at only one time point and there would be no additional data gained by increasing the length of dialysis time as this is a static system. Lesions could be directly dialysed to measure unbound drug concentrations as drug concentration of rifampicin measured in lesions of rabbits were found to be significantly lower than plasma concentrations and penetration of rifampicin into healthy lung tissue was greater than that in lesions[192]. *Ex vivo* dialysis of TB cavities has also been performed in human TB patients with MDR-TB. Interestingly, there was a good correlation between levofloxacin concentrations in the serum and cavities ($r=0.71$, $p=0.01$)[158].

Following establishment of the microdialysis methodology to measure unbound rifampicin concentrations in the lungs of guinea pigs, an experiment was conducted to test the second hypothesis of this thesis that blood and organ drug concentrations would be different. Therapeutic thresholds of rifampicin based on the PK/PD indices Cmax :MIC and AUC:MIC, were not achieved in blood, however the therapeutic thresholds associated with the two ratios were achieved in the lungs. These data were further strengthened by the fact that a dose of 50mg/kg rifampicin provided a therapeutic benefit in aerosol infected guinea pigs (Figure 5.14). The organ-specific PK data associated with the lung indicated that blood concentrations of the drug are not a good representative of drug concentrations at the site of infection (the lungs). These novel organ PK data generated *in vivo* indicate that administration of a dose higher than 50mg/kg rifampicin in guinea pigs would be in effect 'over-dosing' the guinea pigs and therefore it is unsurprising that toxic effects can occur[207]. This conclusion could not be drawn from the PK parameters measured in blood and incorrect assumptions on required doses would be made.

Building on the data generated in this thesis, the main application of the microdialysis methodology in the guinea pig could be centred around dose optimisation studies during pre-clinical drug development. This could be conducted in infected or uninfected guinea pigs.

Initially the microdialysis methodology could be used in guinea pigs that have been administered lower doses of rifampicin (<50mg/kg) to measure if the estimated lung AUC_{0-t} and subsequent PK/PD indices were still within the human range (when corrections for protein binding and probe efficiency are applied). Conversely, higher doses of rifampicin could be administered in guinea pigs in order to match human-like exposures in the blood. Using microdialysis to estimate the subsequent concentration of rifampicin in the lung will give an indication of how 'over-exposed' the lung is to rifampicin. For the studies detailed in this thesis in order to orally administer 50mg/kg rifampicin to the guinea pigs, the rifampicin was mixed with a fruit puree to aid palatability. In other studies that have measured blood PK of rifampicin in guinea pigs, rifampicin was administered in a 40% sucrose solution[220,207]. However, co-administration of rifampicin with food is known to decrease oral bioavailability in humans[242]. Rifampicin could be administered in a non-food based vehicle to understand effects of dosing mixtures on measured PK, or as a tablet (as is in humans) to ensure the full dose was being administered.

An additional parameter to measure could be the effects of the co-administration of rifampicin and probiotic on organ PK parameters. Probiotics often need to be administered to guinea pigs receiving drug treatment due to the sensitivity of their gut[207], however probiotic is known to change PK parameters via changing gut microbiota composition and enzyme activities[209]. Microdialysis could be used to measure organ PK parameters associated with rifampicin following co-administration with a probiotic in guinea pigs. If the measured PK parameters remained unchanged, probiotic could be administered with drugs ensuring no effect on organ PK parameters but also improving guinea pig comfort and welfare. Data generated from these dosing studies (i.e. higher or lower than 50mg/kg rifampicin) can be applied in PBPK predictions or used to generate a 'numerical factor' that can be applied, in the future, to measured drug concentrations in blood to estimate drug concentrations in the lungs without the need for additional microdialysis experiments.

Additional studies can be performed in the guinea pig using the microdialysis methodology to further understand differences between rifampicin PK parameters measured in blood, organ

homogenate and those measured via microdialysis. In Chapter 2, when a dose of 75mg/kg rifampicin was administered to guinea pigs that had previously received a dose of 50mg/kg rifampicin, the associated total systemic exposure (AUC_{0-t}) in blood was lower following the 75mg/kg dose (when compared to the 50mg/kg dose). This indicated that auto-induction of metabolism was occurring in the guinea pig following secondary exposure to rifampicin. Dutta *et al*[220] and Kjellsson *et al*[192] have stated that auto-induction does not occur in guinea pigs or rabbits. Assuming auto-induction of metabolism was occurring following secondary exposure to rifampicin would suggest that total liver concentrations of rifampicin would be highest almost immediately following drug administration. Livers were collected at necropsy during the studies detailed in this thesis and total rifampicin concentrations measured. The highest rifampicin concentration measured in the liver was at one hour post drug administration (Figure 5.12) and the rapid decline after one hour could be associated with the rapid metabolism of rifampicin in the guinea pig which has also been shown in baboons where rifampicin is entirely cleared from the liver by 3 hours post drug administration[115]. In the guinea pig, rifampicin was still detectable in the liver at 4 hours post drug administration in similar concentrations to those measured at 1 and 2 hours.

Microdialysis can be used to understand the effects of repeat administration of rifampicin as although the feasibility of probe implantation into the liver was found to be limited (Chapter 4), there are studies where microdialysis has been conducted in the bile duct of anesthetised rats [243,244] . It is known that rifampicin is excreted via the biliary route[245] in humans and that guinea pigs possess a bile duct and are able to excrete xenobiotics via this mechanism[246]. Consistent with this, rifampicin was measured in the faecal samples of the guinea pigs which were administered rifampicin (Table 5.1). The rifampicin measured in the faeces was approximately 10% of the liver concentration. Although likely to require anaesthesia, measurement of unbound rifampicin in the bile duct following repeated administration of rifampicin would add further information on auto-induction of metabolism (as well as elimination) in the guinea pig. This would provide important information of dosing frequency.

Although able to induce it's own metabolism, rifampicin is also known to affect the metabolism and overarching pharmacokinetics of other drugs, most notably the anti-retrovirals[247]. This has an impact on TB treatment as 25% of all tuberculosis related deaths are due to HIV co-infection[1]. However, the measured changes in PK parameters associated with co-administration of rifampicin with other drugs is based on data generated in the blood. It has been shown that blood is not a reliable surrogate for organ concentrations of rifampicin and it would therefore be important to measure PK parameters in the organs. Microdialysis could be used to understand the effects of co-administration of other drugs with rifampicin on the measured organ PK parameters. Administration of a combination of the four front-line anti-TB drugs (as given in humans) would be an important application of this methodology since it would allow studies to investigate timing of rifampicin administration relative to the other drugs to limit drug-drug interactions, however this would require additional optimisation further than that of calculating probe efficiency, especially in relation to drug interactions at the probe membrane and analytical methods [85,207].

In the future, it would be interesting to use the microdialysis methodology in other animal models associated with TB especially in relation to rifampicin concentrations in infected animals. In infected rabbits, a dose of 30mg/kg rifampicin does not achieve human-like exposures in the plasma (Cmax: 1.2mg/L, AUC_{0-t}: 14.7mg/L*h)[192] whereas in infected mice a dose of 10mg/kg does achieve human-like exposures in plasma (Cmax 11mg/L, AUC_{0-24} 121mg/L*h)[235]. However, as was shown in the guinea pig, measuring the PK parameters associated with the organs may give congruent results to those measured in the blood. There would need to be significant additional development to the microdialysis methodology for use in other animal models, as although most microdialysis-specific parameters could remain the same, in smaller animals some features such as the 10mm probe membrane may prove to be problematic. Although microdialysis has been performed in mice, the probe is usually inserted into the brain and it appears that any peripheral tissue dialysis of mice (which is limited) has occurred under anaesthesia[248]. There seems to be no evidence in the literature of *in vivo*

microdialysis in the peripheral tissues of mice or rabbits associated with measuring the PK of drugs.

Although guinea pigs are the gold standard of animal models for TB vaccine research[205], they are not as frequently used for anti-TB drug development. This is in part due to the high doses required to achieve human-like exposures in guinea pigs and doses of this magnitude have been associated with toxicity. However, use of the microdialysis methodology in the guinea pig has shown that a dose of 50mg/kg rifampicin was sufficient to achieve human-like PK parameters in the lung although not in the blood. Although, it is of vital importance that the PK data generated in the guinea pig (or other model species) are as relevant to humans as possible, it seems these PK parameters should be matched at the clinically relevant site of disease and not in the blood. These results can help refine the use of rifampicin, a very important front-line anti-TB drug, as well as potentially reducing associated drug toxicities in animal models and ultimately may impact the initial dose selection for human clinical trials.

Overall the studies described in this thesis address the two hypotheses. The first hypothesis was centred around the establishment of the microdialysis methodology in guinea pigs to measure the concentration of drugs in the lung. These studies demonstrate that microdialysis in guinea pigs is feasible and that the methodology shows great potential to more accurately define the PK of drugs in organs. These studies also identified some limitations associated with microdialysis and areas for improvement. The second hypothesis was that the concentrations and concentration-time curves (PK curves) of anti-TB drugs within the blood will be significantly different to the concentrations and PK curves in the lungs. The use of the microdialysis methodology in the guinea pig has proven that generation of organ-specific pharmacokinetic data is possible as well as highlighting the relevance of these data when compared to those data generated in blood. In conclusion, the use of microdialysis in guinea pigs can be an integral part of the pre-clinical drug development pipeline especially in relation to dose optimisation studies.

APPENDIX

RELATIVE RECOVERIES FOLLOWING ISONIAZID *IN VITRO* MICRODIALYSIS WITH PHYSIOLOGICALLY RELEVANT DOSE SOLUTIONS (50 AND 5µG/ML)

Replicate	Dose	Time	Conc (µg/ml)	%Relative Recovery	Mean %RR	SD	%CoV
1	Dose Aim:50µg/ml Actual:20.3µg/ml	60	23.5	115.8	92.4	17.2	18.6
		90	17.9	63.9			
		120	23.4	99.6			
		150	18.5	103.4			
		180	18.3	78.2			
		210	19.6	105.9			
		240	14.6	79.8			
2	Dose Aim:50µg/ml Actual:28.0µg/ml	60	23.6	116.3	86.5	15.5	18.0
		90	18.8	67.1			
		120	18.1	77.0			
		150	No Sample				
		180	21.5	91.9			
		210	14.5	78.4			
		240	16.2	88.5			
1	Dose Aim:5µg/ml Actual:5.25µg/ml	30	11.6	221.0	63.0	56.1	89.0
		60	4.15	79.0			
		90	3.33	63.4			
		120	3.87	73.7			
		150	2.80	53.3			
		180	2.97	56.6			
		210	2.73	52.0			
2	Dose Aim:5µg/ml Actual:5.49µg/ml	30	11.8	214.9	81.2	56.0	68.9
		60	4.58	83.4			
		90	3.57	65.0			
		120	3.21	58.5			
		150	3.22	58.7			
		180	2.40	43.7			
		210	2.43	44.3			

ISONIAZID PROBE EFFICIENCIES

INH Conc (µg)	%RR	Probe Efficiency	
5.25	63	61±2%	67.5±3.4%
5.49	59		
20.3	86	83.5±4%	
28.0	81		
949	41	58%±4%	
992	44		
1.00 (mg)	64		

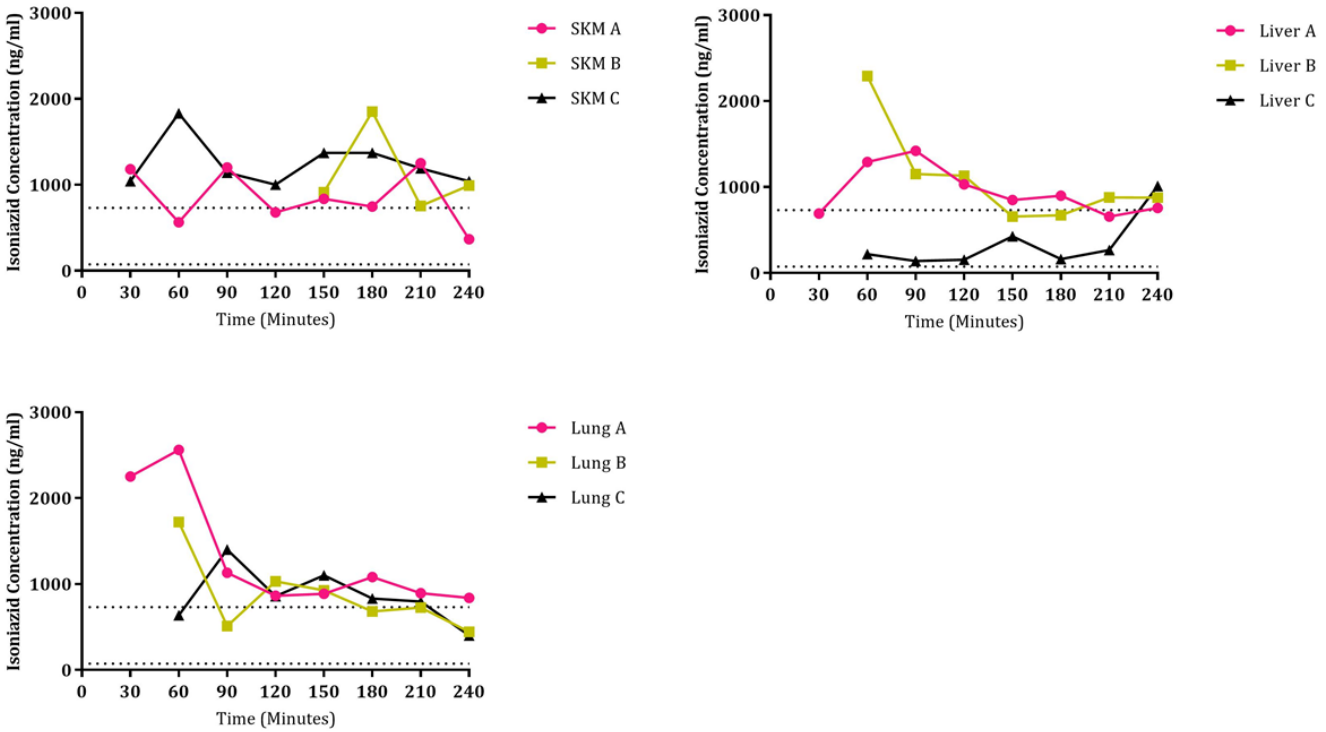

ORGAN EFFECTS ON ISONIAZID RECOVERIES

It was hypothesised that there is 0.12µg (120ng/ 41.5% Fu) of free isoniazid available in the homogenate for collection via microdialysis. Using the calculated probe efficiency of 61% and the proposed free (unbound) drug in the homogenate a line (lower line) was drawn on the graph which shows 61% of 120ng. An additional line has been marked on the graphs at 10 times this proposed efficiency.

REFERENCES

1. WHO | Global tuberculosis report 2018. *WHO* (2018). Available at: https://www.who.int/tb/publications/global_report/en/. (Accessed: 4th February 2019)

2. Daniel, T. M. The history of tuberculosis. *Respir. Med.* **100**, 1862–70 (2006).

3. Frieden, T. R., Sterling, T. R., Munsiff, S. S., Watt, C. J. and Dye, C. Tuberculosis. *Lancet* **362**, 887–899 (2003).

4. The Paradigm Shift. (2016). Available at: http://www.stoptb.org/assets/documents/global/plan/plan2/ExecutiveSummary.pdf. (Accessed: 1st August 2016)

5. Corbett, E. L., Watt, C. J., Walker, N., Maher, D., Williams, B. G., Raviglione, M. C. and Dye, C. The Growing Burden of Tuberculosis. *Arch. Intern. Med.* **163**, 1009 (2003).

6. Kim, S. J., Hong, Y. P., Lew, W. J., Yang, S. C. and Lee, E. G. Incidence of pulmonary tuberculosis among diabetics. *Tuber. Lung Dis.* **76**, 529–33 (1995).

7. Gomez, J. E. and McKinney, J. D. M. tuberculosis persistence, latency, and drug tolerance. *Tuberculosis* **84**, 29–44 (2004).

8. Crofton, J. and Mitchison, D. A. Streptomycin resistance in pulmonary tuberculosis. *Br. Med. J.* **2**, 1009–15 (1948).

9. Kapur, V., Whittam, T. S. and Musser, J. M. Is Mycobacterium tuberculosis 15,000 years old? *J. Infect. Dis.* **170**, 1348–9 (1994).

10. Chae, H. and Shin, S. J. Importance of differential identification of Mycobacterium tuberculosis strains for understanding differences in their prevalence, treatment efficacy, and vaccine development. *J. Microbiol.* **56**, 300–311 (2018).

11. Comas, I., Coscolla, M., Luo, T., Borrell, S., Holt, K. E., Kato-Maeda, M., Parkhill, J., Malla, B., Berg, S., Thwaites, G., Yeboah-Manu, D., Bothamley, G., Mei, J., Wei, L., Bentley, S., Harris, S. R., Niemann, S., Diel, R., Aseffa, A. *et al.* Out-of-Africa migration and Neolithic coexpansion of Mycobacterium tuberculosis with modern humans. *Nat. Genet.* **45**, 1176–1182 (2013).

12. de Jong, B. C., Antonio, M. and Gagneux, S. Mycobacterium africanum--review of an important cause of human tuberculosis in West Africa. *PLoS Negl. Trop. Dis.* **4**, e744 (2010).

13. Firdessa, R., Berg, S., Hailu, E., Schelling, E., Gumi, B., Erenso, G., Gadisa, E., Kiros, T., Habtamu, M., Hussein, J., Zinsstag, J., Robertson, B. D., Ameni, G., Lohan, A. J., Loftus, B., Comas, I., Gagneux, S., Tschopp, R., Yamuah, L. *et al.* Mycobacterial Lineages Causing Pulmonary and Extrapulmonary Tuberculosis, Ethiopia. *Emerg. Infect. Dis.* **19**, 460 (2013).

14. Barnes, D. S. Historical perspectives on the etiology of tuberculosis. *Microbes Infect.* **2**, 431–440 (2000).

15. Unaids. GLOBAL AIDS UP DATE 2016. (2016). Available at: http://www.unaids.org/sites/default/files/media_asset/global-AIDS-update-2016_en.pdf. (Accessed: 23rd April 2019)

16. Narasimhan, P., Wood, J., Macintyre, C. R. and Mathai, D. Risk factors for tuberculosis. *Pulm. Med.* **2013**, 828939 (2013).

17. Esmail, H., Barry, C. E., Young, D. B., Wilkinson, R. J. and Wilkinson, R. J. The ongoing challenge of latent tuberculosis. *Philos. Trans. R. Soc. Lond. B. Biol. Sci.* **369**, 20130437 (2014).

18. Comstock, G. W. The International Tuberculosis Campaign: A Pioneering Venture in Mass Vaccination and Research. *Clin. Infect. Dis.* **19**, 528–540 (1994).

19. Henao-Tamayo, M., Shanley, C. A., Verma, D., Zilavy, A., Stapleton, M. C., Furney, S. K., Podell, B.

and Orme, I. M. The Efficacy of the BCG Vaccine against Newly Emerging Clinical Strains of Mycobacterium tuberculosis. *PLoS One* **10**, e0136500 (2015).

20. Fox, W., Ellard, G. A. and Mitchison, D. A. Studies on the treatment of tuberculosis undertaken by the British Medical Research Council Tuberculosis Units, 1946–1986, with relevant subsequent publications.

21. Raviglione, M. and Pio, A. Evolution of WHO policies for tuberculosis control, 1948–2001. *Lancet* **359**, 775–780 (2002).

22. Lee, S. H. Tuberculosis Infection and Latent Tuberculosis. *Tuberc. Respir. Dis. (Seoul).* **79**, 201–206 (2016).

23. Smith, I. Mycobacterium tuberculosis pathogenesis and molecular determinants of virulence. *Clin. Microbiol. Rev.* **16**, 463–96 (2003).

24. Dartois, V. The path of anti-tuberculosis drugs: from blood to lesions to mycobacterial cells. *Nat. Rev. Microbiol.* **12**, 159–67 (2014).

25. te Brake, L. H. M., de Knegt, G. J., de Steenwinkel, J. E., van Dam, T. J. P., Burger, D. M., Russel, F. G. M., van Crevel, R., Koenderink, J. B. and Aarnoutse, R. E. The Role of Efflux Pumps in Tuberculosis Treatment and Their Promise as a Target in Drug Development: Unraveling the Black Box. *Annu. Rev. Pharmacol. Toxicol.* **58**, 271–291 (2018).

26. Ramakrishnan, L. Revisiting the role of the granuloma in tuberculosis. *Nat. Rev. Immunol.* **12**, 352–366 (2012).

27. Irwin, S. M., Prideaux, B., Lyon, E. R., Zimmerman, M. D., Brooks, E. J., Schrupp, C. A., Chen, C., Reichlen, M. J., Asay, B. C., Voskuil, M. I., Nuermberger, E. L., Andries, K., Lyons, M. A., Dartois, V. and Lenaerts, A. J. Bedaquiline and Pyrazinamide Treatment Responses Are Affected by Pulmonary Lesion Heterogeneity in Mycobacterium tuberculosis Infected C3HeB/FeJ Mice. *ACS Infect. Dis.* **2**, 251–267 (2016).

28. Chest, W. F. Whither short-course chemotherapy? *Br. J. Dis.* (1981).

29. Liu, Y., Pertinez, H., Ortega-Muro, F., Alameda-Martin, L., Harrison, T., Davies, G., Coates, A. and Hu, Y. Optimal doses of rifampicin in the standard drug regimen to shorten tuberculosis treatment duration and reduce relapse by eradicating persistent bacteria. *J. Antimicrob. Chemother.* **73**, 724–731 (2018).

30. Barry, C. E., Boshoff, H. I., Dartois, V., Dick, T., Ehrt, S., Flynn, J., Schnappinger, D., Wilkinson, R. J., Young, D. and Young, D. The spectrum of latent tuberculosis: rethinking the biology and intervention strategies. *Nat. Rev. Microbiol.* **7**, 845–55 (2009).

31. Lobue, P. and Menzies, D. Treatment of latent tuberculosis infection: An update. *Respirology* **15**, 603–622 (2010).

32. Menzies, D., Adjobimey, M., Ruslami, R., Trajman, A., Sow, O., Kim, H., Obeng Baah, J., Marks, G. B., Long, R., Hoeppner, V., Elwood, K., Al-Jahdali, H., Gninafon, M., Apriani, L., Koesoemadinata, R. C., Kritski, A., Rolla, V., Bah, B., Camara, A. *et al.* Four Months of Rifampin or Nine Months of Isoniazid for Latent Tuberculosis in Adults. *N. Engl. J. Med.* **379**, 440–453 (2018).

33. The sandbag and fresh air cure. Available at: http://news.bbc.co.uk/1/hi/health/564540.stm. (Accessed: 1st February 2019)

34. Nunn, A. J., Phillips, P. P. J. and Gillespie, S. H. Design issues in pivotal drug trials for drug sensitive tuberculosis (TB). *Tuberculosis (Edinb).* **88 Suppl 1**, S85-92 (2008).

35. van Ingen, J., Aarnoutse, R. E., Donald, P. R., Diacon, A. H., Dawson, R., Plemper van Balen, G., Gillespie, S. H. and Boeree, M. J. Why Do We Use 600 mg of Rifampicin in Tuberculosis Treatment? *Clin. Infect. Dis.* **52**, e194–e199 (2011).

36. Dorman, S. E., Schumacher, S. G., Alland, D., Nabeta, P., Armstrong, D. T., King, B., Hall, S. L., Chakravorty, S., Cirillo, D. M., Tukvadze, N., Bablishvili, N., Stevens, W., Scott, L., Rodrigues, C., Kazi, M. I., Joloba, M., Nakiyingi, L., Nicol, M. P., Ghebrekristos, Y. *et al.* Xpert MTB/RIF Ultra for

detection of Mycobacterium tuberculosis and rifampicin resistance: a prospective multicentre diagnostic accuracy study. *Lancet. Infect. Dis.* **18**, 76–84 (2018).

37. Nathan, C., Barry, C. E. and III. TB drug development: immunology at the table. **264**, (2015).

38. 99DOTS. Available at: https://www.99dots.org/. (Accessed: 30th January 2019)

39. Rapid Communication: Key changes to treatment of multidrug- and rifampicin-resistant tuberculosis (MDR/RR-TB). (2018). Available at: http://apps.who.int/bookorders. (Accessed: 24th April 2019)

40. Ma, Z., Lienhardt, C., McIlleron, H., Nunn, A. J. and Wang, X. Global tuberculosis drug development pipeline: the need and the reality. *Lancet* **375**, 2100–2109 (2010).

41. Critical Path to TB Drug Regimens (CPTR). Available at: https://www.c-path.org/pdf/CPTR 2010 MARCH.pdf. (Accessed: 26th April 2019)

42. Amikacin - TB DRUG MONOGRAPHS. Available at: http://www.tbdrugmonographs.co.uk/amikacin.html. (Accessed: 14th February 2019)

43. Hayward, R. S., Harding, J., Molloy, R., Land, L., Longcroft-Neal, K., Moore, D. and Ross, J. D. C. Adverse effects of a single dose of gentamicin in adults: a systematic review. *Br. J. Clin. Pharmacol.* **84**, 223–238 (2018).

44. Roy, C. J., Sivasubramani, S. K., Dutta, N. K., Mehra, S., Golden, N. A., Killeen, S., Talton, J. D., Hammoud, B. E., Didier, P. J. and Kaushal, D. Aerosolized Gentamicin Reduces the Burden of Tuberculosis in a Murine Model. *Antimicrob. Agents Chemother.* **56**, 883–886 (2012).

45. Stoffels, K., Traore, H., Vanderbist, F. and Fauville-Dufaux, M. The effect of combined tobramycin-clarithromycin on Mycobacterium tuberculosis isolates. *Int. J. Tuberc. Lung Dis.* **13**, 1041–4 (2009).

46. Cycloserine - TB DRUG MONOGRAPHS. Available at: http://www.tbdrugmonographs.co.uk/cycloserine.html. (Accessed: 18th May 2019)

47. Vora, A. Terizidone. *JAPI* **58**, 267–268 (2010).

48. Yamori, S., Ichiyama, S., Shimokata, K. and Tsukamura, M. Bacteriostatic and bactericidal activity of antituberculosis drugs against Mycobacterium tuberculosis, Mycobacterium avium-Mycobacterium intracellulare complex and Mycobacterium kansasii in different growth phases. *Microbiol. Immunol.* **36**, 361–8 (1992).

49. Scardigli, A., Caminero, J. A., Sotgiu, G., Centis, R., D'Ambrosio, L. and Migliori, G. B. Efficacy and tolerability of ethionamide versus prothionamide: a systematic review. *Eur. Respir. J.* **48**, 946–52 (2016).

50. Chiang, C.-Y., Van Deun, A. and Rieder, H. L. Gatifloxacin for short, effective treatment of multidrug-resistant tuberculosis. *Int. J. Tuberc. Lung Dis.* **20**, 1143–7 (2016).

51. Berning, S. E. The Role of Fluoroquinolones in Tuberculosis Today. *Drugs* **61**, 9–18 (2001).

52. Ahmad, Z., Tyagi, S., Minkowski, A., Peloquin, C. A., Grosset, J. H. and Nuermberger, E. L. Contribution of Moxifloxacin or Levofloxacin in Second-Line Regimens with or without Continuation of Pyrazinamide in Murine Tuberculosis. doi:10.1164/rccm.201212-2328OC

53. Nuermberger, E. L., Yoshimatsu, T., Tyagi, S., O'Brien, R. J., Vernon, A. N., Chaisson, R. E., Bishai, W. R. and Grosset, J. H. Moxifloxacin-containing Regimen Greatly Reduces Time to Culture Conversion in Murine Tuberculosis. *Am. J. Respir. Crit. Care Med.* **169**, 421–426 (2004).

54. Walwaikar, P. P., Morye, V. K. and Gawde, A. S. Ofloxacin in multidrug resistant tuberculosis. *J. Indian Med. Assoc.* **101**, 210–2 (2003).

55. Lubasch, A., Erbes, R., Mauch, H. and Lode, H. Sparfloxacin in the treatment of drug resistant tuberculosis or intolerance of first line therapy. *Eur. Respir. J.* **17**, 641–6 (2001).

56. TB Alliance. FDA Approves New Treatment for Highly Drug-Resistant Forms of Tuberculosis | TB

Alliance. Available at: https://www.tballiance.org/news/fda-approves-new-treatment-highly-drug-resistant-forms-tuberculosis. (Accessed: 9th September 2019)

57. Tasneen, R., Betoudji, F., Tyagi, S., Li, S.-Y., Williams, K., Converse, P. J., Dartois, V., Yang, T., Mendel, C. M., Mdluli, K. E. and Nuermberger, E. L. Contribution of Oxazolidinones to the Efficacy of Novel Regimens Containing Bedaquiline and Pretomanid in a Mouse Model of Tuberculosis. *Antimicrob. Agents Chemother.* **60**, 270–277 (2016).

58. Shaw, K. J. and Barbachyn, M. R. The oxazolidinones: past, present, and future. *Ann. N. Y. Acad. Sci.* **1241**, 48–70 (2011).

59. Crabol, Y., Catherinot, E., Veziris, N., Jullien, V. and Lortholary, O. Rifabutin: where do we stand in 2016? *J. Antimicrob. Chemother.* **71**, 1759–1771 (2016).

60. von Groote-Bidlingmaier, F., Patientia, R., Sanchez, E., Balanag, V., Ticona, E., Segura, P., Cadena, E., Yu, C., Cirule, A., Lizarbe, V., Davidaviciene, E., Domente, L., Variava, E., Caoili, J., Danilovits, M., Bielskiene, V., Staples, S., Hittel, N., Petersen, C. *et al.* Efficacy and safety of delamanid in combination with an optimised background regimen for treatment of multidrug-resistant tuberculosis: a multicentre, randomised, double-blind, placebo-controlled, parallel group phase 3 trial. *Lancet. Respir. Med.* **7**, 249–259 (2019).

61. A Phase 3 Study Assessing the Safety and Efficacy of Bedaquiline Plus PA-824 Plus Linezolid in Subjects With Drug Resistant Pulmonary Tuberculosis - Full Text View - ClinicalTrials.gov. Available at: https://clinicaltrials.gov/ct2/show/NCT02333799?term=nix-tb&rank=1. (Accessed: 1st February 2019)

62. TB Online - P-aminosalicylic acid. Available at: http://www.tbonline.info/posts/2011/8/30/p-aminosalicylic/. (Accessed: 14th February 2019)

63. TB Online - Thioacetazone. Available at: http://www.tbonline.info/posts/2011/9/9/thioacetazone/. (Accessed: 15th February 2019)

64. Clofazimine - TB DRUG MONOGRAPHS. Available at: http://www.tbdrugmonographs.co.uk/clofazimine.html. (Accessed: 14th February 2019)

65. Clarithromycin - TB DRUG MONOGRAPHS. Available at: http://www.tbdrugmonographs.co.uk/clarithromycin.html. (Accessed: 14th February 2019)

66. Walker, N. F., Clark, S. O., Oni, T., Andreu, N., Tezera, L., Singh, S., Saraiva, L., Pedersen, B., Kelly, D. L., Tree, J. A., D'Armiento, J. M., Meintjes, G., Mauri, F. A., Williams, A., Wilkinson, R. J., Friedland, J. S. and Elkington, P. T. Doxycycline and HIV Infection Suppress Tuberculosis-induced Matrix Metalloproteinases. *Am. J. Respir. Crit. Care Med.* **185**, 989–997 (2012).

67. Cicek-Saydam, C., Cavusoglu, C., Burhanoglu, D., Hilmioglu, S., Ozkalay, N. and Bilgic, A. In vitro susceptibility of Mycobacterium tuberculosis to fusidic acid. *Clin. Microbiol. Infect.* **7**, 700–2 (2001).

68. Mitchison, D. A. and Selkon, J. B. The bactericidal activities of antituberculous drugs. *Am. Rev. Tuberc.* **74**, 109–16; discussion, 116–23 (1956).

69. Slayden, R. A. and Barry, C. E. The genetics and biochemistry of isoniazid resistance in Mycobacterium tuberculosis. *Microbes Infect.* **2**, 659–669 (2000).

70. Zhang, Y., Heym, B., Allen, B., Young, D. and Cole, S. The catalase—peroxidase gene and isoniazid resistance of Mycobacterium tuberculosis. *Nature* **358**, 591–593 (1992).

71. Scior, T., Meneses Morales, I., Garcés Eisele, S. J., Domeyer, D. and Laufer, S. Antitubercular isoniazid and drug resistance of Mycobacterium tuberculosis--a review. *Arch. Pharm. (Weinheim).* **335**, 511–25 (2002).

72. Timmins, G. S. and Deretic, V. Mechanisms of action of isoniazid. *Mol. Microbiol.* **62**, 1220–7 (2006).

73. Dessen, A., Quémard, A., Blanchard, J. S., Jacobs, W. R. and Sacchettini, J. C. Crystal structure and function of the isoniazid target of Mycobacterium tuberculosis. *Science* **267**, 1638–41 (1995).

74. Alderwick, L. J., Harrison, J., Lloyd, G. S. and Birch, H. L. The Mycobacterial Cell Wall--Peptidoglycan and Arabinogalactan. *Cold Spring Harb. Perspect. Med.* **5**, a021113 (2015).

75. Bollela, V. R., Namburete, E. I., Feliciano, C. S., Macheque, D., Harrison, L. H. and Caminero, J. A. Detection of katG and inhA mutations to guide isoniazid and ethionamide use for drug-resistant tuberculosis. *Int. J. Tuberc. Lung Dis.* **20**, 1099–104 (2016).

76. De Groote, M. A., Gilliland, J. C., Wells, C. L., Brooks, E. J., Woolhiser, L. K., Gruppo, V., Peloquin, C. A., Orme, I. M. and Lenaerts, A. J. Comparative studies evaluating mouse models used for efficacy testing of experimental drugs against Mycobacterium tuberculosis. *Antimicrob. Agents Chemother.* **55**, 1237–47 (2011).

77. Liu, Y., Pertinez, H., Davies, G. R., Gillespie, S. H., Coates, A. R. and Hu, Y. Moxifloxacin Replacement in Contemporary Tuberculosis Drug Regimens Is Ineffective against Persistent *Mycobacterium tuberculosis* in the Cornell Mouse Model. *Antimicrob. Agents Chemother.* **62**, e00190-18 (2018).

78. Gillespie, S. H., Crook, A. M., McHugh, T. D., Mendel, C. M., Meredith, S. K., Murray, S. R., Pappas, F., Phillips, P. P. J. and Nunn, A. J. Four-Month Moxifloxacin-Based Regimens for Drug-Sensitive Tuberculosis. *N. Engl. J. Med.* **371**, 1577–1587 (2014).

79. Hu, Y., Liu, A., Ortega-Muro, F., Alameda-Martin, L., Mitchison, D. and Coates, A. High-dose rifampicin kills persisters, shortens treatment duration, and reduces relapse rate in vitro and in vivo. *Front. Microbiol.* **6**, (2015).

80. Zhang, Y. and Yew, W. W. Mechanisms of drug resistance in Mycobacterium tuberculosis [State of the art series. Drug-resistant tuberculosis. Edited by C-Y. Chiang. Number 1 in the series].

81. Wehrli, W. Rifampin: mechanisms of action and resistance. *Rev. Infect. Dis.* **5 Suppl 3**, S407-11

82. Miller, L. P., Crawford, J. T. and Shinnick, T. M. *The rpoB Gene of Mycobacterium tuberculosis*. *Antimicrob. Agents Chemother.* **38**, (1994).

83. Mitchison, D. A. and Fourie, P. B. The near future: Improving the activity of rifamycins and pyrazinamide. *Tuberculosis* **90**, 177–181 (2010).

84. Boeree, M. J., Diacon, A. H., Dawson, R., Narunsky, K., du Bois, J., Venter, A., Phillips, P. P. J., Gillespie, S. H., McHugh, T. D., Hoelscher, M., Heinrich, N., Rehal, S., van Soolingen, D., van Ingen, J., Magis-Escurra, C., Burger, D., Plemper van Balen, G. and Aarnoutse, R. E. A Dose-Ranging Trial to Optimize the Dose of Rifampin in the Treatment of Tuberculosis. *Am. J. Respir. Crit. Care Med.* **191**, 1058–1065 (2015).

85. Grosset, J., Truffot-Pernot, C., Lacroix, C. and Ji, B. Antagonism between isoniazid and the combination pyrazinamide-rifampin against tuberculosis infection in mice. *Antimicrob. Agents Chemother.* **36**, 548–51 (1992).

86. Via, L. E., Savic, R., Weiner, D. M., Zimmerman, M. D., Prideaux, B., Irwin, S. M., Lyon, E., Gopal, P., Eum, S., Lee, M., Lanoix, J.-P., Dutta, N. K., Shim, T., Su Cho, J., Kim, W., Karakousis, P. C., Lenaerts, A., Nuermberger, E., Barry III, C. E. *et al.* Host-Mediated Bioactivation of Pyrazinamide: Implications for Efficacy, Resistance, and Therapeutic Alternatives. doi:10.1021/id500028m

87. Zhang, Y. and Mitchison, D. The curious characteristics of pyrazinamide: a review.

88. Konno, K., Feldmann, F. M. and McDermott, W. Pyrazinamide susceptibility and amidase activity of tubercle bacilli. *Am. Rev. Respir. Dis.* **95**, 461–9 (1967).

89. Zhang, Y., Mitchison, D., Shi, W. and Zhang, W. Mechanisms of Pyrazinamide Action and Resistance. *Microbiol. Spectr.* **2**, (2014).

90. Ahmad, Z., Fraig, M. M., Bisson, G. P., Nuermberger, E. L., Grosset, J. H. and Karakousis, P. C. Dose-dependent activity of pyrazinamide in animal models of intracellular and extracellular tuberculosis infections. *Antimicrob. Agents Chemother.* **55**, 1527–32 (2011).

91. Dickinson, J. M. and Mitchison, D. A. Efficacy of intermittent pyrazinamide in experimental murine tuberculosis. *Tubercle* **72**, 110–114 (1991).

92. Steenken, W. and Wolinsky, E. The antituberculous activity of pyrazinamide in vitro and in the guinea pig. *Am. Rev. Tuberc.* **70**, 367–9 (1954).

93. Singapore Tuberculosis Service/British Medical Research Council. Clinical Trial of Six-Month and Four-Month Regimens of Chemotherapy in the Treatment of Pulmonary Tuberculosis. *AJRCCM* **199**, (1978).

94. Ferebee, S. H., Doster, B. E. and Murray, F. J. ETHAMBUTOL: A SUBSTITUTE FOR PARA-AMINOSALICYLIC ACID IN REGIMENS FOR PULMONARY TUBERCULOSIS. *Ann. N. Y. Acad. Sci.* **135**, 910–920 (1966).

95. Lee, R. E., Brennan, P. J. and Besra, G. S. Mycobacterial arabinan biosynthesis: the use of synthetic arabinoside acceptors in the development of an arabinosyl transfer assay. *Glycobiology* **7**, 1121–1128 (1997).

96. Forbes, M., Kuck, N. A. and Peets, E. A. Mode of Action of Ethambutol. *J. Bacteriol.* **84**, 1099–1103 (1962).

97. Moodley, R. and Godec, T. R. Short-course treatment for multidrug-resistant tuberculosis: the STREAM trials. *European respiratory review : an official journal of the European Respiratory Society* **25**, (2016).

98. Pontali, E., Sotgiu, G., Tiberi, S., D'ambrosio, L., Centis, R. and Migliori, G. B. Cardiac safety of bedaquiline: a systematic and critical analysis of the evidence. doi:10.1183/13993003.01462

99. Nuermberger, E., Tyagi, S., Tasneen, R., Williams, K. N., Almeida, D., Rosenthal, I. and Grosset, J. H. Powerful Bactericidal and Sterilizing Activity of a Regimen Containing PA-824, Moxifloxacin, and Pyrazinamide in a Murine Model of Tuberculosis. *Antimicrob. Agents Chemother.* **52**, 1522–1524 (2008).

100. Park, Y., Pacitto, A., Bayliss, T., Cleghorn, L. A. T., Wang, Z., Hartman, T., Arora, K., Ioerger, T. R., Sacchettini, J., Rizzi, M., Donini, S., Blundell, T. L., Ascher, D. B., Rhee, K., Breda, A., Zhou, N., Dartois, V., Jonnala, S. R., Via, L. E. *et al.* Essential but Not Vulnerable: Indazole Sulfonamides Targeting Inosine Monophosphate Dehydrogenase as Potential Leads against *Mycobacterium tuberculosis*. *ACS Infect. Dis.* **3**, 18–33 (2017).

101. BTZ-043 | Working Group for New TB Drugs. Available at: https://www.newtbdrugs.org/pipeline/compound/btz-043. (Accessed: 14th February 2019)

102. Merle, C. RAFA Trial Results: High Dose Rifampicin Tuberculosis treatment regimen to reduce 12 month mortality of TB/HIV co-infected patients. (2018). doi:10.24376/RD.SGUL.5831706.V1

103. Farber, S. M. and Eagle, H. R. Streptomycin Therapy of Tuberculosis. *Calif. Med.* **69**, 6–11 (1948).

104. Gumbo, T., Angulo-Barturen, I. and Ferrer-Bazaga, S. Pharmacokinetic-Pharmacodynamic and Dose-Response Relationships of Antituberculosis Drugs: Recommendations and Standards for Industry and Academia. *J. Infect. Dis.* **211**, S96–S106 (2015).

105. Nestorov, I. Whole Body Pharmacokinetic Models. *Clin. Pharmacokinet.* **42**, 883–908 (2003).

106. Mariappan, T. T. and Singh, S. Positioning of Rifampicin in the Biopharmaceutics Classification System (BCS). *Clin. Res. Regul. Aff.* **23**, 1–10 (2006).

107. Becker, C., Dressman, J. B., Amidon, G. L., Junginger, H. E., Kopp, S., Midha, K. K., Shah, V. P., Stavchansky, S. and Barends, D. M. Biowaiver Monographs for Immediate Release Solid Oral Dosage Forms: Ethambutol Dihydrochloride. A project of the International Pharmaceutical Federation FIP, Groupe BCS, http://www.fip.org/bcs. *J. Pharm. Sci.* **97**, 1350–1360 (2008).

108. Becker, C., Dressman, J. B., Amidon, G. L., Junginger, H. E., Kopp, S., Midha, K. K., Shah, V. P., Stavchansky, S., Barends, D. M. and International Pharmaceutical Federation, Groupe BCS. Biowaiver Monographs for Immediate Release Solid Oral Dosage Forms: Isoniazid**A project of the International Pharmaceutical Federation FIP, Groupe BCS, www.fip.org/bcs. *J. Pharm. Sci.* **96**, 522–531 (2007).

109. Becker, C., Dressman, J. B., Amidon, G. L., Junginger, H. E., Kopp, S., Midha, K. K., Shah, V. P.,

Stavchansky, S. and Barends, D. M. Biowaiver Monographs for Immediate Release Solid Oral Dosage Forms: Pyrazinamide. *Pharm. Assoc. J Pharm Sci* **97**, 3709–3720 (2008).

110. Stott, K. E., Singh, B., Beadsworth, M. B. J., Vaudrey, K., Khoo, S. H., Davies, G. and Stott, K. Adequacy of Rifampin Absorption after Jejunostomy Tube Administration. *Pharmacotherapy* **36**, 23–25 (2016).

111. Dharmadhikari, A. S., Kabadi, M., Gerety, B., Hickey, A. J., Fourie, P. B. and Nardell, E. Phase I, single-dose, dose-escalating study of inhaled dry powder capreomycin: a new approach to therapy of drug-resistant tuberculosis. *Antimicrob. Agents Chemother.* **57**, 2613–9 (2013).

112. Garcia Contreras, L., Sung, J., Ibrahim, M., Elbert, K., Edwards, D. and Hickey, A. Pharmacokinetics of Inhaled Rifampicin Porous Particles for Tuberculosis Treatment: Insight into Rifampicin Absorption from the Lungs of Guinea Pigs. *Mol. Pharm.* **12**, 2642–2650 (2015).

113. Acocella, G. Clinical Pharmacokinetics of Rifampicin. *Clin. Pharmacokinet.* **3**, 108–127 (1978).

114. Lee, C. S., Gambertoglio, J. G., Brater, D. C. and Benet, L. Z. Kinetics of oral ethambutol in the normal subject. *Clin. Pharmacol. Ther.* **22**, 615–621 (1977).

115. Liu, L., Xu, Y., Shea, C., Fowler, J. S., Hooker, J. M. and Tonge, P. J. Radiosynthesis and bioimaging of the tuberculosis chemotherapeutics isoniazid, rifampicin and pyrazinamide in baboons. *J. Med. Chem.* **53**, 2882–91 (2010).

116. Zeitlinger, M. A., Derendorf, H., Mouton, J. W., Cars, O., Craig, W. A., Andes, D. and Theuretzbacher, U. Protein binding: do we ever learn? *Antimicrob. Agents Chemother.* **55**, 3067–74 (2011).

117. Rullas, J. and Ferrer, S. *Evaluate protein binding and blood partitioning (blood-to-plasma ratio) for first and second line drugs (PreDiCT TB WP2 Deliverable No D2.43)*. (2016).

118. Lee, S. Y., Jang, H., Lee, J.-Y., Kwon, K., Oh, S. J. and Kim, S. K. Inhibition of cytochrome P450 by ethambutol in human liver microsomes. *Toxicol. Lett.* **229**, 33–40 (2014).

119. Wen, X., Wang, J.-S., Neuvonen, P. J. and Backman, J. T. Isoniazid is a mechanism-based inhibitor of cytochrome P 450 1A2, 2A6, 2C19 and 3A4 isoforms in human liver microsomes. *Eur. J. Clin. Pharmacol.* **57**, 799–804 (2002).

120. Nishimura, Y., Kurata, N., Sakurai, E. and Yasuhara, H. Inhibitory Effect of Antituberculosis Drugs on Human Cytochrome P450-Mediated Activities. *J. Pharmacol. Sci. J Pharmacol Sci* **96**, 293–300 (2004).

121. Shimada, T., Mimura, M., Inoue, K., Nakamura, S., Oda, H., Ohmori, S. and Yamazaki, H. Cytochrome P450-dependent drug oxidation activities in liver microsomes of various animal species including rats, guinea pigs, dogs, monkeys, and humans. *Arch. Toxicol.* **71**, 401–408 (1997).

122. Lin, J. H. CYP Induction-Mediated Drug Interactions: in Vitro Assessment and Clinical Implications. *Pharm. Res.* **23**, 1089–1115 (2006).

123. Horio, M., Gottesman, M. M. and Pastan, I. ATP-dependent transport of vinblastine in vesicles from human multidrug-resistant cells. *Proc. Natl. Acad. Sci. U. S. A.* **85**, 3580–4 (1988).

124. Gant, T. W., Oconnor, C. K., Corbitt, R., Thorgeirsson, U. and Thorgeirsson, S. S. In Vivo Induction of Liver P-Glycoprotein Expression by Xenobiotics in Monkeys. *Toxicol. Appl. Pharmacol.* **133**, 269–276 (1995).

125. Matheny, C. J., Lamb, M. W., Brouwer, K. L. R. and Pollack, G. M. Pharmacokinetic and Pharmacodynamic Implications of P-glycoprotein Modulation. *Pharmacotherapy* **21**, 778–796 (2001).

126. Yamashita, F., Sasa, Y., Yoshida, S., Hisaka, A., Asai, Y., Kitano, H., Hashida, M., Suzuki, H., Honig, P., Wortham, D., Zamani, K., Conner, D., Mullin, J., Josephson, F., Grub, S., Bryson, H., Goggin, T., Lüdin, E., Jorga, K. *et al.* Modeling of Rifampicin-Induced CYP3A4 Activation Dynamics for the Prediction of Clinical Drug-Drug Interactions from In Vitro Data. *PLoS One* **8**, e70330 (2013).

127. Ng, C.-S., Hasnat, A., Al Maruf, A., Ahmed, M. U., Pirmohamed, M., Day, C. P., Aithal, G. P. and Daly,

A. K. N-acetyltransferase 2 (NAT2) genotype as a risk factor for development of drug-induced liver injury relating to antituberculosis drug treatment in a mixed-ethnicity patient group. *Eur. J. Clin. Pharmacol.* **70**, 1079–86 (2014).

128. Lee, S.-W., Chung, L. S.-C., Huang, H.-H., Chuang, T.-Y., Liou, Y.-H. and Wu, L. S.-H. NAT2 and CYP2E1 polymorphisms and susceptibility to first-line anti-tuberculosis drug-induced hepatitis. *Int. J. Tuberc. Lung Dis.* **14**, 622–6 (2010).

129. Desta, Z., Soukhova, N. V and Flockhart, D. A. Inhibition of Cytochrome P450 (CYP450) Isoforms by Isoniazid: Potent Inhibition of CYP2C19 and CYP3A. **45**, 382–392 (2001).

130. Denti, P., Jeremiah, K., Chigutsa, E., Faurholt-Jepsen, D., PrayGod, G., Range, N., Castel, S., Wiesner, L., Hagen, C. M., Christiansen, M., Changalucha, J., McIlleron, H., Friis, H. and Andersen, A. B. Pharmacokinetics of Isoniazid, Pyrazinamide, and Ethambutol in Newly Diagnosed Pulmonary TB Patients in Tanzania. *PLoS One* **10**, e0141002 (2015).

131. McIlleron, H., Wash, P., Burger, A., Norman, J., Folb, P. I. and Smith, P. Determinants of rifampin, isoniazid, pyrazinamide, and ethambutol pharmacokinetics in a cohort of tuberculosis patients. *Antimicrob. Agents Chemother.* **50**, 1170–7 (2006).

132. Sharma, V. and McNeill, J. H. To scale or not to scale: the principles of dose extrapolation. *Br. J. Pharmacol.* **157**, 907–21 (2009).

133. Nielsen, E. I. and Friberg, L. E. Pharmacokinetic-Pharmacodynamic Modeling of Antibacterial Drugs. *Pharmacol. Rev.* **65**, 1053–1090 (2013).

134. Hatton, G. B., Yadav, V., Basit, A. W. and Merchant, H. A. Animal Farm: Considerations in Animal Gastrointestinal Physiology and Relevance to Drug Delivery in Humans. *J. Pharm. Sci.* **104**, 2747–2776 (2015).

135. Luttringer, O., Theil, F., Poulin, P., Schmitt-Hoffmann, A. H., Guentert, T. W. and Lavé, T. Physiologically Based Pharmacokinetic (PBPK) Modeling of Disposition of Epiroprim in Humans. *J. Pharm. Sci.* **92**, 1990–2007 (2003).

136. Zhuang, X. and Lu, C. PBPK modeling and simulation in drug research and development. *Acta Pharm. Sin. B* **6**, 430–440 (2016).

137. Chen, C., Ortega, F., Alameda, L., Ferrer, S. and Simonsson, U. S. H. Population pharmacokinetics, optimised design and sample size determination for rifampicin, isoniazid, ethambutol and pyrazinamide in the mouse. *Eur. J. Pharm. Sci.* **93**, 319–333 (2016).

138. Schipani, A., Pertinez, H., Mlota, R., Molyneux, E., Lopez, N., Dzinjalamala, F. K., Van Oosterhout, J. J., Ward, S. A., Khoo, S. and Davies, G. A simultaneous population pharmacokinetic analysis of rifampicin in Malawian adults and children. *Br. J. Clin. Pharmacol.* **81**, (2016).

139. Marsot, A., Ménard, A., Dupouey, J., Muziotti, C., Guilhaumou, R. and Blin, O. PHARMACOKINETICS Population pharmacokinetics of rifampicin in adult patients with osteoarticular infections: interaction with fusidic acid. *Br. J. Clin. Pharmacol. Br J Clin Pharmacol* **83**, 1039 (2017).

140. Wilton, J. H., Nix, D. and Schentag, J. J. *Ciprofloxacin concentrations in lung tissue following a single 400 mg intravenous dose Impact of Requiring Reapproval on Day Three of Restricted Antibiotic Therapy View project Clinical Failure Rates With and Without Atypical Coverage in Hospitalized Adul*. *Article in Journal of Antimicrobial Chemotherapy* **43**, (1999).

141. Brunner, M. and Langer, O. Microdialysis versus other techniques for the clinical assessment of in vivo tissue drug distribution. *AAPS J.* **8**, E263-71 (2006).

142. Ungerstedt, U. and Hallström, A. In vivo microdialysis--a new approach to the analysis of neurotransmitters in the brain. *Life Sci.* **41**, 861–4 (1987).

143. Lönnroth, P., Jansson, P. A. and Smith, U. A microdialysis method allowing characterization of intercellular water space in humans. *Am. J. Physiol.* **253**, E228-31 (1987).

144. Scott, D. O., Sorenson, L. R., Steele, K. L., Puckett, D. L. and Lunte, C. E. In vivo microdialysis sampling for pharmacokinetic investigations. *Pharm. Res.* **8**, 389–392 (1991).

145. Plock, N. and Kloft, C. Microdialysis--theoretical background and recent implementation in applied life-sciences. *Eur. J. Pharm. Sci.* **25**, 1–24 (2005).

146. Falcon, E., Maier, K., Robinson, S. A., Hill-Smith, T. E. and Lucki, I. Effects of buprenorphine on behavioral tests for antidepressant and anxiolytic drugs in mice. *Psychopharmacology (Berl).* **232**, 907–915 (2015).

147. Higashino, K., Ago, Y., Umehara, M., Kita, Y., Fujita, K., Takuma, K. and Matsuda, T. Effects of acute and chronic administration of venlafaxine and desipramine on extracellular monoamine levels in the mouse prefrontal cortex and striatum. *Eur. J. Pharmacol.* **729**, 86–93 (2014).

148. Alves, I. A., Staudt, K. J., Carreño, F. O., de Araujo Lock, G., de Miranda Silva, C., Rates, S. M. K., Dalla Costa, T. and De Araujo, B. V. Population Pharmacokinetic Modeling to Describe the Total Plasma and Free Brain Levels of Fluconazole in Healthy and Cryptococcus neoformans Infected Rats: How Does the Infection Impact the Drug's Levels on Biophase? *Pharm. Res.* **35**, 132 (2018).

149. Wei, J., Lai, Q., Shumyak, S. P., Xu, L., Zhang, C., Ling, J. and Yu, Y. An LC/MS quantitative and microdialysis method for cyclovirobuxine D pharmacokinetics in rat plasma and brain: The pharmacokinetic comparison of three different drug delivery routes. *J. Chromatogr. B* **1002**, 185–193 (2015).

150. Rottbøll, L., Skovgaard, K., Barington, K., Jensen, H. E. and Friis, C. Intrabronchial Microdialysis: Effects of Probe Localisation on Tissue Trauma and Drug Penetration into the Pulmonary Epithelial Lining Fluid. *Basic Clin. Pharmacol. Toxicol.* (2015). doi:10.1111/bcpt.12403

151. Rottbøll, L. A. H. and Friis, C. Penetration of antimicrobials to pulmonary epithelial lining fluid and muscle and impact of drug physicochemical properties determined by microdialysis. *J. Pharmacol. Toxicol. Methods* **78**, 58–65 (2016).

152. Tøttrup, M., Bibby, B. M., Hardlei, T. F., Bue, M., Kerrn-Jespersen, S., Fuursted, K., Søballe, K. and Birke-Sørensen, H. Continuous versus short-term infusion of cefuroxime: assessment of concept based on plasma, subcutaneous tissue, and bone pharmacokinetics in an animal model. *Antimicrob. Agents Chemother.* **59**, 67–75 (2015).

153. Çavuş, I., Romanyshyn, J. C., Kennard, J. T., Farooque, P., Williamson, A., Eid, T., Spencer, S. S., Duckrow, R., Dziura, J. and Spencer, D. D. Elevated basal glutamate and unchanged glutamine and GABA in refractory epilepsy: Microdialysis study of 79 patients at the yale epilepsy surgery program. *Ann. Neurol.* **80**, 35–45 (2016).

154. Amato, D., Beasley, C. L., Hahn, M. K. and Vernon, A. C. Neuroadaptations to antipsychotic drugs: Insights from pre-clinical and human post-mortem studies. *Neurosci. Biobehav. Rev.* **76**, 317–335 (2017).

155. Nguyen, H. X., Puri, A., Bhattaccharjee, S. A. and Banga, A. K. Qualitative and quantitative analysis of lateral diffusion of drugs in human skin. *Int. J. Pharm.* **544**, 62–74 (2018).

156. Bodenlenz, M., Dragatin, C., Liebenberger, L., Tschapeller, B., Boulgaropoulos, B., Augustin, T., Raml, R., Gatschelhofer, C., Wagner, N., Benkali, K., Rony, F., Pieber, T. and Sinner, F. Kinetics of Clobetasol-17-Propionate in Psoriatic Lesional and Non-Lesional Skin Assessed by Dermal Open Flow Microperfusion with Time and Space Resolution. *Pharm. Res.* **33**, 2229–2238 (2016).

157. Eslam, R. B., Burian, A., Vila, G., Sauermann, R., Hammer, A., Frenzel, D., Minichmayr, I. K., Kloft, C., Matzneller, P., Oesterreicher, Z. and Zeitlinger, M. Target site pharmacokinetics of linezolid after single and multiple doses in diabetic patients with soft tissue infection. *J. Clin. Pharmacol.* **54**, 1058–1062 (2014).

158. Kempker, R. R., Barth, A. B., Vashakidze, S., Nikolaishvili, K., Sabulua, I., Tukvadze, N., Bablishvili, N., Gogishvili, S., Singh, R. S. P., Guarner, J., Derendorf, H., Peloquin, C. A. and Blumberg, H. M. Cavitary Penetration of Levofloxacin among Patients with Multidrug-Resistant Tuberculosis. *Antimicrob. Agents Chemother.* (2015). doi:10.1128/AAC.00379-15

159. Wang, C., Lu, X., Li, L., Zhang, R., shi, T. and Li, S. Microdialysis combined with liquid chromatography-tandem mass spectrometry for the determination of nimodipine in the guinea pig hippocampus. *J. Chromatogr. B* **1017–1018**, 226–232 (2016).

160. Gulati, G. K., Berger, L. R. and Hinds, B. J. A preclinical evaluation of a programmable CNT membrane device for transdermal nicotine delivery in hairless Guinea pigs. *J. Control. Release* **293**, 135–143 (2019).

161. Wang, G., Zhang, B., Nie, Q., Zang, C. and Zhu, Q. Simultaneous Determination of Four Substances in Plasma and Dermal Microdialysates of Guinea Pig after Different Acupoints Administration of Fufang Baijiezi Gel. *Chinese Herb. Med.* **7**, 365–370 (2015).

162. Shukla, C., Li, J., Lionberger, R. and Bashaw, E. Microdialysis in Drug Development. in *Microdialysis in Drug Development* 67–80 (2012).

163. Cooley, J., Ducey, M., Regel, A., Nandi, P., Lunte, S. M. and Lunte, C. E. Microdialysis in Drug Development. in *Microdialysis in Drug Development* 35–63 (2012).

164. Wu, J.-W., Shih, H.-H., Wang, S.-C. and Tsai, T.-H. Determination and pharmacokinetic profile of pyrazinamide in rat blood, brain and bile using microdialysis coupled with high-performance liquid chromatography and verified by tandem mass spectrometry. *Anal. Chim. Acta* **522**, 231–239 (2004).

165. Nandi, P. and Lunte, S. M. Recent trends in microdialysis sampling integrated with conventional and microanalytical systems for monitoring biological events: a review. *Anal. Chim. Acta* **651**, 1–14 (2009).

166. de Araújo, B. V., Laureano, J. V., Grünspan, L. D., Dalla Costa, T. and Tasso, L. Validation of an efficient LC-microdialysis method for gemifloxacin quantitation in lung, kidney and liver of rats. *J. Chromatogr. B. Analyt. Technol. Biomed. Life Sci.* **919–920**, 62–6 (2013).

167. Bouw, M. R. and Hammarlund-Udenaes, M. Methodological aspects of the use of a calibrator in in vivo microdialysis-further development of the retrodialysis method. *Pharm. Res.* **15**, 1673–9 (1998).

168. Shippenberg, T. S. and Thompson, A. C. Overview of microdialysis. *Curr. Protoc. Neurosci.* **Chapter 7**, Unit7.1 (2001).

169. Stenken, J. A., Lunte, C. E., Southard, M. Z. and Ståhle, L. Factors that influence microdialysis recovery. Comparison of experimental and theoretical microdialysis recoveries in rat liver. *J. Pharm. Sci.* **86**, 958–66 (1997).

170. Kloft, C. and Simmel. Microdialysis feasibility investigations with the non-hydrophilic antifungal voriconazole for potential applications in nonclinical and clinical settings. *Int. J. Clin. Pharmacol. Ther.* **48**, 695–704 (2010).

171. Wang, Y., Wong, S. L. and Sawchuk, R. J. Microdialysis calibration using retrodialysis and zero-net flux: application to a study of the distribution of zidovudine to rabbit cerebrospinal fluid and thalamus. *Pharm. Res.* **10**, 1411–9 (1993).

172. Menacherry, S., Hubert, W. and Justice, J. B. In vivo calibration of microdialysis probes for exogenous compounds. *Anal. Chem.* **64**, 577–83 (1992).

173. Olson, R. J. and Justice, J. B. Quantitative microdialysis under transient conditions. *Anal. Chem.* **65**, 1017–22 (1993).

174. Larsson, C. I. The use of an 'internal standard' for control of the recovery in microdialysis. *Life Sci.* **49**, PL73-8 (1991).

175. Yokel, R. A., Allen, D. D., Burgio, D. E. and McNamara, P. J. Antipyrine as a dialyzable reference to correct differences in efficiency among and within sampling devices during in vivo microdialysis. *J. Pharmacol. Toxicol. Methods* **27**, 135–42 (1992).

176. Mindermann, T., Zimmerli, W. and Gratzl, O. Rifampin concentrations in various compartments of the human brain: a novel method for determining drug levels in the cerebral extracellular space. *Antimicrob. Agents Chemother.* **42**, 2626–9 (1998).

177. Bungay P, M. P. D. R. Steady-State Theory for Quantitative Microdialysis of Solutes and Water In Vivo and In Vitro. *Life Sci.* **46**, 105–119 (1989).

178. Joukhadar, C. and Müller, M. Microdialysis: current applications in clinical pharmacokinetic studies and its potential role in the future. *Clin. Pharmacokinet.* **44**, 895–913 (2005).

179. Davies, M. I., Cooper, J. D., Desmond, S. S., Lunte, C. E. and Lunte, S. M. Analytical considerations for microdialysis sampling. *Adv. Drug Deliv. Rev.* **45**, 169–88 (2000).

180. de Lange, E. Methodological considerations of intracerebral microdialysis in pharmacokinetic studies on drug transport across the blood–brain barrier. *Brain Res. Rev.* **25**, 27–49 (1997).

181. Gumbo, T., Louie, A., Deziel, M. R., Liu, W., Parsons, L. M., Salfinger, M. and Drusano, G. L. Concentration-Dependent Mycobacterium tuberculosis Killing and Prevention of Resistance by Rifampin. *Antimicrob. Agents Chemother.* **51**, 3781–3788 (2007).

182. Williams, A. and Orme, I. M. Animal Models of Tuberculosis: An Overview. in *Tuberculosis and the Tubercle Bacillus, Second Edition* **4**, 131–142 (American Society of Microbiology, 2016).

183. Lanoix, J.-P., Betoudji, F. and Nuermberger, E. Sterilizing Activity of Pyrazinamide in Combination with First-Line Drugs in a C3HeB/FeJ Mouse Model of Tuberculosis. *Antimicrob. Agents Chemother.* **60**, 1091–6 (2016).

184. Grosset, J., Almeida, D., Converse, P. J., Tyagi, S., Li, S.-Y., Ammerman, N. C., Pym, A. S., Wallengren, K., Hafner, R., Lalloo, U., Swindells, S. and Bishai, W. R. Modeling early bactericidal activity in murine tuberculosis provides insights into the activity of isoniazid and pyrazinamide. *Proc. Natl. Acad. Sci. U. S. A.* **109**, 15001–5 (2012).

185. Hu, Y., Pertinez, H., Ortega-Muro, F., Alameda-Martin, L., Liu, Y., Schipani, A., Davies, G. and Coates, A. Investigation of Elimination Rate, Persistent Subpopulation Removal, and Relapse Rates of Mycobacterium tuberculosis by Using Combinations of First-Line Drugs in a Modified Cornell Mouse Model. *Antimicrob. Agents Chemother.* **60**, 4778–85 (2016).

186. Calderon, V. E., Valbuena, G., Goez, Y., Judy, B. M., Huante, M. B., Sutjita, P., Johnston, R. K., Estes, D. M., Hunter, R. L., Actor, J. K., Cirillo, J. D. and Endsley, J. J. A Humanized Mouse Model of Tuberculosis. *PLoS One* **8**, e63331 (2013).

187. Gonzalez-Juarrero, M., Turner, O. C., Turner, J., Marietta, P., Brooks, J. V. and Orme, I. M. Temporal and Spatial Arrangement of Lymphocytes within Lung Granulomas Induced by Aerosol Infection with Mycobacterium tuberculosis. *Infect. Immun.* **69**, 1722–1728 (2001).

188. Driver, E. R., Ryan, G. J., Hoff, D. R., Irwin, S. M., Basaraba, R. J., Kramnik, I. and Lenaerts, A. J. Evaluation of a mouse model of necrotic granuloma formation using C3HeB/FeJ mice for testing of drugs against Mycobacterium tuberculosis. *Antimicrob. Agents Chemother.* **56**, 3181–95 (2012).

189. de Steenwinkel, J. E. M., Aarnoutse, R. E., de Knegt, G. J., ten Kate, M. T., Teulen, M., Verbrugh, H. A., Boeree, M. J., van Soolingen, D. and Bakker-Woudenberg, I. A. J. M. Optimization of the Rifampin Dosage to Improve the Therapeutic Efficacy in Tuberculosis Treatment Using a Murine Model. *Am. J. Respir. Crit. Care Med.* **187**, 1127–1134 (2013).

190. Ji, B., Truffot-Pernot, C., Lacroix, C., Raviglione, M. C., O'Brien, R. J., Olliaro, P., Roscigno, G. and Grosset, J. Effectiveness of rifampin, rifabutin, and rifapentine for preventive therapy of tuberculosis in mice. *Am. Rev. Respir. Dis.* **148**, 1541–1546 (1993).

191. Zapata, A., Chefer, V. I. and Shippenberg, T. S. Microdialysis in rodents. *Current Protocols in Neuroscience* (2009). doi:10.1002/0471142301.ns0702s47

192. Kjellsson, M. C., Via, L. E., Goh, A., Weiner, D., Low, K. M., Kern, S., Pillai, G., Barry, C. E., Dartois, V. and Dartois, V. Pharmacokinetic evaluation of the penetration of antituberculosis agents in rabbit pulmonary lesions. *Antimicrob. Agents Chemother.* **56**, 446–57 (2012).

193. Zimmerman, M., Lestner, J., Prideaux, B., O'Brien, P., Dias-Freedman, I., Chen, C., Dietzold, J., Daudelin, I., Kaya, F., Blanc, L., Chen, P.-Y., Park, S., Salgame, P., Sarathy, J. and Dartois, V. Ethambutol Partitioning in Tuberculous Pulmonary Lesions Explains Its Clinical Efficacy. *Antimicrob. Agents Chemother.* **61**, (2017).

194. Rifat, D., Prideaux, B., Savic, R. M., Urbanowski, M. E., Parsons, T. L., Luna, B., Marzinke, M. A.,

Ordonez, A. A., DeMarco, V. P., Jain, S. K., Dartois, V., Bishai, W. R. and Dooley, K. E. Pharmacokinetics of rifapentine and rifampin in a rabbit model of tuberculosis and correlation with clinical trial data. *Sci. Transl. Med.* **10**, eaai7786 (2018).

195. Wang, Y. and Sawchuk, R. J. Zidovudine transport in the rabbit brain during intravenous and intracerebroventricular infusion. *J. Pharm. Sci.* **84**, 871–6 (1995).

196. Scanga, C. A. and Flynn, J. L. Modeling Tuberculosis in Nonhuman Primates. *Cold Spring Harb. Perspect. Med.* **4**, a018564 (2014).

197. Lin, P. L., Dartois, V., Johnston, P. J., Janssen, C., Via, L., Goodwin, M. B., Klein, E., Barry, C. E. and Flynn, J. L. Metronidazole prevents reactivation of latent Mycobacterium tuberculosis infection in macaques. *Proc. Natl. Acad. Sci.* **109**, 14188–14193 (2012).

198. Galvan, A., Smith, Y. and Wichmann, T. Continuous monitoring of intracerebral glutamate levels in awake monkeys using microdialysis and enzyme fluorometric detection. *J. Neurosci. Methods* **126**, 175–85 (2003).

199. Kumar, N., Vishwas, K. G. G., Kumar, M., Reddy, J., Parab, M., Manikanth, C. L. L., Pavithra, B. S. S. and Shandil, R. K. K. Pharmacokinetics and dose response of anti-TB drugs in rat infection model of tuberculosis. *Tuberculosis* **94**, 282–286 (2014).

200. Li, C. H., Stratford, R. E., Velez de Mendizabal, N., Cremers, T. I., Pollock, B. G., Mulsant, B. H., Remington, G., Bies, R. R. and Bies, R. R. Prediction of brain clozapine and norclozapine concentrations in humans from a scaled pharmacokinetic model for rat brain and plasma pharmacokinetics. *J. Transl. Med.* **12**, 203 (2014).

201. Torres, B. G. S., Helfer, V. E., Bernardes, P. M., Macedo, A. J., Nielsen, E. I., Friberg, L. E. and Dalla Costa, T. Population Pharmacokinetic Modeling as a Tool To Characterize the Decrease in Ciprofloxacin Free Interstitial Levels Caused by Pseudomonas aeruginosa Biofilm Lung Infection in Wistar Rats. *Antimicrob. Agents Chemother.* **61**, (2017).

202. Xu, Y., Zhang, Q., Li, P., Hong, G., Wang, D., Liu, J., Zhou, H., Chai, G., Lu, B., He, S., Zhang, W., Sun, S., Zhang, J. and Mao, J. Nicotine Pharmacokinetics in Rat Brain and Blood by Simultaneous Microdialysis, Stable-Isotope Labeling, and UHPLC–HRMS: Determination of Nicotine Metabolites. *Anal. Chem.* **91**, 2916–2922 (2019).

203. Chang, H.-Y., Morrow, K., Bonacquisti, E., Zhang, W. and Shah, D. K. Antibody pharmacokinetics in rat brain determined using microdialysis. *MAbs* **10**, 843–853 (2018).

204. Massé, I., Moquin, L., Provost, C., Guay, S., Gratton, A. and De Beaumont, L. Running Title: Cerebral microdialysis and concussion combined model Title: In vivo cerebral microdialysis validation of the acute central glutamate response in a translational rat model of concussion combining force and rotation. doi:10.1101/432633

205. Podell BK, Williams A, I. A. and B. *Tuberculosis, Leprosy and Mycobacterial Diseases of Man and Animals: The Many Hosts of Mycobacteria. (Laboratory Models of Tuberculosis Guinea Pigs)*. (2015).

206. Orme, I. M. and Ordway, D. J. Mouse and Guinea Pig Models of Tuberculosis. in *Tuberculosis and the Tubercle Bacillus, Second Edition* **4**, 143–162 (American Society of Microbiology, 2016).

207. Ahmad, Z., Nuermberger, E. L., Tasneen, R., Pinn, M. L., Williams, K. N., Peloquin, C. A., Grosset, J. H. and Karakousis, P. C. Comparison of the 'Denver regimen' against acute tuberculosis in the mouse and guinea pig. *J. Antimicrob. Chemother.* **65**, 729–34 (2010).

208. Dharmadhikari, A. S. and Nardell, E. A. What Animal Models Teach Humans about Tuberculosis. *Am. J. Respir. Cell Mol. Biol.* **39**, 503–508 (2008).

209. Kim, J.-K., Choi, M. S., Jeong, J.-J., Lim, S.-M., Kim, I. S., Yoo, H. H. and Kim, D.-H. Effect of Probiotics on Pharmacokinetics of Orally Administered Acetaminophen in Mice. *Drug Metab. Dispos.* **46**, 122–130 (2018).

210. Lewis, J. H. Comparative hematology: studies on guinea-pigs (Cavia porcellus). *Comp. Biochem. Physiol. Comp. Physiol.* **102**, 507–12 (1992).

211. Hahn, H., Kammerer, B., DiMauro, A., Salt, A. N. and Plontke, S. K. Cochlear microdialysis for quantification of dexamethasone and fluorescein entry into scala tympani during round window administration. *Hear. Res.* **212**, 236–44 (2006).

212. Saunte, D. M., Simmel, F., Frimodt-Moller, N., Stolle, L. B., Svejgaard, E. L., Haedersdal, M., Kloft, C. and Arendrup, M. C. In vivo efficacy and pharmacokinetics of voriconazole in an animal model of dermatophytosis. *Antimicrob. Agents Chemother.* **51**, 3317–21 (2007).

213. Gupta, A., Jansson, B., Chatelain, P., Massingham, R. and Hammarlund-Udenaes, M. Quantitative determination of cetirizine enantiomers in guinea pig plasma, brain tissue and microdialysis samples using liquid chromatography/tandem mass spectrometry. *Rapid Commun. Mass Spectrom.* **19**, 1749–1757 (2005).

214. Wetherell, J. R., Armstrong, S. J., Read, R. W. and Clough, G. F. VX Penetration Following Percutaneous Poisoning: A Dermal Microdialysis Study in the Guinea Pig. *Toxicol. Mech. Methods* **18**, 313–321 (2008).

215. Mumford, H., Docx, C. J., Price, M. E., Green, A. C., Tattersall, J. E. H. and Armstrong, S. J. Human plasma-derived BuChE as a stoichiometric bioscavenger for treatment of nerve agent poisoning. *Chem. Biol. Interact.* **203**, 160–166 (2013).

216. Zhang, K., Li, Q., Xu, J., Liu, J., Ke, J., Kang, W., Li, T. and Ma, F. Unilateral horizontal semicircular canal occlusion induces serotonin increase in medial vestibular nuclei: a study using microdialysis in vivo coupled with HPLC–ECD. *Analyst* **140**, 3846–3851 (2015).

217. Zhang, Y., Huo, M., Zhou, J. and Xie, S. PKSolver: An add-in program for pharmacokinetic and pharmacodynamic data analysis in Microsoft Excel. *Comput. Methods Programs Biomed.* **99**, 306–314 (2010).

218. Burhan, E., Ruesen, C., Ruslami, R., Ginanjar, A., Mangunnegoro, H., Ascobat, P., Donders, R., van Crevel, R. and Aarnoutse, R. Isoniazid, rifampin, and pyrazinamide plasma concentrations in relation to treatment response in Indonesian pulmonary tuberculosis patients. *Antimicrob. Agents Chemother.* **57**, 3614–9 (2013).

219. Smythe, W., Khandelwal, A., Merle, C., Rustomjee, R., Gninafon, M., Bocar Lo, M., Sow, O. B., Olliaro, P. L., Lienhardt, C., Horton, J., Smith, P., McIlleron, H. and Simonsson, U. S. H. A semimechanistic pharmacokinetic-enzyme turnover model for rifampin autoinduction in adult tuberculosis patients. *Antimicrob. Agents Chemother.* **56**, 2091–8 (2012).

220. Dutta, N. K., Alsultan, A., Peloquin, C. A. and Karakousis, P. C. Preliminary pharmacokinetic study of repeated doses of rifampin and rifapentine in guinea pigs. *Antimicrob. Agents Chemother.* **57**, 1535–7 (2013).

221. Müller, M. Science, medicine, and the future: Microdialysis. *BMJ* **324**, 588–91 (2002).

222. Technical Brief. Mass Spectrometry in Bioanalysis. *Part. Sci.* **4**, (2009).

223. Charlwood, P. A. Ultracentrifugal studies of rat, rabbit and guinea-pig serum albumins. *Biochem. J.* **78**, 163–72 (1961).

224. Mindermann, T., Zimmerli, W. and Gratzl, O. Rifampin concentrations in various compartments of the human brain: a novel method for determining drug levels in the cerebral extracellular space. *Antimicrob. Agents Chemother.* **42**, 2626–9 (1998).

225. Taylor, J. R. (John R. *An introduction to error analysis : the study of uncertainties in physical measurements*. (University Science Books, 1997).

226. Charles River. Brains Online. Available at: https://www.criver.com/products-services/discovery-services/vivo-pharmacology/neuroscience-translational-tools/microdialysis?region=3696.

227. Metushi, I., Uetrecht, J. and Phillips, E. Mechanism of isoniazid-induced hepatotoxicity: then and now. *Br. J. Clin. Pharmacol.* **81**, 1030 (2016).

228. Tasso, L., Bettoni, C. C., Oliveira, L. K. and Dalla Costa, T. Evaluation of gatifloxacin penetration

into skeletal muscle and lung by microdialysis in rats. *Int. J. Pharm.* **358**, 96–101 (2008).

229. Liu, P., Fuhrherr, R., Webb, A. I., Obermann, B. and Derendorf, H. Tissue penetration of cefpodoxime into the skeletal muscle and lung in rats. *Eur. J. Pharm. Sci.* **25**, 439–444 (2005).

230. Cooper. *Anatomy of the Guinea Pig*. (1976).

231. Mosaei, H., Molodtsov, V., Kepplinger, B., Harbottle, J., Moon, C. W., Jeeves, R. E., Ceccaroni, L., Shin, Y., Morton-Laing, S., Marrs, E. C. L., Wills, C., Clegg, W., Yuzenkova, Y., Perry, J. D., Bacon, J., Errington, J., Allenby, N. E. E., Hall, M. J., Murakami, K. S. *et al.* Mode of Action of Kanglemycin A, an Ansamycin Natural Product that Is Active against Rifampicin-Resistant Mycobacterium tuberculosis. *Mol. Cell* **72**, 263–274.e5 (2018).

232. Jayaram, R., Gaonkar, S., Kaur, P., Suresh, B. L., Mahesh, B. N., Jayashree, R., Nandi, V., Bharat, S., Shandil, R. K., Kantharaj, E. and Balasubramanian, V. Pharmacokinetics-pharmacodynamics of rifampin in an aerosol infection model of tuberculosis. *Antimicrob. Agents Chemother.* **47**, 2118–24 (2003).

233. Alghamdi, W. A., Al-Shaer, M. H. and Peloquin, C. A. Protein Binding of First-Line Antituberculosis Drugs. *Antimicrob. Agents Chemother.* **62**, (2018).

234. Lenaerts, A. J. *GP-pk-01 (data shared by Anne Lenaerts, Colorado State University)*.

235. Hu, Y., Liu, A., Ortega-Muro, F., Alameda-Martin, L., Mitchison, D. and Coates, A. High-dose rifampicin kills persisters, shortens treatment duration, and reduces relapse rate in vitro and in vivo. *Front. Microbiol.* **6**, 641 (2015).

236. Stott, K. E., Pertinez, H., Sturkenboom, M. G. G., Boeree, M. J., Aarnoutse, R., Ramachandran, G., Requena-Méndez, A., Peloquin, C., Koegelenberg, C. F. N., Alffenaar, J. W. C., Ruslami, R., Tostmann, A., Swaminathan, S., Mcilleron, H. and Davies, G. Pharmacokinetics of rifampicin in adult TB patients and healthy volunteers: a systematic review and meta-analysis. doi:10.1093/jac/dky152

237. Damsma, G., Westerink, B. H., de Vries, J. B., Van den Berg, C. J. and Horn, A. S. Measurement of acetylcholine release in freely moving rats by means of automated intracerebral dialysis. *J. Neurochem.* **48**, 1523–8 (1987).

238. Ho, S. and Future Science Ltd. *Tissue analysis for drug development*.

239. Fiegel, J., Garcia-Contreras, L., Thomas, M., VerBerkmoes, J., Elbert, K., Hickey, A. and Edwards, D. Preparation and in Vivo Evaluation of a Dry Powder for Inhalation of Capreomycin. *Pharm. Res.* **25**, 805–811 (2008).

240. Lenaerts, A. J., Hoff, D., Aly, S., Ehlers, S., Andries, K., Cantarero, L., Orme, I. M. and Basaraba, R. J. Location of Persisting Mycobacteria in a Guinea Pig Model of Tuberculosis Revealed by R207910. *Antimicrob. Agents Chemother.* **51**, 3338–3345 (2007).

241. Oh, J.-H., Park, S.-E., Shim, C.-K. and Lee, Y.-J. Biliary clearance of bromosulfophthalein in anesthetized and freely moving conscious rat. *Biopharm. Drug Dispos.* **30**, 94–98 (2009).

242. Zent, C., Smith, P. and Zent, C. *Tubercle and Lung Disease Study of the effect of concomitant food on the bioavailability of rifampicin, isoniazid and pyrazinamide*. *Tubercle and Lung Disease* **76**, (1995).

243. Tsai, T. H., Huang, C. T., Shum, A. Y. and Chen, C. F. Simultaneous blood and biliary sampling of esculetin by microdialysis in the rat. *Life Sci.* **65**, 1647–55 (1999).

244. Tsai, T. H., Hung, L. C. and Chen, C. F. Microdialysis study of biliary excretion of chloramphenicol and its glucuronide in the rat. *J. Pharm. Pharmacol.* **51**, 911–5 (1999).

245. Acocella, G. Clinical pharmacokinetics of rifampicin. *Clin. Pharmacokinet.* **3**, 108–27 (1978).

246. Gad, S. *Animal Models in Toxicology*. (2015).

247. Maartens, G., Decloedt, E. and Cohen, K. Effectiveness and safety of antiretrovirals with rifampicin: crucial issues for high-burden countries. *Antivir. Ther.* **14**, 1039–1043 (2009).

248. Watanabe, C., Mizoguchi, H., Bagetta, G. and S, S. The involvement of the spinal release of glutamate and nitric oxide in peripheral noxious stimulation-induced pain-related behaviors—Study in mouse spinal microdialysis. *Neurosci. Lett.* **515**, 111–114 (2012).